50272-101

REPORT DOCUMENTATION PAGE	1. REPORT NO. BuMines OFR 188-82	2.	3. Recipient's Accession No. PB83 137091
4. Title and Subtitle: Haulroad Berm and Guardrail Design Study and Demonstration. Volume I			5. Report Date: June 1981
7. Author(s): Gary L. Stecklein and John Labra			8. Performing Organization Rept. No.
9. Performing Organization Name and Address: Southwest Research Institute, 6220 Culebra Rd., San Antonio, TX 78284			10. Project/Task/Work Unit No.
			11. Contract(C) or Grant(G) No. (C) H0282028 (G)
12. Sponsoring Organization Name and Address: Office of Assistant Director--Minerals Health and Safety Technology, Bureau of Mines, U.S. Department of the Interior, Washington, DC 20241			13. Type of Report & Period Covered: Contract research, 9/78--5/81
			14.

15. Supplementary Notes: Supplements BuMines OFR 189-82 (PB83-137109). Approved by the Director, Bureau of Mines, for placement on open file, November 3, 1982.

16. Abstract (Limit: 200 words)

This report presents the findings of the test programs, simulations, and analyses performed to determine the requirements for the effective application of berms and guardrails as truck restraint systems for elevated mine roadways. Included are criteria for effective vehicle restraints for guardrail applications and recommendations for berm applications based on scale model tests and computer simulations. Full-scale haulage vehicle-berm interaction field tests were performed to correlate the results of these model tests and computer simulations. Recommendations for the construction of berms were made on the basis of tests of berm-bearing strength, response of the vehicle to different berms, and predictions based on the obtained correlation.

17. Document Analysis a. Descriptors

Mining
Haul road
Berm
Trucks

b. Identifiers/Open-Ended Terms

c. COSATI Field/Group: 08I

18. Availability Statement: Release unlimited by NTIS.	19. Security Class (This Report)	21. No. of Pages: 186
	20. Security Class (This Page)	22. Price

(See ANSI-Z39.18) See Instructions on Reverse OPTIONAL FORM 272 (4-77) (Formerly NTIS-35) Department of Commerce

FOREWORD

This report was prepared by Southwest Research Institute, Department of Engine and Vehicle Research, Mining Technology Section, San Antonio, Texas under USBM Contract Number H0282028. The contract was initiated under the Health and Safety/Industrial Hazard/Haulage and Material Handling Program. It was administered under the technical direction of the Spokane Research Center with Mr. Lester Crow and later Mr. Gregory G. Miller acting as technical project Officer. Mr. David J. Askin was the contract administrator for the Bureau of Mines. This report is a summary of the work recently completed as part of this contract during the period September 1978 through May 1981. This report was submitted by the authors on June 30, 1981.

The authors wish to acknowledge the assistance of Mr. James Burkes, section manager, Mining Technology Section for his efforts in reviewing and critiquing this report, Mr. Ronald Mathis, former project manager, for his efforts in initiating and organizing the development of this project, and Sherry Boyd for for her secretarial contribution to this report.

In addition, the authors would like to recognize the contributions made by members of the industrial community, especially Parker Brothers Company, Inc., who through Mr. Richard Hammond, the mine superintendent, provided a site and equipment to perform the first series of tests, and H.B. Zachry Company, who through Mr. Fred Grothaus, the equipment superintendent, provided equipment for perform tests at the SwRI testing facility.

(THIS PAGE INTENTIONALLY LEFT BLANK)

TABLE OF CONTENTS

Section			Page
ABSTRACT			1
FOREWORD			2
LIST OF ILLUSTRATIONS			6
LIST OF TABLES			9
1. INTRODUCTION			11
	1.1	PRESENT RESTRAINT PRACTICES	11
	1.2	MSHA STANDARDS	11
	1.3	ACCIDENT DATA	13
	1.4	PROGRAM OBJECTIVES	15
2. BACKGROUND INFORMATION			16
	2.1	FIELD INVESTIGATIONS	16
	2.2	MECHANISMS OF VEHICLE INTERACTION AND RESTRAINT	32
		2.2.1 Vault	32
		2.2.2 Penetration and Climb	33
		2.2.3 Rollover	33
		2.2.4 Redirection	37
	2.3	METHODS OF VEHICLE-BARRIER ANALYSIS	37
		2.3.1 Geometric Scale Model Simulation	37
		2.3.1.1 Vehicle Considerations	37
		2.3.1.2 Material Considerations	42
		2.3.2 Full Scale Field Tests	45
		2.3.3 Computer Simulations	46
		2.3.3.1 HVOSM Computer Simulations	46
		2.3.3.2 Barrier VII Computer Simulations	49
3. TECHNICAL DISCUSSION			54
	3.1	BERMS	54
		3.1.1 Geometric Scale Modeling	54
		3.1.1.1 Rigid Berm Simulations	55
		3.1.1.2 Deformable Berm Simulations	56

Preceding page blank

TABLE OF CONTENTS, cont'd.

Section			Page
	3.1.2	Field Test Results.	64
		3.1.2.1 Test Site 1	64
		3.1.2.2 Test Site 2	69
	3.1.3	HVOSM Computer Simulations.	78
		3.1.3.1 Cornering Stiffness Coefficients.	79
		3.1.3.2 Tire Stiffness.	80
		3.1.3.3 Steering Parameters	81
	3.1.4	Correlation Analysis.	87
		3.1.4.1 Model Correlation	87
		3.1.4.2 Computer Correlation.	88
	3.1.5	Simulation Predictions.	94
	3.1.6	Berm Requirements	100
3.2	GUARDRAILS.		105
	3.2.1	Collision Severity Index (CSI).	106
	3.2.2	Barrier VII Computer Simulations.	107
3.3	ESCAPE LANES.		112
	3.3.1	Escape Lane Requirements.	112
	3.3.2	Resistance Forces	117
		3.3.2.1 Rolling Resistance.	117
		3.3.2.2 Sinkage Resistance.	117
		3.3.2.3 Aerodynamic Drag Resistance	119
		3.3.2.4 Roll Back	119
	3.3.3	Escape Lane Limitations	120
	3.3.4	Model Tests of Escape Lanes	123
	3.3.5	Median Berms on Escape Lanes.	127
	3.3.6	Construction of Escape Lanes.	127
3.4	MEDIAN BERMS.		131
	3.4.1	Median Berm Model Tests	131
	3.4.2	Construction of Median Berms.	133

TABLE OF CONTENTS, cont'd.

Section		Page
3.5	BARRIERS	136
3.6	BOULDERS	145
3.7	COST EFFECTIVENESS OF RESTRAINT SYSTEMS	153
4.	CONCLUSIONS AND RECOMMENDATIONS	156
5.	RECOMMENDATIONS FOR FUTURE RESEARCH	160
	REFERENCES	161
	APPENDIX A - DETERMINATION OF MODEL VEHICLE MASS MOMENT OF INERTIA	163
	APPENDIX B - HAULAGE VEHICLE DATA	168
	APPENDIX C - HVOSM COMPUTER PROGRAM SYMBOLOGY	174

LIST OF ILLUSTRATIONS

Figure		Page
1	LOCATION OF MINES VISITED DURING STUDY.	17
2	STATIC FORCES ACTING ON HAULAGE VEHICLE	35
3	PLAN OF VEHICLE POSITIONED ON A BERM AT AN APPROVED ANGLE (β). .	36
4	DETAILED VEIW OF MODEL SUSPENSION SYSTEM.	41
5	FIELD TEST CONFIGURATION AND DATA RECORDED.	47
6	BERM QUALIFICATIONS TEST DESCRIPTION.	48
7	WHEEL CLIMB OF RIGID BERM (MODEL SIMULATION).	58
8	35-TON VEHICLE RESPONSE FOR TEST 1A ON AN AXLE HEIGHT, UNCONSOLIDATED PIT RUN MATERIAL BERM.	67
9	35-TON VEHICLE RESPONSE FOR TEST 1B ON A THREE AXLE HEIGHT, UNCONSOLIDATED PIT RUN MATERIAL BERM.	68
10	35-TON VEHICLE RESPONSE FOR TEST 1C ON A THREE AXLE HEIGHT, COMPACTED PIT RUN MATERIAL BERM	70
11	35-TON EMPTY VEHICLE RESPONSE FOR TEST 1D ON A THREE AXLE HEIGHT, COMPACTED PIT RUN MATERIAL BERM	71
12	35-TON VEHICLE RESPONSE FOR TEST 2A ON AN AXLE HEIGHT, UNCONSOLIDATED SELECTED MATERIAL BERM	74
13	35-TON VEHICLE RESPONSE FOR TEST 2B ON A THREE AXLE HEIGHT, UNCONSOLIDATED SELECTED MATERAIL BERM	75
14	35-TON VEHICLE RESPONSE FOR TEST 2C ON A THREE AXLE HEIGHT, COMPACTED SELECTED MATERIAL BERM.	76
15	35-TON VEHICLE RESPONSE FOR TEST 2D ON A THREE AXLE HEIGHT, BANK CUT BERM	77
16	TIRE STIFFNESS COEFFICIENTS	82
17	EFFECT OF TIRE STIFFNESS ON BERM CLIMB.	85
18	RIGID BERM MODEL TEST COMPARED TO TEST 2C	89
19	MODEL TEST - FIELD TEST COMPARISON.	90

LIST OF ILLUSTRATIONS, cont'd.

Figure		Page
20	COMPUTER SIMULATION, MODEL TEST, AND FIELD TEST 2C DATA COMPARISON FOR 35-TON VEHICLE.	93
21	PREDICTED RESPONSE OF 85-TON HAULAGE VEHICLE	97
22	PREDICTED RESPONSE OF 170-TON HAULAGE VEHICLE.	98
23	GENERAL BERM SIZE REQUIREMENT AS A FUNCTION OF BERM STRENGTH . .	101
24	BERM SIZE REQUIREMENT AS A FUNCTION OF STRENGTH FOR 35-TON VEHICLE.	102
25	BERM SIZE REQUIREMENT AS A FUNCTION OF STRENGTH FOR 85-TON VEHICLE.	103
26	BERM SIZE REQUIREMENT AS A FUNCTION OF STRENGTH FOR 170-TON VEHICLE.	104
27	DOUBLE TUBULAR THRIE/WOOD POST GUARDRAIL	108
28	WIDE FLANGE/WOOD POST GUARDRAIL.	109
29	CONCRETE POST/WIDE FLANGE GUARDRAIL (MODEL K).	109
30	SINGLE WIDE/FLANGE/WOOD POST GUARDRAILS.	110
31	WIDE FLANGE/DUAL LEG CONCEPT (MODEL O)	110
32	TYPICAL VEHICLE TRAJECTORY (CASE NO. 24)	115
33	TYPICAL VEHICLE ACCELERATION-TIME TRACE (CASE NO. 24).	115
34	FORCES ACTING ON INCLINED VEHICLE.	121
35	EFFECT OF ROAD SURFACES ON TOTAL ROLLING RESISTANCE.	122
36	ILLUSTRATION OF ESCAPE LANE TEST CONFIGURATION	125
37	ESCAPE LANE STOPPING DISTANCE FOR VARIOUS MATERIALS FOR 85-TON VEHICLE	126
38	COMPARISON OF MODEL TEST RESULTS AND THEORY FOR ESCAPE LANES FOR 85-TON VEHICLE	128

LIST OF ILLUSTRATIONS, cont'd.

Figure		Page
39	STOPPING DISTANCE USING MEDIAN BERM ON ESCAPE LANE (MODEL TEST RESULTS).	129
40	MEDIAN BERM DESIGN CONFIGURATION.	132
41	STRENGTH CHARACTERISTICS OF MODEL MEDIAN BERMS.	134
42	STOPPING DISTANCE FOR CURRENTLY RECOMMENDED MEDIAN BERMS OF VARIOUS STRENGTHS AND ZERO PERCENT GRADE.	135
43	COMPARISON OF STOPPING DISTANCES.	137
44	BARRIER COMBINATION I	139
45	BARRIER COMBINATION II.	140
46	BARRIER COMBINATION DESIGNS III AND III-A	141
47	BARRIER COMBINATION DESIGNS IV AND V.	142
48	BARRIER COMBINATION DESIGN VI	143
49	VEHICLE-BOULDER IMPACT.	147
50	VEHICLE IMPACTING BOULDER BERM.	149
51	VEHICLE STOPPING DISTANCE FOR BOULDER IMPACTS BY 85-TON VEHICLE	152

LIST OF TABLES

Table		Page
1	SUMMARY OF HAULAGE ACCIDENTS.	13
2	CONTRIBUTING FACTORS ASSOCIATED WITH HAULAGE ACCIDENTS.	14
3	SUMMARY OF HAULAGE ACCIDENTS RELATING TO BERM LOCATION.	14
4	SUMMARY OF MINE VISITS.	19
5	PARAMETERS FOR BERM IMPACT.	38
6	PI TERMS FOR BERM IMPACT.	38
7	SCALE FACTORS FOR MODELING BERM IMPACT.	40
8	LOADED VEHICLE MOMENTS OF INERTIA	43
9	GENERAL HAULAGE VEHICLE	44
10	HVOSM INPUT PARAMETERS FOR FULL-SCALE 35-TON HAULAGE VEHICLE	50
11	HVOSM INPUT PARAMETERS FOR FULL-SCALE 85-TON HAULAGE VEHICLE	51
12	HVOSM INPUT PARAMETERS FOR FULL-SCALE 170-TON HAULAGE VEHICLE	52
13	MODEL VEHICLE FRICTION COEFFICIENT/CRITICAL TIPPING ANGLE	55
14	RIGID BERM MODEL TEST RESULTS	57
15	EFFECT OF BERM STRENGTH ON VEHICLE RESPONSE FOR 30 MPH IMPACT AT 30° APPROACH ANGLE	60
16	DEFORMANCE SOIL BERM TEST RESULTS FOR 30 MPH IMPACT AT 30° APPROACH ANGLE.	61
17	EFFECT OF APPROACH CONDITIONS ON DEFORMANCE BERM COMPOSITIONS.	63
18	35-TON HAULAGE VEHICLE FIELD TEST MATRIX, TEST SITE 1, LIMESTONE QUARRY.	66

LIST OF TABLES, cont'd.

Table		Page
19	35-TON HAULAGE VEHICLE FIELD TEST MATRIX, TEST SITE 2, SwRI TEST SITE.	72
20	EFFECT OF TIRE CORNERING AND CHAMBER STIFFNESS COEFFICIENTS FOR AN 85-TON VEHICLE.	80
21	COMPUTER SIMULATION SUMMARY FOR 35-TON VEHICLE.	83-84
22	STEERING DEGREE-OF-FREEDOM (DOF) EFFECT ON VEHICLE/BERM INTERACTION	86
23	COMPUTER SIMULATION, MODEL TEST, AND FIELD TEST DATA COMPARISON FOR 35-TON VEHICLE	92
24	HVOSM PREDICTIONS OF 85-TON HAULAGE VEHICLE-BERM INTERACTION	95
25	HVOSM PREDICTIONS OF 170-TON HAULAGE VEHICLE-BERM INTERACTION	96
26	MAXIMUM RESULTANT TIRE LOAD PREDICTION BY HVOSM COMPUTER SIMULATIONS	99
27	HAULAGE VEHICLE PARAMETERS FOR CSI.	107
28	SUMMARY OF GUARDRAIL DESIGN CONCEPTS.	111
29	120-TON HAULAGE VEHICLE FLEXIBLE BARRIER INTERACTION. . . .	113
30	235-TON HAULAGE VEHICLE FLEXIBLE BARRIER INTERACTION. . . .	114
31	TYPICAL ROLLING RESISTANCE FACTORS (R_r)	118
32	VEHICLE BOULDER PARAMETERS.	151
33	ESTIMATED INSTALLED COST OF 1000 FEET OF VARIOUS SYSTEMS TO RESTRAIN 170-TON VEHICLE, 30 MPH, 30°.	154

1. INTRODUCTION

1.1 PRESENT RESTRAINT PRACTICES

Currently a wide variety of restraint systems are used to reduce damage resulting from accidents on surface mine haul roads. These systems include the use of edge of the road berms, guardrails, boulders, concrete barriers, median berms and escape lanes. Mines overwhelmingly prefer to use berms constructed of waste material because they feel that berms are the least costly of alternatives.

Guardrails are used in locations where the installation is thought to be permanent, such as at mine entrances. They can also be found where the road width is not sufficient to provide room for the construction of berms.

Boulders are used where they are a natural product of the mine operation. Found in areas where large rock formations comprised a significant portion of the overburden, their application as a restraint system is a result of an attempt to reduce the cost of rehandling the material.

Concrete barriers are the least common of the restraint systems to be applied to the mine environment. Reasons for their unpopularity include large initial cost, high cost of removal, and inflexibility for reuse.

Median berms provide an alternate to edge of the road restraint systems where adequate length of the roadway exists to utilize the relatively small deceleration rate which may exist. They are used in conjunction with escape lanes to reduce escape lane length requirements.

Escape lanes are the most advantageous restraint system when minimizing damage is the prime consideration. Utilized in steeply sloped terrain, they can be found to be constructed with a firm base where an upward slope is available, but usually are constructed with a loose base to reduce the length requirement.

1.2 MSHA STANDARDS

Government regulations specifying requirements for restraint systems applicable to surface mining operations are contained in the Code of Federal Regulations, Title 30(1)* - Mineral Resources, Promulgated by the Federal Metal and Nonmetallic Mine Safety Act (30 U.S.C. 725). These regulations must be complied with by mine operators for protection of life, promotion

*Number in parenthesis refer to items in the list of references at the end of this report.

of health and safety, and prevention of accidents in open-pit metal and nonmetallic mines. To ensure compliance with these regulations, MSHA inspectors periodically inspect each mining operation. The specific area of concern to this project is the relative degree of industry compliance with the regulations governing berms and signage on open-pit metal and nonmetallic mines and surface coal mines.

The regulations governing the safety standards for various types of mine operations are specified in individual sections of CFR 30. Those standards applicable to Metal and Nonmetallic open-pit mines are contained in Part 55, of which the only item pertinent to this study is as follows:

> 55.9-22 Mandatory. Berms or guards shall be provided on the outer bank of elevated roadways.

An identical set of regulations is contained in CFR 30 for sand, gravel, and crushed stone operations, and for both the underground and surface operations of underground mines.

Part 77 of the Code of Federal Regulations contains the mandatory safety standards for surface coal mines and surface work areas of underground coal mines. The section applicable to this study is as follows:

> 77.1605(k) Berms or guards shall be provided on the outer bank of elevated roadways.

Mine operators are aware of the problems which exist in complying with these regulations. At present, they have no guidelines, recommendations, procedures, etc., which define the requirements of a berm or guard which will not only insure compliance with the regulation but will insure the safety of personnel. The only actual guideline available is the definition of a "berm" as given in CFR 30 - "a pile or mound of material capable of restraining a vehicle". The actual size or composition of the material required to restrain a vehicle is not known. The alternatives for the mine operator are to individually conduct tests to determine the requirements for berms which will restrain the size haulage vehicle used or to construct the berms to satisfy MSHA inspectors.

Mine operators have a vast amount of working experience with their equipment. They probably know more about the capabilities of their equipment than the respective manufacturers. Numerous interviews with mine personnel have indicated the perceived ineffectiveness of berms constructed to the current "rule of thumb" recommendations (current rule of thumb recommendations indicate that the berm should be built to the axle height of the largest haulage truck using the haul road). Mine operators, therefore, tend to have one of the following three distinct attitudes toward berm construction.

- Current rule of thumb (axle height) recommendations are judged to be inadequate and to compensate, mine personnel construct berms to a height of between two and three times the axle height, hoping to improve berm effectiveness.

- Current rule of thumb recommendations are accepted or at least not questioned and built to current recommendations in order to avoid confrontation.

- Current rule of thumb recommendations are judged to be inadequate, but operators continue to construct berms to minimum standards.

1.3 ACCIDENT DATA

Prior to initiation of this project, it was anticipated that a significant amount of vehicle/berm encounter data would become available through review of MESA/MSHA accident reports. Federal law requires that each fatal accident be investigated and an appropriate accident report form prepared. To determine the exact information that is available and the means of obtaining this information, an investigation team worked with the MSHA Health and Safety Analysis Center, (HSAC) in Denver. Only those accidents which have occurred from January 1975, through December 1977, were investigated.

Computer listings provided coded information as to location of mine, date accident occurred, type of equipment involved, job held by injured party, length of experience of the injured party on the job, activity of injured party at the time of the accident, and degree of injury. The listings are compiled according to type of mine.

Table 1 is a summary of all the haulage accidents which have occurred in surface or open-pit mines, both coal and metal/nonmetal (including metallic minerals, nonmetallic minerals, and quarrying) for the years 1975 through 1977, classified according to the existing coding system.

Table 1
Summary of Haulage Accidents

YEAR	TYPE OF MINE	FATAL	NON FATAL INJURY	NON INJURY	TOTAL
1975	Coal	16	264	200	480
	Metal/Nonmetal	9	455	245	709
1976	Coal	12	318	238	568
	Metal/Nonmetal	12	402	166	580
1977	Coal	11	327	229	567
	Metal/Nonmetal	17	359	149	525

Table 2 presents the statistics based on the contributing factor associated with accidents which occurred on haulage roads.

Table 2

Contributing Factors Associated with Haulage Accidents

Year	Type of Mine	Barrier Berms	Median Berms
1975	Coal	12	2
	Metal/Nonmetal	26	2
1976	Coal	17	3
	Metal/Nonmetal	35	3
1977	Coal	12	3
	Metal/Nonmetal	44	5

Incidents associated with berms occurred in two primary areas of mining operations, berms located along the edge of a haul road, i.e., those being investigated by this study, and berms located along the edge of a dump site. The summary of the haulage data pertaining to berms, presented in Table 2, is further divided between these two areas, and is presented in Table 3.

Table 3

Summary of Haulage Accidents Relating to Berm Location

	COAL				METAL/NONMETAL			
YEAR	HAUL ROAD	PERCENTAGE OF TOTAL HAULAGE ACCIDENTS	DUMP SITE	PERCENTAGE OF TOTAL HAULAGE ACCIDENTS	HAUL ROAD	PERCENTAGE OF TOTAL HAULAGE ACCIDENTS	DUMP SITE	PERCENTAGE OF TOTAL HAULAGE ACCIDENTS
1975	7	1.5	59	1.0	2	.3	5	.7
1976	8	1.4	9	1.6	24	4.1	11	1.9
1977	8	1.4	4	.7	29	5.5	15	2.9

1.4 PROGRAM OBJECTIVES

Current regulation inadequacies may be viewed as the primary reasons why stringent, acceptable restraint systems are not unilaterally found in mine environments. A more realistic reason is the lack of information which has existed for the proper design of restraint systems.

To alleviate this situation, this project was initiated with the specific objectives of determining the kind, size, and construction of berms, guardrails, or a combination of both, for mine haulroads to be effective in controlling runaway or run-off of any size mobile haulage vehicle.

(THIS PAGE INTENTIONALLY LEFT BLANK)

2. BACKGROUND INFORMATION

2.1 FIELD INVESTIGATIONS

Before suitable restraint systems were designed, a certain amount of background knowledge of mine lay-outs, present methods of haulage vehicle operations, effects of terrain and climate on a mining operation, etc., was obtained. Each of these areas was investigated by judiciously selecting representative mining operations, visiting each mine site, and discussing problems with the appropriate personnel. Selection of candidate mine sites provided a representative cross-sectional sampling of each type of mining operation which will be affected by any proposed recommendations resulting from this program.

Figure 1 shows the location of the various sites inspected throughout the course of this study. Three were metal mines, three were coal mines, and three were quarry operations.

Selection of mine sites was based on one or more of the following factors:

- Geographical location
- Type of mining operation
- Relative size of operation
- Past safety of mine

The primary concern regarding the geographical location was the requirement for snow removal equipment on the haulage road and the influence of both median and edge-of-the-road berms on the operation of such equipment. Erosion of berms due to rain, while being an area of importance in berm and road construction, was treated as a secondary influence on mine selection.

The type of mining operation, e.g., open-pit, surface, contour, or quarry, defines the width and length of the haulage route. The haulage route in a surface mining operation is longer and utilizes larger size haulage vehicles than a quarry operation. Consequently, the requirement for berms and the material generally available for berm construction will be a function of the specific mining operation. Mine sites were, therefore, selected to obtain a representative sampling of the various operations.

The relative size of the mining operation becomes a significant factor considering that any proposed recommendations resulting from this project will affect all mining operations. Since the regulations that apply to the major mining corporations will also apply to the small independent organizations, another criteria for mine site selection was the size of the company. Therefore, the views, opinions, and limitations of various size operations were obtained.

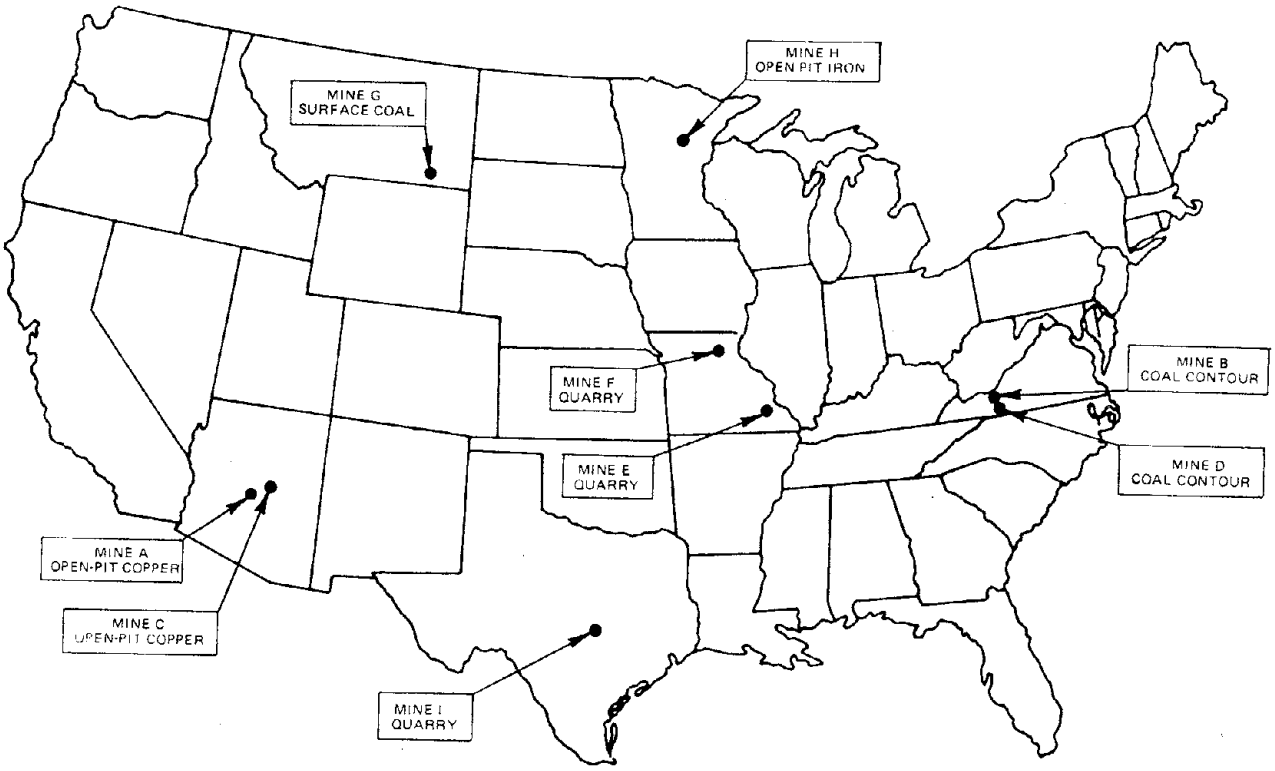

FIGURE 1. LOCATION OF MINES VISITED DURING STUDY

A portion of the work effort was devoted to review of existing accident data. Review of this data indicated the existence of several mining operations which experienced a past history of haulage accidents as well as some operations which were considered very safety conscious. The extremes from both mine situations were chosen for visits.

Mine Visits

General characteristics, observations, operator comments, and types of berm construction for each mine visited were obtained. Table 4 summarizes the types, locations, operational characteristics, and berm composition observed at the various sites. As originally anticipated, berm materials range from fine waste material to 4 ft boulders. The use of the boulders, however, was more evident in quarry type operations. The majority of berms observed were a mixture of overburden soil and drill/blasted rock material, the general type of mixture resulting from blasting operations. Several of the mine operators were selective in the choice of material for use in berms, mentioning that they preferred a mixture of soil and rock rather than rock only.

Opinions of the mine operators regarding the effectiveness of a berm to restrain a haulage vehicle varied from a feeling of confidence in the restraint capability of a berm to the opinion that their effect is totally psychological. One operator commented that the berms only provide a false sense of security for the drivers.

The cost associated with construction of a berm was not immediately known by mine personnel, the general remark being that cost is insignificant because overburden material has to be relocated at some distance along the haulage road anyway.

Most operators were of the opinion that something could be done to the berm to minimize the potential danger of having the vehicle ride up and vault the berm. The ideas of compacting and shaping the berm to provide redirection of the vehicle and the use of specific grades or mixtures of available overburden material were discussed as possible solutions.

The use of guardrails or portable barrier systems was discussed and initially dismissed by mine operators as being uneconomical or technically unfeasible. Further discussion of these types of restraint systems generally resulted in a concession that for certain specific situations a guardrail system may be a viable solution. These situations might be in instances in which an errant haulage vehicle could cause additional damage if it vaulted a berm. From an economic viewpoint, the installation of a guardrail system does not appear feasible when the haul road may be mined within six months to a year.

TABLE 4

Summary of Mine Visits

MINE	LOCATION	TYPE OF MINE	NO.-SIZE OF HAULAGE VEHICLE	MAXIMUM HAULAGE SPEED, MPH	LENGTH OF HAULROAD, MILES	MAXIMUM ROAD GRADE	TRAFFIC PATTERN	EDGE-OF-ROAD BERM HEIGHT, FT	BERM COMP.
A	Arizona	Open-Pit-Copper	34-120 ton 6-235 ton	26	1/2-2-1/2	8-10%	Left Hand	8-10	Soil plus small rock
B	West Virginia	Contour-Coal	85 ton 50 ton 35 ton	20	4	10%	Right Hand	4- 5	Sandy clay
C	Arizona	Open-Pit-Copper	15-150 ton 5-170 ton	22	1-1/3-1-1/2	8-10%	Left Hand	8-10	Soil plus 12-18 inch rock
D	West Virginia	Contour-Coal	5- 35 ton 3- 50 ton	25	3-6		One Way	4	Soil plus small rock
E	Missouri	Quarry	3- 35 ton 1- 50 ton		1/4—1/2		One Way	4- 8	Large rock 18-24 in. large boulder, soil and small rocks
F	Missouri	Quarry	6- 35 ton		1/4	6%	Left Hand	4	Rock 12-18 in. Boulder 3-4 ft
G-1	Montana	Surface-Coal	6- 80 ton 9-150 ton	25		4-6%	One Way as required		Overburden Material Coal
G-2	Montana	Surface-Coal	19-170 ton	26	1-1/2	<6%	Switching	5	Waste material small rock
H	Minnesota	Open-Pit-Iron	80-120 ton		3-15	6-8%	Right Hand	6	Waste Material large rock
I	Texas	Quarry	3- 15 ton 3- 35 ton	24		<6%	Right Hand	4	Crushed rock 3/4 in. Boulders 3-4 ft

Mine A

Mine A, located in Arizona, represents a major open-pit metal mine. The annual precipitation rate is eight inches with an approximate temperature range from 26 to 116°F. The mine was selected as one which successfully utilized median berms as a retard mechanism for large haulage trucks.

The general configuration of this mine is a multiple bench operation for the mining of copper ore. The overburden material is drilled and blasted and removed by a shovel/truck operation. The benches are maintained at a 40 foot height and the overall stripping ratio maintained at 3:1. The entire mining operation is located in a valley between two mountains, the benches being located on the slope of each mountain with mining progressing outward. Overburden material is transported by haulage vehicles to the dump sites located at each end of the valley.

The tour of the mine haulage roads was conducted by the Mine Safety Engineer. He explained the training program employed for new drivers, the general operation of the mine, and his opinion of guardrails and portable barrier systems. Basically, he feels the edge-of-the-road berms and median berms presently employed by the mine are sufficient, and that guardrails or portable barriers would not be economically feasible for the size of haulage vehicles used at the mine. The company does not have a specific set of safety guidelines for general use at the mines, but leaves the safety policy and compliance with MSHA regulations as the responsibility of the Safety Engineer.

Specific Information

Edge-of-Road Berms - The berms along the edge of the road are constructed from overburden material to a height of 8-10 feet (2-2.5 times the axle height of the 85-ton haul truck). These berms are considered sufficient to restrain a haulage vehicle if impacted at a shallow angle. The company has had a driver fall asleep and impact these berms without serious consequences. When it is determined which vehicle was involved, the operator will be suspended.

Median Berms - Median berms are used wherever the steep grades occur. These are constructed from a finer grade of overburden material, not containing any big rocks. These berms are normally 4-5 feet high with a base width of 8-10 feet. Periodically these median berms require rebuilding since the edges are often cut away by the blade on the road grader.

These median berms are a constant height with the length varying from 125-175 feet. A specific method of construction, e.g., tapering the entrance ramp, widening out the base, etc., is not used. If the safety people feel that a median berm is too long, they instruct a dozer or front-end loader to install an opening. If a driver experiences a brake failure, he would probably turn into the berm rather than wait for an opening to

occur in lieu of allowing his speed to increase. Previously, 120-ton vehicles have been stopped by straddling these berms and allowing the front-end and undercarriage to plow up the berm. Information on damage to the truck undercarriage was unobtainable. The width of these berms is considerably less than the spacing between the vehicles' front wheels.

Escape Lane - The mine did have an escape lane; however, it has never been utilized. The mine favors use of the median berm over the escape lane since the operator can take evasive action immediately without having to wait for an escape lane to appear or having just passed one. A median berm is used in the escape lane with soft material on each side. No special maintenance is performed on the escape lane. The soft material is probably soft compared to the haul road. The length of the escape lane was approximately 100-150 feet, with the lane having a steep upgrade. A conventional berm totally enclosed the sides and end of the lane.

General Comments - The predominate feature of this mine was median berms, which did not possess any special, readily apparent design factors such as sloping entrance ramps or side slopes, etc. The edge-of-the-road berm contained larger rocks than the median berms. Both appeared to be constructed in typical mining fashion. Several loads of overburden material are placed at a specific location along the roadway and a front-end loader performs the final shaping of the berm. Occasionally, an opening is installed in the outer berm for drainage.

Mine B

This mining operation, located in West Virginia, is representative of a relatively large contour coal mine. The temperature range at this location varies between 11 to 92°F with the annual precipitation being 43 inches, the annual sleet or snowfall being 27 inches.

The operation of the mine was discussed with the Mine Safety Engineer, with the tour of the mine conducted by a mine representative. The comments of these individuals are included in the appropriate sections of this mine visit report.

The mining method employed at the site consists of mountain top removal. The overburden material located above the coal seam is drilled, blasted and hauled off to a valley fill location. The haulage vehicles used at the location are 85 ton capacity haul trucks loaded by front-end loaders. The haul distance is 1/4 mile or less. The coal is loaded on 35 to 50 ton capacity rear dump coal haulers and transported a maximum of four miles to a dump location. The mine operates two 9-hour shifts six (6) days a week.

Specific Information

Haul Roads - The haul road used at this mining operation is wide enough for two lanes of operation. The traffic pattern employed along

the road is a conventional right hand pattern. Drainage of the road is directed towards the highwall and road grades restricted to below 10 percent. However, in some localized areas the grade did exceed this limit.

Speeds along the haul road were limited to 20 mph as recommended by the company's mining engineers. Road maintenance is presently performed on an "as required" basis. As the road progresses, a full-time crew will eventually be designated for this function. In conjunction with the road maintenance, a rock crusher is available for production of road repair material.

Berms - The berms used on the haul road are constructed from the available overburden material. This berm material appears to be a sandy clay substance containing a noticeable lack of rock fragments, more nearly resembling topsoil rather than material which has been drilled and blasted.

The berms were constructed to existing MSHA standards, i.e., axle height; however, the base width of the berm was wider than that previously observed at other mining operations. The slope of these berms is approximately 1:1. During this visit, the construction of these berms was observed with the following sequence of operation: a rear dump truck backs perpendicular to the edge of the road and dumps successive mounds of material along the edge. The final "shaping" of the berm is then performed by a small front-end loader. Erosion of these berms is a problem, particularly during the fall season due to frequent rains. Along one section of the roadway, the berm was seeded to minimize erosion damage.

Boulders were used for berms in some areas of the mine but only when they were available. These boulder type berms were normally located in the valley fill area where a rock core is used for water drainage. The comment was made that the mine does not make a practice of using the boulders as berms.

Guardrails - The use of guardrails and portable barrier concepts were discussed with the general comment being that the cost would be prohibitive, particularly to the smaller, independent operators. The life expectancy of the haulage road was also mentioned as being a factor against guardrails. The possibility of utilizing a guardrail in a specific location where loss of a vehicle over the edge may result in further incident was discussed, e.g., near a public road, adjacent to houses, etc. This appeared to be the only area where they felt the cost of a guardrail would be justified.

General Comments - The general ability of a berm to stop a haulage vehicle was discussed. The concern is that the berm would act as a ramp for an errant vehicle. We discussed the possibility of constructing the berm in layers, compacting each layer with a sheepsfoot or similar compacting device, then cutting or shaping the inboard side to a specific slope. The Safety Engineer thought this could easily be done and indicated that cutting the steep angle on a berm would minimize the ramp effect of a berm.

The weather was cited as being a significant factor in the condition of the berms at this operation. While the statement was made that a full-time road crew was not presently employed, the condition of the haulage road itself did not appear to be deteriorated even in view of the recent rains.

Mine C

Mine C, located in Arizona, was selected as being representative of a large surface metal mining operation. The annual precipitation rate at this location is approximately eight inches with a temperature range from 25 to 115°F.

General Information

The primary product mined at this operation is copper ore. The operation consists of multiple benches, with the overburden material drilled and blasted. Removal of both the overburden and ore is performed by the shovel/truck method.

The general purpose of the project was discussed with the Director of Safety and the mine tour was conducted by the Safety Engineer.

The mining operation is located at the site of a previous copper mining operation where the ore was removed by contour mining methods. Since then, the entire mountain has been removed and the surrounding area is being mined. The entire operation consists of numerous 45-foot benches, with the majority of the overburden material hauled out one end of the pit.

The general use of guardrails and portable barrier systems was discussed. The general comment was that the cost would be prohibitive and the haul roads are not permanent. Some roads remain in operation for four months, others for four to nine years. In addition, these roads are not always in constant use. The mine maintains a stripping ratio of 1.5:1; therefore, the major operation changes location in the pit to provide this ratio of overburden removal to ore removal.

Specific Information

Haul Trucks - The haulage fleet presently consists of fifteen 150 ton, five 170 ton, with two more 170 tons on order. The mine has six electric shovels, with four, at the most, in operation at one time. The vehicles are in operation three shifts daily seven days per week. The processing plant, crushers, etc., are shut down for maintenance one day per week, and during this time the trucks are engaged only in overburden removal.

The maximum level or upgrade speed of the vehicles is 22 mph, governed speed, and maximum downgrade speed, either empty or loaded, is 10 mph.

Haul Roads - The length of the haulage routes range from 1.3 to 1.5 miles, and consist of curved roads leading up out of the pit to the dump site. Grades range from 8-10 percent, with a left hand traffic pattern used throughout the pit.

The haul roads are crowned for drainage, because without proper drainage too much time would have to be spent in berm and road repair. The operation had recently received several inches of rain prior to our visit, with no evidence of road or berm deterioration.

Edge-of-the-Road Berms - The berms located along the edge of the road were 8 to 10 feet in height and constructed from overburden material. The material at the edge of the base of the berm was loose and muddy as a result of the recent rains; however, there was no evidence of erosion. The overburden material used for these berms consists of rock 12 to 18 inches in size mixed with soil. No special grading procedure is used in selecting berm material.

Escape Lane - One escape lane is available for use at the mine. This lane is located at the base of a downgrade where the haul road makes a 180° turn. The lane is an extension of the road and contains a median berm of four to five feet in height. The lane was positioned at this location based on the judgment of the safety officer. The lane has never been used. The lane is approximately 150 feet in length and eventually runs-out onto a level grade. Eventually, mining in this level area will result in removal of the escape lane.

General Comments - This mine site was representative of a large open-pit mining operation. The haulage roads only require a berm on one side, the opposite side being a bench. The mine personnel feel confident about the berms ability to restrain an errant haulage vehicle.

Mine D

Mine D, located in West Virginia, is representative of a smaller contour coal mining operation. The annual precipitation for this area is 44 inches with an annual sleet or snowfall of 27 inches.

General Information

The mining activity is presently at two contour mining locations, with both having the same general mining method, topography, and operating policies. The tour of both mine sites was conducted by the Mine Superintendent. It had previously rained in the area and began raining as we initiated the tour of the mine; consequently, the condition of the haulage road was quite muddy.

Specific Information

Haul Roads - The haul roads at both sites are essentially identical. The road is narrow, 15 to 20 feet in width, which requires oncoming vehicles to stop at a widened area along the road. A berm is located on the outside edge of the road and a water drainage ditch adjacent to the reclaimed hillside on the other. Normally a full-time scraper operator keeps the roadway in good condition; however, the person generally involved with this function has been off for the past month and deterioration of the road was evident. At some locations, 12 to 18 inch-deep tire tracks were worn into the muddy road. A four percent superelevation is normally maintained for drainage; however, the lack of road maintenance made this feature ineffective at some locations.

Snow is removed from the road by dozers or scrapers and generally piled along the side; only being hauled away if necessary. Special additives were used with the water spray to seal the road surface; however, no solution was used in winter time to prohibit freezing.

Maximum haulage speed on the road is 25 mph. With the number of turns along the road, this speed is probably only reached under ideal conditions. The maximum allowable grade (according to State Regulations) along the road is 12 percent over a specific distance. However, no adverse grades were in existence at either site.

The haulage road at these two sites will only remain in operation for a period of approximately one year. The mining permit expires after that period and the land will then be reclaimed. The roadway is presently advancing at the rate of 60 ft/day.

Berms - The only berms employed were along the edge of the road and constructed from overburden material, a mixture of topsoil and rock. The berm height is approximately four feet. The method of initial roadway construction results in a level area, six to eight feet wide, located approximately 10 feet below the road grade. The intent is that if a vehicle leaves the haul road and goes over the berm, it may be restrained on this lower surface. Adjacent to this lower surface is the treeline which will provide some additional restraint.

No special maintenance is performed on these berms and by the amount of water present in the drainage ditch and the general condition of the road, erosion is not a problem. Inquiries were made concerning the cost of berm construction. No dollar figure was available, but the cost was considered to be insignificant.

General Comments - The mine superintendent seemed convinced of the ability of the berm to restrain the haulage vehicles. There have not, however, been any incidents in which the vehicles ran into the berms,

except that of a dozer, having a mechanical failure during reclamation, rolled backwards down the slope and was stopped by the berm. Vehicles occasionally slide into the drainage ditch. In the event of an emergency, the operator would turn the vehicle into the drainage ditch.

The guardrail and portable barrier concepts were discussed, but the ability of a guardrail to stop a haulage vehicle and also the cost of these systems was questioned.

Mine E

Mine E, located in Missouri, is representative of a typical quarry operation. The temperature ranges between -10 and 100°F, with an annual precipitation of 37 inches, annual sleet or snowfall in the area is approximately 19 inches. This mining operation was selected as one which utilizes boulders for berms.

General Information

The mining operation is located in an area susceptible to snow and icing conditions on the haul road. Prior to this visit, the municipal airport was closed for a three day period due to a recent ice storm. During this time, the mine remained in operation. The tour of the quarry operation, discussion of operating procedures, and general comments on berms, signs, and guardrails were obtained from the Mine Safety Officer.

Specific Information

Haul Roads - The primary haulage road at this site was relatively short, 1500 to 2000 feet in length. This road went from the hopper location down to the quarry floor with a spur road located midway along the main road. The grade of the road was 10 to 12 percent, with the road crowned for drainage. The width of the road was approximately 1.5 vehicle widths; therefore, only one vehicle could operate on the road during a given period. Loaded vehicles had the right-of-way and the entire roadway could be viewed from either end of the haulage route. During the visit, loading was being performed from an area serviced by the spur road; consequently, the vehicles would wait in this area, slightly wider than the main road, for loading by the front-end loader. Traveling out of this area the vehicle would travel down-grade or negotiate a tight 180° turn and proceed up-grade. View of trucks coming out from this area was restricted when viewed from the top of the haulage road; however, there were only three trucks operating along the haulage route. Each operator was aware of the position of the other trucks.

The mine operation was not closed during the recent ice storm. If the road becomes covered with snow or ice a fine material, maybe 1.5 inches or less, is deposited along the road surface. As the condition improves, the ice and rock material is dozed off. The rock material is used to prevent the snow from packing on the road.

Berms - The berms located on each side of the haul road were constructed from overburden material, large rocks 18 to 24 inches of irregular shape and at some locations large boulders intermixed with the smaller rocks. Generally, the mine prefers smaller rocks mixed with soil; however, the large boulders are present and, consequently, placed alongside the roadway. The mine personnel feel that more damage will result if a vehicle inadvertently impacts one of the boulders. The berms were located several feet from the edge of the road surface, approximately four to eight feet.

General Comments - The possibility of using a guardrail or portable barrier system was discussed; however, the Mine Safety Officer feels the economics of the system would be prohibitive and also mentioned the haul roads were only temporary. The possibility of utilizing specific size rock or packing the material in the berms was discussed as being feasible. No cost data was available regarding berm construction; however, the method of construction was typical. A load of material is dumped in a desired position and the front-end loader is used to construct the berm. If necessary, the bucket of the loader would be used to tramp the berm material.

Mine F

Mine F is also located in Missouri and subject to similar climatic condition as the previously discussed mine. This mine was selected as being representative of a larger quarry operation.

Specific Information

Haul Roads - The haulage roads used at the mine are approximately 1/4 mile in length. The vehicles operate in a left hand traffic pattern with the maximum grade being six percent. Several escape lanes or "relief valves" as they were called were located along the haulage route. These were positioned at the base of the downgrade wherever a turn was located. The lanes provided an optional pathway for a vehicle which lost power or failed to negotiate a turn. No median berms, signs, or soft pits were used in conjunction with these lanes.

In general, the road surface was in good condition, being constantly maintained by a grader. Snow or ice on the road is removed by either a loader or dozer. To prevent snow from being packed, 1.5 inch of material is deposited along the road surface; consequently, the road is slightly higher during the winter season. During muddy road conditions, layers of the road surface are removed.

Berms - The berms located along the edge of the roadway were constructed from overburden material consisting of rock 12 to 18 inches in diameter and occasionally large boulders three to four feet in diameter. As in the previous quarry operation, the boulders were available and, consequently, utilized as berms.

The mine site has had two separate incidents in the past of vehicles being restrained by the boulder type berms. In both cases the vehicle was unloaded and appears to have been stopped by hi-centering on the boulder.

General Comments - The use of guardrails or barrier systems were discussed with the general opinion of the mine personnel being that the cost would be prohibitive. Some of these haulage roads will be in existence for several years and others for only a short period. Shaping of the berm or using specific grade (size) of material for berm construction was considered feasible; however, the majority of the berms observed contained a considerable amount of rock and very little soil. Shaping of these berms would be difficult.

Mine G

Mine G is considered representative of the larger surface coal mining operations located in Montana. The temperature at this location ranges from -35 to 96°F , with an annual precipitation of 10 inches. The annual sleet or snowfall is 24 inches. This mine was selected for its geographical location and the large size of the haulage vehicles. There are two adjacent mining operations, each operated and managed separately. The observations and comments from each mine are discussed separately.

General Information (Mine G-1) - This mine operation utilizes two draglines, both with approximately 70 yard capacity buckets, to remove 100 feet of drilled and blasted overburden to uncover a 52-foot single coal seam. Topsoil is removed prior to this by scrapers, stock-piled and later replaced. Reclamation is performed by standard tracked dozers.

The coal is hauled out of the pit by a fleet of nine 150-ton, bottom-dump, coal haulage trucks. In addition, six 80 ton trucks are used. The shot coal is loaded on the trucks by a shovel which operates on the coal seam at a grade below the truck haulage road. Working the seam in this manner eliminates the congestion of turning the vehicles around in the pit, which may not be wide enough.

The basic layout of the mine is similar to a half-section of spoked wheel. The dragline operates along the circumference-spoiling inward, spokes form the haulage roads leading to the stock pile located at the center of the wheel. The vehicle enters the pit down a one-way spoke, is loaded in the pit, and driven out of the pit on an adjacent one-way spoke to the stock pile location.

Haul Road Information (Mine G-1) - The operating procedure for this mine was discussed with the Safety Manager. Due to the type of operation, loading out of the pit, there are few elevated roadways which require a berm. If a vehicle lost control going down into the pit, it would be

restrained by the highwall on both sides of the road. Average grade is four to six percent, with the one ramp being 10 percent. However, hauling is not done on this steep ramp.

Once in the pit area, the vehicles drive along the coal seam which constitutes an elevated roadway. The berm along this road is constructed completely from coal to eliminate contamination of the coal seam.

This situation is probably a common occurrence in thick seam operations. Shovels have a maximum reach of 40 feet and the haul trucks have a loading height of 15 feet. Therefore, a 25-foot bench height or seam thickness would be maximum with a shovel/truck operation. No type of guardrails, escape lanes, or median berms are used at this site.

Prior to each shift, the drivers report to a central briefing room where they are instructed as to the location of the shovel, which ramp they will enter on, and which one they will haul out of. In addition, a line drawing layout of the various haulage roads is displayed with arrows indicating the traffic pattern for the day. If a change occurs, the pit foreman will stop every haul truck and inform the driver of the change.

We did not have the opportunity to interview any of the vehicle operators at this site. However, we did talk to the person who trains the vehicle drivers. All the personnel are given a general safety briefing, the drivers are instructed to wear seat belts and stay with the vehicle in the event of an accident. The general comments concerning berms, signs, etc., of the Safety Officer will be discussed in a later section of this report.

General Information (Mine G-2) - This mine is a typical shovel/truck operation. Two 40 yd^3 shovels are used to remove the 40 feet of blasted overburden which uncovers the first of two seams. Each seam at this location is approximately 25 feet and the seams eventually run together. The two shovels load a fleet of 19 rear dumps, all having 170 ton capacity. The blasted overburden material is then transported approximately 1.5 miles to the dump area. At this dump area the trucks make a fishhook turn, back-up to the edge and dump the material over. A dozer, referred to as a cat-skinner, is constantly pushing the material over the edge, while maintaining a 5 foot protective berm. Coal is presently being removed from a separate pit by center dumps, transported to the stockpile, and shipped out by rail.

Haul Road Information (Mine G-2) - The haul road for the overburden removal trucks runs from the pit area, up a gradual grade, along one edge of a pit where coal is being removed, and up a slight grade to the dump site. The road along the edge of the pit has a 5 foot berm. The haul truck travels along the road at 26 mph, governed vehicle speed. A similar berm is constructed along the outer edge of the road leading to the dump site location.

A median berm was previously used on the section of haul road next to the pit, when the enter haulage road then used a left hand pattern. However, this median berm trapped snow during the winter and caused considerable problems. The median berm was subsequently removed. At present, there are no median berms or escape lanes utilized at this mine.

When asked about road conditions, the driver mentioned that the water truck sometimes gets the road too wet, but it wasn't a big problem. During the winter season, the mine uses a salt solution to prevent the water from freezing on the road surface.

General Comments on Mine G-1 and G-2 - Both mine Safety Officers spent some time discussing the general purpose of our visit. They do not feel that berms or guardrails would be beneficial in preventing a runaway for the haul trucks at their mine. They are of the opinion that the berm has more of a psychological effect than a safety value.

Mine H

Mine H, located in Minnesota, represents a large metal mining operation. The mine site was selected on the basis of its geographical location, the large size of the operation, and the reputation of the company's safety consciousness. The annual precipitation in this area is 25 inches, with an annual sleet or snowfall of approximately 70 inches. The temperature ranges from 31 to 92°F. The tour of this operation was conducted by the company's Mine Safety Engineer.

General Information

The haulage fleet consists of 80 rear dumps having carry capacities of approximately 120 tons. The haulage trucks at the mine are used for two purposes, transporting overburden material to a dump site or hauling tailing material (fine grade material not containing iron) from the processing plant to a dump site. The mine operates three shifts per day seven days per week.

The maximum loaded speed of these trucks is approximately 20 mph. The drivers are not restricted to any specific speed but are instructed to drive according to road conditions. Maximum no grade speed for these types of vehicles, listed in the manufacturers literature, is 32 mph. The length of the haulage route varies from 3 to 15 miles.

Haul Road Information

Haul Roads - The haul roads at this mine, while maintained by graders and water trucks, were rougher than those observed at other sites. These roads were well bermed; in fact, the policy is almost, when in doubt, berm it. Berms are used on both elevated haulage roads and service roads. The material used for these berms is either the overburden material--blasted,

large rock type material or tailing material--a fine grade substance. Those berms constructed from tailing material are higher than those made from the overburden material with the idea that both berms are capable of stopping a slow vehicle impacting at a shallow angle but that the finer material possesses less resistance.

The berms are constructed by dumping the material from the haulage trucks at the specified location. If the operator feels a berm is inadequate or if it has been eroded, he reports it and the berm is repaired.

Berms constructed from overburden or waste material are the only type of vehicle restraining device used on the mine. The mine personnel feel their effect is psychological and will only restrain a vehicle impacting at a slow, shallow angle. They have had a haul truck go over a regulation size berm constructed from the tailing material. This particular incident occurred as the vehicle came over a hill, applied the brakes, and the vehicle skidded on ice, turned 90 degrees, and went over/through the berm, down a 25-foot embankment. The accident, fortunately, was non-fatal.

Use of a guardrail system or portable barrier concept was discussed with the mine personnel. They don't think anything will stop a loaded haulage truck impacting at 90°. They mentioned that the economics of the suitable restraining system will be a primary factor for acceptance of this type of system. For their particular operation, they do not have many elevated roadways and think barriers other than berms may be more significant in a contour mining operation.

Mine I

Mine I, located in Texas, was selected as being representative of a typical quarry operation. The annual precipitation in this area is 37 inches with the temperature ranging from 22 to 100°F. The mine tour was conducted by the quarry Superintendent with most of the pertinent comments being supplied by the works manager.

General Information

The primary product of the mine is high calcium limestone, obtained from a 26-foot seam. The material is loaded on 15 to 35 ton capacity haulage trucks by front-end loaders. The material is then dumped into a crusher, grader, separator, kiln, etc., eventually producing high concentrate lime. The 50 feet of overburden material is drilled/blasted and sold to a subcontractor who hauls it off with his own trucks.

The mine personnel were interested in this present study but indicated that they do not think a berm will stop a 35-ton vehicle. The general thinking is that berms serve more as a guide than a safety feature. They feel that the economics of barrier systems will be a primary factor in their acceptance. While they could not supply a cost for berm construction or maintenance they considered it as being insignificant.

Specific Information

Haul Trucks - The haulage fleet consists of three 35 ton rear dump trucks. The vehicles are operated in two shifts per day, except Sunday.

The speed of the haul trucks is at the discretion of the driver. Maximum rated speed is 32 mph. The Superintendent mentioned the average speed is 24 mph.

Haul Roads - The haul roads on this mine were winding and undulating; this may have been due to the seam configuration, outcroppings, etc. The general path of the roadway was not conducive to a maximum speed operation. The road surfaces are maintained by the typical water truck and grader operation. Due to the geographical location of the mine, the major problem is rain, which causes erosion of the berms.

The berms utilized at this location are constructed from existing available material. The size ranges from boulders approximately four to five feet in diameter to waste material 3/4 inch and under. This type of operation can easily construct berms from crushed material which are fairly uniform in size.

General Comments - The predominant feature of this mine was the difference in the material size used in the construction of berms. The boulder type of berm will probably be more prevalent at the quarry type operation.

Table 4 summarizes the general characteristics of the mining operations visited during this project.

2.2 MECHANISMS OF VEHICLE INTERACTION AND RESTRAINT

The purpose of any restraint system is to prevent the vehicle from leaving the elevated roadway. The methods of restraint include a combination of berm penetration and vehicle climb, redirecting the vehicle, or causing the vehicle to roll over. Restraint, therefore, is a desired effect of the vehicle's interaction with the restraint system.

2.2.1 Vault

Loss of the vehicle from the haul road will almost always result in an uncontrolled accident at the bottom of the elevated road. It is for this very reason that the other interactions are acceptable.

Defining vaulting as the condition where the vehicle has the potential of leaving the elevated roadway does not precisely describe the vehicle's acceptable location during an accident situation. The likelihood of rear slope failure of the roadway dictates the distance from the edge of the road that should be maintained during the interaction.

Because of the inconsistent nature of the road construction material, it is impossible to determine exactly the distance which would be safe for each road condition. When berms are used, preventing the leading tire that contacts the berm from penetrating more than halfway through the berm can be used as the criterion for vaulting. When guardrails are used, keeping all tires at least two axle height distances from the edge of the roadway can be used as the design criterion. This same tread criterion can also be applied to concrete barriers and boulders since it may be the only convenient measure for these restraint systems.

2.2.2 Penetration and Climb

Penetration and climb are interactions which primarily occur between vehicles and berms although some small aspects are present in the interactions with other restraint systems.

As the leading tire of the vehicle contacts the berm, the tire begins to penetrate into the berm. If the bearing strength of the berm is of sufficient value, the tire will also begin to climb up the berm's surface. At the lower end of the possible berm strength, penetration of the tires and also of the vehicle's body will be the predominent interaction. When this occurs, the size of the berm must be sufficient to prevent the leading tire from penetrating more than halfway through the berm.

Increasing the berm's bearing strength will cause the vehicle to climb the berm. In this case, the combination of penetration and the change in the vehicle's elevation will cause the vehicle to come to a stop.

2.2.3 Rollover

Rollover may not seem to be a desirable method of restraining a runaway haulage vehicle. Indeed, it is probably the least desirable method of restraint, but there are conditions where it may be the only practical means of restraint.

Field investigations revealed that 20 mph was the typical recommended speed for use on haul roads, but that 32 mph was the maximum speed recommended by manufacturers. If a vehicle was traveling at 30 mph and interacted with a berm, the required changes in height to totally dissipate the vehicle's kinetic energy would be 30 feet. It would be impractical to build a berm to this height requirement.

Penetration into the berm would reduce this height requirement, but during times of prolonged cold weather, the likelihood of penetration decreases. Rollover may be the only restraint option available.

For rollover to occur, the line of action of the vehicle's weight must fall outside of the vehicle's tire footprint. Figure 2 indicates the static forces operation on the vehicle. Equation (1) indicates a method of determining the static tipping angle of a vehicle.

$$\theta = \tan^{-1} \frac{(t/2)}{h} \qquad (1)^*$$

where:

Wx = vehicle weight, component parallel to road slope (lb)
Wy = vehicle weight component normal to road slope (lb)
s = side force on vehicle wheels (lb)
t = horizontal track width (in.)
h = vertical location of c.g. from ground level (in.)
θ = side slope of road.

When a vehicle is positioned on a berm at an approach angle (β) as shown in Figure 3, the body roll angle can be determined according to Equation (2). The approach angle

Vehicle Slope Angle (γ) = Berm Slope Angle (θ) x cosine (Approach Angle (β)) (2)

of a haulage vehicle will, at the minimum value, be zero degrees. It can be expected to increase to some practical limit which will be governed by the width of the road, the radius of curvature of the road, and the turning radius of the vehicle. Physical limitations of the mine sites noted during the field investigations indicated that an approach angle of 30° would be possible. Since the body roll angles presented in Figure 2 indicated the maximum vehicle slope angles required for instability, it is possible by using Equation (2) to derive the berm slope angle required for instability.

For a vehicle slope angle of 30° at an approach angle of 30°, the required berm slope angle for rollover is 35°. When the vehicle slope angle is 40° at an approach angle of 30°, the required berm slope angle for rollover is 46°.(Figure 3)

Vehicles operating on a berm experience a vehicle slope angle (γ) greater than that expressed in Equation (2) because of suspension system deflections of the vehicle. These values were found to range as much as 20° with a minimum value of at least 10°. Because of this additional amount of vehicle slope angle, the minimum berm slope angle to achieve rollover can be obtained. For example, when the approach angle is 30° and the

*Numbers in parenthesis and underlined refer to equations, some of which are referenced when their derivation is not obvious.

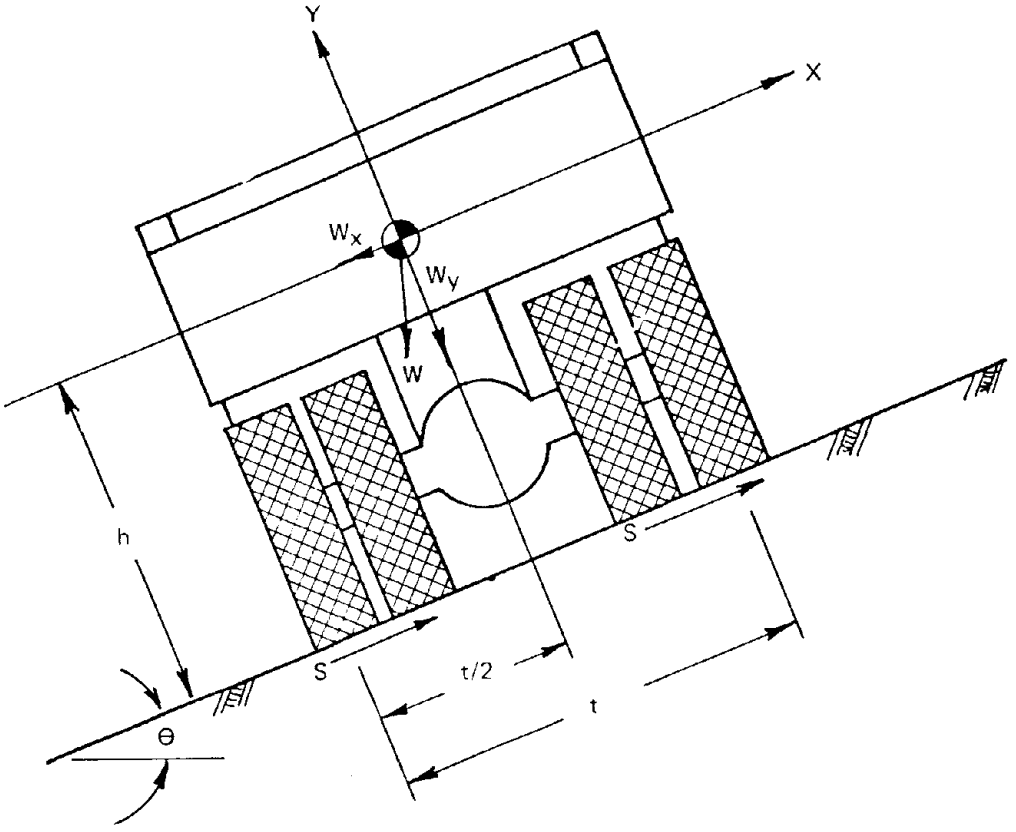

VEHICLE SIZE CARRY CAPACITY (tons)	HALF TRACK WIDTH in. (t/2)	LOADED c.g. LOCATION in. (h)	VEHICLE SLOPE ANGLE Deg. (θ)	EMPTY c.g. LOCATION in. (h)	VEHICLE SLOPE ANGLE Deg. (θ)
23	48	66	36	60	39
35	48.5	86	29	60	39
35	43	60	36	54	39
40	43	69	32	63	34
45	53	66	39	60	41
50	54	95	30	63	41
50	53	78	34	72	36
85	66.5	117	30	76	41
100	85.5	122	35	78	48
120	71.5	115	32	79	42
170	81	152	28	101	39

FIGURE 2. STATIC FORCES ACTING ON A HAULAGE VEHICLE*

*Obtained from manufacturer's data

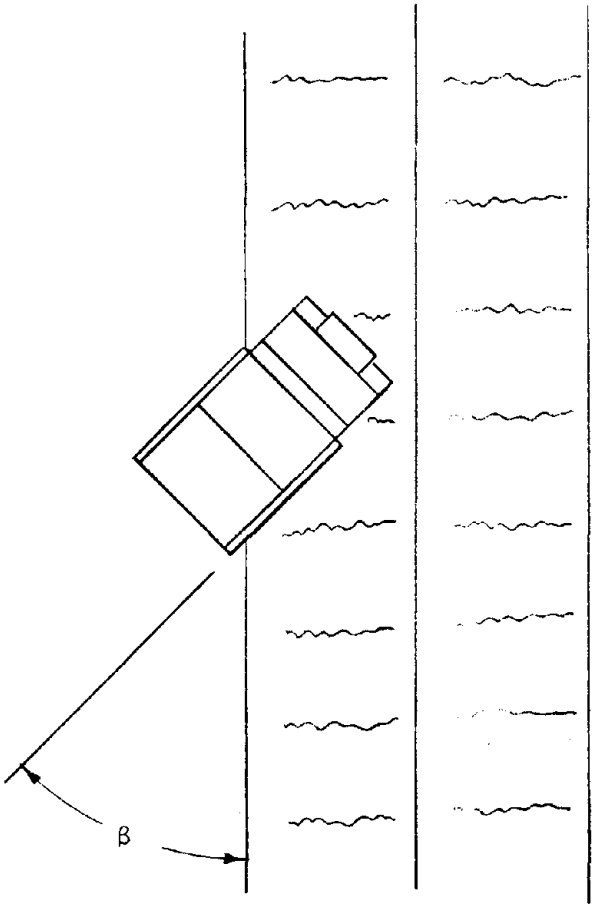

FIGURE 3. PLAN OF VEHICLE POSITIONED ON A BERM AT AN APPROACH ANGEL (β)

total required vehicle slope angle is 40°, the berm slope angle is determined as follows:

$$(40° - 10°) = \text{Berm Slope Angle } (\theta) \times \cos 30° \quad (3)$$

$$\therefore \text{ Berm slope Angle } (\theta) = 35°$$

Therefore, berm slope angle of 40° will provide a conservative design which should produce rollover for all but one of the vehicles listed in Figure 2.

2.2.4 Redirection

Redirection occurs when the frictional forces which exist between the vehicle's tires and the barrier are of insufficient magnitude so that the vehicle slides down the barrier and thus is redirected in the direction of the haul road. This interaction is typified by the use of concrete median barriers on highways.

As the vehicle interacts with the barrier, it initially climbs the barrier only to slide down again. This process can continue or the vehicle's body might contact the barrier. Restraint of the vehicle occurs by the combination of energy dissipation by vehicle climb and/or frictional dissipation of energy by the vehicle's body and/or tires in contact with the barrier.

2.3 METHODS OF VEHICLE-BARRIER INTERACTION ANALYSIS

To determine the effectiveness of the various restraint systems, the following approach was initiated:

- Geometric scale model simulations of the interactions were performed to evaluate the significant parameters controlling the interaction.
- Full scale field tests were performed to correlate and validate the results of the simulation. Predictive computer simulations were made to determine the recommendations for restraint system construction for various haulage vehicle sizes.
- Analytical evaluations of guardrails and boulders were performed.

2.3.1 Geometric Scale Model Simulation

2.3.1.1 Vehicle Considerations - The model analysis considered only rigid body motion of the vehicle, i.e., deformation of the vehicle was not considered. Using this assumption, the gross vehicle kinematics during and after interaction with a restraint system is dependent upon the parameters listed in Table 5. Using these parameters and the principle of similarity(2), the dimensional analysis yielded the relevant "pi" terms listed in Table 6.

Table 5

PARAMETERS FOR BERM IMPACT

PARAMETER	SYMBOL	FUNDAMENTAL UNITS OF MEASURE
Characteristic Length	d	L
Other Length Ratios	d_i	—
Vehicle Mass	m	FT^2/L
Vehicle Mass Moment of Inertia	I	FT^2L
Other Mass Moment of Inertia Ratios	I_i	—
Accelerations of gravity	g	L/T^2
Spring Constants	K	F/L
Viscous Damping	β	FT/L
Coefficient of Friction	f	—
Berm Mass Density	ϱ_s	FT^2L^4
Berm Inherent Strength Parameters	σ_s	F/L^2
Impact Velocity	v	L/T
Resulting Displacements	X	L
Resulting Rotations	θ	—
Resulting Decelerations	a	L/T^2
Time	t	T

Baker, W.E., Westine, P.S., and Dodge, F.T., "Similarity Methods in Engineering Dynamics", Spartan Books, Rochelle, New Jersey, 1973.

Table 6

PI TERMS FOR BERM IMPACT

$$\pi_1 = d_i$$

$$\pi_2 = I_i$$

$$\pi_3 = \frac{M}{\rho_s d^3}$$

$$\pi_4 = \frac{I}{\rho_s d^5}$$

$$\pi_5 = f$$

$$\pi_6 = \frac{\beta}{\rho_s g^{1/2} d^{5/2}}$$

$$\pi_7 = \frac{k}{\rho_s g d^2}$$

$$\pi_8 = \frac{\sigma_s}{\rho_s g d}$$

$$\pi_9 = \frac{V}{g^{1/2} d^{1/2}}$$

$$\pi_{10} = \frac{x}{d}$$

$$\pi_{11} = \theta$$

$$\pi_{12} = \frac{a}{g}$$

$$\pi_{13} = \frac{tg^{1/2}}{d^{1/2}}$$

(2)

A model system and a prototype system are equivalent if the pi terms are the same in both systems. This is accomplished by equating pi terms in both systems to each other. The ratio of the model parameter to the prototype parameter is by definition the scale factor. By mathematically equating the pi terms and rearranging the terms to include the ratio of model length to prototype length, each parameter can be expressed in terms of this length ratio. The results of this analysis and the corresponding scale factors for a model berm impact are illustrated in Table 7.

The relationship between the scale factors and vehicle parameters establishes the requirements for fabrication of the physical models. The categories of haulage vehicles operating in the mines ranges from single rear axle, rear dump to dual rear axle, bottom dump, articulated coal haulers. Selection of representative vehicles for simulation was, therefore, based on the most frequently employed configurations used in a surface mining operation. Based on information provided in Government Census Documents(3-5) the single rear axle, rear dump type vehicles represented the most frequently used type of surface vehicle. Of this category, the 35-, 85-, and 170-ton capacities were selected as being a representative cross section of the haulage vehicle population.

The suspension system used on most vehicles consists of suspension cylinders which use oil and nitrogen gas under pressure to absorb road shocks. For modeling purposes, this suspension system was replicated by using small commercially available double-acting cylinders as illustrated in Figure 4. With the extension port of the cylinders uncovered, the cylinders were extended and the valve closed, the trapped volume of air resulting in a variable spring rate common to this type of system as the cylinder is compressed. However, in the fully loaded condition, the effectiveness of this system became insignificant. The weight compressed the cylinder to the point of eliminating any additional travel. Hence, the vehicle acted as if it were on a solid axle. This same condition is, of course, present in an actual loaded vehicle.

The tires used on the model were for practical purposes rigid rather than scale pneumatic wheels. Likewise, the tread design was not considered influential on the resulting trajectory of the vehicle. The wheels utilized for the model were commercially available hard rubber wheels ground to a specific diameter and bearing mounted on the axles.

An initial area of concern in the fabrication of the models was the influence of the steering mechanism and its effect upon vehicle redirection. Initially, the steering systems were designed with a tensioning device which would allow simulation of the mechanical resistance of the steering system. However, the magnitude of this resistance or frictional force was not available from the manufacturers.

Table 7

SCALE FACTORS FOR MODELING BERM IMPACT

QUANTITY	SYMBOL	SCALE FACTOR
Length, Displacement	d,x	λ
Velocity	v	$\sqrt{\lambda}$
Acceleration	a,g	1.0
Rotations	θ	1.0
Time	t	$\sqrt{\lambda}$
Vehicle Mass	M	λ^3
Mass Moment of Inertia	I	λ^5
Mass Density	ϱ_s	1.0
Coefficient of Friction	f	1.0
Viscous Damper	β	$\lambda^{5/2}$
Spring Constants	k	λ^2
Stress parameter	σ_s	λ

Baker, W.E., Westine, P.S., and Dodge, F.T., "Similarity Methods in Engineering Dynamics", Spartan Books, Rochelle Park, New Jersey, 1973.

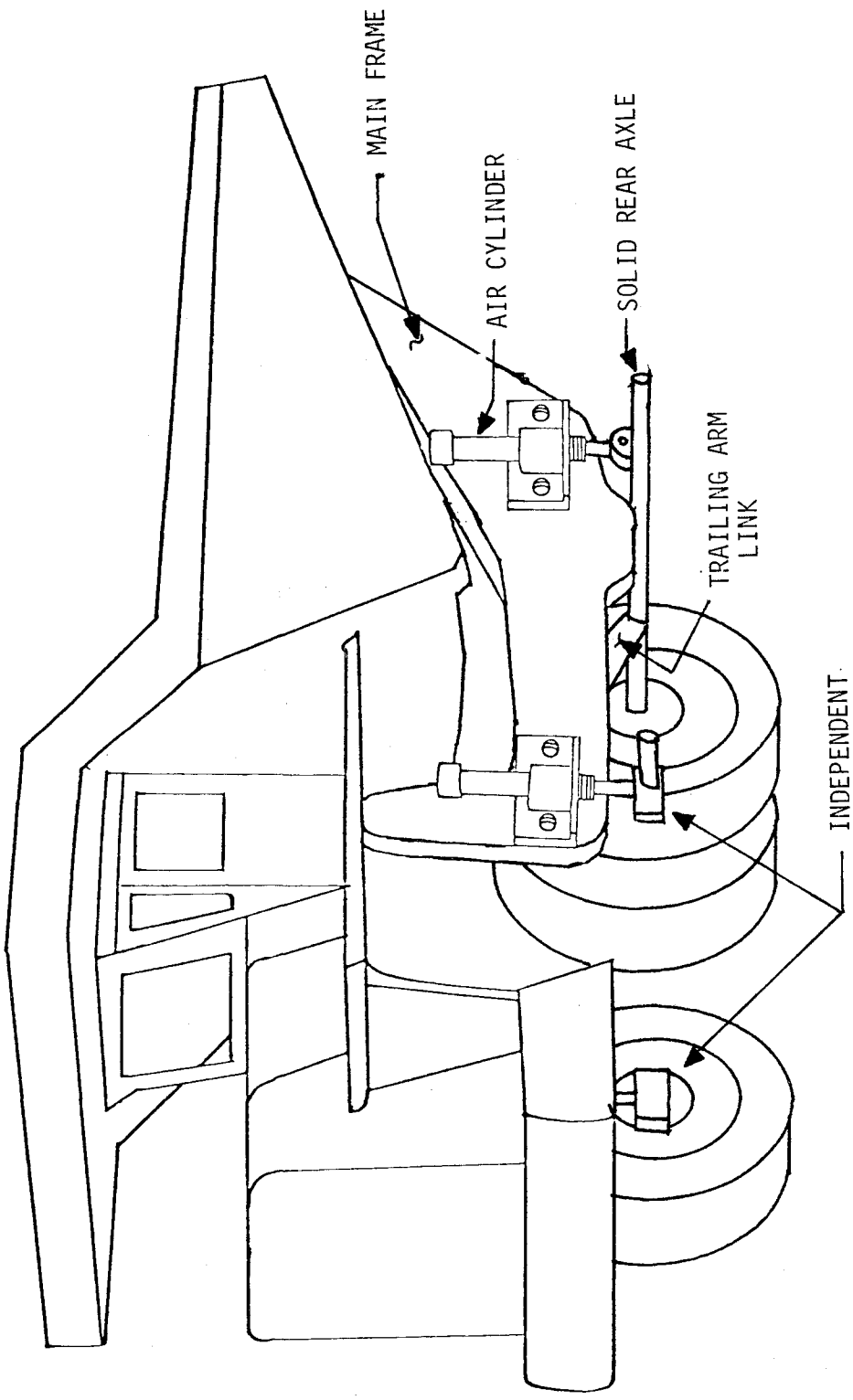

FIGURE 4. DETAILED VIEW OF MODEL SUSPENSION SYSTEM

Investigation into the various steering systems employed on surface haulage vehicles(5) provided a further insight into the types of steering systems used. Two basic types are found: a hydrostatic steering system with mechanical feedback as used on several vehicles, and a hydrostatic steering system using hand metering pump/valve without feedback, used on other vehicles. For either type of steering system, the self-correction from a turn may not be incorporated into the vehicle's steering geometry. Consequently, if an operator inadvertently turned a vehicle into a berm, the vehicle would continue to travel in that direction until either corrective action was initiated, side slippage of the wheels changed the vehicle's direction, structural failure occurred, or excessive side forces on the wheel exceeded the pressure relief valve setting for the steering system forcing the wheels to turn. Therefore, a locked steering system, one having the wheels retained in a fixed position, is more representative of a typical vehicle operating mode.

The vehicle bodies used on the models were of plywood construction attached to the metal framework of the chassis. No attempts were made to model the structural strength of the body, bumpers, or axles. The primary concern was that the general exterior dimensions and ground clearances were representative for the various vehicle categories. The general configuration of these models was not intended to be representative of a specific manufacturer but rather a general representation of the vehicle's dimensions for a certain category of haulage vehicles.

The primary parameters of interest in a vehicle stability problem is the mass moment of inertia about the roll, pitch, and yaw axes of the vehicle. With the exception of one value, the manufacturers have no idea as to the magnitude of these terms. Ideally, knowing the inertia values of the vehicles and the center-of-gravity (c.g.) locations, the vehicle's mass could then be properly distributed to represent that of the actual vehicle.

While the physical models required the inertia term to ensure a representative weight distribution, the need for these terms in a mathematical representation of the vehicle is even more imperative. Therefore, the model vehicles were fabricated according to the manufacturer's data, the weight distribution about the c.g. position, and the mass moment of inertia of these models determined experimentally. The scale inertia terms for each category of haulage vehicle and the corresponding calculated full-scale values are illustrated in Table 8. The experimental procedure used to determine the inertia terms is delineated in Appendix A. The resulting vehicle parameters for both the 1/20 scale model and full-scale haulage vehicle based on manufacturer's data and the inertia terms as previously described, are illustrated in Table 9.

2.3.1.2 Material Considerations - Reproduction of the material employed for representation of model berms, as they exist in actual mining operations, is complicated due to the wide variation in berm material composition.

Table 8. Loaded Vehicle Moments of Inertia

Vehicle	Inertia Term	*1/20 Scale	Full Scale	Mfr. Data
35-ton	Ix	.25 in-lb-sec^2	0.8 X 10^6 in-lb-sec^2	.8 x 10^6 in-lb-sec^2
	Iy	.78 in-lb-sec^2	2.5 X 10^6 in-lb-sec^2	2.5 x 10^6 in-lb-sec^2
	Iz	.56 in-lb-sec^2	1.8 X 10^6 in-lb-sec^2	1.8 x 10^6 in-lb-sec^2
85-ton	Ix	1.16 in-lb-sec^2	3.7 X 10^6 in-lb-sec^2	3.9 X 10^6 in-lb-sec^2
	Iy	2.31 in-lb-sec^2	7.4 X 10^6 in-lb-sec^2	Not Available
	Iz	2.70 in-lb-sec^2	8.6 X 10^6 in-lb-sec^2	Not Available
170-ton	Ix	1.56 in-lb-sec^2	5.0 X 10^6 in-lb-sec^2	Not Available
	Iy	4.60 in-lb-sec^2	14.7 X 10^6 in-lb-sec^2	Not Available
	Iz	5.34 in-lb-sec^2	17.1 X 10^6 in-lb-sec^2	Not Available

*See Appendix A.

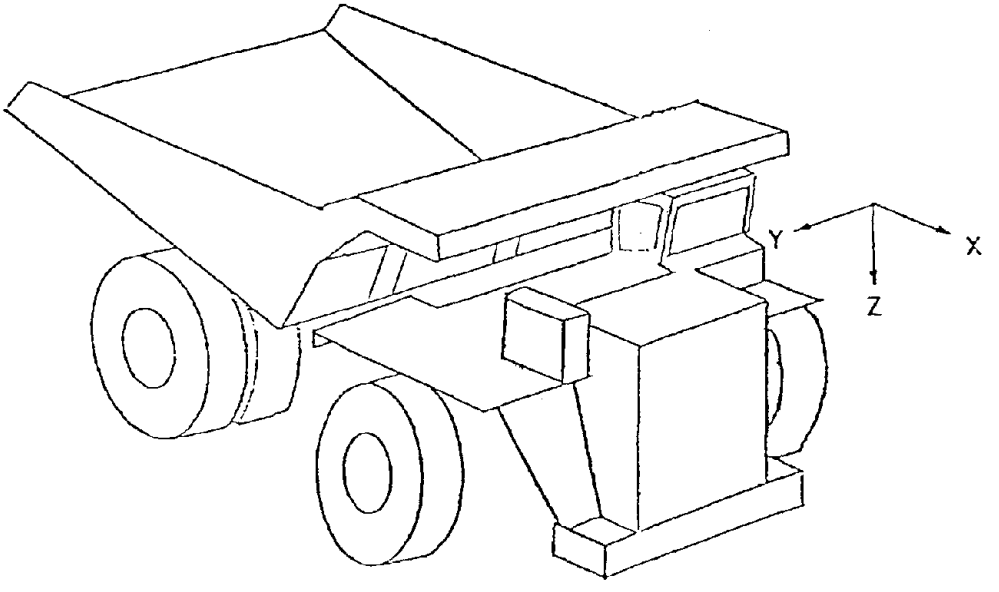

TABLE 9

General Haulage Vehicle Parameters

Characteristic Lengths	35-ton Model	35-ton Full-Scale**	85-ton Model	85-ton Full-Scale**	170-ton Model	170-ton Full-Scale**
Length, in	15.4	307	19.3	385	24.3	456
Width, in	7.2	144	9.6	192	12.5	262
Height, in	7.7	154	9.5	193	11.2	224
Ground Clearance, in	0.9	16	2.5	29.5	1.5	34
Wheel Base, in	6.7	142	9.0	180	11.1	222
Wheel Diameter, in	3.0	60	5.0	92	5.8	115
Turning Circle	31.5	630	47.7	954	49.2	984
C.G. Location						
Verticle Empty, in	-	60	-	76	-	87
Horizontal Empty, in*	-	72	-	83	-	110
Vertical Loaded, in	4.2	86	5.5	119	6.5	130
Horizontal Loaded, in*	2.5	50	2.8	55	2.8	74
Vehicle Mass						
Suspended Mass Empty, lb-sec /in	-	-	-	-	-	-
Suspended Mass Loaded, lb-sec /in	.0377	302	.0887	710	.1517	1214
Unsuspended Mass Front, lb-sec /in	.0018	14.8	.0041	33	.0064	51
Unsuspended Mass Rear, lb-sec /in	.0047	38	.0125	100	.0167	134
Moment of Inertia (Loaded)***						
I_{x-x} Empty, lb-sec^2-in	-	-	-	1.5×10^6**	-	-
I_{x-x} Loaded, lb-sec^2-in	.25	0.8×10^6	1.16	3.9×10^6**	1.56	5.0×10^6
I_{y-y} Loaded, lb-sec^2-in	.78	2.5×10^6	2.31	7.4×10	4.60	14.7×10^6
I_{z-z} Loaded, lb-sec^2-in	.56	1.8×10^6	2.70	8.6×10	5.34	17.1×10^6

*Distance from $\mathbb{L}$ of rear axle

**Manufacturer's data

***From Table 8

Visits to numerous mine sites clearly indicated that berms, for both practical and economical reasons, are being constructed from the most readily available waste material located at the mine site. The material will normally range from relatively fine grain tailing particles to overburden soil to drilled and blasted rock. Boulders four feet and larger in diameter are also frequently employed for berms in quarry operations or whenever boulders of this size are encountered which are too large to break up or transport to a waste site.

Model representation of the various berm compositions observed at various mining operations would be an endless task. To minimize this requirement, berms encompassing the edges of the spectrum, unconsolidated to rigid, were investigated. An unconsolidated berm was represented by a loose deposit of soil uniformly distributed to a specific height. The rigid type soil berm was prepared by packing the berm material to a specific density level. In actual practice, a totally rigid berm was not obtained, i.e., some berm deformation always resulted from the impact.

The primary difficulty encountered with modeling soil is the representation of the test material and the repeatability of the test site conditions. This problem was not completely solved during this test period. Initially, a mixture of sand and oil was employed for the berm composition. Oil was added to obtain a degree of cohesiveness and to minimize the effects of humidity. This combination was totally ineffective in producing the desired berm response. The model vehicle simply plowed completely through the material. Increasing the volume and compaction of this material made little difference. The use of artificial materials such as styrofoam, etc., was investigated, however, the failure characteristics of these materials did not produce the expected response.

The use of a clay material having increased bearing strength compared to the sand was then investigated. By packing this material, its compressive strength increased and the resulting material failure models began resembling those observed in actual vehicle-berm impacts. To minimize the variations expected in repeating the tests, two techniques were employed; 1) record the compressive strength of the test berm, and 2) perform a complete series of tests before changing the soil conditions. The soil conditions were prone to change due to the soil's moisture content variation, particularly when the berm was reconstructed. Consequently, performing a particular series of model tests within a half-day period appeared acceptable.

2.3.2 Full Scale Field Tests

Included as a necessary step in the determination of the adequate restraint systems, and particularly berm design criteria, was the validation of the simulation techniques used. Full Scale field tests were performed to provide information which describes the interaction between the vehicle and a berm.

Tests were performed with a 35-ton single rear axle, rear dump truck. A wide range of soil constituents with various degrees of compaction provide the range of berm materials which can be expected in operating mines.

A matrix of test runs were performed on each berm composition with the approach conditions varied. The approach angles were 10°, 20°, and 30°. Approach velocities of 5, 2.5, 10, 12.5, and 15 mph were obtained with the maximum velocity at each angle limited by the likelihood that increased velocity might result in damage.

Tests were performed in the following manner; the operator was instructed as to the test velocity and a guide string was placed at the appropriate angle. As the operator obtained the appropriate speed, he would shift the truck's transmission into neutral just prior to contact with the berm. The weight was allowed to interact naturally with the berm as the steering wheel was maintained in the neutral, straight ahead position. When the vehicle came to a stop either after climbing the berm or being redirected, the operator would stop the vehicle so that documentary photographs could be obtained. Upon removal of the vehicle, interaction data was obtained.

Figure 5 indicates the general test configuration of the interaction and explains the data taken. Data which depicts the amount of wheel climb, tire sinkage, and penetration along the direction of travel were recorded.

Additionally, for each berm composition, a special qualification test was performed to relate acceptable berm strength values. This is illustrated in Figure 6. This test involved driving the loaded vehicle forward up the berm at both 90° and 45° to the axle height of the vehicle. This height was chosen because it represented an easily reproducible test procedure. The tire sinkage values were recorded which provided the baseline strength values for eventually determining the berm design requirements for various strength levels.

2.3.3 Computer Simulations

Extensive investigations have been undertaken in the past to develop computer simulation programs to define the behavior of a vehicle interacting with a median or barrier. Presently, the two computer programs that have been used in this project to evaluate the performance of vehicle restraint systems and to determine the trajectories of vehicles are the HVOSM and BARRIER VII.

2.3.3.1 HVOSM Computer Simulations - The Highway-Vehicle-Objective-Simulation Model (HVOSM)(6) was developed by the Calspan Corporation (formally Cornell Aeronautical Laboratory, Inc.). This program represents the characteristics of a vehicle by a mathematical model and predicts the response of a vehicle and the forces generated during the vehicle's interaction with a rigid non-deflecting surface, as a function of vehicle impact speed and approach angle.

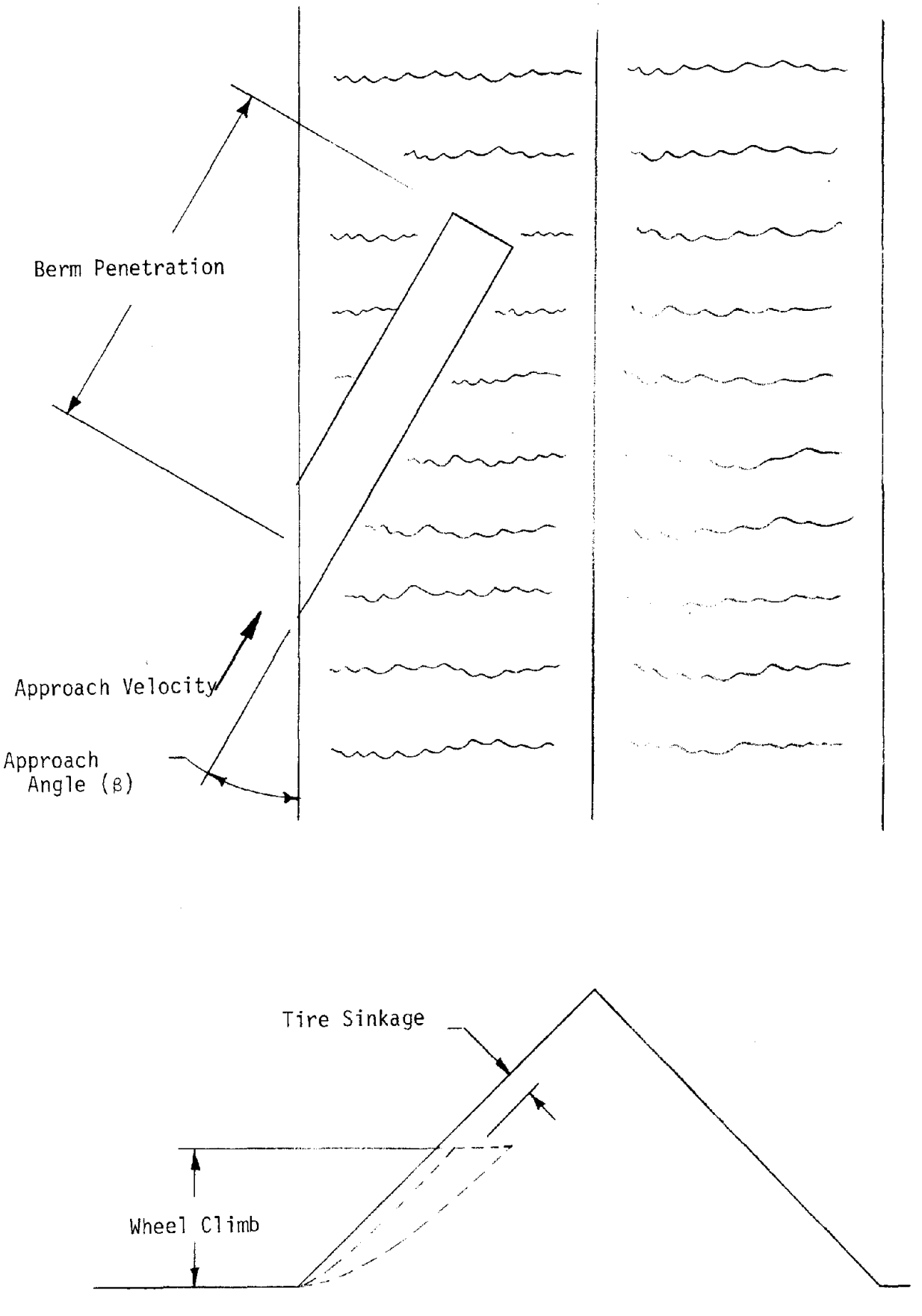

FIGURE 5. FIELD TEST CONFIGURATION AND DATA RECORDED

Berm Qualification Test at 90°

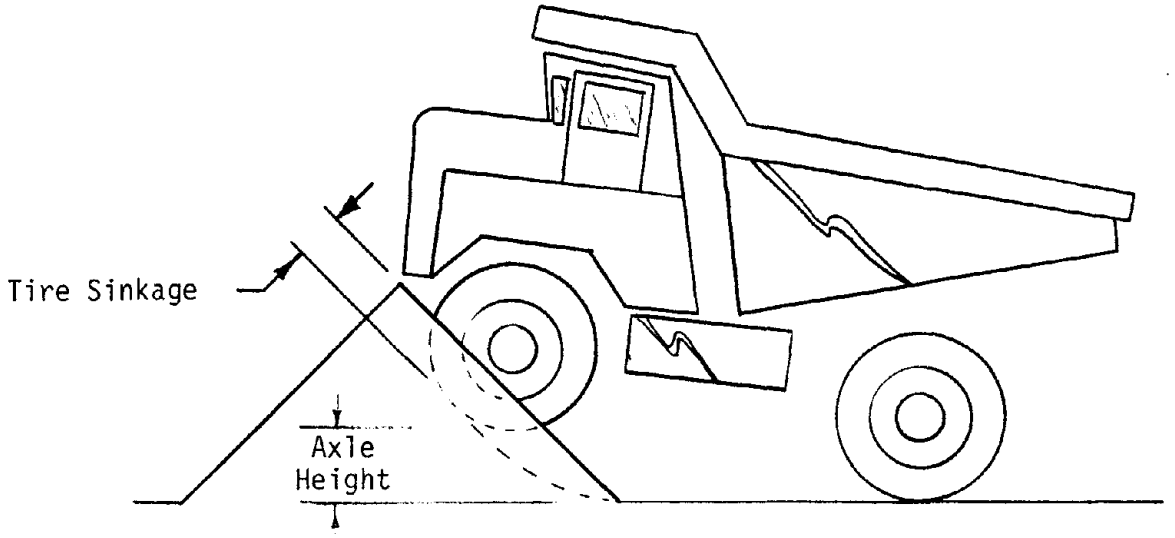

Berm Qualification Test at 45°

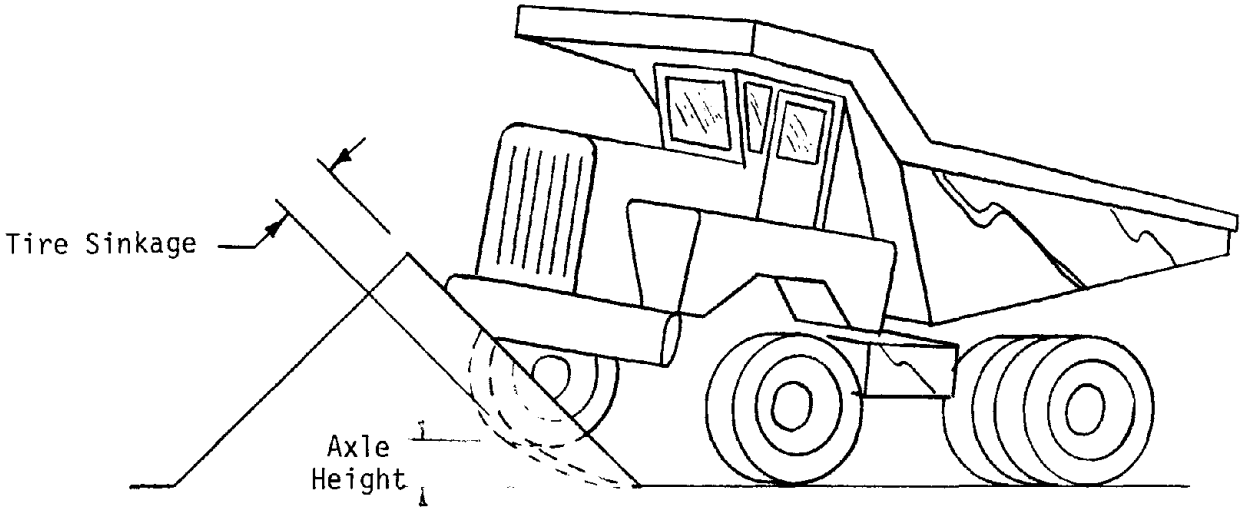

FIGURE 6. BERM QUALIFICATION TEST DESCRIPTION

The mathematical model of the vehicle dynamics represented by this simulation includes the general three-dimensional motion resulting from specific vehicle control inputs, traversal over irregular terrain, or from the interaction with simple roadside barriers, e.g., berms, concrete structure, etc. As a consequence of this type of simulation, extensive vehicle parameters are required for input to the program. The accuracy of this program in predicting a vehicle's response has been validated by full-scale testing of passenger-type vehicles. The accuracy is, however, a direct function of the vehicle input data. Appendix B represents manufacturer's data which was obtained for the 35-, 85-, and 170-ton haulage vehicles. The various vehicle input parameters associated with usage of this program are summarized in Appendix C. A review of these parameters illustrates the quantity of vehicle data needed to fully utilize the capability of the program.

The advantage of a computer simulation program lies in the ease of performing numerous simulations in a relativley short time period and, therefore, predicting the vehicle's response for various conditions. However, the current limitation of the computer simulation is the general unavailability of the input parameters, specifically the significant basic parameters such as the vehicle inertia terms. Prior to performing these full-scale tests, parameters of the selected test vehicle were accurately determined, their values were compared to those used in the simulation, and the program was rerun with parameters more closely representing those of the test vehicle.

The parameters employed in the HVOSM program represent a combination of available manufacturer's data, extropolated highway vehicle data, and engineering estimates of unavailable input parameters. The input data used in these simulations were not intended to replicate a particular manufacturer's vehicle but rather provide a representation of the general parameters associated with either a 35-, 85-, or 170-ton vehicle. Representative computer input data for these vehicles, as used in a specific computer simulation run are summarized in Tables 10, 11, and 12 for each vehicle category.

2.3.3.2 Barrier VII Computer Simulation - Computer modeling of a haulage vehicle interacting with a guardrail was performed using existing computer programs. The interaction of a vehicle with a restraining device such as a guardrail, concrete barrier, or soil backed barrier, was simulated by the BARRIER VII Program.(7) This program restricts the vehicle to a two-dimensional plane, the type of interaction expected from a guardrail. In this program, the vehicle is modeled as a plane body of arbitrary shape encompassed by inelastic springs. Springs are also used to simulate the vehicle's crush characteristics, tires, and any additional hard points of the vehicle. The guardrail is represented by an arbitrary plane assemblage of beams, cables, posts, springs, links, and damping devices. A two-dimensional dynamic structural analysis problem is then solved using a step-by-step

TABLE 10
HVOSM INPUT PARAMETERS FOR 35-TON HAULAGE VEHICLE
(Full Scale)

VEHICLE DIMENSIONS

Length:	309 inches
Width:	143 inches
Height:	153 inches
Front Track (TF):	104 inches
Rear Track (TR):	92 inches
Wheel Radius (RW):	30 inches

CENTER-OF-GRAVITY LOCATIONS

Horizontal from Front Axle (A):	84 inches
Horizontal from Rear Axle (B):	50 inches
Vertical from Front Axle (ZF):	55 inches
Vertical from Rear Axle (TR):	55 inches
Distance from Axle Center & Axle Roll Center (RHO):	-4 inches

TIRE DATA

Tire Stiffness (KT):	10,000 lb/in.
Linear Defl. Range (SIGT):	5.0 inches
Tire Stiffness Multiple (XLAMT):	5
Tire Coefficient (AO):	44,000
Tire Coefficient (A1):	82.76
Tire Coefficient (A2):	29,000
Tire Coefficient (A3):	17.80
Tire Coefficient (A4):	39,000
Tire-Terrain Friction (AMU):	.65
Multiple of A (OMEGT):	1.0

INERTIA DATA

Sprung Mass (XMS):	302 lb-sec^2/in.
Front Unsprung Mass (XMUF):	14.8 lb-sec^2-in.
Rear Unsprung Mass (XMUR):	38 lb/sec^2/in.
Mass Moment of Inertia (XIX):	.8 x 10^6 lb-sec^2-in.
(XIY):	2.5 x 10^6 lb-sec^2-in.
(XIZ):	1.8 x 10^6 lb-sec^2-in.
Spring Mass Roll-Yaw Product (XIXZ):	0
Rear Unsprung Mass Inertia (XIR):	6.9 x 10^4 lb-sec^2-in
Acceleration Due to Gravity (G):	386.4 in/sec^2

SUSPENSION DATA

Suspension Load-Deflection Rates:	Front (AKF)	= 2,175 lb/in.
	Rear (AKR)	= 38,000 lb/in.
Coulomb Damping per Wheel:	Front (CFP)	= 10,000 lbs.
	Rear (CRP)	= 1 lb.
Viscous Damping per Wheel:	Front (CF)	= 5 lb-sec/in.
	Rear (CR)	= 5 lb-sec/in.
Suspension Friction Lag:	Front (EPSF)	= .001 in/sec.
	Rear (CR)	= .001 in/sec.

LINEAR COEFFICIENT OF SUSPENSION BUMPER TERMS

Front Comp. (AKFC)	= 2,175	Rear Comp. (AKRC)	= 38,000 lb/in.
Front Ext. (AKFE)	= 2,175 lb/in.	Rear Ext (AKREP)	= 38,000 lb/in.

CUBIC COEFFICIENT OF BUMPER TERMS

Front Comp. (AKFCP)	= 4,350 lb/in^3	Rear Comp. (AKRCP)	= 76,000 lb/in^3
Front Ext. (AKFEP)	= 4,350 lb/in^3	Rear Ext. (AKREP)	= 76,000 lb/in^3

SUSPENSION DEFLECTION AT BUMPER CONTACTS

Max. Front Comp. (OMEGAF)	= 6.0 in.	Max Rear Comp. (OMEGAR)	= 3.0 in.
Front Ext. (OMEGFC)	= 5.0 in.	Front Ext. (OMEGFE)	= 7.0 in.
Rear Comp. (OMEGRC)	= 5.25 in.	Rear Ext. (OMEGRE)	= 5.25 in.

RATIO OF CONSERVED TO ABSORBED SUSPENSION ENERGY

Front (XLAMF) = .5 Rear (XLAMR) = .5

SUSPENSION ROLL STIFFNESS

Front (RF) = 226,000 in-lb/rad Rear (RR) = 61,000 in-lb/rad

Distance between Spring Mounts and Rear Axle (TS) = 72 in.
Rear Axle Roll-Steer Coefficient (AKRS) = .07

Impact Conditions with Berm: Vehicle Velocity = 30 mph, Approach Angle = 20°, Case No. 19

TABLE 11
HVOSM INPUT PARAMETERS FOR 85-TON HAULAGE VEHICLE
(Full Scale)

VEHICLE DIMENSIONS

Length:	385 inches
Width:	190 inches
Height:	193 inches
Front Track (TF):	156 inches
Rear Track (TR):	133 inches
Wheel Radius (RW):	50 inches

CENTER-OF-GRAVITY LOCATIONS

Horizontal from Front Axle (A):	125 in.
Horizontal from Rear Axle (B):	55 in.
Vertical from Front Axle (ZF):	60 in.
Vertical from Rear Axle (ZR):	67 in.
Distance from Axle Center & Axle Roll Center (RHO):	-4 in.

TIRE DATA

Tire Stiffness (KT):	10,000 lb/in.
Linear Defl. Range (SIGT):	1.0 inches
Tire Stiffness Multiple (XLAMT):	10
Tire Coefficient (AO):	44,000
Tire Coefficient (A1):	82.76
Tire Coefficient (A2):	29,000
Tire Coefficient (A3):	17.80
Tire Coefficient (A4):	39,000
Tire-Terrain Friction (AMU):	.65
Multiple of A (OMEGT):	1.0

INERTIA DATA

Sprung Mass (XMS):	622 lb-sec^2/in.
Front Unsprung Mass (XMUF):	72 lb-sec^2-in.
Rear Unsprung Mass (XMUR):	144 lb/sec^2/in.
Mass Moment of Inertia (XIX):	3.7×10^6 lb-sec^2-in.
(XIY):	7.4×10^6 lb-sec^2-in.
(XIZ):	8.6×10^6 lb-sec^2-in.
Spring Mass Roll-Yaw Product (XIXZ):	0
Rear Unsprung Mass Inertia (XIR):	6.9×10^4 lb-sec^2-in
Acceleration Due to Gravity (G):	386.4 in/sec^2

SUSPENSION DATA

Suspension Load-Deflection Rates:	Front (AKF)	= 14,200 lb/in.
	Rear (AKR)	= 100,000 lb/in.
Coulomb Damping per Wheel:	Front (CF)	= 10,000 lb
	Rear (CR)	= 1 lb.
Viscous Damping per Wheel:	Front (EPSF)	= 5 lb-sec/in.
	Rear (CR)	= 5 lb-sec/in.
Suspension Friction Lag:	Front (EPSF)	= .001 in/sec.
	Rear (CR)	= .001 in/sec.

LINEAR COEFFICIENT OF SUSPENSION BUMPER TERMS

Front Comp. (AKFC)	= 14,200 lb/in.	Rear Comp. (AKRC)	= 100,000 lb/in.
Front Ext. (AKFE)	= 14,200 lb/in.	Rear Ext (AKRE)	= 100,000 lb/in.

CUBIC COEFFICIENT OF BUMPER TERMS

Front Comp. (AKFCP)	= 28,400 lb/in^3	Rear Comp. (AKRCP)	= 200,000 lb/in^3
Front Ext. (AKFEP)	= 28,400 lb/in^3	Rear Ext. (AKREP)	= 200,000 lb/in^3

SUSPENSION DEFLECTION AT BUMPER CONTACTS

Max. Front Comp. (OMEGAF)	= 6.0 in.	Max Rear Comp. (OMEGAR)	= 3.0 in.
Front Comp. (OMEGFC)	= 5.5 in.	Front Ext. (OMEGFE)	= 7.0 in.
Rear Comp. (OMEGRC)	= 1.25 in.	Rear Ext. (OMEGRE)	= 5.25 in.

RATIO OF CONSERVED TO ABSORBED SUSPENSION ENERGY

Front (XLAMF) = .5 Rear (XLAMR) = .5

AUXILIARY SUSPENSION ROLL STIFFNESS

Front (RF) = 266,000 in-lb/rad Rear (RR) = 61,900 in-lb/rad

Distance between Spring Mounts and Rear Axle (TS) = 100 in.
Rear Axle Roll-Steer Coefficient (AKRS) = .07

Impact Conditions with Berm:
Vehicle Velocity = 30 mph, Approach Angle = 15°, Case Number 11

TABLE 12
HVOSM INPUT PARAMETERS FOR 170-TON HAULAGE VEHICLE
(Full Scale)

VEHICLE DIMENSIONS

Length:	468 inches
Width:	274 inches
Height:	240 inches
Front Track (TF):	212 inches
Rear Track (TR):	174 inches
Wheel Radius (RW):	57.5 inches

CENTER-OF-GRAVITY LOCATIONS

Horizontal from Front Axle (A):	140 inches
Horizontal from Rear Axle (B):	74 inches
Vertical from Front Axle (ZF):	72.5 inches
Vertical from Rear Axle (ZR):	72.5 inches
Distance from Axle Center & Axle Roll Center (RHO):	-4 in.
Total Weight	540,300 lbs

TIRE DATA

Tire Stiffness (KT):	15,000 lb/in.
Linear Defl. Range (SIGT):	5.0 inches
Tire Stiffness Multiple (XLAMT):	5
Tire Coefficient (AO):	88,000
Tire Coefficient (A1):	165.52
Tire Coefficient (A2):	58,000
Tire Coefficient (A3):	35.6
Tire Coefficient (A4):	78,000
Tire-Terrain Friction (AMU):	.65
Multiple of A2 (OMEGT):	1.0

INERTIA DATA

Sprung Mass (XMS):	1,213.7 lb-sec^2/in.
Front Unsprung Mass (XMUF):	51.3 lb-sec^2-in.
Rear Unsprung Mass (XMUR):	134 lb/sec^2/in.
Mass Moment of Inertia (XIX):	6.0×10^6 lb-sec^2-in.
(XIY):	14.7×10^6 lb-sec^2-in.
(XIZ):	17.1×10^6 lb-sec^2-in.
Spring Mass Roll-Yaw Product (XIXZ):	0
Rear Unsprung Mass Inertia (XIR):	6.9×10^4 lb-sec^2-in
Acceleration Due to Gravity (G)	386.4 in/sec^2

SUSPENSION DATA

Suspension Load-Deflection Rates:	Front (AKF)	=	29,762 lb/in.
	Rear (AKR)	=	24,921 lb/in.
Coulomb Damping per Wheel:	Front (CFP)	=	10,000 lb.
	Rear (CRP)	=	1 lb.
Viscous Damping per Wheel:	Front (CF)	=	5 lb-sec/in.
	Rear (EPSR)	=	5 lb-sec/in.
Suspension Friction Lag:	Front (EPSF)	=	.001 in/sec.
	Rear (CR)	=	.001 in/sec.

LINEAR COEFFICIENT OF SUSPENSION BUMPER TERMS

Front Comp. (AKFCP)	= 29,762 lb/in.	Rear Comp. (AKRC)	= 124,921 lb/in.
Front Ext. (AKFE)	= 29,762 lb/in.	Rear Ext (AKRE)	= 124,921 lb/in.

CUBIC COEFFICIENT OF BUMPER TERMS

Front Comp. (AKFCP)	= 59,524 lb/in^3	Rear Comp. (AKRCP)	= 249,842 lb/in^3
Front Ext. (AKFEP)	= 59,524 lb/in^3	Rear Ext. (AKREP)	= 249,842 lb/in^3

SUSPENSION DEFLECTION AT BUMPER CONTACTS

Max. Front Comp. (OMEGAF)	= 6.0 in.	Max Rear Comp. (OMEGAR)	= 3.0 in.
Front Ext. (OMEGFC)	= 8.8 in.	Front Ext. (OMEGFE)	= 8.8 in.
Rear Comp. (OMEGRC)	= 7.1 in.	Rear Ext. (OMEGRE)	= 7.1 in.

RATIO OF CONSERVED TO ABSORBED SUSPENSION ENERGY

Front (XLAMF) = .5 Rear (XLAMR) = .5

SUSPENSION ROLL STIFFNESS

Front (RF) = 266,000 in-lb/rad Rear (RR) = 61,900 in-lb/rad

Distance between Spring Mounts and Rear Axle (TS)	=	72 in.
Rear Axle Roll-Steer Coefficient (AKRS)	=	.07

Impact Conditions with Berm: Vehicle Velocity = 25 mph Approach Angle = 15°, Case No. 3

integration method. During the simulated impact, the vehicle slides along the barrier. Forces between the vehicle tires and roadway are taken into account as well as interaction forces between the vehicle and guardrail. The resultant barrier deformation, vehicle trajectory, and impact loads are then computed. This analysis is two-dimensional in the horizontal plane. Out-of-plane effects, which include vertical displacements of either the vehicle and barrier, are not considered. The results predicted by the BARRIER VII computer program for impacts with various restraint systems have been examined.

3. TECHNICAL DISCUSSION

3.1 BERM INTERACTIONS

3.1.1 Geometric Scale Modeling

Scale model testing of haulage vehicles were performed to

- provide a correlation between physical testing and the computer simulation results
- determine the vehicle's reaction in a deformable berm composition
- determine any additional inputs that require further full-scale testing.

The computer simulation program used for determining the response of a haulage vehicle interacting with a berm, the HVOSM program is, by its development, limited to analyzing vehicles interacting with a rigid structure. Consequently, to verify the results of this program, the scale model testing was initially performed on a rigid berm and the results compared to those predicted by the computer simulation. By judiciously adjusting specific input variables in the computer program, the results approximated those produced by the scale model.

Deformable berms were examined by impacting the vehicle into various berm material compositions, each test berm having a different strength level. As expected, the higher strength berm more closely approximated the results of a rigid berm interaction. The influence of the berm strength and composition is, however, a significant factor in providing the proper response.

The data acquisition technique employed on the deformable berm test was limited to physical measurements and photographic documentation. The primary measurements recorded were maximum wheel climb, maximum penetration normal to the berm measured from the point where the berm and roadway meet, and representative berm compressive strength. The gross response of the vehicle, e.g., rollover, etc., were recorded on test data sheets.

Berm configurations investigated were limited to straight segments having a slope of 45° with the road surface. While most haulage roads contain some degree of curvature, vehicle impacts in curved sections were considered analogous to steep angle impacts.

The actual height of the rigid berms was immaterial since the primary variable being investigated was wheel climb as influenced by impact speed and approach angle. Therefore, if the resultant wheel climb exceeded some arbitrary rigid berm height, the vehicle would either vault or straddle the berm -- either case being an unacceptable restraint condition. More important was the actual wheel climb associated with realistic approach

conditions. It is these conditions which dictate the height requirements of a berm.

3.1.1.1 - Rigid Berm Simulations - A rigidly constructed berm represents an approximation of the minimum berm height required to restrain an errant haulage vehicle. Impacting of a similar size berm constructed from a deformable material will result in the vehicle either penetrating the berm or vaulting over. While the deformable material will offer an increased rolling resistance, its reduced strength may allow a shear failure of the berm tip resulting from the vehicle loading. Therefore, the rigid berm was assumed to represent an optimum configuration.

The significant parameters associated with a vehicle interacting with any type of restraint system are the encroachment conditions and the restraining system's configuration. To provide a feasible test condition while still being slightly conservative, the approach conditions of 30 mph and a 30° impact were considered a maximum. While the speed of most haulage vehicles is lower, a berm designed to withstand these impact conditions will perform satisfactorily for either a lesser speed or shallower impact angle. The configuration of the berm selected was one having a 1:1 slope, i.e., a 45° incline relative to the roadway. This slope was representative of the berms observed at the surface mine sites. Berms having a lesser slope would require an increased base width to obtain the desired height. An errant vehicle under power will continue to climb a shallow inclined berm, while the same vehicle will roll over back onto the roadway for a steeper berm.

The height requirements for the rigid berm to restrain the various categories of haulage vehicle were determined by positioning an excessively high plywood berm at the base of the launching ramp and recording the maximum vehicle climb for the appropriate impact conditions. Prior to performing these tests, the sliding coefficient of friction between each model vehicle and the plywood surface was determined and also the static tipping angle of the vehicles positioned parallel to the roadway. Table 13 delineates these results.

Table 13

Model Vehicle Friction Coefficient/Critical Tipping Angle

Vehicle Size	Sliding Friction Angle	Coeff. of Friction	Tipping Angle
35 - ton	31°,33°,33°.	.65	41°,42°
85 - ton	33°,33°.	.65	40°,42°
170 - ton	--	0	32°,33°

The coefficient of sliding friction, 0.65, is equivalent to the published value for sliding friction between rubber tires and an earthen surface.

The 170-ton, due to its higher center of gravity position, began to tip before sliding down the plane.

The results of these rigid berm tests are summarized in Table 14 with the results given in model dimensions and illustrated graphically in Figure 7 using the equivalent full-scale dimensions. The results of these rigid berm tests imply that a berm height of 3-4 times the axle height is necessary to restrain a haulage vehicle impacting a rigid berm at 30 mph and 30°. Reducing the impact velocity to 20 mph reduces the berm height equivalent to that of twice the axle height. This reduction in wheel climb would also signify a reduction in berm height for the less severe impact conditions. By neglecting the rolling resistance of each vehicle, the kinetic energy is dissipated by an increase in potential energy as the vehicle climbs the berm. This energy balance is given by the following:

$$1/2\ M\ V^2 = Mgh \qquad (4)$$

where,

M = mass of the vehicle, lbm
h = vertical travel up the berm
V = impact velocity, ft/sec.
g = gravitational constant, ft/sec^2

This relation implies that all vehicles operating at the same speed and impact angle will travel up the berm an identical distance. Vehicle mass should not influence vehicle climb unless rolling resistance is a significant factor. Examination of test data illustrated in Figure 7 indicates approximately the same wheel climb for both the empty and loaded conditions. An influencing factor on the maximum vehicle climb is that the vehicle is rolling over prior to completely dissipating its kinetic energy; otherwise, the 35-ton loaded vehicle would have traveled the same vertical distance as the 85-ton. The 170-ton vehicle, having a slightly higher center-of-gravity position, traveled nearly the same distance as the 85-ton vehicle before rolling over. The results obtained with these rigid berm tests provided the guidelines for construction of the deformable berms. Tests performed at lower speeds and less critical approach angles showed the vehicle would be redirected.

3.1.1.2 Deformable Berm Simulations - The ability of a deformable berm to restrain a haulage vehicle is dependent upon structural properties, which determine the ability of the berm to generate sufficient bearing strength to cause the vehicle to act as if operating on a rigid berm. This strength requirement will vary for each category of haulage vehicle and will be a function of vehicle weight, not the vehicle's axle height. This conclusion is obvious when one considers the axle height on a 170-ton vehicle is 15 percent larger than on a 85-ton vehicle while the corresponding loaded vehicle gross weight is nearly 50 percent greater.

TABLE 14

RIGID BERM* TEST RESULTS

TEST NO.	VEHICLE	VEHICLE WEIGHT lb.	IMPACT SPEED mph	IMPACT ANGLE deg.	VERTICAL CLIMB in.	CLIMB MULTIPLE OF	VEHICLE RESPONSE
1	35-ton	17.2	20	30	2.8	1.8	Rolled Up/Down Berm
2	"	"	25	20	3.5	2.4	Reverse Rollover†
3	"	"	"	25	4.2	2.8	Reverse Rollover
4	"	"	"	30	4.2	2.8	Reverse Rollover
5	"	"	30	20	4.2	2.8	Reverse Rollover
6	"	"	"	25	4.9	3.2	Reverse Rollover
7	"	"	"	30	4.9	3.2	Reverse Rollover
8	85-ton	21.4	25	25	7.6	3.0	Reverse Rollover
9	"	"	"	30	8.3	3.4	Reverse Rollover
10	"	"	30	25	9.2	3.6	Reverse Rollover
11	"	"	"	30	9.9	4.0	Reverse Rollover
12	"	40.5	20	30	6.4	2.6	Rolled Up/Down Berm
13	"	"	25	25	7.7	3.0	Reverse Rollover
14	"	"	"	30	9.2	3.6	Reverse Rollover
15	"	"	30	25	8.5	3.4	Reverse Rollover
16	"	"	"	30	9.9	4.0	Reverse Rollover
17	170-ton	67.5	20	30	6.5	2.2	Rolled Up/Down Berm
18	"	"	25	25	8.5	3.0	Reverse Rollover
19	"	"	"	30	9.2	3.2	Reverse Rollover
20	"	"	30	25	8.7	3.0	Reverse Rollover
21	"	"	"	30	9.4	3.2	Reverse Rollover

* Berm Slope of 1:1
† Vehicle Rolled Over Onto Roadway

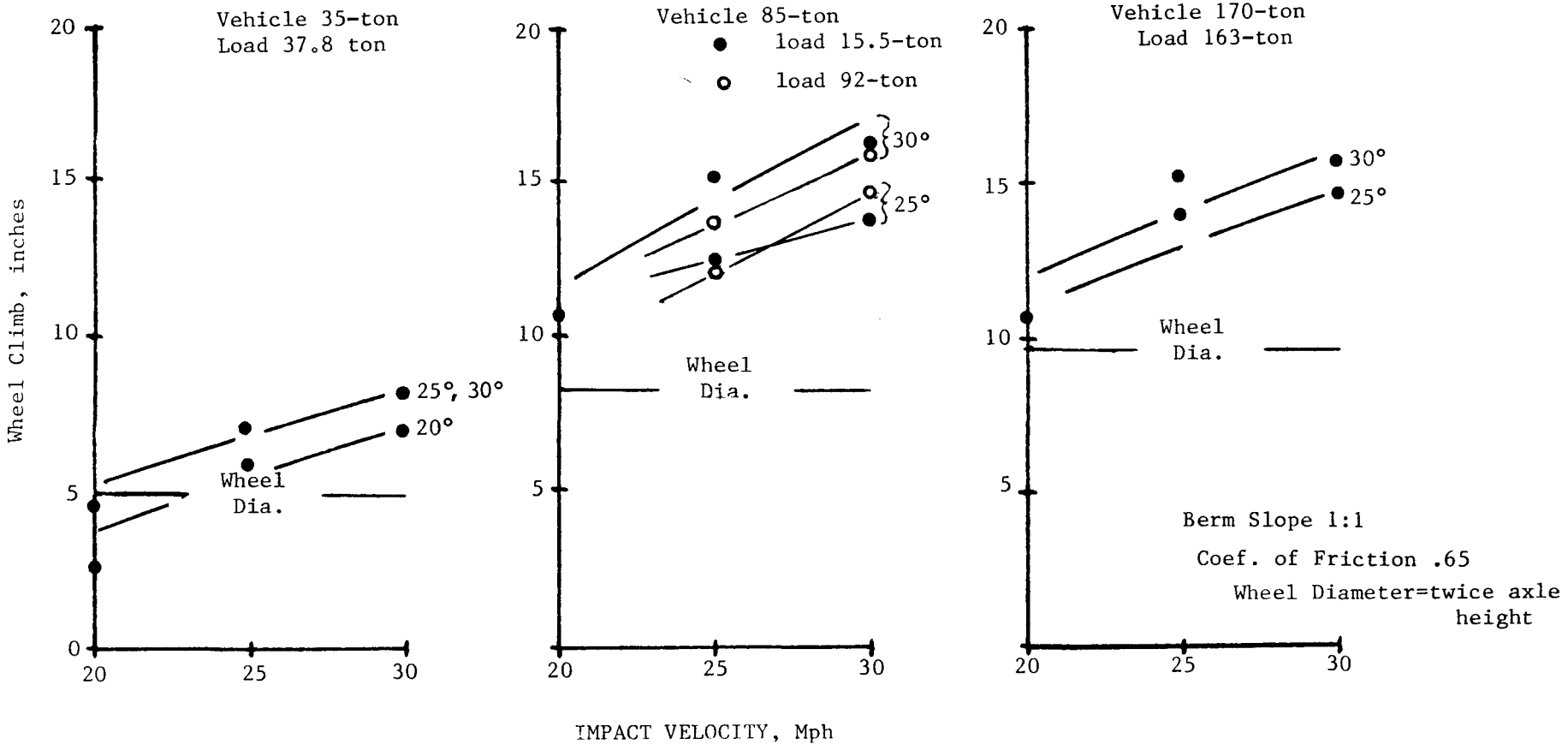

FIGURE 7. WHEEL CLIMB ON RIGID BERM (MODEL SIMULATION)

Soil berms were initially constructed to the height requirement determined by rigid berm testing, and the resulting unconfined bearing strength consisted of depressing a circular plate normal to the berm surface to a depth of 1/4 inch and recording the penetration force. The diameter of the circular plate was equivalent to the wheel width of each test vehicle, a .75 inch diameter plate for the 35-ton and a 1.25 inch diameter plate for the 85- and 170-ton vehicles. This technique is analogous to the California Bearing Ratio test. These forces must not be interpreted as full-scale strength requirements but used only as a relative comparison between berms. A suitable field technique for determining the berm strength will be evaluated later in the report.

Since a loaded vehicle would impose the more stringent strength requirements on the berm, only the responses of loaded vehicles were evaluated. The adequacy of a soil berm requires that some acceptance criteria be established to evaluate the restraint capability of the test berm. Therfore, a reverse roll of the vehicle back onto the roadway or redirection of the vehicle was deemed acceptable. Penetration of the vehicle less than one half the width of the berm base was also considered acceptable. By establishing this criteria, two options are available to the mine operator; (1) the berm can be compacted with a relatively narrow base width, or (2) an unconsolidated berm of adequate width can be used. This second choice, however, would appear to have inherent maintenance problems for areas experiencing excessive rains, resulting in erosion of the berm and/or limited roadbed width.

The results of soil berm model impacts for 30 mph and 30° approach angle are presented in Table 15. Berms were constructed to the height and slope which corresponded to the rigid berm requirements and each category of vehicle evaluated for various berm strengths. Additional deformable berm tests were performed to evaluate different strength levels and berm cross-sectional changes on vehicle response; these results are summarized in Table 16. The results obtained during these tests confirmed what was expected. A berm height of twice the axle height, either unconsolidated or only moderately compacted, will be ineffective in restraining any size haulage vehicle impacting a 30 mph and a 30° angle. Deformable berms must possess some degree of compaction and the compaction must be based on the weight of the vehicle, not on a linear dimension.

The influence of relative berm strength is evident from these test results. Simply constructing a berm to a given height, width, and slope will not produce a safe response. Likewise, the strength requirement is increased for each larger size vehicle. The test berm evaluated with a compressive strength of 1.54 psi represented the loose, unconsolidated strength of the soil berm. The remaining tow strengths represent some increased degree of berm compaction. Full-scale representation of these strengths would be equivalent to 30, 400, and 1080 psi at a penetration depth of five inches. Lower compressive strength berms would not possess the inherent strength to perform satisfactorily at an equivalent penetration.

TABLE 15
EFFECT OF BERM STRENGTH ON VEHICLE RESPONSE 30 MPH IMPACT AT 30° APPROACH ANGLE

COMPRESSIVE STRENGTH		o 1.54 psi* (30 psi full scale)			o 20 psi** (400 psi full scale)			σ 54 psi** (1080 psi full scale)		
VEHICLE LOAD		35-ton	85-ton	170-ton	35-ton	85-ton	170-ton	35-ton	85-ton	170-ton
BERM CONFIGUR'N	Height, in.	5.2	8	8.5	5.25	8	8	5.25	8	8
	Width, in.	12	17	17	10.5	16	16	10	16	16
	Slope	41	43	45	45	45	45	46	45	45
BERM HEIGHT / AXLE HEIGHT		3.5	3.2	3.0	3.5	3.2	2.8	3.5	3.2	2.8
VEHICLE PENETRATION, IN.		12	17	>20	5	—	—	—	—	—
WHEEL CLIMB, IN.		—	2	—	2	5	5.5	4	6.2	7.8
BERM DESIGN		Unsafe	Unsafe	Unsafe	Safe	Safe	Unsafe	Safe	Safe	Safe
VEHICLE RESPONSE		Vault†	Vault	Vault	Penetration‡	Reverse Roll	Vault	Reverse Roll	Reverse Roll	Reverse Roll

* Unconsolidated Strength Measured at 1/4 in. Penetration with 1.25 in. Diameter Plate.

** Compacted Strength Measured at 1/4 in. Penetration with 1.25 in. Diameter Plate.

*** Axle height of 35-ton, 85-ton, and 170-ton trucks were 30, 50, and 57 inches.

† Vault occurred when leading tire penetrated more than halfway through berm

‡ Penetration occurred when leading tire penetrated less than halfway through berm

TABLE 16

DEFORMABLE SOIL BERM TEST RESULTS FOR 30 MPH IMPACT AT 30° APPROACH ANGLE

TEST NO.	VEHICLE (Loaded)	BERM CONFIGURATION HT.	WID. (in.)	SLOPE (in.)	RELATIVE STRENGTH OF BERM	COMP. PENETR'N DISTANCE* (in.)	MAX. BERM CLIMB**	MAX. VEHICLE RESPONSE	BERM DESIGN	AXLE HEIGHT
1	35-ton	5	10	1:1	1.1	5	—	Penetration	Safe	3.4
2	"	"	"	"	1.2	5	—	Penetration	Safe	3.4
3	"	5	"	"	3.5	—	3.75	R.R.	Safe	3.4
4	"	"	"	"	3.7	—	4	R.R.	Safe	3.4
5	"	3	6	"	1.1	6	—	Penetration	Unsafe	2
6	"	"	"	"	1.1	7	—	Penetration	Unsafe	2
7	"	"	"	"	3.2	—	2	Vault	Unsafe	2
8	"	3	10	1:1	1.0+	12	—	Penetration	Unsafe	2
9	85-ton	5	10	1.1	1.9	—	4	Vault	Unsafe	2
10	"	"	"	"	4.7	—	5	Vault	Unsafe	2
11	"	10	20	1:1	2.1	—	8	R.R.	Safe	4
12	"	"	"	"	3.9	—	8	R.R.	Safe	4
13	"	5	14	1:1	2.3	—	5	Vault	Unsafe	2
14	"	10	20	1:1	1.0++	12	6	R.R.	Safe	4
15	170-ton	10	20	1:1	1.0+++	20	3	Penetration	Unsafe	1.8
16	"	"	"	"	1.6	—	6	Vault	Unsafe	1.8
17	"	"	"	"	2.1	—	8	R.R	Safe	1.8

* Penetration of front wheel measured normal to edge of berm.

** Climb of front wheel measured above road surface.

\+ Actual compressive strength of 47 psi at 1/4" penetration of 3/4 in. dia. plate.

\+ + Actual compressive strength of 15 psi at 1/4" penetration of 1-1/4 in. dia. plate.

\+ + + Actual compressive strength of 31 psi at 1/4" penetration of 1-1/4 in. dia. plate.

Examination of the 35-ton test data implies that the restraining mode, either stopping the vehicle by plowing the soil (penetration) or having the vehicle climb the berm and perform a reverse roll, will depend upon the berm strength. A weak berm of suitable size will allow the vehicle to penetrate the material, eventually being stopped by the soil resistance forces. A compacted berm must dissipate the vehicle's energy by having the vehicle ride up the berm, eventually resulting in a rollover. Therefore, even though the berm may be compacted and extremely wide, if it is of sufficient height, it will not be effective in restraining the vehicle.

The results obtained with the 85-ton were similar. However, penetration into the berm was less evident. For an inadequately sized berm, the vehicle would simply vault the berm. Berms constructed to the recommended height of four times the axle height were effective in restraining the vehicle by causing it to roll over rather than vault. The influence of compaction strength is reflected in the increased sinkage, i.e., decreased berm climb, for the lower strength berm. The 170-ton vehicle, while being relatively close to the 85-ton in the physical dimension of the wheel width and diameter, is considerably more massive. Consequently, a minimum strength berm capable of resisting the impact forces of an 85-ton vehicle would not be considered effective in restraining a 170-ton vehicle. The 170-ton simply penetrated through the berm which stopped the 85-ton. By suitably compacting the berm to a sufficient strength level to resist wheel sinkage, the berms were capable of causing the vehicle to roll over onto the roadway.

The influence of the approach condition on berm requirements was examined for the 85- and 170-ton vehicles for the less severe impact condition with the results indicated in Table 17. The 85-ton vehicle responded in a safe mode for either a decrease in impact velocity or a decrease in impact angle, provided the berm was of appropriate size. Reducing both the speed to 25 mph and angle to 25°, however, did not reduce the berm height requirements.

The 170-ton demonstrated a similar decrease in strength requirements for less severe encroachments. However, speeds of 30 mph with a 25° impact angle produced an unsafe response. By reducing <u>both</u> the speed and the angle while maintaining an adequate berm strength, the vehicle did produce a safe response by either rolling over or being stopped by the soil resistance.

The influence of the berm size and relative strength on vehicle response has been illustrated by the previously described series of tests. The berms were constructed to the height specified by the rigid berm test and, when adequately compacted, produced a safe restraining mechanism. The actual vehicle climb associated with these tests was less than that predicted by a rigid berm. Essentially the vehicle was experiencing the influence of rolling resistance from wheel sinkage due to the deformable material. Consequently, the results predicted by a rigid berm analysis

TABLE 17
EFFECT OF APPROACH CONDITIONS ON DEFORMABLE BERM COMPOSITION

TEST NO.	VEHICLE SIZE	BERM CHARAC'SICS HT.	WID.	SLOPE	IMPACT VELOCITY	APPROACH ANGLE	MAX. PENETRATION DISTANCE	MAX. BERM CLIMB	RELATIVE COMP. STRENGTH	VEHICLE RESPONSE	BERM DESIGN
	(Loaded)	(in.)	(in.)		(mph)	(Deg.)	(in.)	(in.)	(PSI)		
18	85-ton	10	20	1:							
		1			25	30°	—	9	2.1	Rolled Down Berm	Safe
19	"	"	"	"	"	25°	—	8.5	2.1	Remained on Berm	Safe
20	"	"	"	"	30	25	—	8	2.1	Reverse Roll	Safe
21	"	"	"	"	25	30	—	9.5	3.9	Reverse Roll	Safe
22	"	"	"	"	"	25	—	10	3.9	Reverse Roll	Safe
23	"	"	"	"	30	25	—	9.5	3.9	Reverse Roll	Safe
24	"	5	14	"	25	30	—	5	2.0	Straddle	Unsafe
25	"	"	"	"	"	25	—	5	2.1	Vault	Unsafe
26	"	"	"	"	30	25	—	5	2.0	Vault	Unsafe
27	"	10	20	1:							
		1			25	30	11	4.7	1.3	Rolled Down	Safe
28	"	"	"	"	"	25	10	4.5	1.0	Berm Penetration	Safe
29	"	"	"	"	30	25	11	5	1.0	Reverse Roll	Safe
30	170-ton	10	20	1:							
		1			25	30	12	4.5	2.0	Berm Penetration	Unsafe
31	"	"	"	"	"	25	10.5	4	2.0	Berm Penetration	Safe
32	"	"	"	"	30	25	—	8.0	2.0	Vault	Unsafe
33	"	"	"	"	25	30	—	8.0	3.3	Reverse Roll	Safe
34	"	"	"	"	"	25	—	8	3.3	Reverse Roll	Safe
35	"	"	"	"	30	25	—	7	3.3	Vault	Unsafe

will provide a conservative height estimate for a deformable berm. This further implies that a computer simulation technique would also yield a conservative approach provided the input parameters are suitably selected.

The strength of a berm can be determined by specifying its exact constituents or arbitrarily using available material that, by compaction or physical characteristics, yields the desired strength. Since the available material composition will vary significantly for the different types of mines and geographic locations, meeting certain strength requirements is a more practical solution to the problem. This assumes that an acceptable technique can be developed which will readily evaluate the strength of the berm and hopefully will consist of something as simple as driving a loaded vehicle up the berm, recording the wheel penetration, and comparing this reading to an established guideline.

While the relative size of berms and the vehicle response capable of being predicted by the computer simulation has been tentatively established through model testing, the exact berm strength necessary to produce the desired results is still uncertain. We have demonstrated that the compaction strength must be a multiple of the unconsolidated strength. The magnitude of this strength can be estimated by scaling the berm strength specified in the previous tables. The berm strengths specified in these tables were easily obtained and readily measured. Actual berms will require the compaction of soil-type materials to obtain the desired strength level of the mixture of soil and rock to increase the compressive strength. Regardless of how the mine operators obtain the desired strength level, a technique is still required to evaluate the berm. A limited amount of model tests were performed using loose gravel and mixtures of soil and gravel. These tests indicated a mixture of 50 percent soil and gravel (equivalent to 6 inch diameter rock) by weight was more effective in increasing wheel climb than either soil or gravel alone. As long as the mines can construct and maintain a berm conforming to a given size and strength, regardless of the type or composition of the material employed, it will safely restrain a haulage vehicle.

3.1.2 Field Test Results

3.1.2.1 Test Site No. 1. - The field test program was initiated in the summer of 1980 with tests conducted in a limestone quarry located in south central Texas. This site was chosen because the material available for testing consisted of pit run gravel, five inches in diameter and smaller, which is representive of materials found in many mine sites. The relative ability of this material to restrain a 35-ton haul truck under varying approach conditions, berm height, and compaction conditions was tested.

An economic constraint of the field test program prohibited testing that would result in damage to the vehicle. As a result, small approach velocities were tested first and then increased to the point where safety of the test was questionable.

Data presented includes the matrix of tests performed, measured tire sinkage, wheel climb, and penetration along the direction of travel. In addition, data obtained from testing the strength of the berm is recorded to correlate the test results to berm strength.

A goal of this phase was to determine the acceptability of testing techniques used during the course of the field test program. The results of two methods are presented in the section on vehicle field test responses. These results include static tire penetration and cone penetration test data.

Tire sinkage qualification tests were performed for each berm composition. These tests were performed by driving the vehicle up the berm, either perpendicular or at an angle of 45° to the berm to a height equal to the axle height. In the former situation, both tires contacted the berm, and in the latter case only one tire made contact. Tire penetration values normal to the surface of the undisturbed berm were recorded.

Table 18 presents the matrix of tests performed at Field Test Site 1. Test 1A was performed to evaluate the interaction between the vehicle and a berm constructed to the current rule of thumb (axle height) specifications. Tests 1B-1D were performed to evaluate the interaction between the vehicle and berm when the size and the amount of compaction of the berm varied.

Figure 8 presents the results of Test 1A, the current rule of thumb berm test. The test results which are reported were previously explained and include the maximum penetration distance along the direction of travel, the maximum tire sinkage value and the maximum wheel climb value for each combination of approach angle and velocity. In addition, the tire sinkage values of the berm qualification are presented for both the 90° and 45° test condition. For each approach angle, the allowable penetration distance where the leading tire would penetrate more than halfway through the berm is presented.

The results of these tests indicate failure of the berm to restrain the vehicle from penetrating more than halfway through the berm. Data collected for berm qualification is also presented in Figure 8.

After the test of the berm constructed to current rule of thumb standards was complete, Test 1B was performed on a berm of non-compacted pit run material constructed to a height of three times the axle height, or 90 inches. Vehicle response and berm qualification test results are illustrated in Figure 9.

This information reveals that tire sinkage values were less than those experienced during Test 1A. This is attributed to the fact that this test berm had been constructed sometime before the actual test run and had probably experienced some consolidation whereas the berm in Test 1A

Table 18. 35-ton Haulage Vehicle Test Matrix
Test Site 1, Limestone Quarry

Test Case	Berm Characteristics: Composition	Berm Characteristics: Height	Berm Characteristics: Slope*	Vehicle Condition	Approach Condition: Speed(mph)	Approach Condition: Angle(deg)
1A	Unconsolidated Pit-run Material†	Axle Height (30 inches)	Angle of Repose**	Loaded	5,10	10,20,30
1B	Unconsolidated Pit-run Material	3 times Axle Height (90 inches)	Angle of Repose	Loaded	5,10	10,20,30
1C	Compacted Pit-run Material	3 times Axle Height (90 inches)	1:1	Loaded	5,10,12.5 5,7.5,10	10 20,30
1D	Compacted Pit-run Material	3 times Axle Height (90 inches)	1:1	Empty	5,10,12.5 5,7.5,10	10 20,30

*Ratio of Rise to Run
**35 Degrees

†Material consisted of 3% larger than .5 inches, 31% between .19 and .5 inches and 65% smaller than .19 inches in diameter

Berm Qualification Test Data

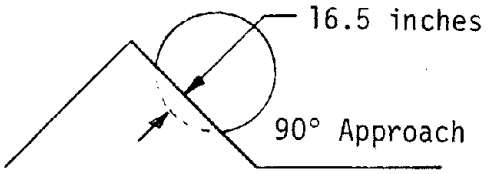

Tire Penetration Data

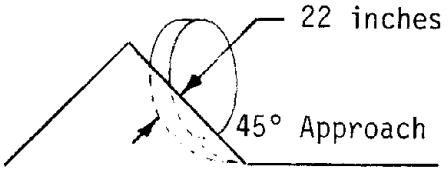

Berm Height 30 inches, Berm Width 86 inches

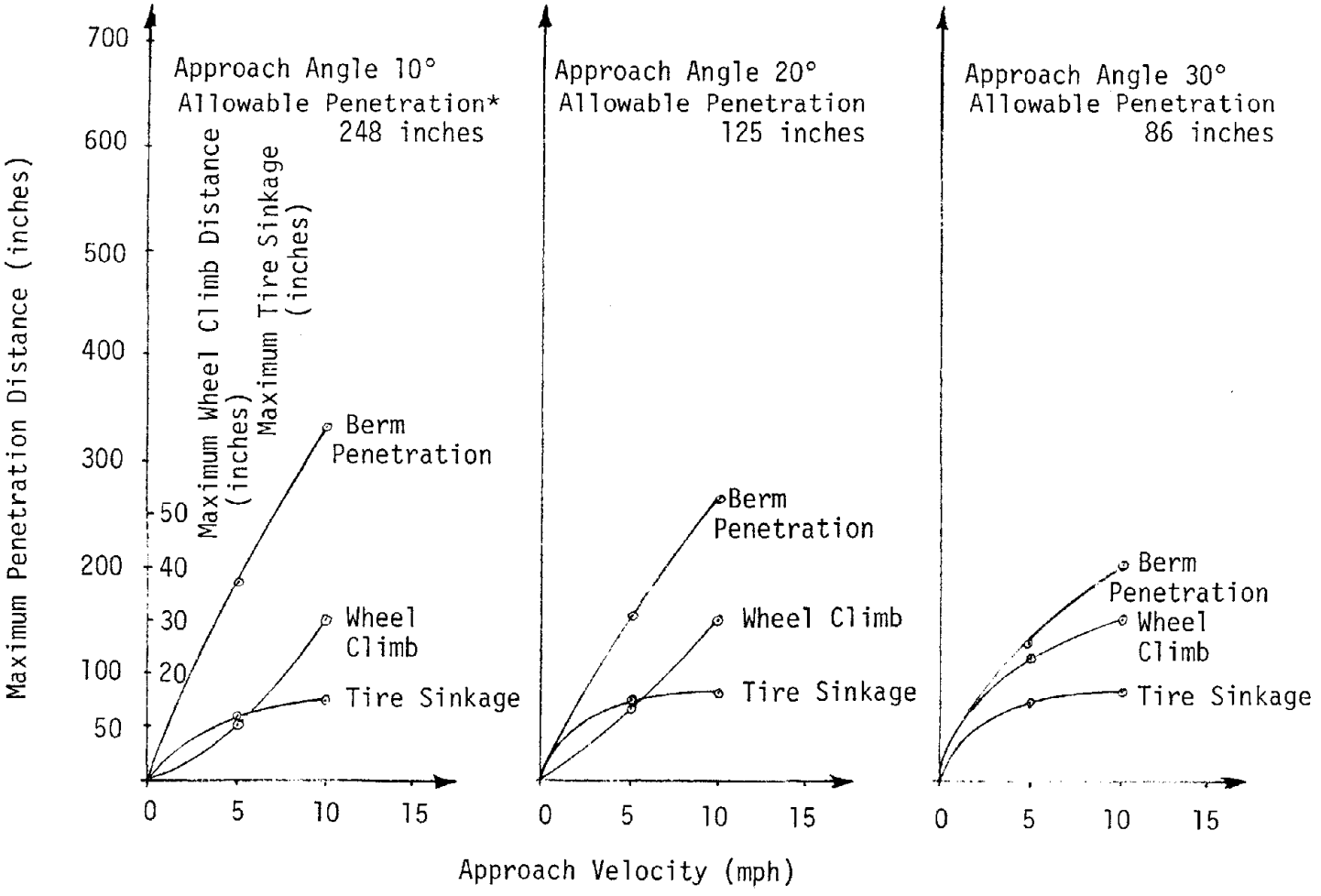

*Allowable Penetration = Berm Width/(2)(sin(approach angle)

FIGURE 8. 35-TON VEHICLE RESPONSE FOR TEST 1A ON AN AXLE HEIGHT, UNCONSOLIDATED PIT RUN MATERIAL BERM

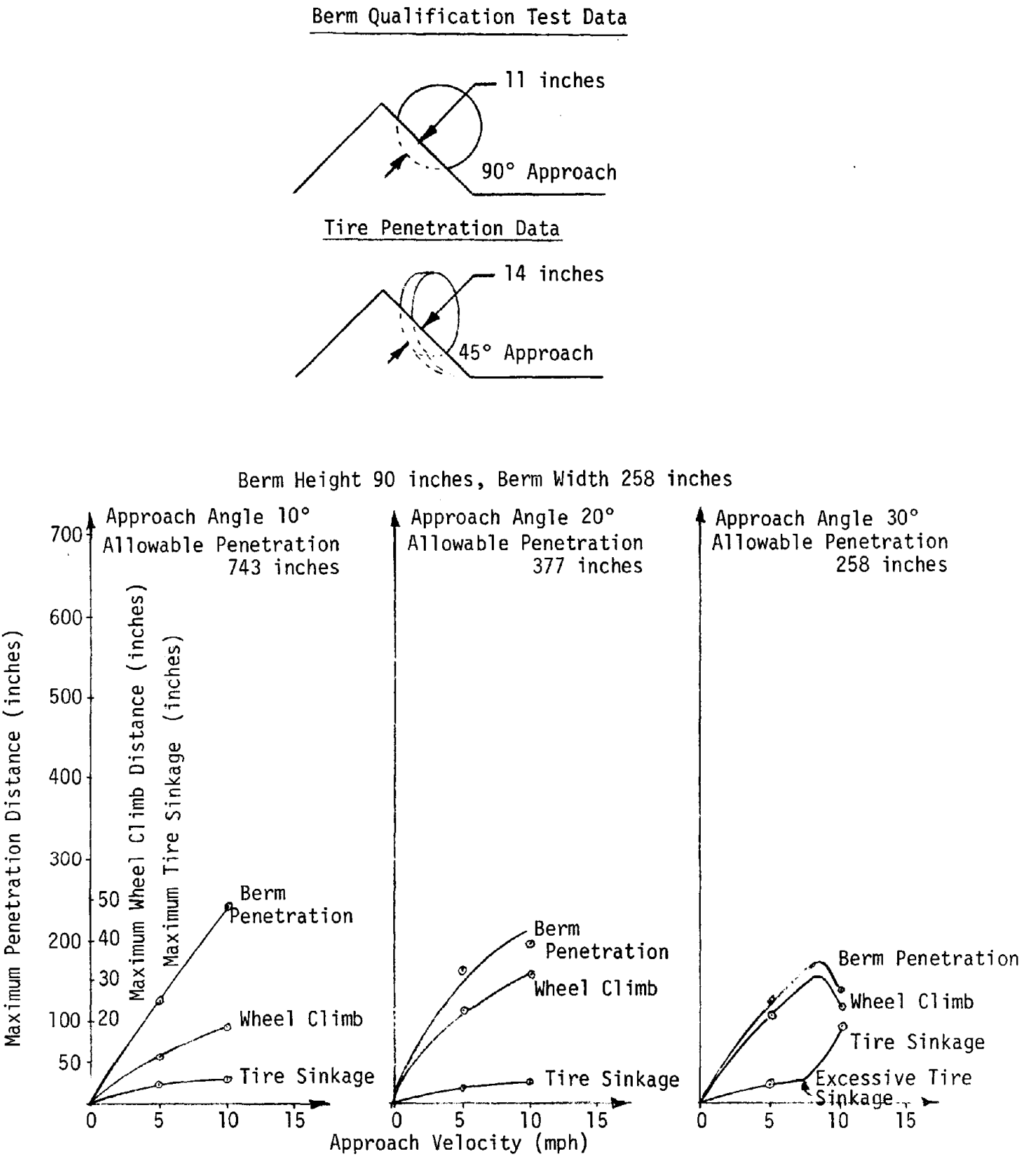

FIGURE 9. 35-TON VEHICLE RESPONSE FOR TEST 1B ON A THREE AXLE HEIGHT, UNCONSOLIDATED PTI RUN MATERIAL BERM

was constructed just prior to the test. The most significant result of this set of tests was the interaction observed for the approach conditions of 10 mph and 30°. It is obvious that the trend of the various values was altered abruptly during this test.

Tests to determine the acceptability of compacted pit run material for use as berm material were also run during this first field test. The results of the vehicle responses and berm qualification tests are given in Figures 10 and 11 for Tests 1C and 1D, respectively. The results presented for Test 1C indicates the preferred response of the vehicle for these approach conditions.

A particularly significant aspect of these tests is revealed when the wheel climb and tire sinkage values associated with the approach conditions of 10 mph and 30° are compared to the results obtained for the same approach conditions in Test 1B. Whereas in Test 1B, gross compressive failure of the berm was experienced, no such berm failure was experienced for Test 1C. Comparing the tire penetration and cone penetrometer results for these cases reveals a proportionate increase in berm strength, the result of the difference in compaction of the berms tested.

Test 1D, Figure 11, related the interaction between an empty haulage vehicle and a compacted berm. Comparing the results presented for a loaded vehicle (Test 1C) and an empty vehicle (Test 1D) indicates generally similar values of berm penetration and wheel climb although the empty vehicle exhibited less tire sinkage. Since the energy dissipation description for this system is a function of both tire drag and vehicle climb, the results are indicative of the similarity of responses which should be exhibited.

The test results previously presented provided some substantial findings regarding the acceptability of certain constructed berms to restrain a haulage vehicle from leaving an elevated roadway. Additional testing was required to finalize the berm requirements and provide data on the range of berm compositions to complete correlation between field tests, model tests, and computer simulations. Although it was initially planned that a larger haul truck be used for this additional testing, none of these larger vehicles could be obtained.

3.1.2.2 Test Site 2 - Because of the limitation of the availability of material used at the first test site,the material was pit run gravel generally .5 inches in diameter and smaller; additional tests were performed with additional material. The conditions of the tests and material descriptions are presented in Table 19, the Haulage Vehicle Field Test Matrix for Test Site 2.

Test 2A was performed to determine the acceptability of the rule of thumb construction specifications currently in practice. Test 2B was performed to determine the acceptability of an uncompacted berm construction

Berm Qualification Test Data

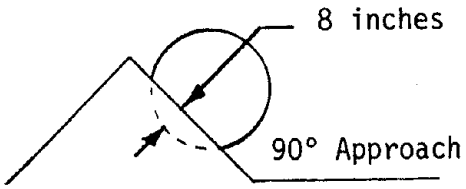

Tire Penetration Data

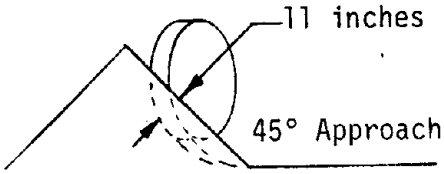

Berm Height 90 inches, Berm Width 180 inches

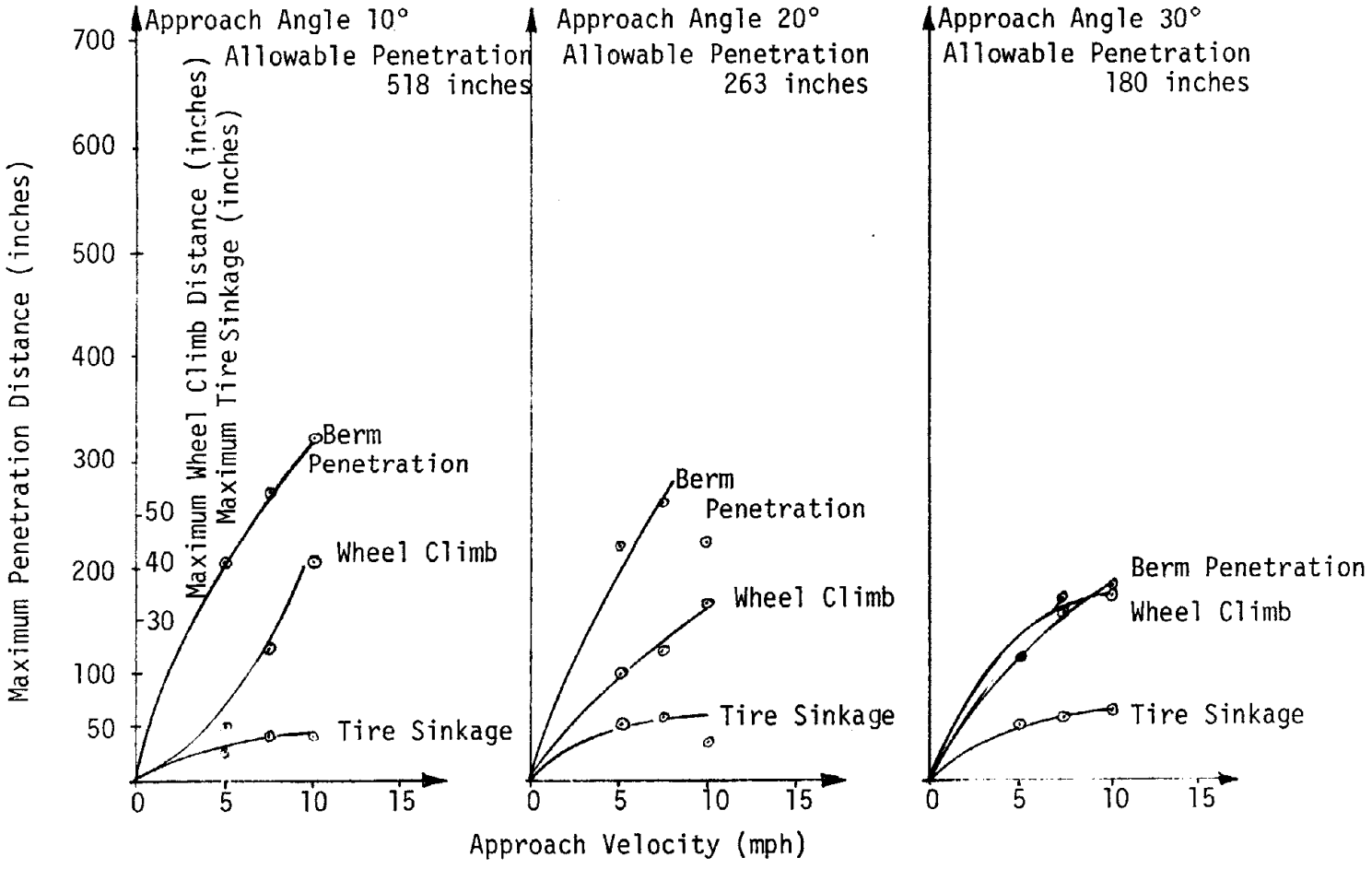

FIGURE 10. LOADED 35-TON VEHICLE RESPONSE FOR TEST 1C ON A THREE AXLE HEIGHT, COMPACTED PIT RUN MATERIAL BERM

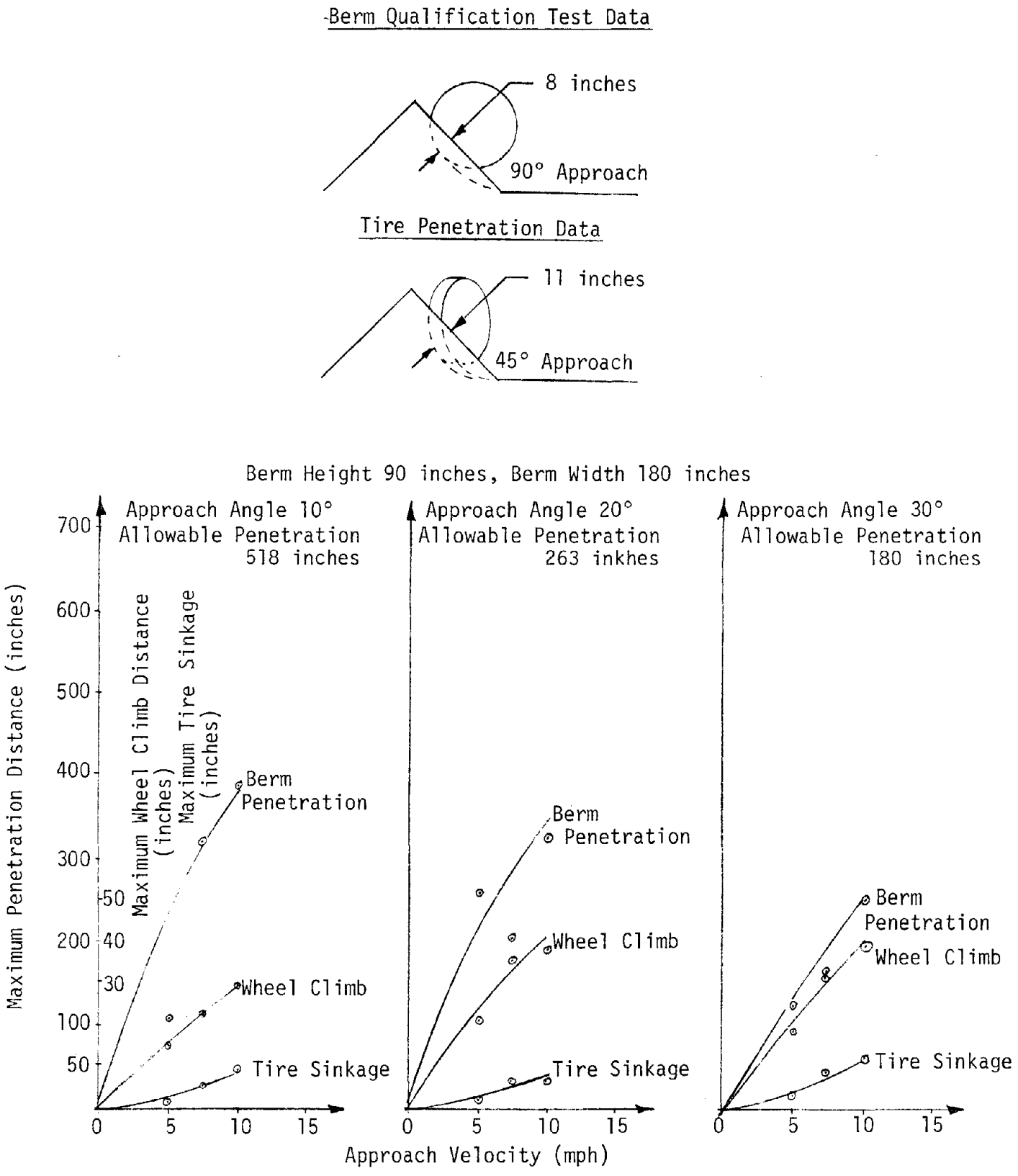

FIGURE 11. EMPTY 35-TON VEHICLE RESPONSE FOR TEST 1D ON A THREE AXLE HEIGHT, COMPACTED PIT RUN MATERIAL BERM

Table 19. 35-ton Haulage Vehicle Test Matrix
Test Site 2, SwRI Test Site

Test Case	Berm Characteristics: Composition	Height	Slope*	Vehicle Condition	Approach Condition: Speed(mph)	Angle(deg)
2A	Unconsolidated Selected Material†	Axle Height (30 inches)	Angle of Repose	Loaded	5,10,12.5 5,7.5,10	10 20,30
2B	Unconsolidated Selected Material	3 times Axle Height (90 inches)	Angle of Repose	Loaded	5,10,12.5 5,7.5,10	10 20,30
2C	Compacted Selected Material	3 times Axle Height (90 inches)	1:1	Loaded	5,10,12.5 5,7.5,10	10 20,30
2D	Bank Cut Berm‡	3 times Axle Height (90 inches)	1:1	Loaded	5,10,12.5 5,7.5,10	10 20,30

*Slope of Rise to Run
†Selected material consisted of 10% larger than 1.0 inch, 25% between .5 and 1.0 inches, 20% between .25 and .5 inches, and 46% less than .25 inches
‡Bank cut berm consisted of 16% larger than 1.0 inch, 17% between .5 and 1.0 inches, 21% between .25 and .5 inches, and 46% less than .25 inches

to the height recommendation of three times the axle height, or 90 inches in this case. Test 2C was designed to determine the acceptability of a berm constructed of compacted selected material built to this same height specification. Finally, Test 2D was conducted to determine the vehicle response to the practical limit of rigidity found in mines.

Presentation of the results obtained has the same format as the results reported for Test Site 1. Included are plots of the vehicle response as a function of approach conditions and the associated berm strength characteristics.

Figure 12 presents the results of Test 2A, the response of a haulage vehicle to a berm constructed of selected material built to the axle height. Penetration values exceed the overall values for each approach angle for approach velocities of only 10 mph. This is unacceptable because penetration of 60 inches or more results in loss of the vehicle. Figure 12 also presents the results of the qualification tests performed on this berm. It should be noted that when comparing the results of this test to those of Test 1A, there exists a substantial increase in the berm strength. This can be observed by comparing the tire sinkage values.

The purpose of Test 2B was to determine the acceptability of an unconsolidated berm constructed to a height of three times the axle height with selected material. The results of this test are presented in Figure 13. The results indicate that according to the tire sinkage values, this berm is roughly equivalent to the compacted pit run material tested in Test 1C. This illustrates the relative significance that berm composition can have on macroscopic strength even when external compaction is neglected.

Testing the response of a haulage vehicle and berm constructed of compacted selected material to a height of three times the axle height was performed under Test 2C. The results obtained are presented in Figure 14 and represent the practical, economical construction limit of berms achievable in mines.

Test 2C illustrates the relative ability of the berm to support a loaded vehicle and, if necessary, cause vehicle rollover. Tire sinkage values, when compared, illustrate the relative improvement in bearing strength that can be accomplished by selecting and compacting certain materials. Tire sinkage exhibited during the test reflects the improved berm strength. Only when these results are correlated to the scale model tests and computer simulations will the acceptability of this or any other berm finally be determined.

The final test performed at the second test site illustrates the response of a haulage vehicle against a berm constructed to the practical limits of rigidity. This berm was cut from a virgin bank at a slope of 45°. The results of the vehicle's response and berm qualification test are presented in Figure 15.

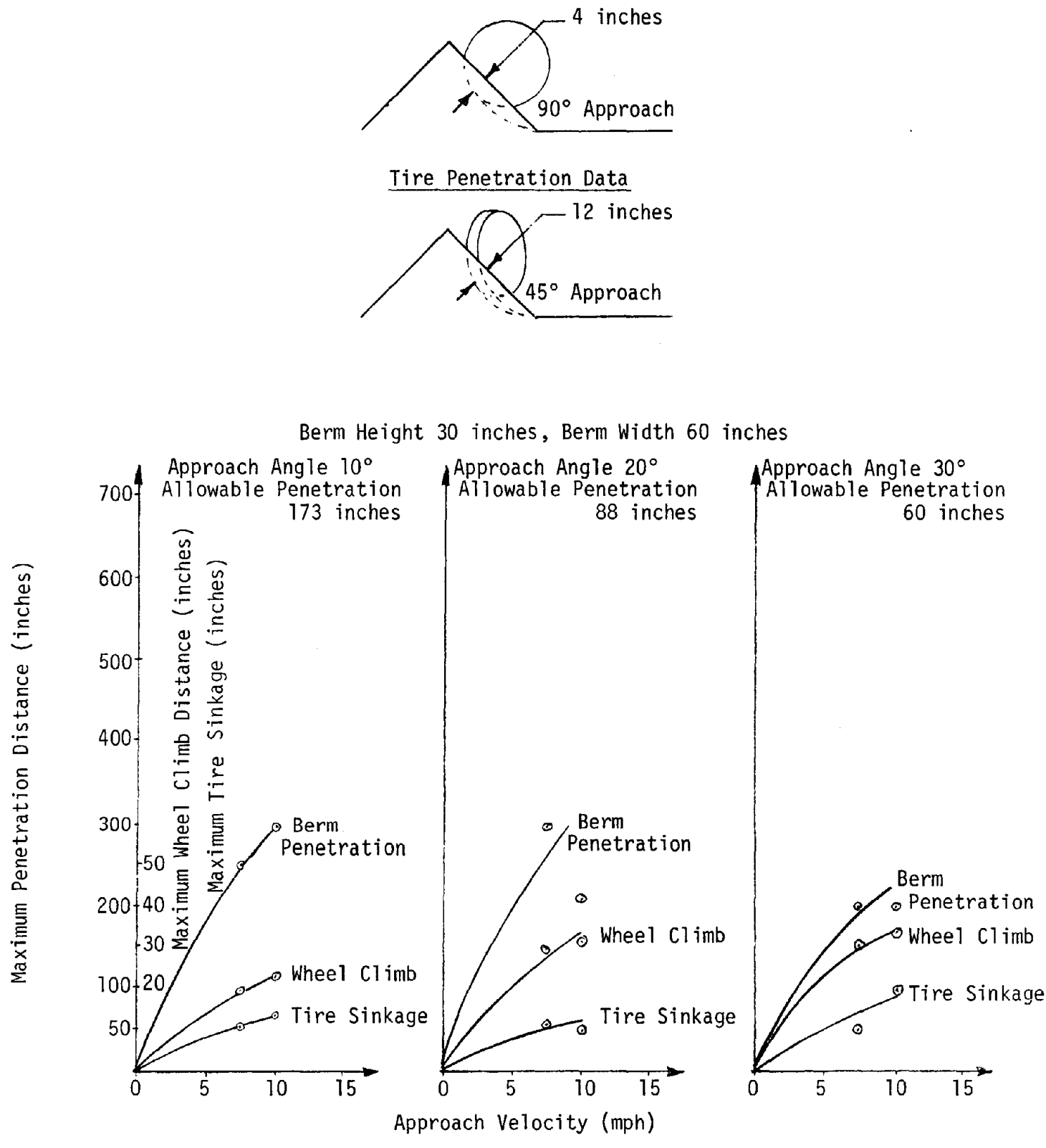

FIGURE 12. LOADED 35-TON VEHICLE RESPONSE FOR TEST 2A ON AN AXLE HEIGHT UNCONSOLIDATED SELECTED MATERIAL BERM

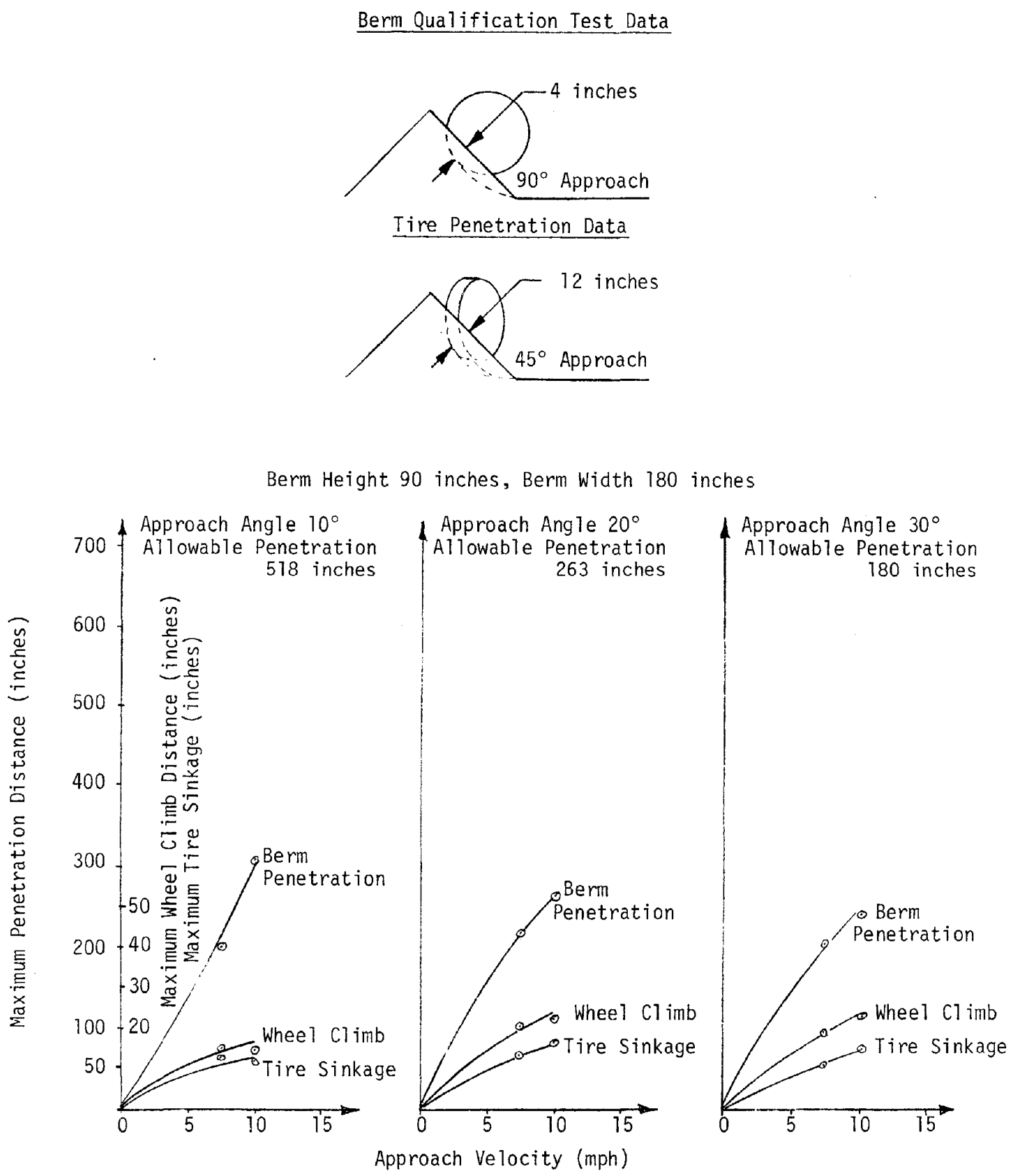

FIGURE 13. LOADED 35-TON VEHICLE RESPONSE FOR TEST 2B ON A THREE AXLE HEIGHT, UNCONSOLIDATED SELECTED MATERIAL BERM

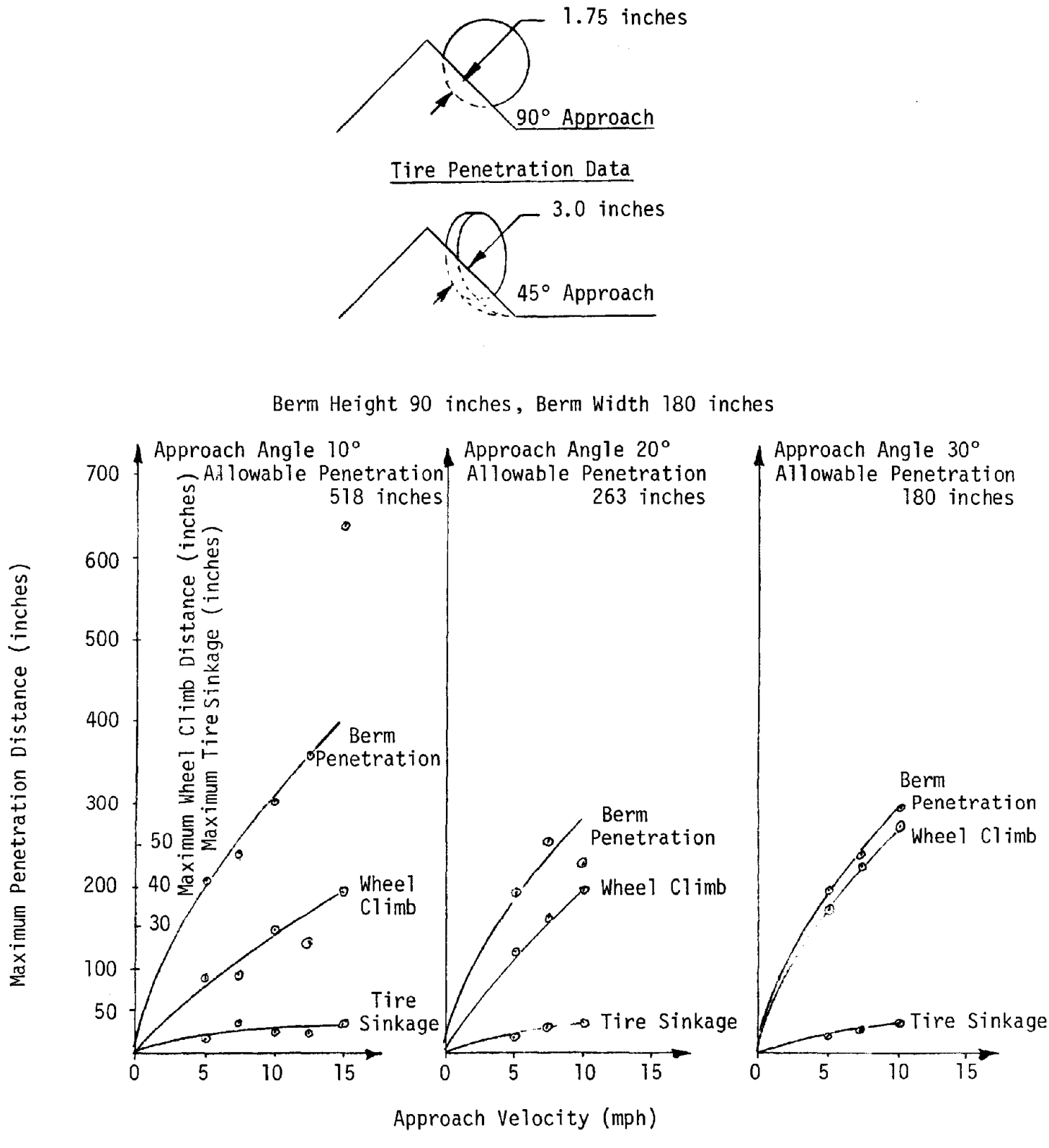

FIGURE 14. LOADED 35-TON VEHICLE RESPONSE FOR TEST 2C ON A THREE AXLE HEIGHT COMPACTED SELECTED MATERIAL BERM

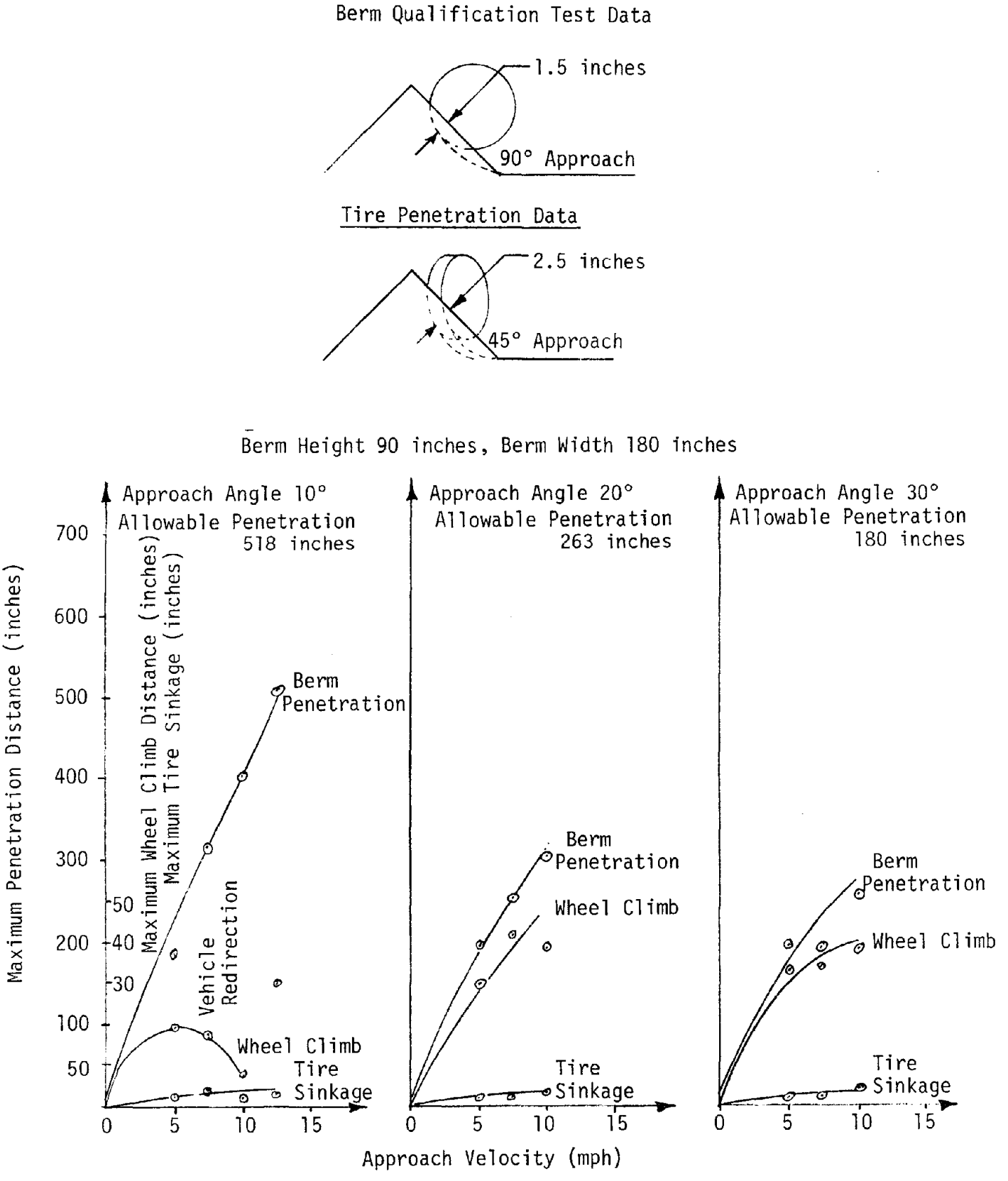

FIGURE 15. LOADED 35-TON VEHICLE RESPONSE FOR TEST 2D ON A THREE AXLE HEIGHT, BANK CUT BERM

Previously, redirection was considered as a possible response of the haulage vehicle under the conditions of a rigid berm with steep slope. This response was exhibited in the model tests when the tests were performed on a rigid berm. Theory holds that these approximate conditions would have to exist during full scale testing to repeat this response.

When testing was performed on this bank cut berm, redirection was exhibited for very small approach angles. Redirection occurs when the frictional forces developed by the front tires is insufficient to hold the vehicle on the berm. This results when either the ground conditions become slippery, thus limiting the coefficient of friction, or the approach angle is sufficiently small so as to limit the load on the front tires.

The field test results described the interactions for the various berms. These tests have indicated that the current rule of thumb construction guidelines are inadequate to restrain a runaway vehicle. They have also shown that non-compacted berms will result in sinkage during dynamic interactions. In addition, the field test results indicated that redirection is limited to small approach angles.

Results obtained from the field test did not provide the information to predict the approach conditions at which rollover will occur. The information is, however, the basis for determining the correlation which exists between the computer simulations and the scale model simulations. On the basis of the obtained correlations, predictions of the approach conditions which will result in rollover are derived.

3.1.3 HVOSM Computer Simulations

Computer simulations of vehicles interacting with edge-of-the-road berms were performed using the HVOSM three-dimensional computer program. Vehicles ranging in size from 35- to 170-ton were simulated impacting a sloping, rigid plane at various approach conditions. The results obtained through these simulations provide detailed information regarding the

- Vehicle trajector
- Forces generated during impact
- Acceleration factors experienced by vehicle and operator.

Use of this program is, however, restricted to the simulation of vehicles interacting with a non-deformable structure which will not be laterally displaced during the impact.

A computer simulation allows the detailed examination of any particular input variable; however, the influence of certain variables on vehicle response is more pronounced than others. Consequently, only those variables which significantly influence the wheel climb on a rigid berm were varied. Other vehicle parameters which corresponded to the parameters used on the model vehicle, e.g., inertia terms, vehicle weight, etc., remained constant. The primary parameters investigated were:

- Cornering stiffness coefficients
- Tire stiffness
- Steering parameters

3.1.3.1 Cornering Stiffness Coefficients - The ability of a vehicle to maintain a position on an inclined surface, such as a berm, is a function of the side forces developed at the tire-terrain contact patch. In the computer program, the side force calculations are a function of the small angle (slip and camber) properties of the tire which are "saturated" or limited in magnitude at large angles. Variations in the small-angle cornering and camber stiffness (C_{SO} and C_{CO}) produced by changes in tire loading are approximated by parabolic functions fitted to experimental data. These cornering stiffnesses vary by the following relationship:

$$C_{SO} = A_0 + A_i F'_{R_i} - \frac{A_1}{A_2} (F'_{R_i})^2 \quad (5)$$

$$C_{CO} = A_3 F'_{R_i} - \frac{A_3}{A_4} (F'_{R_i})^2 \quad (6)$$

(F'_{R_i}) is the component of tire radial force normal to the terrain; the side forces are

$$(F_{S_i})_{camber} = C_{CO}\, \phi_{CG_i} \quad (7)$$

$$(F_{S_i})_{slip} = C_{SO} \frac{v_{S_i}}{u_{G_i}} - \psi'_i \quad (8)$$

where

A_0, A_1, A_2 are constant coefficients for tire side force due to slip angle

A_3, A_4 are constant coefficients for tire side force due to camber angle

F_{S_i} is tire side force produced by slip angle and camber angle

$\phi\, CG_i$ is camber angle of wheel (i) relative to terrain

ψ'_i is steer angle of wheel (i) in its tire-terrain contact plane

u_{G_i}, v_{G_i} are forward and lateral wheel (i) center velocities, respectively.

The parabolic curves associated with Equations (5) and (6) are assumed valid for a specific range of tire loadings (F'R). Once this range is extended beyond the limiting value specified in the program, the side force properties, Equations (5) and (6), are then treated as being independent of tire loading. The influence of these tire side force coefficients on maximum wheel climb is illustrated in Table 20 for an 85-ton vehicle impacting a 45° rigid berm at a speed of 25 mph and approach angle of 20°. The tire stiffness coefficients, A_0 through A_4 for Case 2, are the values associated with passenger car tire data. Varying these tire coefficients, as illustrated, will significantly increase the wheel climb for identical impact conditions.

Table 20 - Effect of Tire Cornering and Camber Stiffness Coefficients for an 85-Ton Vehicle

Case No.*	Tire Cornering and Camber Stiffness Coefficients					Max. Tire Deformation (in.)	Max. Tire Climb (in.)
	A_0	A_1	A_2	A_3	A_4		
2	4,400	8,276	2,900	1.78	3,900	6	22
3	4,400	82.76	29,000	17.8	39,000	6	34
4	44,000	82.76	29,000	17.8	39,000	6	34
5	440,000	827.6	290,000	178	390,000	8	67

* All cases with rigid 1:1 berm, 25 mph, 20° impact
Constants associated with tire-side force loadings
Scale model test demonstrated 50-inch wheel climb (vertical) on berm

Since these coefficients, A_0 through A_4, were not available from the tire manufacturers, nor are contract funds available to experimentally determine their magnitudes, several computer runs were performed using multiples of the passenger car tire data. Using coefficients multiplied by a factor of 10 for the 35- to 85-ton class of haulage vehicle provided a close correlation with rigid berm model tests for impact speeds ranging from 20-30 mph, and impact angles ranging from 12-25°. Likewise, using a coefficient multiple of 20 for the 170-ton vehicle provided a close correlation with the rigid berm model test.

3.1.3.2 Tire Stiffness - Tire load-deflection characteristics were obtained using manufacturer's data. This data provided the tire stiffness coefficient, KT, for computer simulation of the various sizes of haulage vehicles. The physical model by comparison, used molded rubber wheels which exhibit little, if any, deformation characteristics. Therefore, comparing the initial computer simulations using a deformable wheel on a rigid surface with the model tests using a rigid wheel on a rigid surface produced a

substantial variation in maximum wheel climb. To obtain a correlation between the data, it was necessary to mathematically simulate a stiffer wheel. This is obtained by specifying an initial linear tire-deflection rate over a certain deflection range, followed by a multiplier to increase the tire stiffness for any further deflection outside the specified range. These tire stiffness characteristics are indicated by the following notation, 15 (5/5). The first number of this notation represents the initial tire stiffness, 15 Kips/in. equivalent to 15,000 lbs/in. The first number in parentheses signifies five inches of tire deflection for the initial tire stiffness. The second number in parentheses represents a multiple of the initial load-deflection and remains constant for any additional tire displacement after exceeding the initial deflection range, i.e., 15,000 lbs/in. x 5 or 75, 000 lbs/in. The various tire notations and representative manufacturers' test data are illustrated in Figure 16.

The influence of tire stiffness on berm climb is illustrated in Table 21 for a 35-ton vehicle; also illustrated in this table is the effect of tire side force parameters. By experimentally selecting the magnitude of these input parameters, a correlation between model test and computer simulation has been obtained. To obtain a similar correlation between full-scale vehicle trajectories and the computer predictions, it is expected that these tire stiffness characteristics will be adjusted to a more deformable range as indicated by the tire manufacturer's data.

The effect of tire stiffness alone, on maximum vertical berm climb, is illustrated in Figure 17 for a 35-ton vehicle impacting a rigid berm, the tire stiffness coefficients (A_0 through A_4) being the same for both conditions illustrated. By increasing the tire stiffness parameter to produce a more rigid wheel, the vehicle exhibited a reduction in berm climb. Consequently, in an actual situation the combination of tire deformation associated with a "real" tire operating on a rigid surface, e.g., a concrete berm, would result in a berm climb greater than predicted by the computer simulations.

3.1.3.3 Steering Parameters - The test data previously illustrated in Table 21 incorporated a locked steering mode. This mode maintains the front wheels of the vehicle in a fixed position throughout the entire berm-vehicle interaction period. Impacts of this nature would be representative of a driver nodding while holding the steering wheel stationary and eventually impacting the berm. As previously discussed, the hydraulic steering system generally used on haul trucks does not contain any type of terrain feedback or self-correction characteristics. Therefore, in actual practice, the front wheels will remain in a fixed position until the steering wheel is turned.

Simulation of a system which is not locked, one which allows the front wheels to be directed by external forces on the wheels, is illustrated in Table 22. The steering parameters used for this evaluation were not

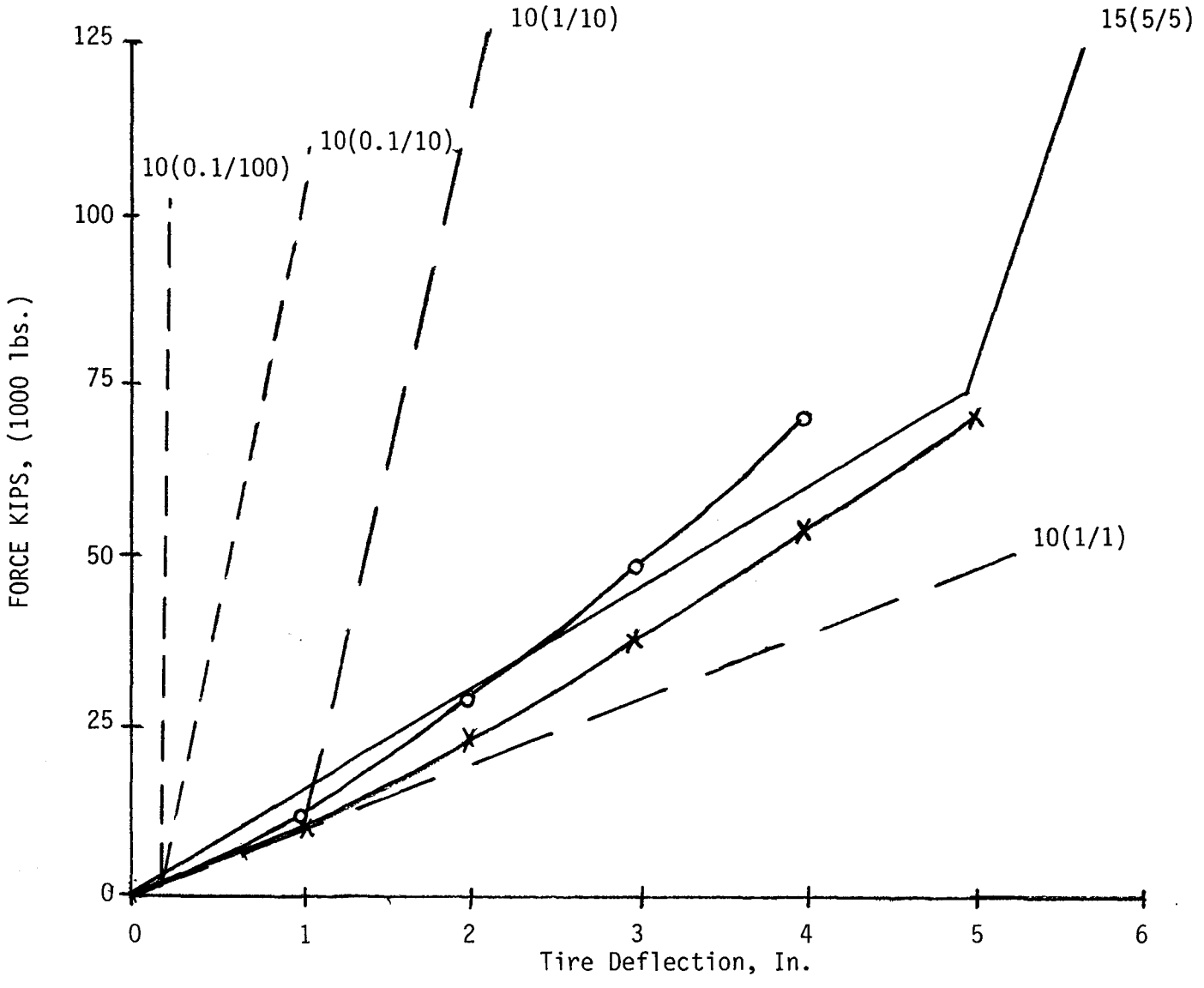

FIGURE 16. TIRE STIFFNESS CHARACTERISTICS

TABLE 21

COMPUTER SIMULATION SUMMARY FOR 35-TON VEHICLE

Case	Speed (mph)	Angle (deg)	HVOSM PREDICTIONS	Scale*** Model	HVOSM Tire Stiffness Coefficient A_0	A_1	A_2	A_3	A_4	Multiple of Sedan Tire Data	Tire Stiffness (kips/in.)
1	25	20	23†/20‡	38	44,000	82.76	29,000	17.8	39,000	10	10(1/10)**
2	25	20	40/31	38	66,000	124.1	43,500	26.7	58,500	15	10(1/10)
3	20	20	32/27	8	66,000	124.1	43,500	26.7	58,500	15	10(1/10)
4	30	20	Straddles	46	66,000	124.1	43,500	26.7	58,500	15	10(1/10)
5	20	20	19/18	8	44,000	82.76	29,000	17.8	39,000	10	10(1/10)
6	30	20	27/22	46	44,000	82.76	29,000	17.8	39,000	10	10(1/10)
7	20	20	32/25	8	66,000	124.1	43,500	26.7	58,500	15	10(0.1/10)
8	20	20	42/40	8	66,000	124.1	43,500	26.7	58,500	15	10(10/10)
9	20	20	14/13	8	66,000	124.1	43,500	26.7	58,500	15	10(0.1/100)
10	25	20	21/21	38	66,000	124.1	43,500	26.7	58,500	15	10(0.1/100)
11	30	20	26/26	46	66,000	124.1	43,500	26.7	58,500	15	10(0.1/100)

* 45° rigid berm (overall height; 50 in.)
† Maximum wheel vertical elevation (in.) above roadway (after contact loss with berm).
‡ Maximum wheel ground contact point terrain elevation (in.).
** Linear tire force-deformation range (in.) - nonlinear stiffness multiplier.
***Models were of 1/20 geometric scale

Table 21 (Cont'd)

Case	Speed (mph)	Angle (deg)	Berm Climb (in.) HVOSM PENETRATION	Scale*** Model	HVOSM Tire Stiffness Coefficients A_0	A_1	A_2	A_3	A_4	Multiple of Sedan Tire Data	Tire Stiffness (kips/in.)
12	20	15	23/20	5	66,000	124.1	43,500	26.7	58,500	15	10(1/10)
13	25	25	79*/27	55†	66,000	124.1	43,500	26.7	58,500	15	10(1/10)
14	25	20	29/26	38	44,000	82.76	29,000	17.8	39,000	10	10(5/10)
15	25	20	34/32	38	44,000	82.76	29,000	17.8	39,000	10	10(5/5)
16	25	20	36/32	38	44,000	82.76	29,000	17.8	39,000	10	10(10/10)
17	20	20	27/27	8	44,000	82.76	29,000	17.8	39,000	10	10(5/5)
18	30	20	65/25‡	46	44,000	82.76	29,000	17.8	39,000	10	10(5/5)

* Program terminated @ time limit of 750 msec; vehicle roll orientation was 41° (reverse) with an increasing roll velocity; reverse rollover probable.
† Reverse rollover occurred.
‡ Vehicle redirected with max wheel elevation occurring after vehicle was redirected @ run termination reverse roll angle of 40° recorded; with increasing roll angular velocity - reverse rollover could occur.
**Linear tire force-deformation range (in.) - nonlinear stiffness multiplier.
***Models were of 1/20 geometric scale

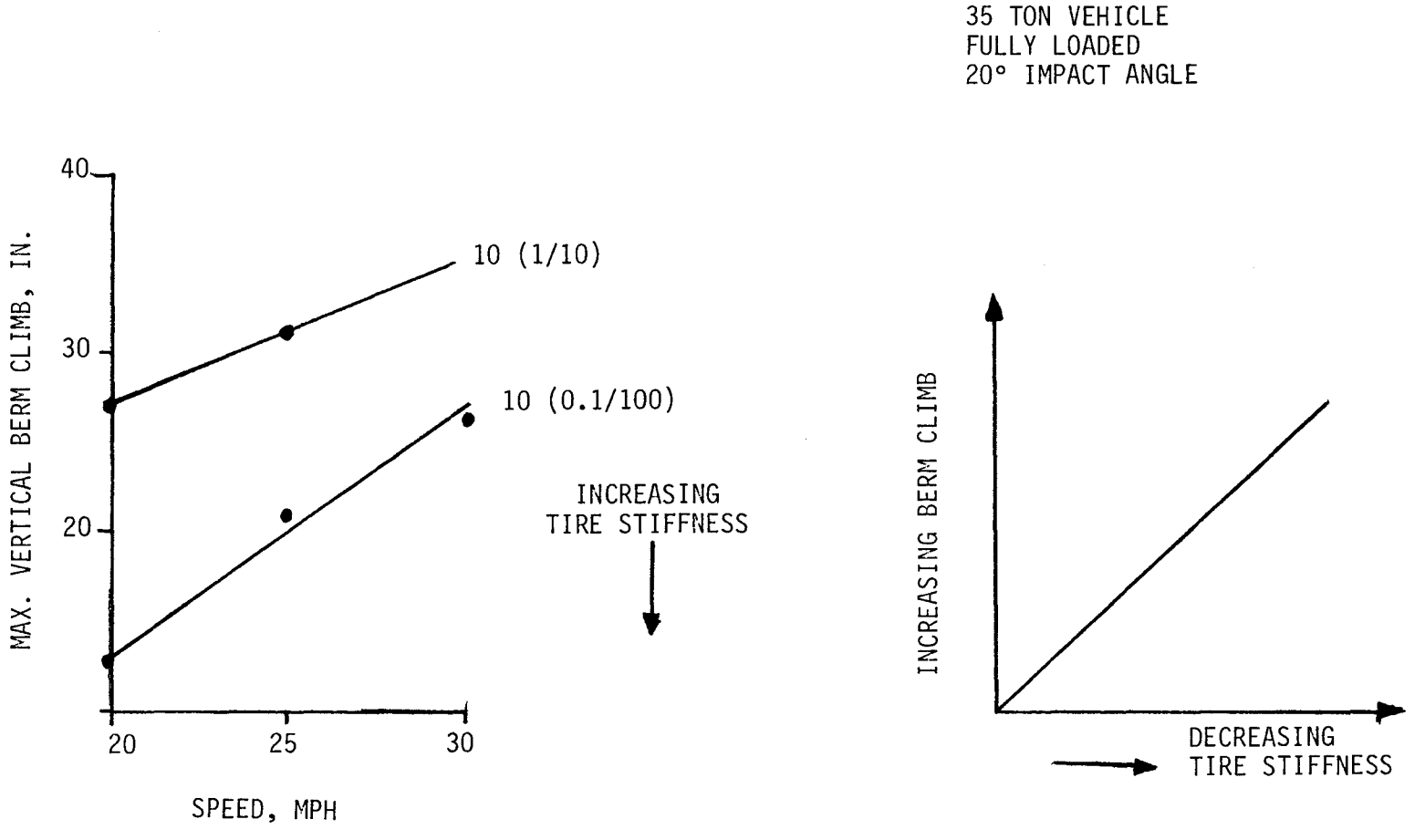

FIGURE 17. EFFECT OF TIRE STIFFNESS ON BERM CLIMB

available from vehicle manufacturers. Therefore, the parameters listed in the table represent extrapolated data based on passenger car and highway truck data. While the actual values of these parameters for haulage vehicles are not known, their relative influence on a vehicle's redirection is still significant.

Table 22
Steering Degree-of-Freedom (DOF) Effect
on Vehicle*Berm Interaction

	HVOSM Steering Parameters*						
Case	I_ψ	C'_ψ	$\Omega\psi$	K_ψ	$\varepsilon\psi$	Berm Climb (in.)	Max. Steer Angle (deg)
17			- LOCKED STEERING -			27	0
22	50,000	60,000	0.4	500,000	0.075	35	-49†
23	50,000	60,00	0.4	5,000,000		32	-32
24	50,000	600,000	0.4	5,000,000		27	- 8

* 35-Ton vehicle impacting at 20 mph, 30° approach angle
† Negative sign - tire turns away from berm.

The five steering parameters incorporated in the HVOSM program to represent the vehicles' steering systems are defined as follows:

I - Moment of inertia of steering system effectiveness at front wheels (both sides included), lb-sec^2-in

C - Coulomb resistance in steering system effective at the wheels, lb-in

$\Omega\psi$ - Angular deflection of the steering system when elastic stops are encountered, radians

$K\psi$ - Load-deflection rate of elastic stops in steering system, effective at wheels, lb-in/radian

$\varepsilon\psi$ - Friction lag in steering system, rad./sec.

Of the five steering parameters listed, the $C'\psi$ term is the most significant in the sense that it represents the steering system's resistance to change in wheel direction. The ultimate magnitude of this resistance is obtained with the locked steering condition, the resistance for this condition being infinite. The remaining steering parameters represent the mass moment of inertia of the steering system, properties of the elastic stops at the end of wheel travel, and the friction lag in the total steering system. While these terms may collectively influence the maximum steering

angle experienced during impact, the primary factors is the coulomb resistance, the C'_ψ, parameter. An increase in this steering resistance term corresponds to a reduction in the steering angle as the wheel impacts the berm.

The corresponding berm climb associated with the various resistance terms listed in Table 22 must be interpreted in terms of what is occurring as the vehicle impacts the berm. The function of a rigid berm or barrier is redirection of the vehicle. This is attainable by either a smooth or an abrupt transition, and is dependent upon the barrier configuration. The side forces generated by the barrier and causing redirection can be minimal or substantial. Highway barriers, banked curves, etc., are designed to minimize the redirection forces, hence, the vehicle follows a smooth trajectory throughout the redirection period. In contrast, altering the configuration of a berm or barrier will produce a corresponding increase in the redirection forces, resulting in an abrupt redirection with a minimum amount of berm climb. These situations are illustrated in Cases 22, 23, and 24 of Table 22.

The steering system with the least resistance to change is encountering lower side forces or less redirectional force and experiencing a smoother transition, allowing the vehicle to travel further up the berm. The stiffer steering, Case 24 compared to Case 23, has a higher redirectional force and experiences a more abrupt change with less berm climb. Case 23 exhibits an increased berm climb due to a difference in elastic stops assumed in the steering system (K_ψ).

Ideally, a haul road berm or barrier would have a configuration which allows the wheel to assume a specific trajectory as does the design of highway barriers to provide a smooth transition back onto the main roadway. Unfortunately, mine haulage road berms are not readily suited to specific shapes nor is there adequate space available to generate a smooth redirection. However, the impact velocity experienced by a mine haul truck, probably 20 mph, is considerably less than the 60 mph impacts which occur on highways. Therefore, the smooth redirectional requirement for either a guardrail system or berm configuration is reduced.

3.1.4 Correlation Analysis

The correlation which exists between the field tests, model tests, and computer simulations is determined by the direct comparison of the results of each test in respect to the vehicle size, approach conditions, and berm construction. By comparing the data obtained during each of the tests and normalizing the data to the geometrically defined height of the axle, the amount of correlation can be demonstrated. This correlation provides the basis for the prediction of larger haulage vehicle-berm interactions.

3.1.4.1 Model Test Correlation

- Model test results presented earlier showed the response of the various vehicles to different approach conditions and berm compactions. To be meaningful, the comparison of these results must be done for berms of equivalent bearing strength.

Tests were performed during the model test program on rigid berms (Table 14). During the field test program, tests were performed on a compacted berm, Test 2C, which was considered relatively rigid. The comparison of these test results is presented in Figure 18. By reviewing the comparison of these tests, results appear to be within reasonable agreement.

The modeled berm strength determined to be acceptable for all vehicles according to Table 15 had an equivalent full scale berm strength of 1080 psi for a flat circular plate penetration of five inches. The field test cases performed whose berm strength approximates the model test results are Test 1C and Test 2B. Illustration of this comparison can be found in Figure 19.

Figure 19(a) illustrates the comparison of the model test results with those obtained in Test 1C of the field test program. Test 2B of the field test program is compared to this same model test results, Figure 19(b). When comparing the tire sinkage values for these tests, the berm in Test 1C has higher sinkage values at 90°, but slightly lower sinkage values at 45°. This indicates relative equivalency in total berm strength. Field test results show that the wheel climp values for Test 1B is somewhat greater than for Test 2B.

As is indicated in Figure 19, the positive offset exhibited in Test 1C and the negative offset exhibited for Test 2B average to be representative of the model test results. This indicates that the tire sinkage values obtained during the field tests are representative of the berm strength and can be used for quantifying the berm size requirements. The tire sinkage values are, however, somewhat subject to the surface condition of the berm.

Care must be taken to assure that the surface effects are negligible when compared to the overall test results. This may be accomplished by maintaining a full load in the vehicle during the tire sinkage tests and by removing the surface layer of the berm causing erroneous strength values to be indicated.

Since the offset illustrated in Test 1C is positive, indicating decreased tire sinkage, the berm size requirements can be expected to be the same as the model test. Test 2B, however, has a negative offset which indicates that tire sinkage will be more of a factor in restraining the vehicle. The berm size must be suitably increased for the experienced field berm strength level.

3.1.4.2 Computer Simulation Correlation - During the performance of this project, computer simulations were used to portray the interaction between haulage vehicles and berms during impacts. The accuracy of the simulations was found to be a direct result of the amount of detail to which the vehicle system is modeled and the quantity and quality of information which describes the system.

The computer simulations of vehicles interacting with edge-of-the-road berms were performed using the HVOSM three-dimensional computer program. Vehicles ranging in size from 35 to 170 tons were simulated impacting a sloping, rigid plane at various approach conditions.

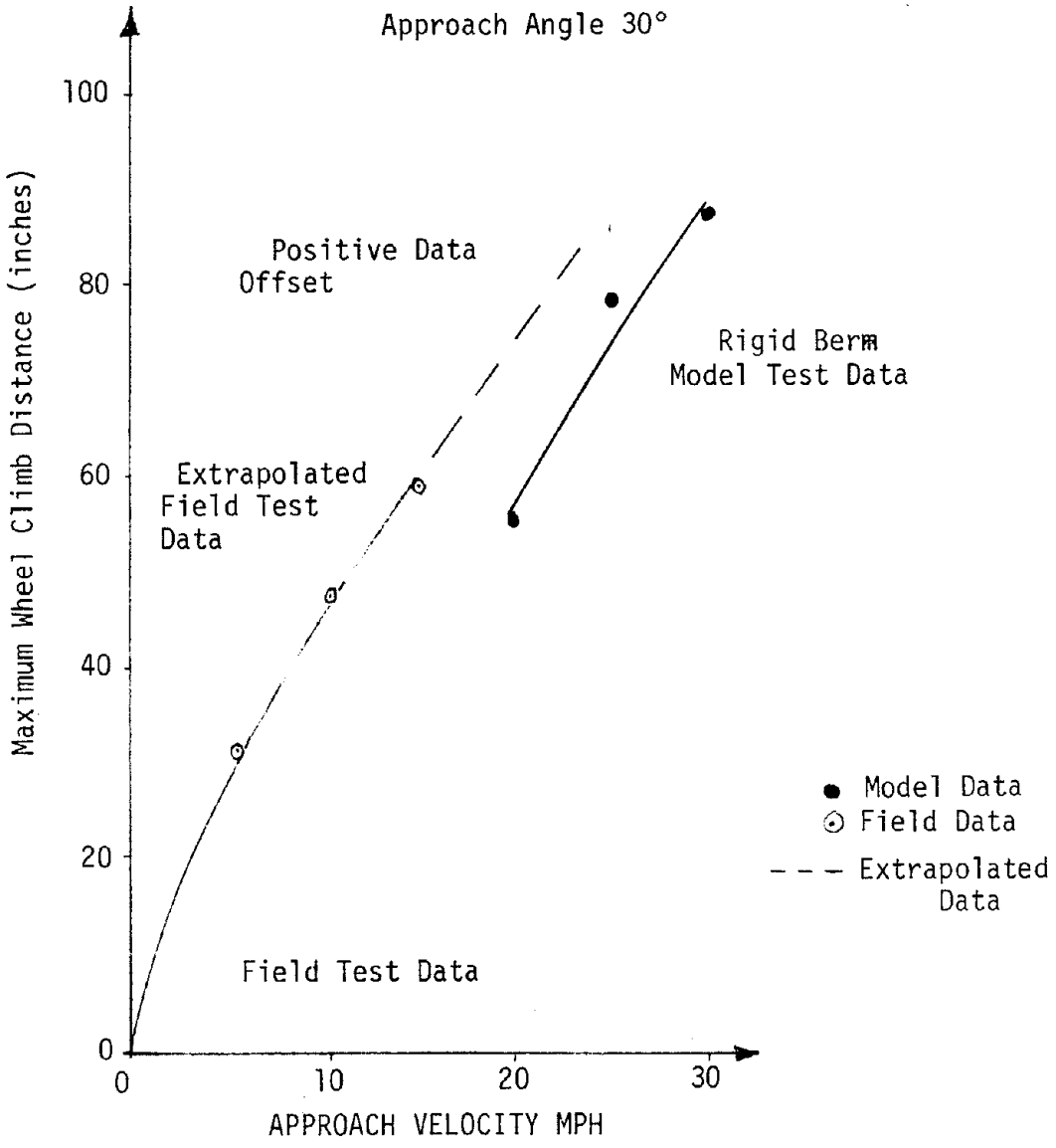

FIGURE 18. RIGID BERM MODEL TEST COMPARED TO FIELD TEST 2C

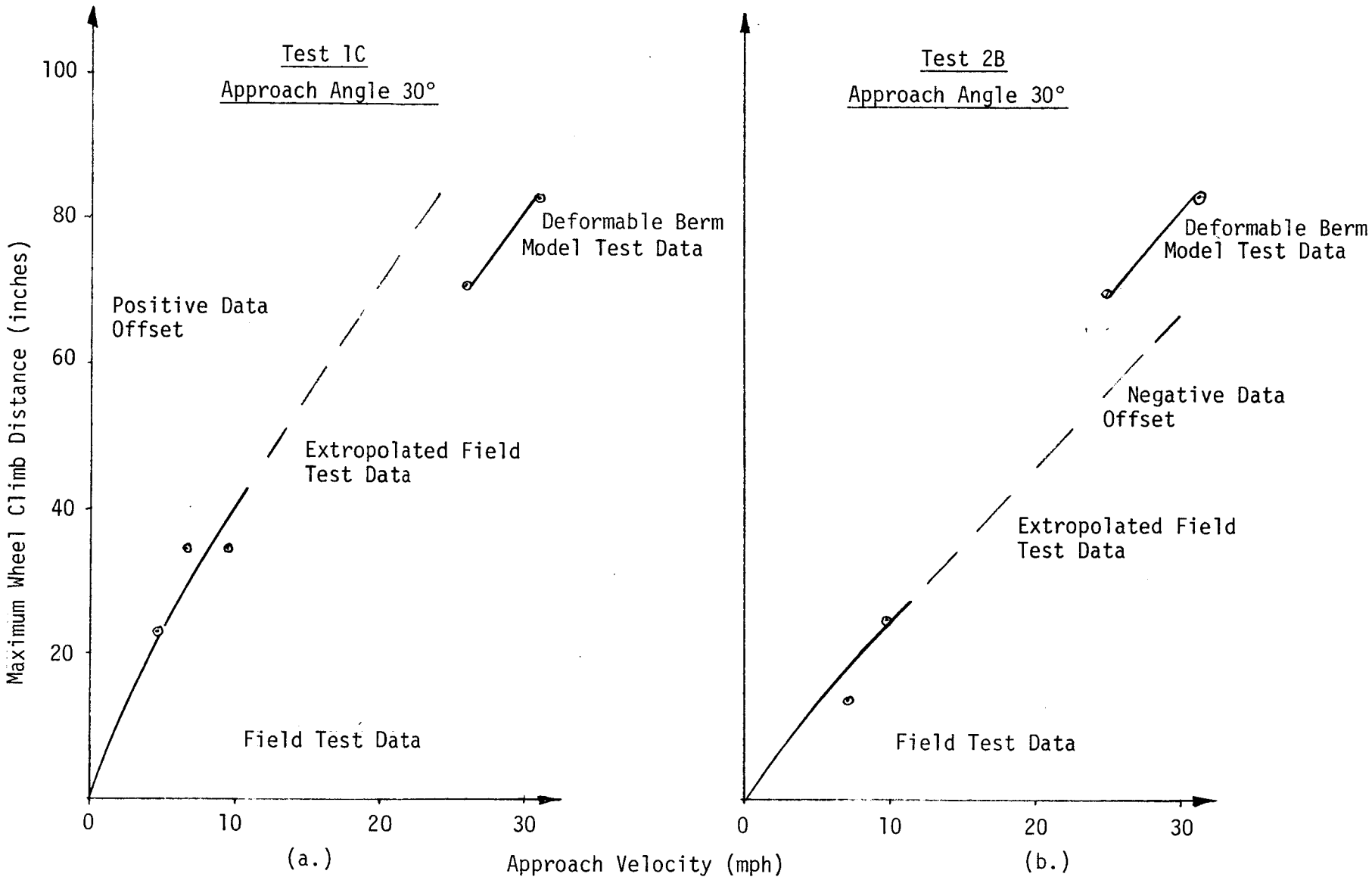

FIGURE 19. MODEL TEST-FIELD TEST COMPARISON

Computer simulations have been performed to improve the correlation with the field tests by increasing the cornering coefficients and more accurately modeling the tire deflection characteristics. These simulations depict the interaction between a 35-ton haul truck and a rigid berm constructed to a height of three times the axle height with a slope of 45°. The vehicle input parameters for these simulations were given in Table 10.

Changes to the vehicle input data which were made included changes in the vehicle suspension load-deflection rates which were originally modeled low as compared to actual load-deflection data obtained. In addition, suspension roll stiffness values originally used were input as multiples of automobile data. Most haulage vehicle size categories do not contain additional roll stiffness components such as anti-sway bars. As a result, these auxiliary suspension roll stiffness values were omitted from further simulations.

These observations regarding these vehicle parameter data indicates the requirement for accurate information for use with computer simulations. The determination of these parameters and a discussion of the implications of this study on the development of haulage vehicles are included in the recommendations.

The results of the computer simulation and pertinent model tests, and field tests are presented in Table 23. This data is presented in graphical form in Figure 20.

The graphical illustration best portrays the correlation obtained between the computer simulation and the field test results. Field test results for small approach velocities are greater than predicted by the computer simulations. This is attributed to the amount of redirection which was exhibited in the computer simulations for small approach velocities. At greater approach velocities the computer simulations predicted greater approach velocities and greater wheel climb values than were exhibited during the field tests. This was the expected result because the computer simulations did not include the transformation of kinetic energy into drag energy dissipation due to tire sinkage.

Predictions of the rollover condition as represented by the wheel climb values are consistently less than the experienced values obtained during the scale model test program. This is attributed to differences in the absolute berm strength levels for the different tests.

Wheel climb values of approximately 75 inches were consistently obtained at the rollover condition. Recommendations for the berm height to be three times the axle height (90 inches for this vehicle) is sufficient to restrain the vehicle from leaving an elevated roadway at the maximum approach conditions of 30 mph and 30°.

Table 23. Computer Simulation, Model Test, and Field Test 2C Data Comparison for 35-ton Vehicle

Speed (mph)	Approach Angle (deg)	WHEEL CLIMB VALUES (inches) HVOSM	Scale Model	Field Test
5	10	7	-	19.5
7.5	10	13	-	20.75
10	10	16	-	30.25
12.5	10	-	-	27.25
15	10	-	-	42.5
20	10	34	-	-
25	10	-	-	-
30	10	71†	-	-
5	20	17	-	27
7.5	20	32	-	35.75
10	20	48	-	43.5
20	20	71†	-	-
25	20	-	72*	-
30	20	72†	84*	-
5	30	25	-	35.5
7.5	30	47	-	45
10	30	60	-	56.5ǂ
20	30	73†	54	-
25	30	-	84*	-
30	30	75†	96*	-

† Program terminated; vehicle roll orientation was 28° (reverse) with an increasing roll velocity; reverse rollover begun.

* Reverse rollover occurred.

ǂ Reverse rollover potential experienced.

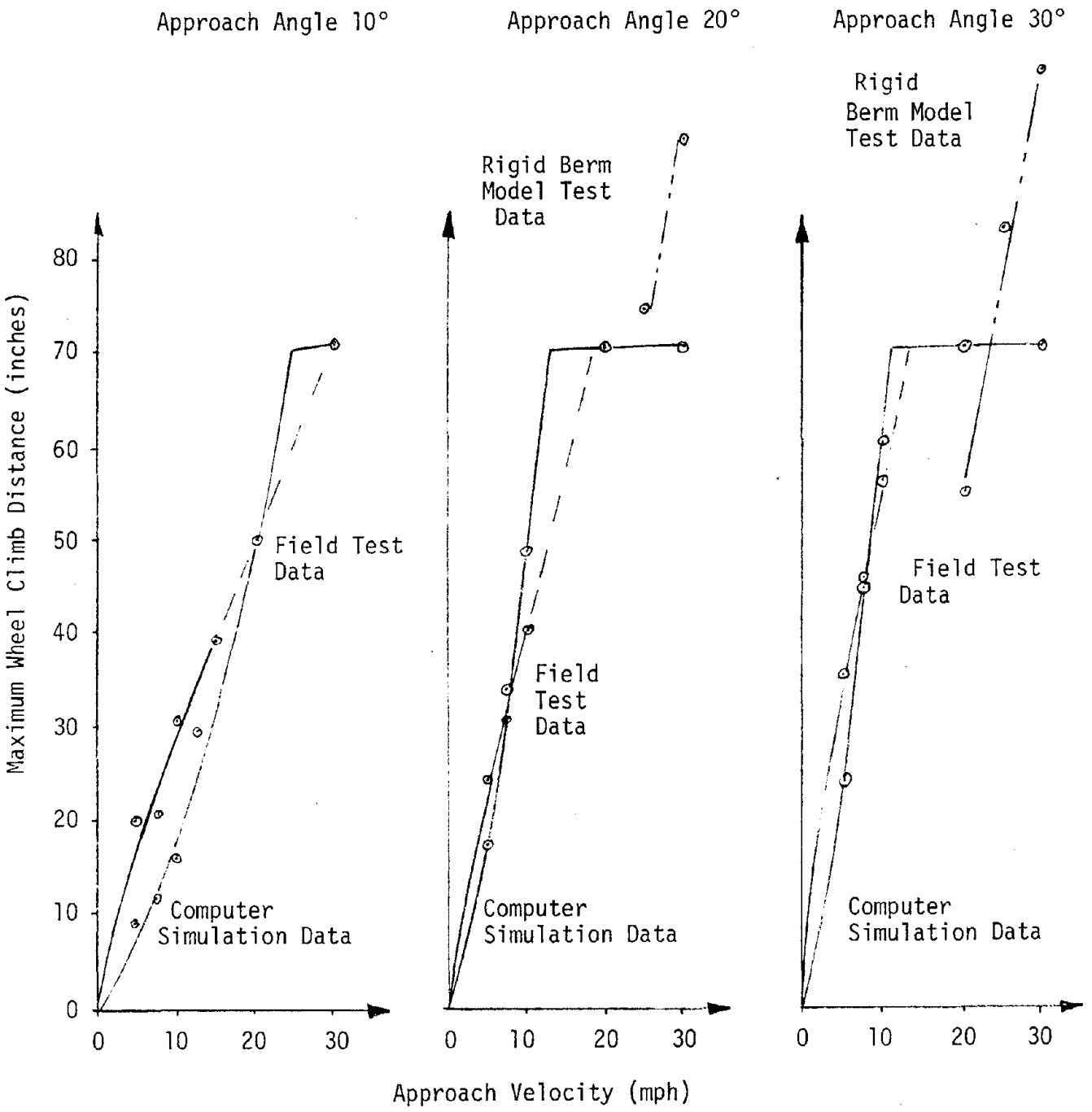

FIGURE 20. COMPUTER SIMULATION, MODEL TEST, AND FIELD TEST 2C DATA COMPARISON FOR 35-TON VEHICLE

——————— Computer
. . . . . Field Test
— — — — Model Test Data (rigid berm)

The demonstrated correlation for the 35-ton haul truck interactions provides the basis for the predictions of larger vehicle-berm interactions. Vehicle input parameters, while not directly obtained, have been estimated to present a conservative view of the resulting berm construction requirements.

3.1.5 Simulation Predictions

HVOSM computer simulations predicted the interactions for larger haul trucks, specifically 85- and 170-ton haulage vehicles. These vehicle size catagories complete the general range of haulage vehicles used presently in the mining industry.

Tables 11 and 12 presented the HVOSM input data for these simulations. Significant parameter values of particular significance include tire coefficient parameters and auxiliary roll stiffness parameters. Tire coefficient values were modeled as a multiple of 15 of the sedan vehicle tire data for the 85-ton haulage vehicles and a multiple of 20 for the 170-ton haulage vehicles. Auxiliary roll stiffness values of zero were used as input to reflect the lack of these devices on haulage vehicles.

Results of these simulations are presented for the 85-ton haulage vehicle in Table 24 and for the 170-ton haulage vehicle in Table 25. These computer simulations indicated that redirection occurred in both vehicles for the approach angles of 10 and 20°. For the 30° approach condition, redirection was not a factor. The vehicles climbed the berms until the rollover condition was reached. Maximum resultant tire loads for these interactions as predicted by HVOSM simulation are presented in Table 26.

Maximum wheel climb values are presented for each approach condition. The 85-ton haulage vehicle obtained a maximum wheel climb value of 78 inches. This is below the berm height recommendation of three times the axle height and provides a conservative construction guideline. The 170-ton haulage vehicle obtained a maximum wheel climb value of 149 inches. This is equivalent to 2.6 times the axle height and requires a recommendation of four times the axle height to maintain a conservative factor of safety.

This simulation data is presented in graphical form in Figure 21 for the 85-ton haulage vehicle and in Figure 22 for the 170-ton haulage vehicle. The limited redirection aspect is viewed by the change in slope of the curves as the approach velocity increases. Although more apparent for the 85-ton haulage vehicle, this is also true of the 170-ton haulage vehicle.

The basic design of 85- and 170-ton haulage units differ from the 35-ton haulage vehicle. Proportionately, neither the vertical height location is higher, nor are the tires larger for these heavier vehicles. This provides a much improved dynamic stability which accounts for the redirection of the larger vehicles.

TABLE 24
HVOSM PREDICTIONS OF 85-TON HAULAGE VEHICLE - BERM INTERACTIONS

Test No.	Vehicle	Berm Configuration			Approach Conditions		Max. Wheel Climb*	Vehicle Response	Berm Design	Berm Height / Axle Height
		Height	Width	Slope	Velocity	Angle				
	(Loaded)	(in.)	(in.)		(mph)	(Deg.)	(in.)			
1	85-ton	150	300	1:1	10	10	14	Climbed Berm	Safe	3.0
2	"	"	"	"	15	10	17	"	"	"
3	"	"	"	"	20	10	19	Redirection	"	"
4	"	"	"	"	25	10	20	"	"	"
5	"	"	"	"	30	10	28	"	"	"
6	85-ton	150	300	1:1	10	20	25	Climbed Berm	Safe	3.0
7	"	"	"	"	15	20	36	"	"	"
8	"	"	"	"	20	20	37	Redirection	"	"
9	"	"	"	"	25	20	46	"	"	"
10	"	"	"	"	30	20	48	"	"	"
11	85-ton	150	300	1:1	10	30	34	Climbed Berm	Safe	3.0
12	"	"	"	"	15	30	60	"	"	"
13	"	"	"	"	20	30	70	"	"	"
14	"	"	"	"	25	30	78+	Reverse Rollover	"	"

*Climb of Front Wheel Measured Above Road Surface.
+ Reverse Rollover Condition Exists as Roll Angle Attains Static Roll Equilibrium with Increased Roll Velocity.

TABLE 25
HVOSM PREDICTION OF 170-TON HAULAGE VEHICLE - BERM INTERACTIONS

Test No.	Vehicle	Berm Configuration			Approach Conditions		Max. Wheel Climb*	Vehicle Response	Berm Design	Berm Height AXLE HEIGHT
	(Loaded)	Height (in.)	Width (in.)	Scope	Velocity (mph)	Angle (Deg.)	(in.)			
1	170-ton	173	346	1:1	10	10	14	Climbed Berm	Safe	3.0
2	"	"	"	"	15	"	21	"	"	"
3	"	"	"	"	20	"	27	"	"	"
4	"	"	"	"	25	"	32	Redirection	"	"
5	"	"	"	"	30	"	38	"	"	"
6	170-ton	173	346	1:1	10	20	32	Climbed Berm	Safe	3.0
7	"	"	"	"	15	"	43	"	"	"
8	"	"	"	"	20	"	52	"	"	"
9	"	"	"	"	25	"	60	Redirection	"	"
10	"	"	"	"	30	"	70	"	"	"
11	170-ton	173	346	1:1	10	30	48	Climbed Berm	Safe	3.0
12	"	"	"	"	15	"	64	"	"	"
13	'	"	"	"	20	"	84	"	"	"
14	"	"	"	"	25	"	105	"	"	"
15	"	"	"	"	30	"	149 +	Reverse Rollover	"	"

*Climb of Front Wheel Measured Above Road Surface.
+ Reverse Rollover Condition Exists as Roll Angle Attains Static Roll Equilibrium with Increased Roll Velocity.

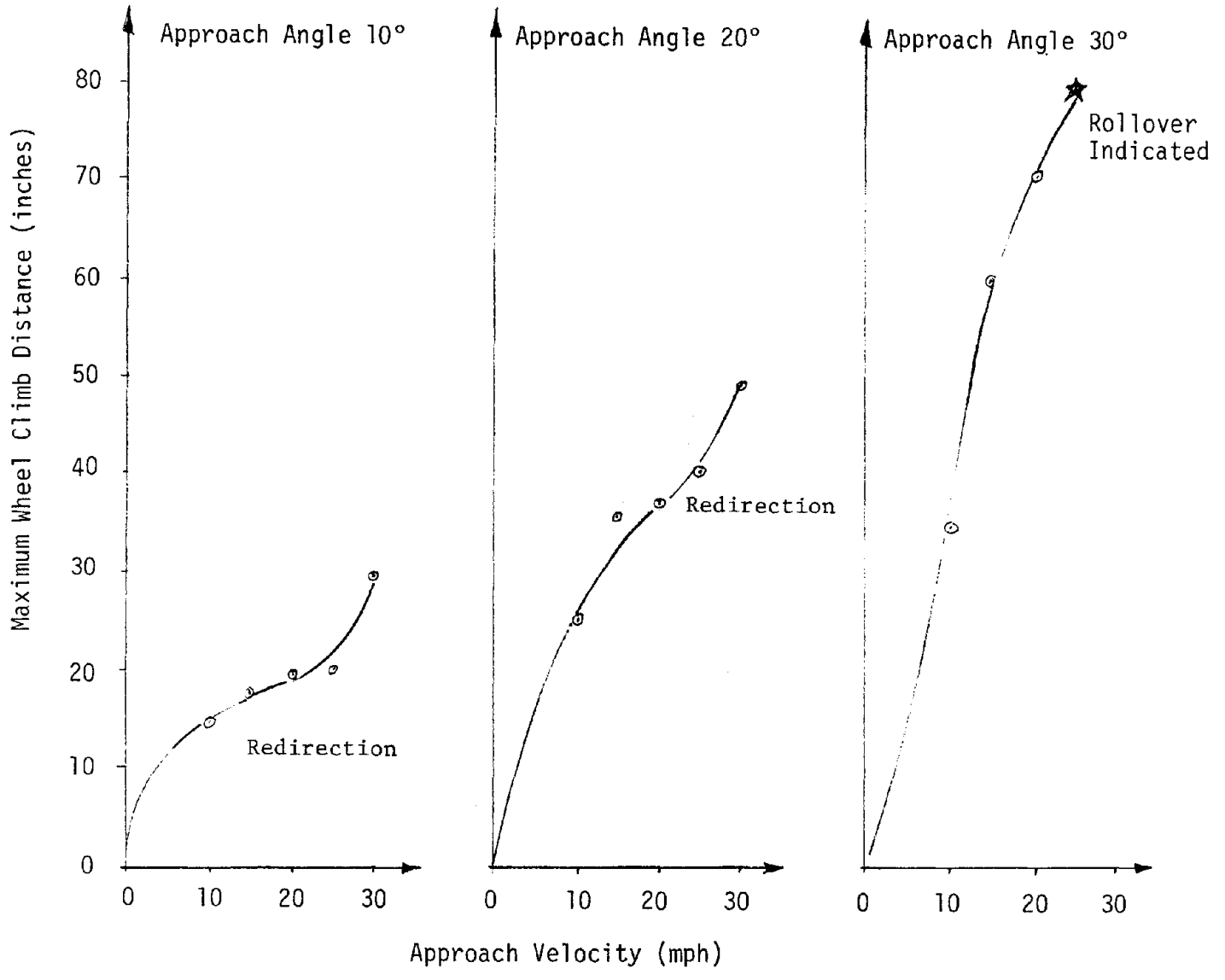

FIGURE 21. PREDICTED RESPONSE OF 85-TON HAULAGE VEHICLE

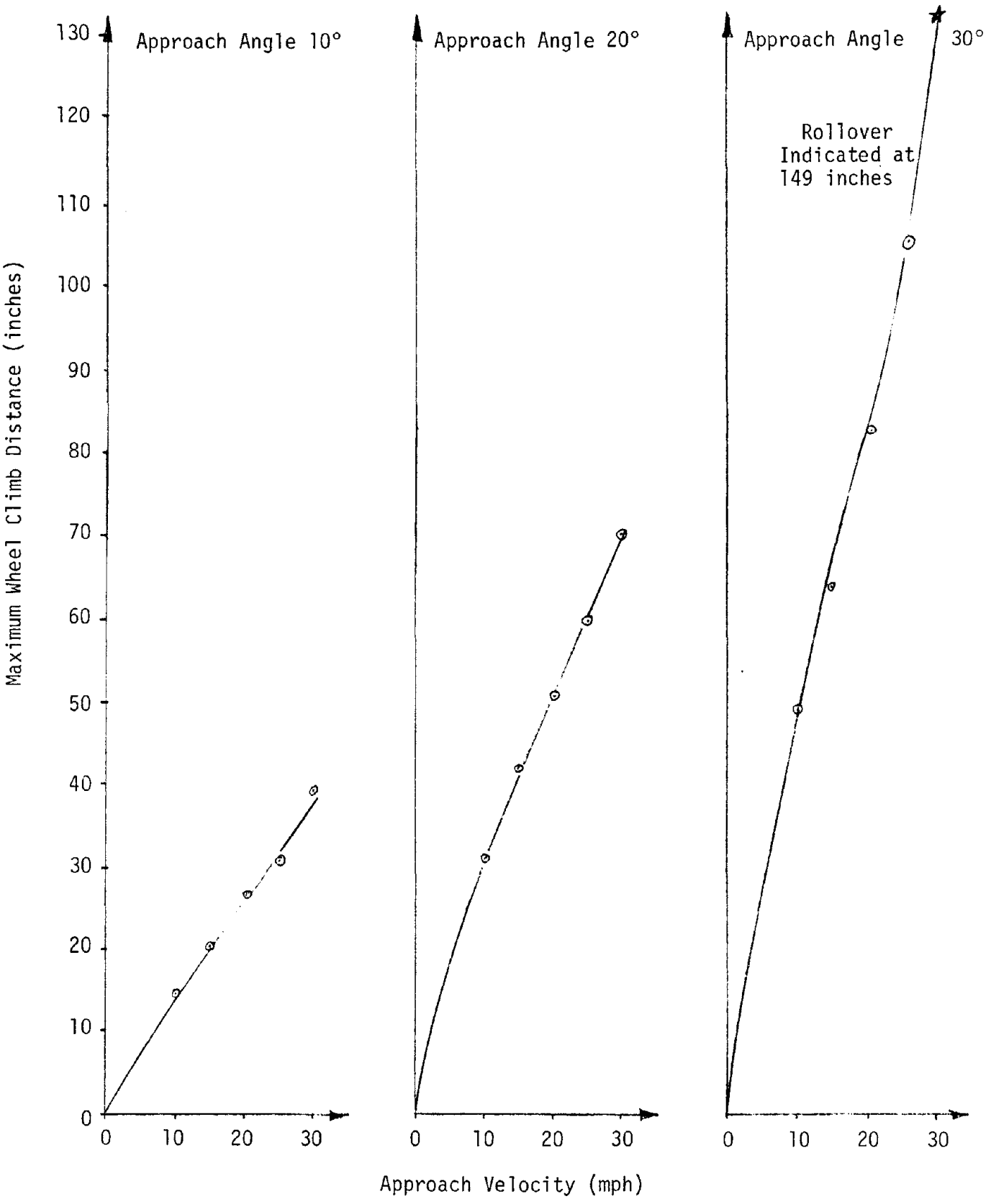

FIGURE 22. PREDICTED RESPONSE OF 170-TON HAULAGE VEHICLE

Table 26. Maximum Resultant Tire Load Prediction by HVOSM Computer Simulation

		Haul Truck Size		
Approach Angle 10°		35-Ton	85-Ton	170-ton
Approach Speed	10 mph	95,000 lb	134,000 lb	324,000 lb
	20 mph	196,000 lb	320,000 lb	369,900 lb
	30 mph	116,000*lb	381,000 lb	563,000 lb
Approach Angle 20°				
Approach Speed	10 mph	103,000 lb	365,000 lb	447,000 lb
	20 mph	376,000 lb	472,000 lb	728,000 lb
	30 mph	506,000 lb	636,000 lb	945,000 lb
Approach Angle 30°				
Approach Speed	10 mph	310,000 lb	545,000 lb	557,000 lb
	20 mph	474,000 lb	704,000†lb	957,000 lb
	30 mph	651,000 lb	1,062,000†lb	1,282,000 lb

* Rapid Redirection Exhibited
† Rollover Potential Evident

As a result of these simulations, berm requirements can be categorized by the vehicle size. Vehicles larger than 85 tons are proportional in size to the 170-ton haulage category. For vehicles whose load carrying capacity is 85 tons or less, the berm height requirement is specified to be three times the axle height for haulage vehicles larger than 85 tons, the berm requirement is four times the axle height.

These simulations produced the resultant tire loads presented in Table 26. Berm bearing strength requirements can be evaluated according to these maximum resultant tire loads. To restrict tire sinkage to 5.0 inches, for example, a bearing strength at 5.0 inches of sinkage, of 1000 psi would be required for 35- and 85-ton trucks and 800 psi for 170-ton trucks.

3.1.6 Berm Requirements

Information obtained from the geometric model simulations, computer simulations and field tests can be combined to present the berm requirements, size as a function of strength, to restrain a runaway haulage vehicle. Berm size will be presented in terms of the height required, expressed as a multiple of axle height, and slope for a triangular cross-section. Strength requirements will be given in terms of the tire sinkage values associated with the berm qualification tests which were utilized.

The form of the relationship between size and strength is presented in Figure 23. Minimum berm size corresponds to maximum strength representative of a rigid berm. Restraint for this berm configuration is in terms of rollover, redirection, or berm climb as the berm strength decreases, there is a corresponding requirement for increased size. Restraint changes from redirection to penetration with rollover and berm climb still evident. As berm strength further decreases, rollover is not evident because penetration becomes predominant although berm climb is still evident.

The berm size requirements for the maximum practical berm strength, representative of a rigid berm, is presented in Figures 24, 25, and 26 for 35-ton, 85-ton, and 170-ton vehicles, respectively. These figures were prepared to restrain these haulage vehicles at the maximum approach conditions of 30 mph and 30°.

The relationship represented in Figure 24 for the 35-ton truck was obtained by fitting a curve to the data obtained from the scale model simulations, computer simulations, and full scale field test results. This included the tire sinkage data obtained in Test 2C of 3.0 inches at 45° and the corresponding berm height requirement of three times the axle height as obtained from the correlation depicted in Figure 20. Additionally, the tire sinkage value of 11.0 inches as obtained from the results of Test 1C of 11.0 inches at 45° is related to the geometric model test results depicted in Table 15 from which a conservative height requirement of four times the axle height is obtained.

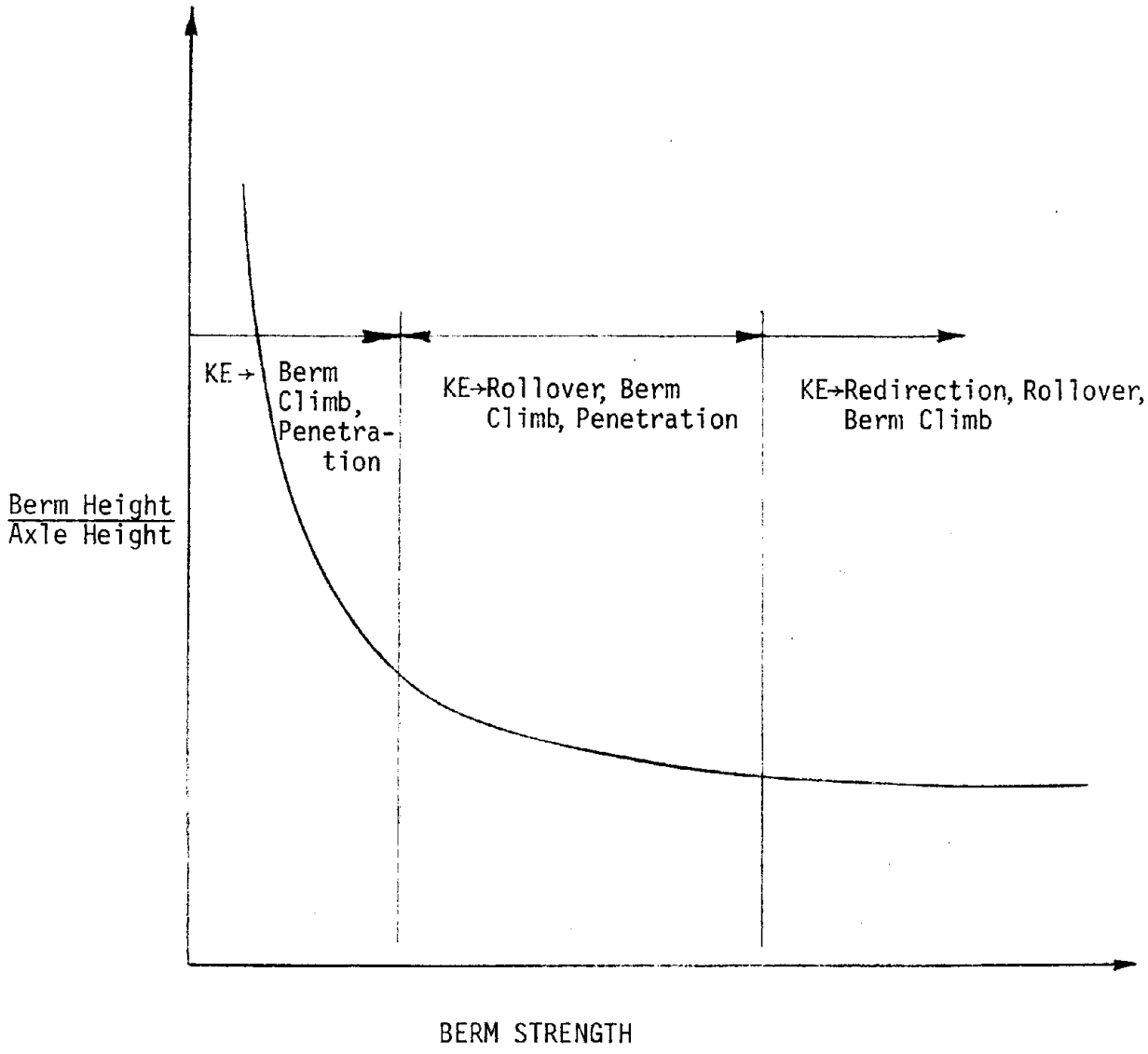

FIGURE 23. GENERAL BERM SIZE REQUIREMENT AS A FUNCTION OF BERM STRENGTH

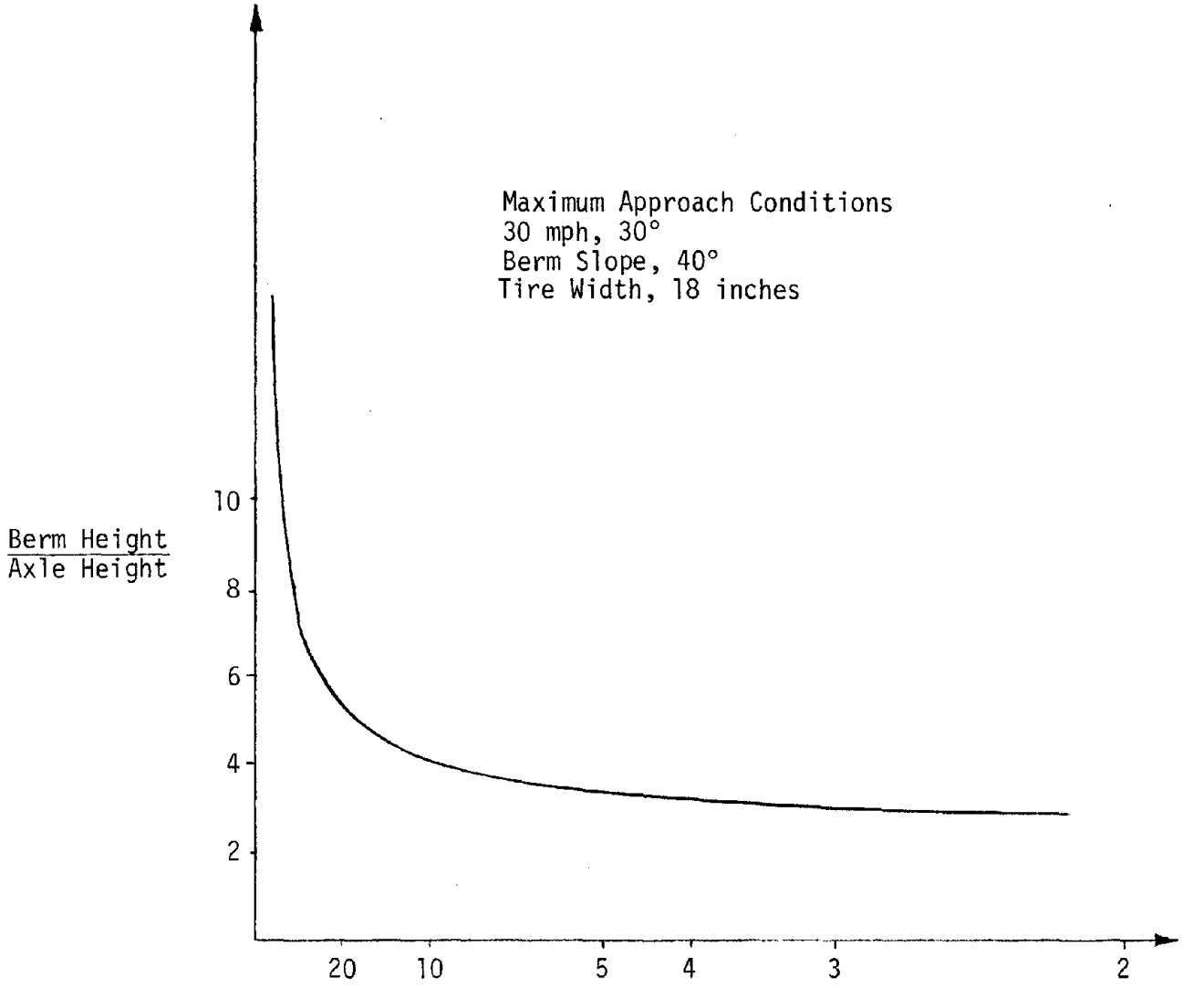

FIGURE 24. BERM SIZE REQUIREMENT AS A FUNCTION OF BERM STRENGTH FOR 35-TON HAULAGE VEHICLE

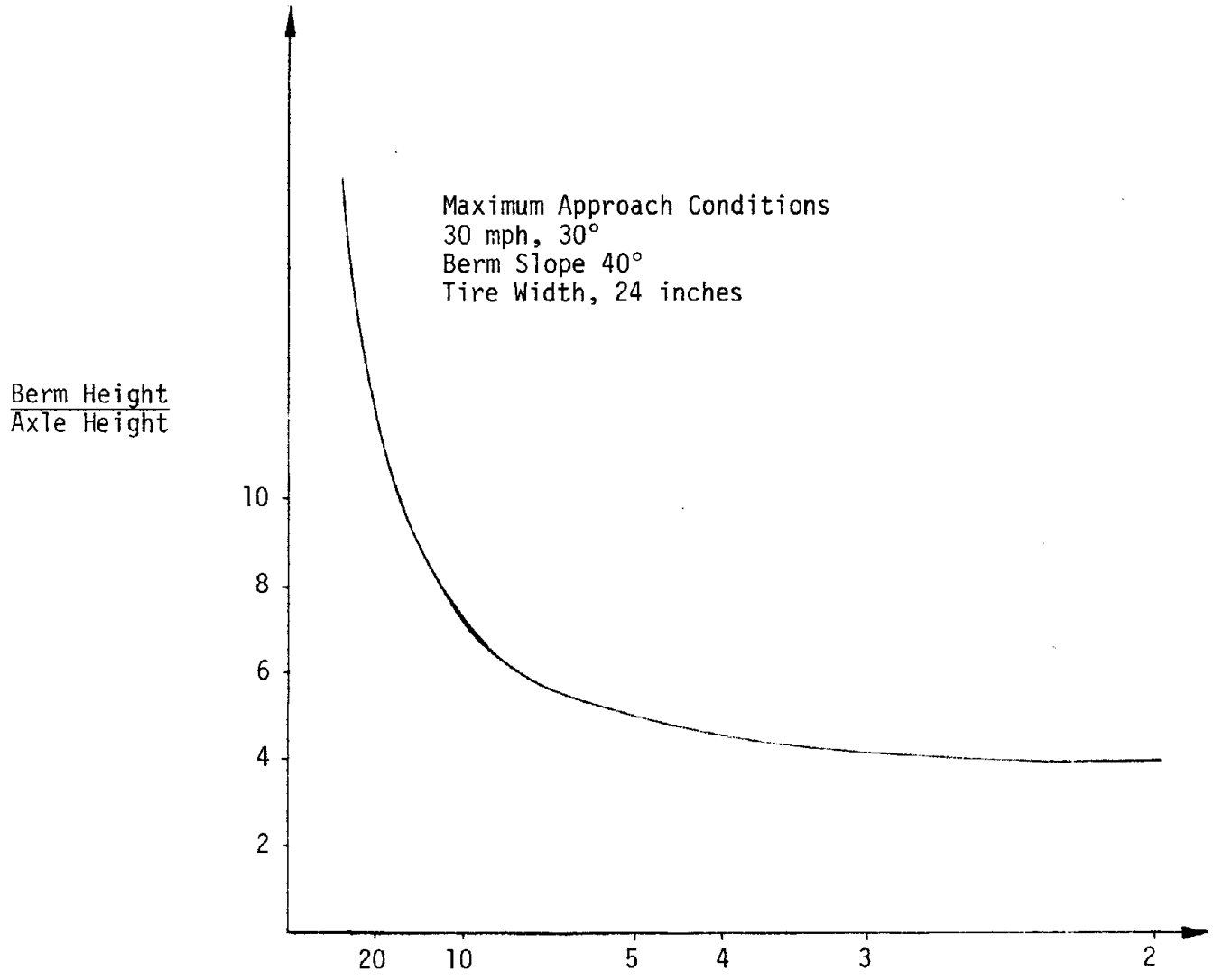

FIGURE 25. BERM STRENGTH AS A FUNCTION OF BERM STRENGTH FOR 85-TON HAULAGE VEHICLES

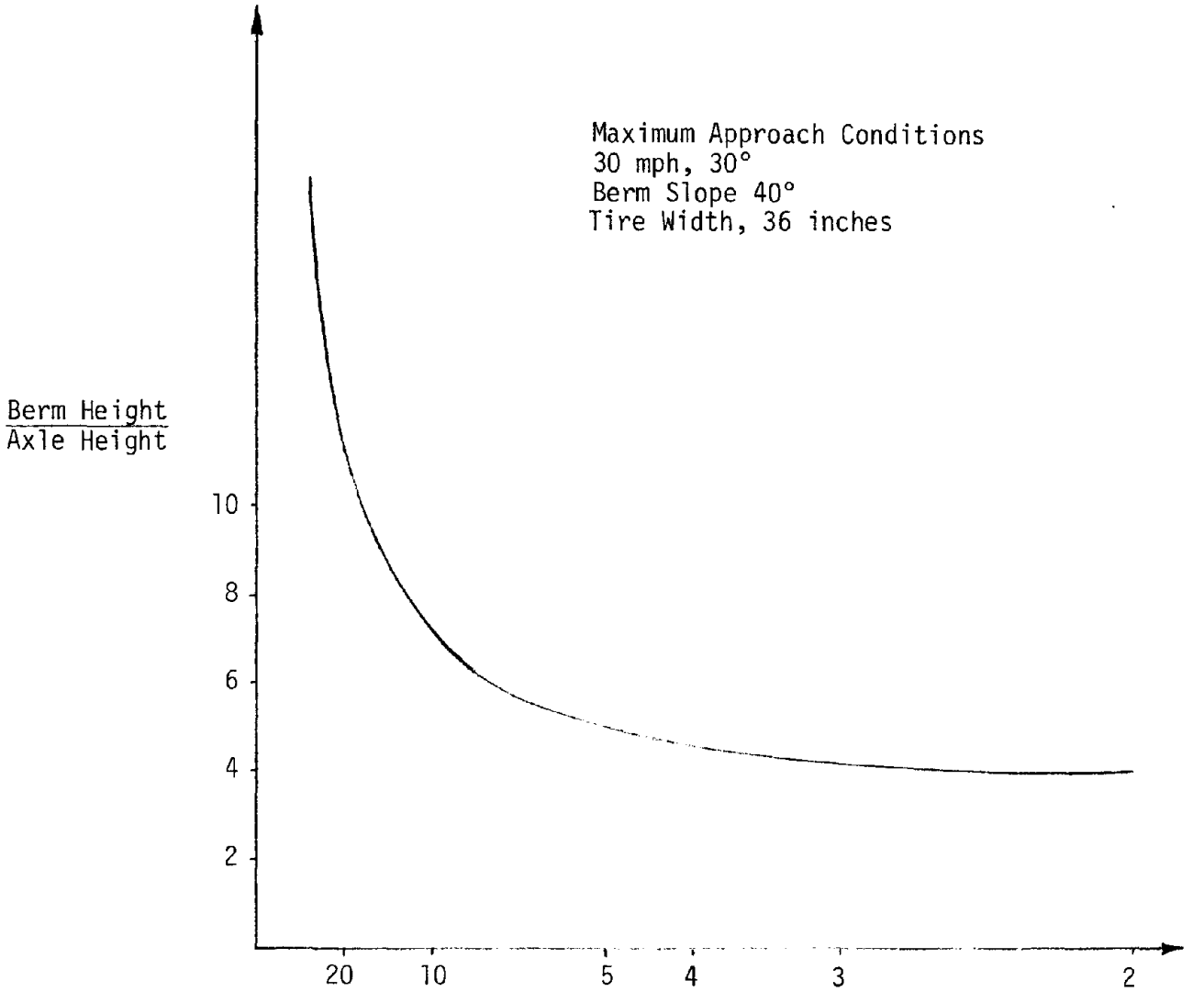

FIGURE 26. BERM SIZE REQUIREMENT AS A FUNCTION OF BERM STRENGTH FOR 170-TON HAULAGE VEHICLES

For the berm requirements of the 85-ton haulage vehicle presented in Figure 25 the relationship was obtained by fitting a curve to the data, presented in part, in the predictive simulation results. For a rigid berm according to Figure 21, rollover was predicted by computer simulations to occur at a wheel climb value of almost two times the axle height from which the conservative requirement of three times the axle height was obtained. The tire sinkage value of the qualification test was obtained by taking the ratio of the maximum tire loads for the 85-ton truck as compared to the 35-ton truck and multiplying it by the ratio of the tire widths of the 35-ton truck as compared to the 85-ton truck and multiplying by the experienced tire sinkage value of Test 2C (3.0 inches). The resultant sinkage value of 2.3 inches was obtained.

Additional data was obtained by determining the tire sinkage value which corresponded to the 11.0 inches of penetration obtained for the 35-ton truck. By applying the same tire load and tire width ratios to this value, a tire sinkage value of 8.44 inches was obtained. The corresponding berm height was obtained from the geometric model test results, conservatively estimating a berm height of six times the axle for penetration to be effective.

Developing the berm requirements for the 170-ton haul truck, the results of which are presented in Figure 26 was accomplished by fitting a curve to data obtained similar to that obtained for the 35-ton truck. For a rigid berm, rollover was predicted by computer simulation to occur at a wheel climb value of just under three times the axle height from which the conservative requirement of four times the axle height was obtained. The tire sinkage value of the qualification test was obtained by applying the load and tire width ratios to the sinkage value obtained for the 35-ton truck in Test 2C. The resulting sinkage value of 2.3 inches was obtained.

The additional data corresponding to the other vehicle sizes was determined similarly. By applying the same tire load and tire width ratios to the value of 11.0 inches, previously related, a tire sinkage value of 8.44 inches was obtained. A conservative estimate of the berm height of six times the axle height was obtained from the geometric scale model results.

The data presented in Figures 24 to 26 therefore represent conservative requirements to restrain these vehicles at the maximum approach conditions of 30 mph and 30°. Appying these design guidelines to berms will yield additionally conservative restraint capability if the approach conditions are reduced.

3.2 GUARDRAILS

The primary intent of a highway guardrail system is to restrain and redirect a vehicle within a specified region. For mining applications, the primary criteria is vehicle restraint; redirection, while desirable,

is of secondary importance. Ideally, restraint should occur in a stable manner as the vehicle interacts with the barrier. Utilization of a near vertical structure minimizes the possibility of the vehicle climbing the structure and potentially rolling over it. Typical highway barriers, specifically the concrete median barriers, are designed with an external configuration which controls vehicle climb during impact, and also provides a controlled redirection of the vehicle. While the general shape of any of the guardrail or concrete barrier designs considered in our computer analysis displays redirectional capability, the actual effectiveness of these shapes to perform a controlled redirection would require detailed investigation, preferably using full-scale testing.

Several guardrail configurations ranging from conventional wooden post and metal beam arrangements to reinforced concrete posts utilizing wide flange steel beam elements were evaluated for various impact conditions. The technical feasibility of each system in restraining 35- to 235-ton capacity haulage vehicles has been demonstrated through the use of the BARRIER VII computer program.

The acceptability and practicality of using a guardrail system can be evaluated by several criteria such as cost, reliability, expected operating life, required maintenance, etc. Each of these factors will vary depending on the type of mining operation and length of time the haul road will be in service.

It is generally conceded that berms constructed from available mine waste material will be less expensive than a guardrail installation. However, in some instances, a guardrail may fulfill a requirement not met by conventional berm design. A realistic example is a haulage road too narrow to construct an adequate sized berm. In this situation, the installation of a guardrail may be a more logical choice when compared to the cost of widening the roadway.

3.2.1 Collision Severity Index (CSI)

When considering a given guardrail system, it is necessary to examine its performance over a variety of vehicle sizes and impact conditions. An empirically-derived relationship is commonly used for guardrail evaluation which provides a numerical comparison of the demands placed on a barrier system under various impact conditions. This relationship is referred to as the Collision Severity Index (CSI) and is a function of the vehicle's mass, mass moment of inertia, impact speed, and approach angle.

The CSI for any set of impact parameters is calculated as follows:

$$CSI = 0.122\ M^{(0.24)}\ I_z^{(0.28)}\ V^{(1.04)}\ \sin_\theta{}^{(1.32)} \qquad (9)$$

where:

CSI = Collision Severity Index
M = Vehicle weight (lb)
V = Impact speed (mph)
θ = Approach angle (degrees)
I_z = Vehicle yaw mass moment of inertia (lb-ft-sec^2)

3.2.2 BARRIER VII Computer Simulation

The BARRIER VII computer program used to evaluate the guardrail designs predicts, along with the response characteristics of the vehicle, the deformation of the restraining structure and the damage generated by the impact of the haulage vehicle, i.e., number of posts damaged and length of rail damaged. Consequently, by defining an acceptable damage limit or a maximum guardrail deflection distance, the corresponding CSI value for an acceptable guardrail design is determined. Using this same CSI value, effects of an impact at different impact speeds, approach angles, or vehicle sizes, can be evaluated and the adequacy of the guardrail design estimated.

Consider the following representative vehicle parameters listed in Table 27.

Table 27

Haulage Vehicle Parameters for CSI

Vehicle Capacity	Loaded Weight tons	Vehicle Yaw Mass Moment of Inertia in-lb/sec^2	CSI (approx) 20 mph, 20°	CSI 20 mph, 15°
35-ton	68.5	1.5×10^5	700	200
85-ton	161.9	7.2×10^5	600	400
170-ton	270.5	14.3×10^5	800	600

If a particular guardrail design had been considered satisfactory for a CSI of 600, the structure would not function satisfactorily for a 170-ton vehicle impacting at 20 mph and a 20° approach angle. The same vehicle at a less severe approach angle of 20 mph and 15° would have a CSI of 600; the guardrail would therefore perform satisfactorily. Using this technique, the influence of different vehicle sizes and approach angles is readily evaluated.

Figures 27 to 31 illustrate the various guardrails and soil backed guardrail restraint systems analyzed during this project. The effectiveness of these systems to restrain various size haulage vehicles impacting at different approach angles is summarized in Table 28. Each configuration

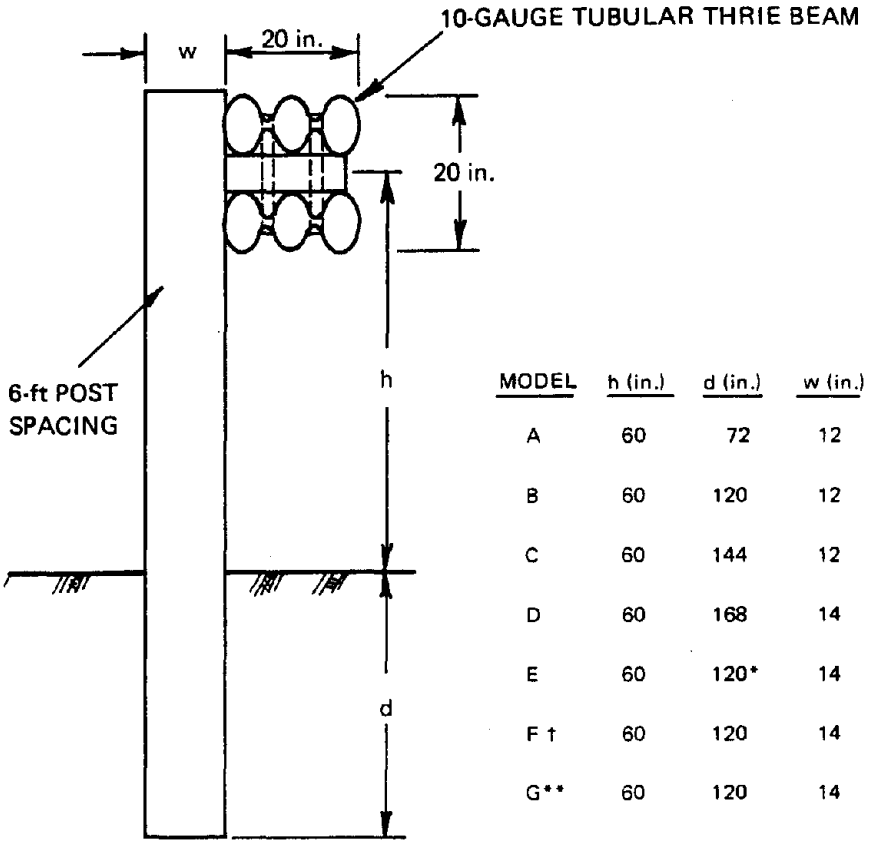

MODEL	h (in.)	d (in.)	w (in.)
A	60	72	12
B	60	120	12
C	60	144	12
D	60	168	14
E	60	120*	14
F †	60	120	14
G**	60	120	14

* WITH 10-ft x 28-in. SOIL PLATE.
† WITH SOIL BACKUP MASS OF 10 KIPS/ft ALONG BARRIER LONGITUDINAL AXIS.
** SAME AS MODEL F WITH 20 KIPS/ft SOIL BACKUP MASS.

FIGURE 27. DOUBLE TUBULAR THRIE/WOOD POST GUARDRAILS

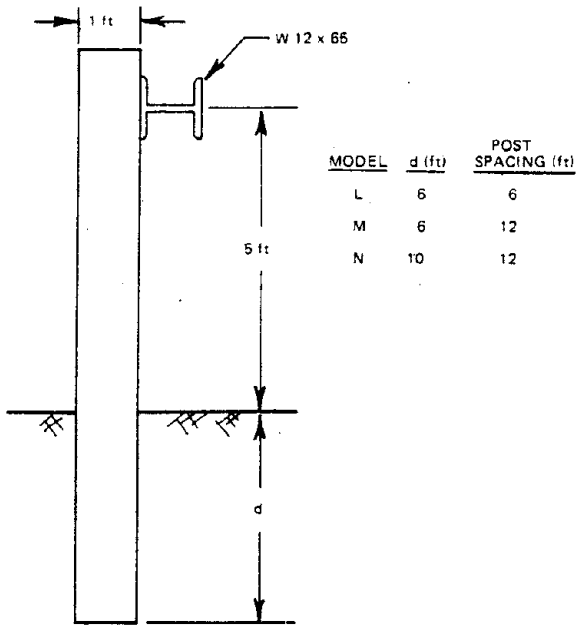

MODEL	d (ft)	POST SPACING (ft)
L	6	6
M	6	12
N	10	12

FIGURE 28. WIDE FLANGE/WOOD POST GUARDRAILS

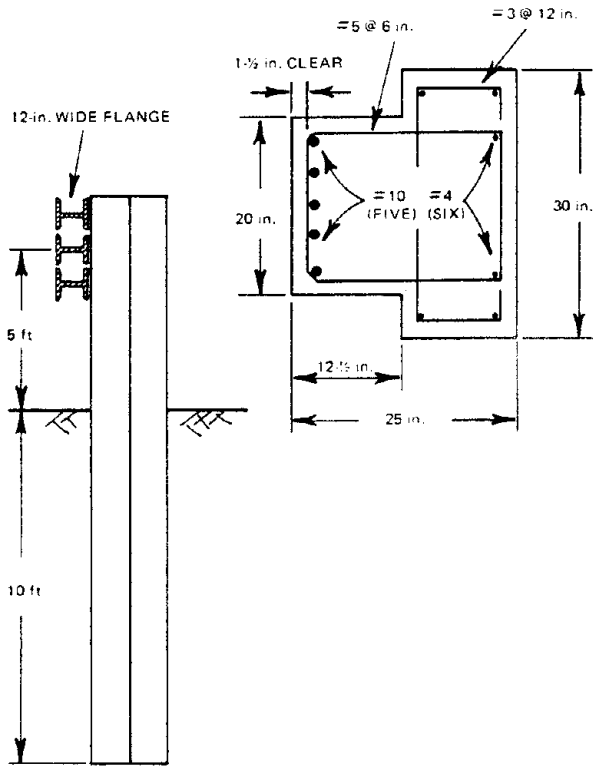

FIGURE 29. CONCRETE POST/WIDE FLANGE GUARDRAIL (MODEL K)

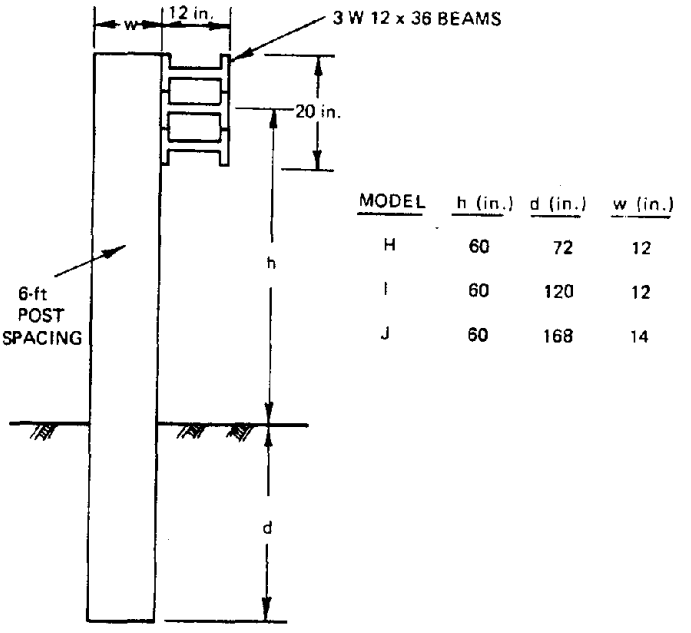

MODEL	h (in.)	d (in.)	w (in.)
H	60	72	12
I	60	120	12
J	60	168	14

FIGURE 30. SINGLE WIDE/FLANGE/WOOD POST GUARDRAILS

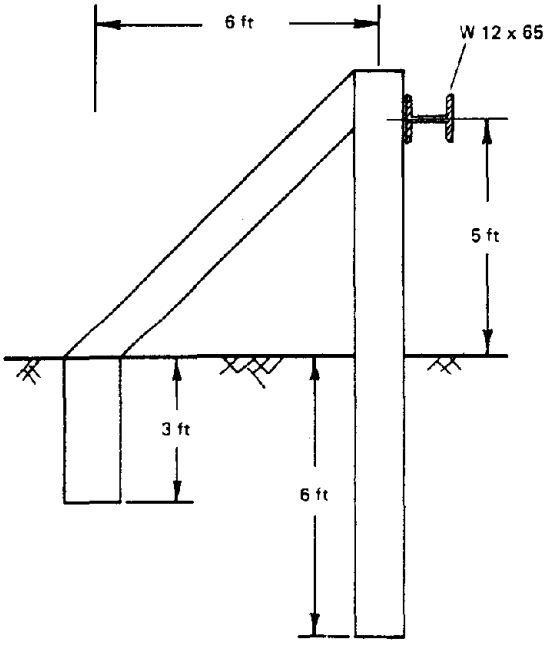

FIGURE 31. WIDE FLANGE/DUAL LEG CONCEPT (MODEL 0)

Table 28. Summary of Guardrail Design Concepts

GUARDRAIL CONFIG.	CSI	Rear Dump Mine Haulage Trucks (lb)		
		137,000 GVW 35-TON CAPACITY	323,800 GWV 85-TON CAPACITY	541,000 GVW 170-TON CAPACITY
A	100	10 mph at 14°	10 mph at 8°	10 mph at 7°
B,H	500	20 mph at 28°	20 mph at 17°	20 mph at 13°
C,I	1000	30 mph at 36°	30 mph at 21°	30 mph at 16°
D	2000	35 mph at 62°	35 mph at 33°	30 mph at 29°
E,F	3000		35 mph at 47°	35 mph at 35°
J,K	4000		35 mph at 65°	35 mph at 46°
	5000			35 mph at 58°

is related to a specific CSI range representing the estimated minimum system warranted to safely redirect the various size haulage vehicles for the specified approach angles. A guardrail system was considered safe if its maximum rail deflection did not exceed half the width of the vehicle track. The feasibility of utilizing any of the guardrail systems illustrated in an operational mining environment will be determined by the specific mine requirements and the effectiveness and economic factors associated with alternative restraint systems.

Each guardrail system was evaluated in terms of damage, maximum dynamic deflection (rail/post), vehicle exit angle (after redirection), and speed. As illustrated in Tables 29 and 30, the degree of damage to each system was dependent upon the severity of the impact (speed, approach angle, vehicle size) and the structural strength of each system.

For all 30 cases, the errant vehicle was redirected. Results were deemed satisfactory with the exception of Case No. 30. In the latter, the vehicle was being redirected, but the first 23 posts were destroyed, which could result in rollover. For the systems with shallow embedded posts, the barrier damage was more extensive than those with extreme post depth. Furthermore, as anticipated, the larger vehicle caused more extensive damage to the system. Systems H, I, J, K, and L performed better because of overall greater beam strength characteristics (M_{max} and F_{max}). Systems M and N with the large (12-foot) post spacing resulted in larger post-impact response than System L.

Figure 32 illustrates the vehicle trajectory for Case Number 24 of Table 30, the corresponding lateral acceleration force acting on the vehicle is illustrated in Figure 33.

3.3 ESCAPE LANE

Escape lanes present an extremely advantageous method for restraining a runaway haulage vehicle. They ideally perform their function without causing the vehicle to roll over. The application of median berms on escape lanes reduce the length requirement, but imposes additional requirements for uniformity of the median berm. The construction, requirements and limitations of escape lanes must be evaluated to assure their safe application in the mine situation.

3.3.1 Escape Lane Requirements

The requirements for escape lanes were investigated to verify the escape lane requirements present in USBM IC 8758, "Design of Surface Mine Haulage Roads - A Manual."(14) The requirements presented in that report are based on the rolling resistance factor of one specific type of material, essentially a soft, muddy roadway. While the analysis is correct, the selection of a high rolling resistance factor is questionable. Therefore,

TABLE 29
120-TON HAULAGE VEHICLE FLEXIBLE BARRIER INTERACTION

CASE NO.	BARRIER	IMPACT ANGLE (DEG)	IMPACT SPEED (MPH)	CSI	BARRIER DAMAGE FT OF RAIL	BARRIER DAMAGE NO. OF POSTS	MAX DYNAMIC DEFLECTION (FT)	EXIT ANGLE/REMARKS
1	A	7	20	27	21.7	0	0.74	-0.7° — contact loss at 19.4 mph
2	A	7	40	153	58.8[1]	10[1]	3.22[1]	At run termination 2.2° at 39.0 mph — secondary impact
3	B	7	40	153	29.5	2	1.40	5° at 37.8 mph secondary impact
4	B	10	40	442	46.8[1]	6[1]	3.48[1]	At run termination 7.6° at 37.4 mph — secondary impact
5	C	10	40	442	32.4[1]	4[1]	2.13	7.5° at 36.8 mph — secondary impact
6	C	15	35	1048	42.1[1]	6[1]	3.92[1]	At run termination 8.4° at 31.3 mph — secondary impact
7	D	15	35	1048	40.0[2]	3	2.78	At run termination 9.5° at 30 mph — secondary impact
8	D	15	40	1464	53.9[2]	6[2]	4.07	At run termination 12.4° at 34.1 mph — secondary impact
9	D	20	33	2088	49.7[2]	6[2]	5.4[2]	At run termination 14.7° at 26.4 mph — secondary impact
10	D	20	38	2972	66.5[2]	9[2]	7.1	At run termination 15.4° at 30.4 mph — secondary impact
11	E	20	38	2972	69.6[2]	9[2]	7.1	At termination 17.9° at 29.9 mph — secondary impact
12	F	20	38	2972	29.9	5	5.5	-2.2°; contact loss at 31.3 mph
13	F	20	38	2972	23.9	3	3.9	0.5°, contact loss at 32.8 mph
14	G	20	45	4535	21.8	3	5.5	At termination 1.5° at 37.8 mph — contact loss at -14.3°
15	G	25	40	6374	71.3[3]	11[3]	9.1[3]	At termination 5.4° at 25.6 mph — contact loss at -14.0°

NOTES. Structural properties corresponding to BARRIER MODELS (i.e., A, B, etc.) are given in Table 12.

[1] At program termination — 1 s real time.
[2] At program termination — 1.2 s real time.
[3] At program termination; further damage possible due to dynamic effect.

TABLE 30
235-TON HAULAGE VEHICLE FLEXIBLE BARRIER INTERACTION

CASE NO.	BARRIER	IMPACT ANGLE (DEG)	IMPACT SPEED (MPH)	CSI	BARRIER DAMAGE FT OF RAIL	BARRIER DAMAGE NO. OF POSTS	MAX DYNAMIC DEFLECTION (FT)	EXIT ANGLE/REMARKS
16	D	7	40	482	38.0	0	1.4	At run termination (1.2 s) 2.9° at 37.5 mph—secondary impact [3]
17	D	10	40	1394	56.0[1]	5[1]	3.0[1]	At run termination (1.2 s) 6.7° at 36.6 mph—secondary impact
18	D	15	40	4615	87.8[1]	12[1]	6.3[1]	At run termination (1.2 s) 3.4° at 35.5 mph—secondary impact
19	H	7	40	482	140.8[1]	17[1]	3.7[1]	At run termination 2.4° at 38.9 mph—secondary impact
20	I	7	40	482	33.6	0	1.3	At run termination 2.5° at 37.6 mph—secondary budget
21	I	10	40	1394	62.1[1]	11[1]	5.0[1]	At run termination 7° at 37.4 mph—secondary impact
22	J	10	40	1394	32.6	0	1.5	3.3° at 36.3 mph—secondary impact
23	J	15	40	4615	57.6[1]	8[1]	5.5[1]	At run termination 8.9° at 34.7 mph—secondary impact
24	K	15	40	4615	54.2	7	5.4	At run termination 9.5° at 34.5 mph—secondary impact
					(120-TON VEHICLE)			
25	L	10	40	442	119.0[1]	19[1]	6.5[1]	At run termination 6.7° at 38.2 mph—secondary impact
26	M	10	40	442	109.5[1]	12[1]	6.1[1]	At run termination 2.6° at 38.8 mph—secondary impact
27	M	15	40	1462	132.0[1]	19[1]	11.7[1]	At run termination -3.9° at 38.7 mph— at t= 1.2 s, no secondary impact
28	N	15	40	1462	66.4[1]	8[1]	8.8[1]	At run termination 9.5° at 36.4 mph—secondary impact
29	N	20	38	2972	184.0[2]	17[2]	13.0[2]	At run termination 10.7° at 32.4 mph—secondary impact
30	O	20	38	2972	181.7[2]	23	14.7[2]	5.7° at 34.1 mph—secondary impact failed first 23 posts

[1]At computer run termination; 1.2s real time
[2]At run termination; 1.5s real time
[3]Secondary impact occurred as vehicle reinteracts with guardrail after initial deflection

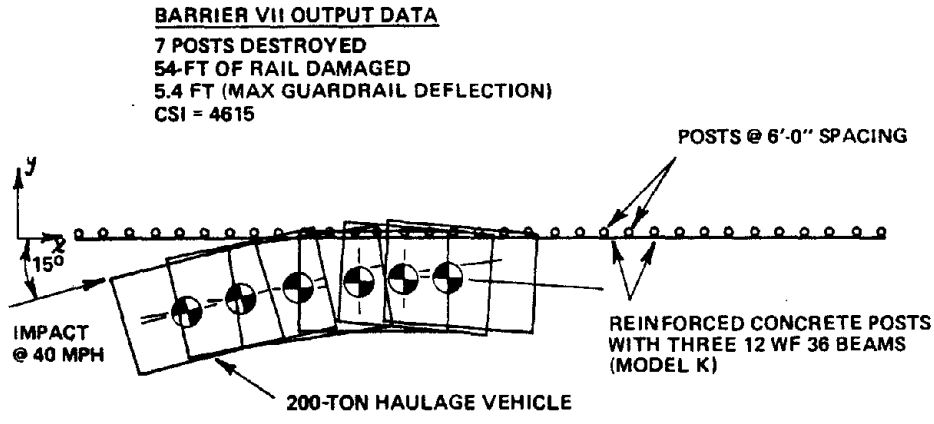

FIGURE 32. TYPICAL VEHICLE TRAJECTORY (CASE NO. 24)

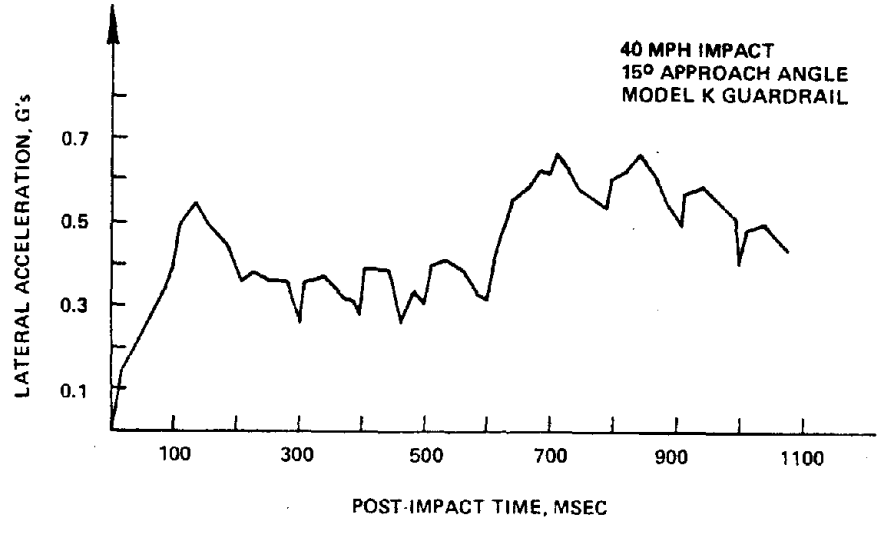

FIGURE 33. TYPICAL VEHICLE ACCELERATION—TIME TRACE (CASE NO. 24)

the analysis has been expanded to account for a different range of resistance factors and their influence on escape lane length requirements. Additionally, model testing of an 85-ton vehicle was performed to explore the action of a vehicle's interaction with an escape lane and a median berm.

Use of an escape lane or ramp to stop a runaway vehicle is commonplace in both the highway community and many surface mining operations. Escape ramp designs in current use consist of one of the following.

Rolling resistance generated by the vehicle's movement along the roadway represents a frictional force opposing forward motion. It is composed of internal tire friction (hysteresis), internal friction in the drive components, and friction developed between the tire tread and road surface. The resistance for radial tires is less than bias tires, approximately 25 percent(9), due to the method of tire construction which allows the sidewalls to deflect radially to absorb roadway irregularities.

The resistance due to wheel sinkage or flexing of the roadway surface results from the force necessary to overcome the compaction resistance of the roadway. Essentially, the wheel is constantly traveling uphill and to do so must compact the material in its path. It is not necessary that permanent soil deformation or penetration occur; flexing of the surface produces the same uphill travel requirement. The magnitude of this resistance force is directly related to the material and methods employed in the road construction and on extremely hard, smooth surfaces, this component of resistance is minimal.

The grade component effect on the vehicle is obvious. An increasing or positive road slope corresponds to increased resistance resulting from the gravity force vector. Likewise, a downgrade or negative road slope will produce a reduction in the overall resistance to vehicle motion.

The length requirements of a safe stopping distance along an escape lane can be approximated by equating the kinetic energy of the vehicle to the energy dissipated by the resistance forces over the stopping distance. This relationship is expressed algebraically by the following equation:

$$S = \frac{V^2}{2g(\sin\theta + \frac{Rr + Rs + Ra}{W})} \qquad (10)$$

where,

S = required stopping distance, ft.

V = entry velocity of vehicle, fps.

Ra = aerodynamic drag resistance force, lbs. (insignificant at 30 mph)

Rr = rolling resistance force, lbs.

Rs = sinkage force, lbs.

R_f = Ra + Rr + Rs

g = acceleration of gravity, fps

W = weight of vehicle, lbs

angle of ascent$^{(+)}$/descent$^{(-)}$, (deg)

Knowing the magnitude of the resistance forces opposing the vehicle motion, the length of the escape lane for various entry velocities and road slopes can be determined using Equation (10).

3.3.2 Resistance Forces

3.3.2.1 Rolling Resistance - The rolling resistance force on the vehicle, particularly after it leaves the well constructed haul road, is dependent upon the type and condition of the material employed in the escape lane. Estimates of average resistance factors have been compiled(9,10), and are summarized in Table 31 for various types of road surfaces and soil conditions. By use of the appropriate resistance factor the rolling resistance force Rr in Equation (10) is determined by the following equation:

Rr = (rolling resistance factor, lb/ton) X (vehicle weight, ton) (11)

3.3.2.2 Sinkage Resistance - The resistive force acting on a vehicle resulting from the sinkage into the surface material has been estimated as 30-lb/ton/inch.(9) This sinkage resistance force can be expressed as:

Rs = (30-lb/ton/inch) X (vehicle weight, ton) X (sinkage, in.) (12)

Use of this factor assumes that the depth of sinkage is known or can be estimated; however, for most situations, it is not only unknown but is a function of the material properties which themselves are subject to periodic changes. Techniques are available for determining the motion resistance and sinkage resulting from the operation of a vehicle in homogeneous and non-homogeneous solids.(11,12) While the correlation between the predicted and actual resistance force utilizing these techniques shows close agreement, it is not a method which would be readily acceptable to the mining industry. Interpretation of measured data, variations in soil conditions, and mathematical manipulation can easily produce a significant error.

Table 31. Typical Rolling Resistance Factors (Rr)

Type of Road Surface	Pounds per ton of Gross Vehicle, Rr	Equivalent % Grade
Concrete and Asphalt.	30 lb/ton	1.5%
Hard, smooth, stabilized, surfaced roadway without penetration under load, well maintained.	40 lb/ton	2.0%
Dry dirt and gravel. Not firmly packed. Some loose material.	60 lb/ton	3.0%
Firm, smooth, rolling roadway with dirt or light surfacing, flexing slightly under load or undulating, maintained fairly regularly, watered.	65 lb/ton	3.0%
Soft, unplowed dirt, poorly maintained.	80 lb/ton	4.0%
Wet, muddy surface on firm base.	80 lb/ton	4.0%
Snow, packed.	50 lb/ton	2.5%
Snow, 4-inch, loose.	90 lb/ton	4.5%
Dirt roadway, rutted, flexing under load, little if any maintenance, no water, 1 to 2-inch tire penetration.	100 lb/ton	5.0%
Rutted dirt roadway, soft under travel, no maintenance, no stabilization, 4 to 6-inch tire penetration.	150 lb/ton	7.5%
Soft, plowed dirt on unpacked dirt fills.	160 lb/ton	8.0%
Loose sand or gravel.	200 lb/ton	10.0%
Deeply rutted, or soft, spongy base.	320 lb/ton	16.0%
Soft, muddy, rutted roadway, no maintenance	200-400 lb/ton	10-12.0%

3.3.2.3 Aerodynamic Drag Resistance - In addition to the rolling and sinkage forces retarding the motion of the vehicle, aerodynamic drag will also produce a resisting force. This force is a function of the drag coefficient, frontal area and vehicle velocity. The magnitude of this force is approximated by the following relationship for a square plate:

$$Ra = 0.26\ Ca\ A\ (\frac{Va}{10})^2 \qquad (13)$$

where

A = projected vehicle area in drive direction sq. ft.

Ca = coefficient of air resistance, dimensionless

Va = vehicle velocity, mph

The air resistance coefficient, Ca, is a function of the geometric shape of the vehicle. For standard atmospheric conditions, this coefficient for a tractor-trailer is 1.3 and for a square plate is 1.2. The influence of this particular resistance force is more significant at higher velocities; for example, for velocities below 30 mph, it represents only 10 percent of the total resistive force normally acting on an 85-ton category haulage vehicle operating on a typical surface mine haul road. The overall effect of this resistive force is considered insignificant when compared to the rolling resistance force and usual haulage vehicle road speeds.

Omission of both the sinkage and aerodynamic drag resistance factors in Equation (10) will result in a conservative estimate of the stopping distance refinement. This information is similar to the results presented in the literature(14); the exception being the total resistance coefficient depending upon both the road grade and surface condition of the roadway.

The rolling resistance factors listed in Table 31 indicate a typical magnitude of 100 to 400 lb/ton for escape lane material ranging from a dirty roadway to a soft, muddy, rutted area. These resistance factors expressed in proper dimensionless units are 0.05 to 0.20, equivalent to the resistance developed by a vehicle traveling a well-maintained haul road having a positive grade of 5 to 20 percent, respectively. In effect, a steep upgrade in the escape lane area would produce a decelerating force on a runaway vehicle equivalent to that of a high resistance surface material. If the terrain of the mine operation permits use of a steep lane grade, this would be the preferred construction method. Soft areas consisting of sand mud pits would be effective in stopping the vehicle, but periodic maintenance would be required to ensure their condition after rains or freezes. Changes in climatic conditions would alter the stopping capabilities for various types of materials. Ideally, the escape lane should be constructed in a soft, plowed, or ripped area at a steep, ascending grade of a length in excess of that required to stop a vehicle entering at the maximum estimated speed.

3.3.2.4 Roll Back - Assuming that a vehicle enters the escape lane due to a complete loss of braking capability and the lane is constructed with a steep grade, provisions must be made to prevent the vehicle from rolling back down the lane after losing forward velocity. From Equation (11),

the rolling resistance force acting on the vehicle is determined by the type of material used on the road surface and the vehicle weight. Using the equations of static equilibrium for the vehicle illustrated in Figure 34, the maximum ascent angle, θmax, which would prevent rollback of the vehicle is defined as follows:

$$\theta max = \sin^{-1}\left(\frac{R_f}{W}\right) \qquad (14)$$

Consequently, the resistance factor (Rf), from Equation (10), dictates the maximum angle for various types of soil or soil conditions to prevent the vehicle from rolling back down the escape lane. This assumes that the resistance factor remains constant as the vehicle rolls back down the lane. The percent grade, corresponding to the various resistance factors for the different surface conditions, is included in Table 31 as an equivalent grade percent for R_r. This equivalent grade percent represents a conservative estimate of the maximum grade at which an escape lane should be constructed to provide sufficient resistance to minimize the likelihood of the vehicle rolling backward down the grade. Grades in excess of this slope will require the driver to perform some type of steering maneuver to prevent this roll back action.

An alternative to limiting the percent grade is to alter the resistance of the material in the lane, by using a mud pit, or a deep, soft area which would allow the vehicle to sink to the undercarriage structure. This arrangement would dissipate the vehicle energy as it travels up the lane and also serve as a means of restraining the vehicle from rolling backwards. It is imperative that any type of restraining pits used in conjunction with steep grades be placed not only at the end of the escape lane, but also at several locations along the length of the lane. The distance traveled by the vehicle will be a function of its entry velocity; consequently, a slower moving vehicle can enter the escape lane and stop before reaching a restraining area located at the far end of the lane.

3.3.3 Escape Lane Limitations

The previous discussion of escape lanes provides a general insight into the requirements for the stopping distance as a function of vehicle entry speed, type of material, and grade utilized in the construction of the lane. Limitations imposed by these requirements are the means of accurately estimating the resistance offered by different types of soil and their surface conditions. Values listed in Table 31 represent only average resistance factors obtained from previous test data and generally accepted by industry.

Review of soil dynamics and technical papers(15,16,17) indicates that resistance force is a function not only of soil conditions, but also vehicle weight, wheel diameter, and wheel width. Figure 35, illustrates the effect of different types of road surfaces on the total rolling resistance

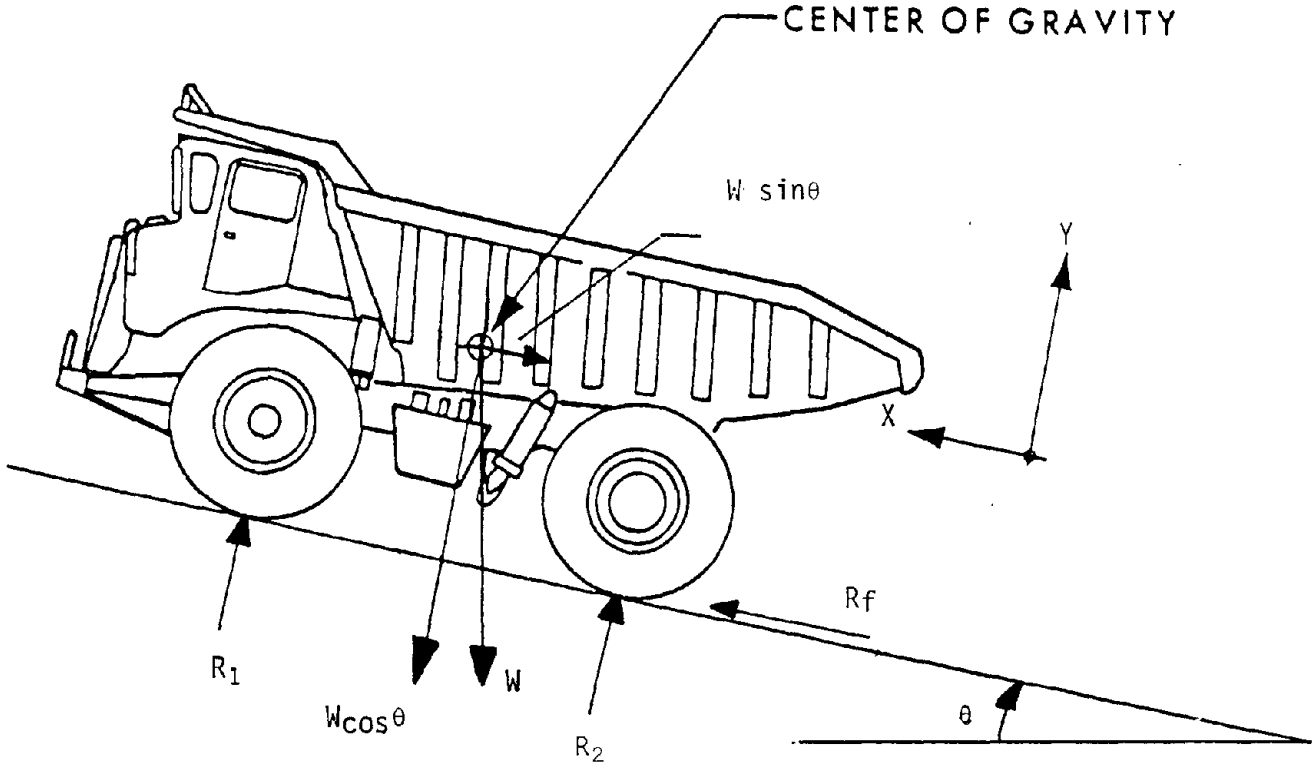

At the limit of static equilibrium:

$$R_f = W \sin\theta_{max}$$

$$\therefore \quad \theta_{max} = \sin^{-1} \frac{R_f}{W}$$

FIGURE 34. FORCES ACTING ON INCLINED VEHICLE

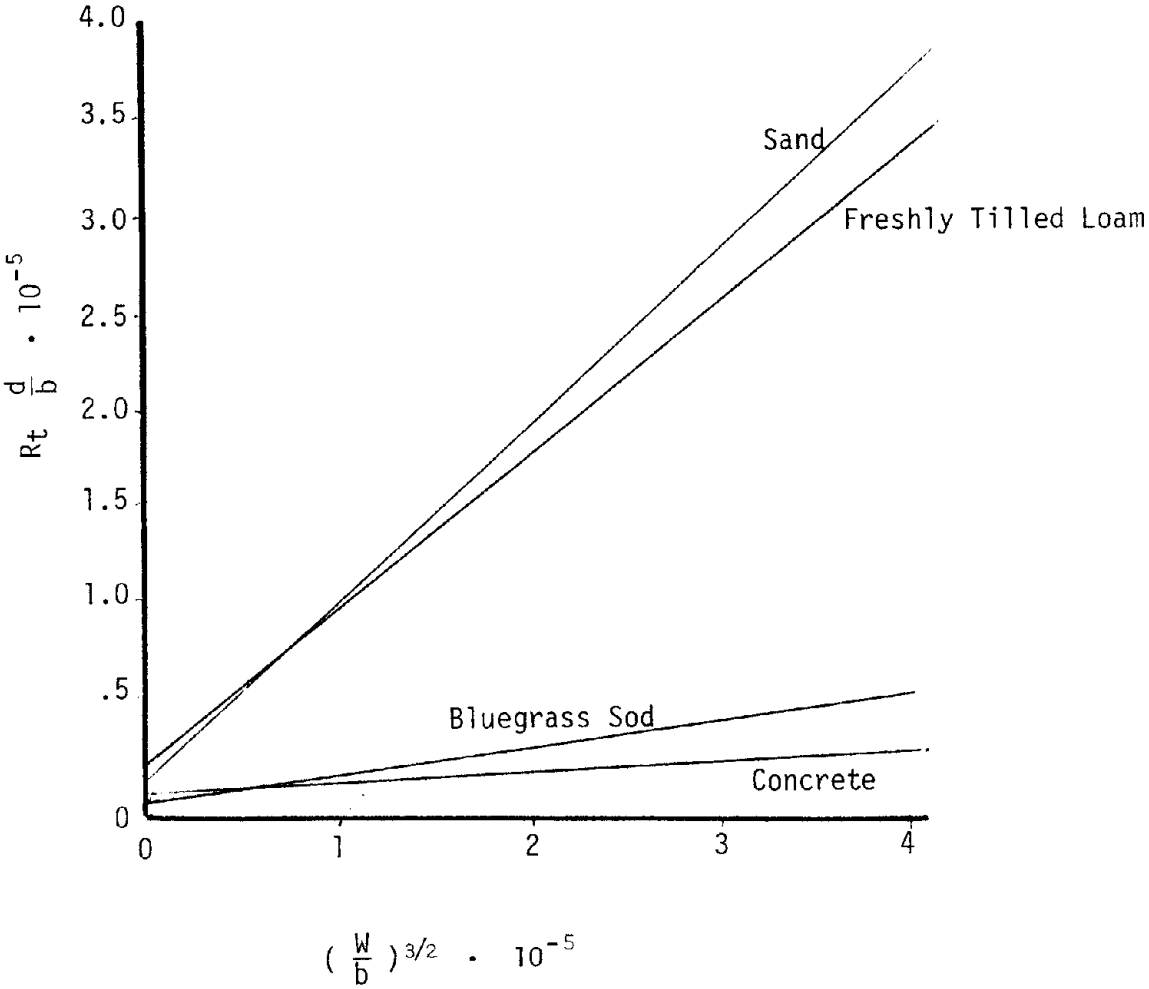

where,

b = tire width
d = tire diameter
Rt = total rolling resistance
W = weight on tire

FIGURE 35. EFFECT OF ROAD SURFACES ON TOTAL ROLLING RESISTANCE

as a function of various sizes of rigid wheels. The mathematical relationship represented by these curves is expressed as:

$$R\left(\frac{d}{b}\right) = K\left(\frac{W}{b}\right)^{3/2} + C \qquad (15)$$

where,

R = rolling resistance force, lb.

d = wheel diameter, in.

b = wheel width, in.

W = weight on wheel, lb.

K = proportionality factors reflecting soil conditions

C = soil condition constant

Regardless of the soil condition factors K and C, the effects of composite design factors of wheel width, diameter and load, can be demonstrated by rearranging the terms in Equation (15) to:

$$R = \frac{1}{d}\left(\frac{K\,W^{3/2}}{b^{1/2}}\right) + bc) \qquad (16)$$

Examination of Equation (16) indicates the influence of tire design factors on rolling resistance for increases in wheel loading, diameter and width. Increasing the wheel diameter, d, results in a decrease of the resistance force. The effect of wheel width, b, however, is not readily evident. For values of wheel width at infinity and zero, the resistance force becomes infinitely large, and at some intermediate value it is a minimum.

The effects of soil conditions on rolling resistance is illustrated by actual test data in Figure 35. Reexamining the rolling resistance factors listed in Table 31 would indicate that these specific values could only represent an average resistance factor for a representative tire geometry and wheel loading. In a typical passenger car operation, the variation in wheel loading as a function of the number of passengers or added cargo weight is negligible compared to the initial loading on each wheel. However, for a typical haulage vehicle, the wheel loading will more than double for the loaded condition without appreciably altering the tire geometry, the tire being designed for maximum capacity. Consequently, the resistance force will nearly triple for a fully loaded vehicle.

3.3.4 Model Tests of Escape Lanes

The influence of vehicle weight on stopping distance is easily demonstrated through the use of scale model testing.

A geometric model of representative 85-ton haulage vehicles was constructed in accordance with the modeling parameters discussed in the previous section of this report. Vehicle weight distribution, sprung and unsprung masses, and suspension characteristics were scaled from the values obtained from various manufacturers. Tires used on the model are representative in both diameter and width of the standard tires commonly used on each vehicle. They are, however, rigid and without tread designs. The effect of either of these characteristics is considered insignificant in relation to that of the type of material the model or the full-scale vehicle would encounter when operating in an escape lane.

The arrangement for model testing, shown in Figure 36, consisted of a vertically curved ramp approximately tangent at its lower terminus to a flat test bed, the slope and material of which could be varied to simulate various full scale escape lane configurations. Velocity of the scale model vehicle as it entered the escape lane was varied up to 40 scale mph, governed by the vehicle starting point on the ramp. Two types of artificial soil were chosen to represent trafficability characteristics of two distinctly different materials which might conceivably be used in constructing an actual escape lane. One of the test soils was a fine grain, dry, homogeneous sand, the other was compacted fire clay.

The relationship between artificial or selectively prepared and conditioned test soil used for model evaluation and the type of material commonly experienced in actual operation has always been an area of concern in the interpretation of model test data. The test materials employed in this testing sequence were specifically selected and prepared to eliminate the probability of introducing an uncontrolled variable into the problem being investigated. This can only be accomplished by using a homogeneous material having constant and readily repeatable soil parameters, such as density, angle of internal friction, and cohesion. In actual practice, the condition of the material will be a non-homogeneous composite, dependent upon climatic and geographic variations, number and types of vehicles traversing the area, and the maintenance and reconditioning performed on the escape lane. Consequently, the soil properties presented in the model simulation, while encompassing a broad range, will generally not represent any readily definable conditions that will occur in actual practice. Utilizing these two extreme types of soils, a frictional and a cohesive material, the gross influence of soil or escape lane material on vehicle response can be observed and general results formulated.

The escape lane model tests were initially performed using the dry, uniform size, sand. This material was placed in the soil test bed to a depth of approximately four inches, graded, and slightly compacted with a roller. The results of these model tests for various vehicle loading conditions, escape lane grades, and roadway materials are illustrated in Figure 37. The influence of both vehicle weight and type of road surface on the stopping distance is evident from this comparison. The sand, which

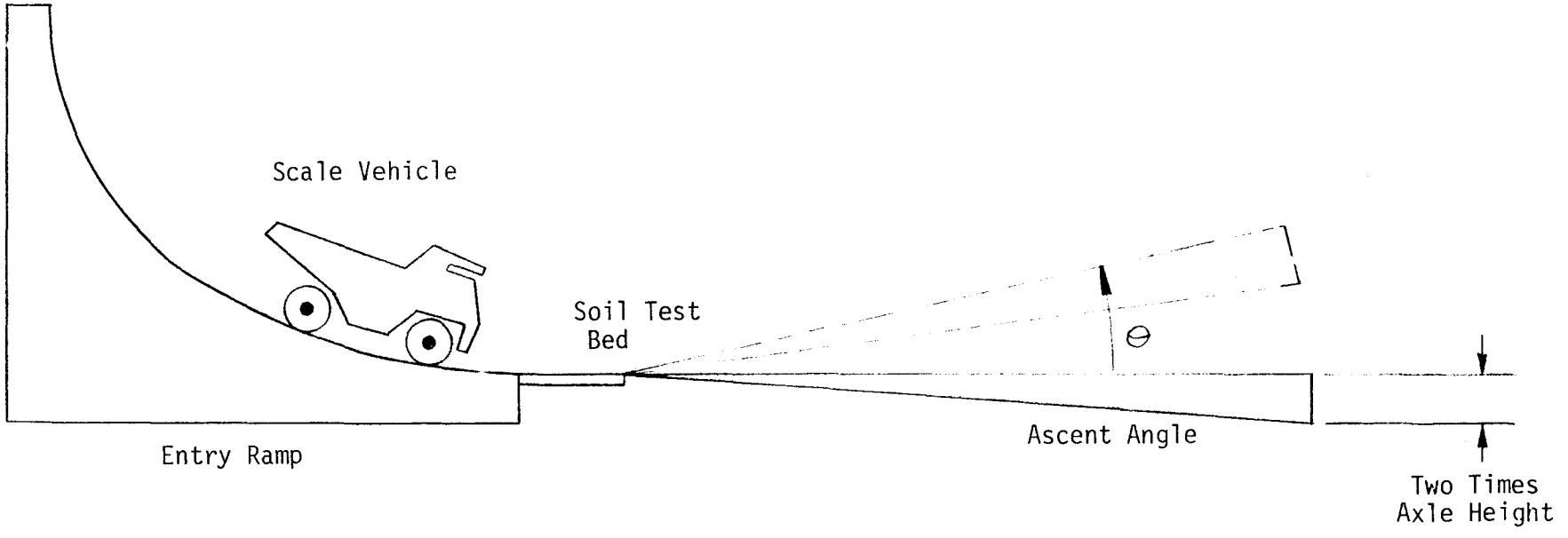

FIGURE 36. ILLUSTRATION OF ESCAPE LANE TEST CONFIGURATION

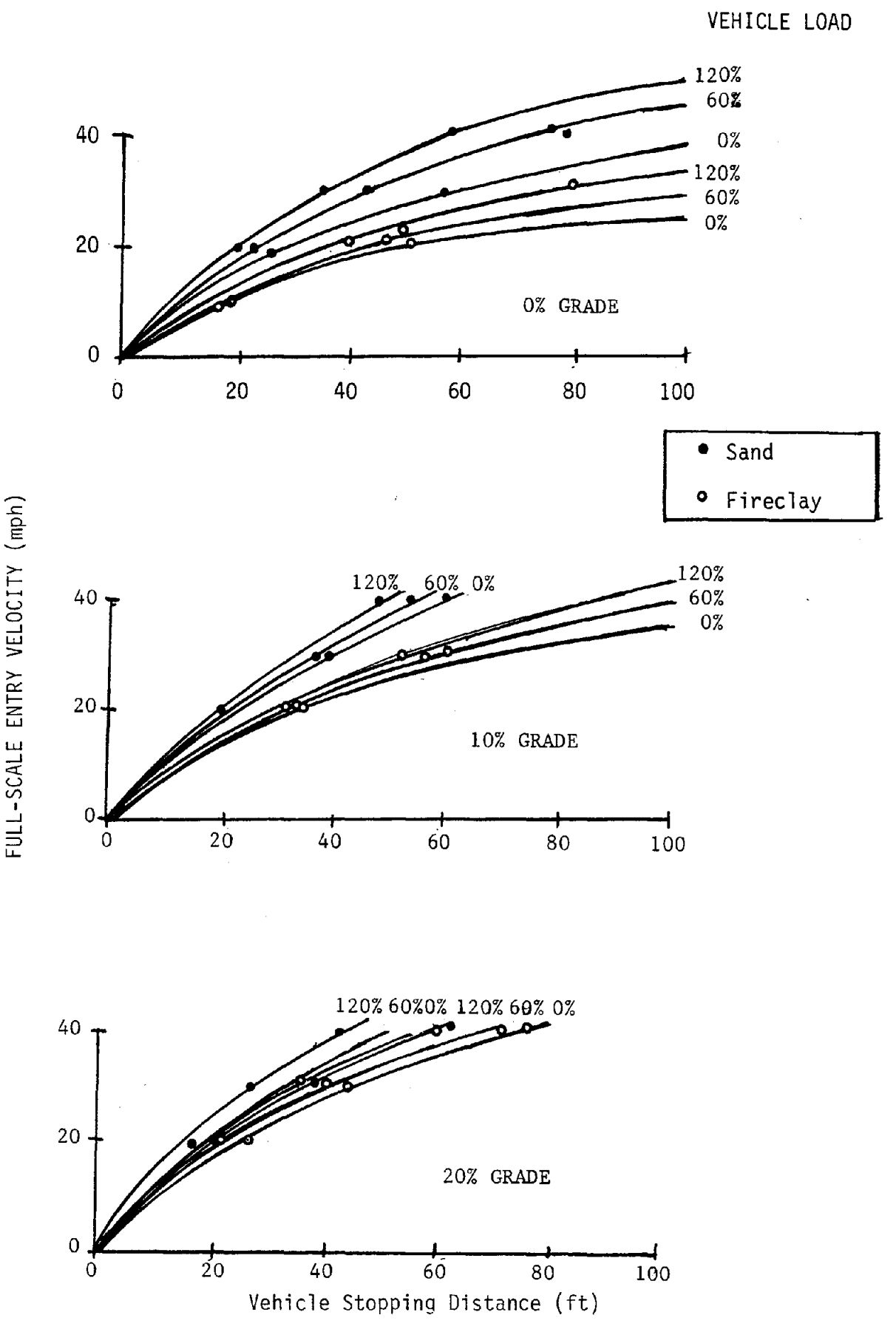

FIGURE 37. ESCAPE LANE STOPPING DISTANCE FOR VARIOUS MATERIALS FOR 85-TON VEHICLE

allowed greater vehicle sinkage, produced a higher resistance force and a shorter stopping distance than the fireclay material.

Figure 38 illustrates a comparison of the theoretical and model test results for an 85-ton vehicle operation on a 20 percent positive grade. In this figure, the theoretical stopping distance is found as follows:

R_t for an 85-ton fully loaded truck is found from Figure 35 as follows:

$$(\frac{W}{b})^{3/2} \cdot 10^{-5} = 1.06 \quad (17)$$

W = 323,800 lbf/6 tires
b = 24 inches
d = 100 inches

For sandy material according to Figure 35

$$R_t \frac{d}{b} \cdot 10^{-5} = 1.05 \quad (18)$$

therefore,

$$R_t = 25200 \text{ lbf/tire} \quad (19)$$

or

$$R_t = 151200 \text{ lbf/vehicle} \quad (20)$$

The stopping distance can be obtained from Equation (10) where R_a is assumed zero as follows:

$$S = \frac{V^2}{2(32.2)(\sin 11.31 + \frac{151200}{323800})} \quad (21)$$

Data from these model tests indicated that Equation (10) will provide a realistic estimate of the necessary distance. A certain amount of discretion is, however, required in the selection of the proper rolling distance coefficient for both the type and condition of the escape lane material.

3.3.5 Median Berms on Escape Lanes

Model tests conducted with a median berm along the escape lane roadway substantially reduced the vehicle stopping distance compared to the escape lane without a berm. The results of the model test with and without the median berm on the escape lane are illustrated in Figure 39. While a median berm reduced the stopping distance approximately 50 percent for a fully loaded vehicle traveling 40 mph, the grading, shaping, and consolidation of an escape lane to insure ideal conditions did not prove to be a feasible alternative to the simple construction of a lane having the length as previously specified.

3.3.6 Construction of Escape Lanes

The physical location and size of the escape lane will depend upon the mine size, terrain, and vehicle sizes employed by the mine, but ideally,

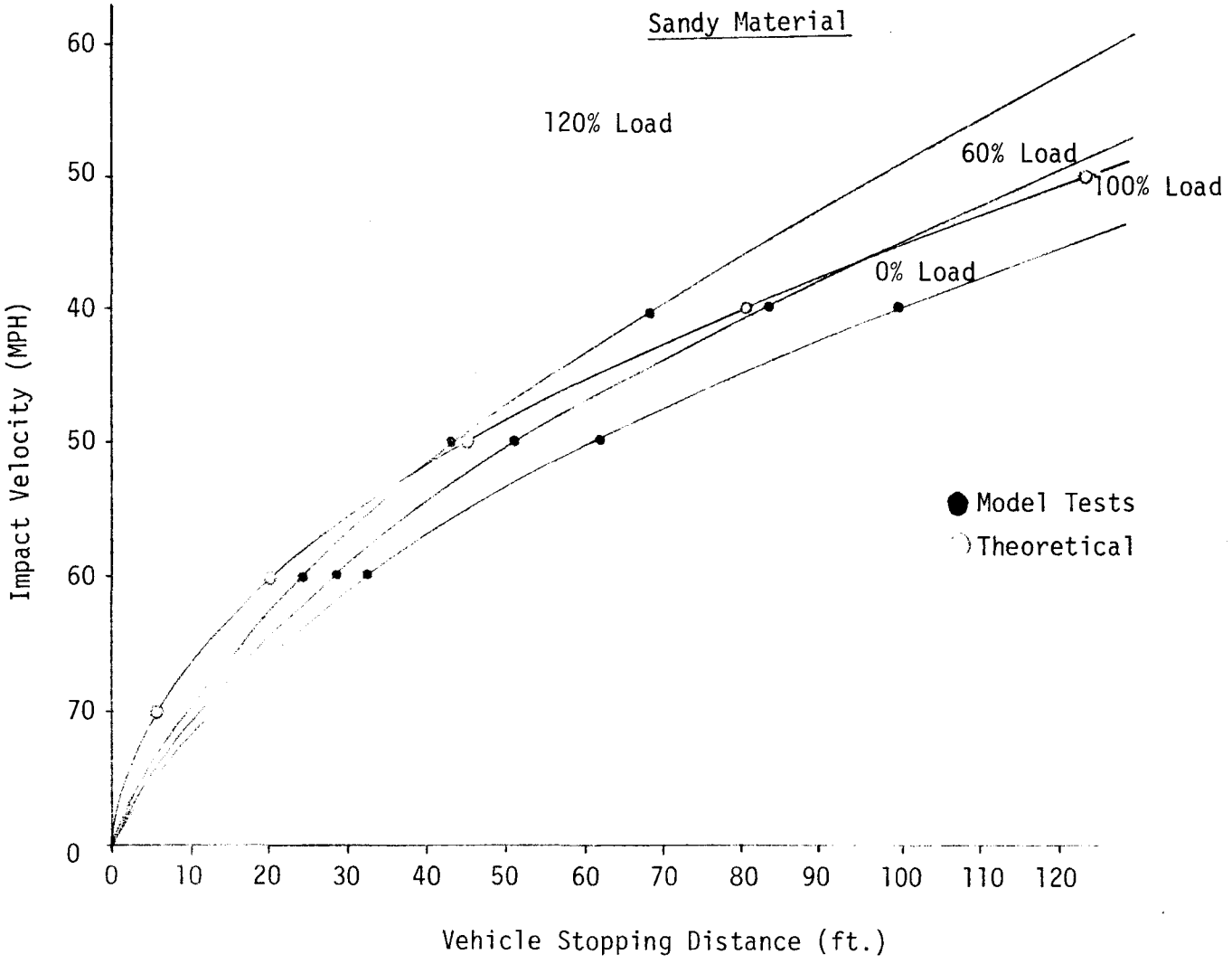

FIGURE 38. COMPARISON OF MODEL TEST RESULTS AND THEORY FOR ESCAPE LANES FOR 85-TON HAULAGE VEHICLE

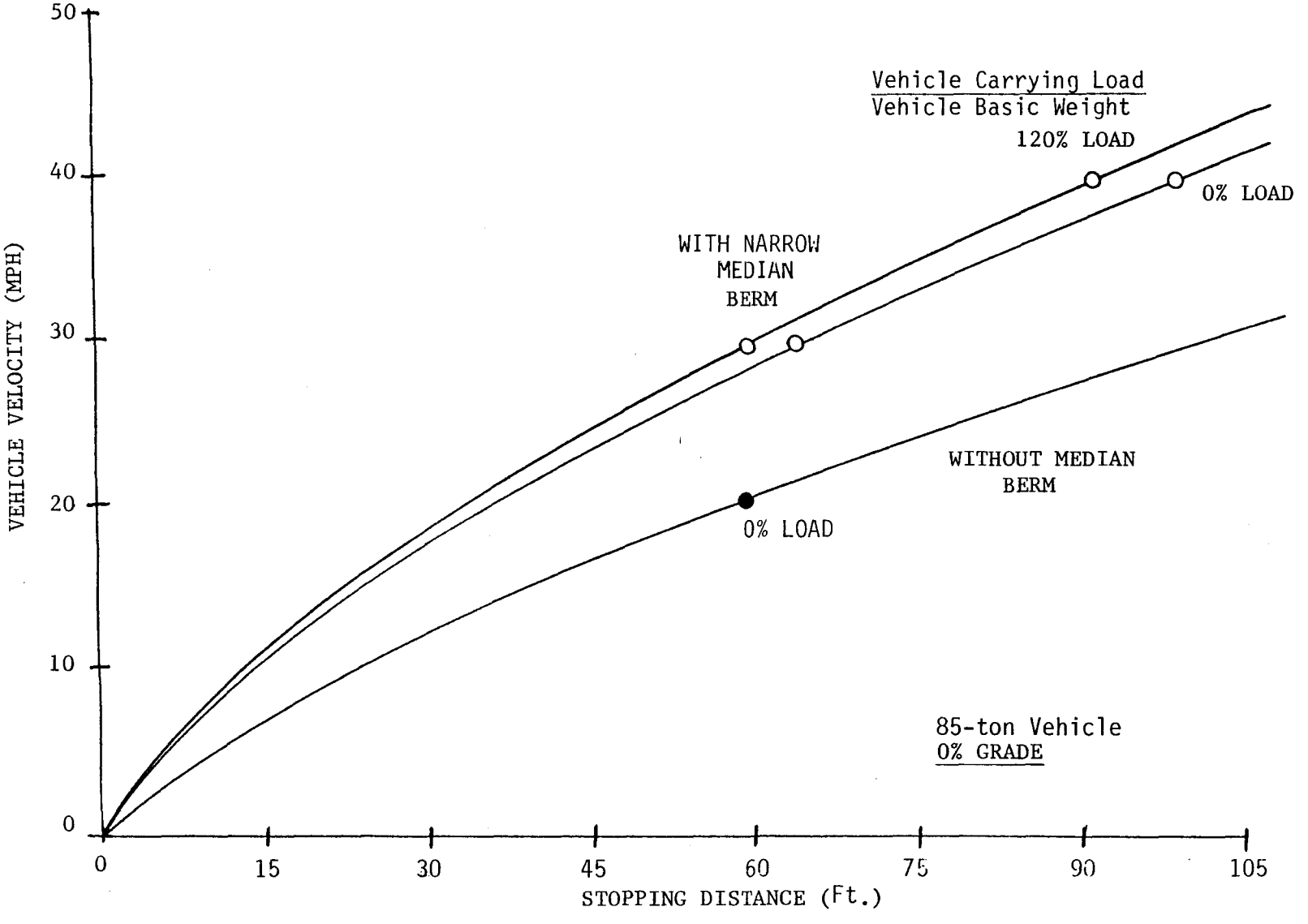

FIGURE 39. STOPPING DISTANCE USING MEDIAN BERM ON ESCAPE LANE (MODEL TEST RESULTS)

the lane should be constructed immediately ahead of the area deemed most hazardous by the mine safety engineer. This location may be at the end of a long downgrade or it may precede a sharp turn in the haulage road. In either case, the hazardous area or areas must be identified and appropriate remedial action taken.

The optimum escape lane would consist of an uphill grade constructed from high energy absorbing material. The entryway should be on a smooth tangent with the haulage road, adequately signed both ahead of the entry and at the point of entrance, and of a width in excess of the largest haulage vehicle being used by the mine. In actual practice, the required location may be along a downgrade area having a minimum length for stoppage of the vehicle. Each situation will be different for the various types of mines.

There are several significant facets of escape lane designs which have been developed during this project and which must be adhered to for the lane to perform its intended function. These basic requirements are:

- Entry to the lane should be marked by appropriate signage.
- Entrance to the lane should be a smooth transition from the haulage road, thereby minimizing the steering requirements of the operator.
- Width of the lane should be reasonably wider than the width of the largest haulage vehicle.
- Depth of loose gravel or sand material should taper from a minimum at the entryway to a depth of two times the maximum ground clearance of any vehicle expected to utilize the escape lane.
- The depth of the arresting material should be graduated along the initial entryway of the ramp so that a vehicle will not be stopped too abruptly.
- Material used in the escape lane should be of an unconsolidating nature; pea gravel is the most common material used in public highway construction. Regardless of the material used, it must be free draining so that freezing will be delayed during periods of cold weather and will not readily compact. It must also be a material that can be readily smoothed out after use and can be maintained with a minimum of effort.
- The length of the escape lane should be based on the largest size vehicle traveling at a realistic maximum speed. The length of the lane will also be a function of the terrain; a lane located on a downslope would be longer than a lane located along an upgrade.

- A barrier constructed from sand, gravel, or any available overburden material should be positioned at the end of the escape lane to prevent a vehicle from traveling over an embankment in the event the vehicle is not stopped in the escape lane area.

- The arrester bed material should also insure that once a vehicle is stopped it will not roll back. Maintenance is necessary to keep the ramp in the proper condition. The ruts must be smoothed out and the surfacing material loosened frequently. As the material becomes infiltrated with dirt and other fine materials it must be removed and replaced with clean material.

The design of highway arresting beds recommends the use of large, round, uniformly graded gravel, free from fines. The use of uniformly graded and washed material will maximize the percentage of voids in the material, thereby providing the optimum drainage and minimizing interlocking and compaction.

3.4 MEDIAN BERMS

Median berms are frequently employed in mining operations in conjunction with escape lanes or as road traffic dividers, and are constructed in a manner which will allow a runaway vehicle to straddle the berm, eventually coming to rest. The design requirements for this type of berm have been presented(14). However, the adequacy of this type berm in physically stopping a haulage vehicle is unknown. Field testing of the concept may have been performed by individual mining operations, but no published data is available to justify the previously proposed design parameters. Verification of these parameters for economic purposes have, therefore, been investigated through scale-model testing in a soil test bin. The test procedure was analogous to the previously described technique utilized for evaluation of the escape lane requirements. The only material used in the construction of the median berm was the commercially available fire clay used in the escape lane testing. Scale median berms were constructed on a prepared surface in accordance with specifications tabulated in Figure 40(14). The model vehicle used for these tests corresponded to the 85-ton category.

3.4.1 Median Berm Model Tests

The ability of median berms to arrest a vehicle is related to the energy dissipated in shearing off that portion of the berm above the vehicle undercarriage, the rolling resistance, and the frictional drag forces on the vehicle's structure. The shearing force required which will cause the berm to fail is, however, dependent upon the soil properties and in situ condition of the berm. Initially, median berms are generally constructed of fine-grain, unconsolidated materials. With changes in climatic conditions, repair, or filling-in of low spots along the berm, it becomes quite probable that the strength of the berm will increase slightly over its original state due to material settling. Various strength model berms were constructed, by lightly packing the berm material (fire clay) during the construction

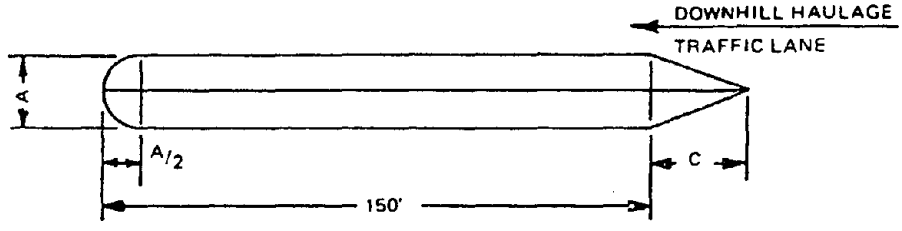

PLAN

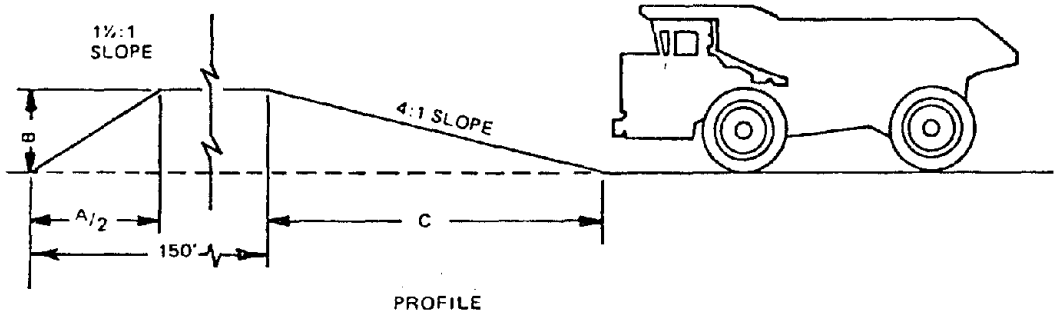

PROFILE

	A	B	C
CATEGORY 1 13 TO 25 TONS < 100,000 lb	11'-12'	3.5'-4'	14'-16'
CATEGORY 2 28 TO 50 TONS 100,000-200,000 lb	12'-15'	4'-5'	16'-20'
CATEGORY 3 55 TO 120 TONS > 200,000-400,000 lb	15'-18'	5'-6'	20'-24'
CATEGORY 4 120 TO 250 TONS > 400,000 lb	18'-32'	6'-11'	24'-44'

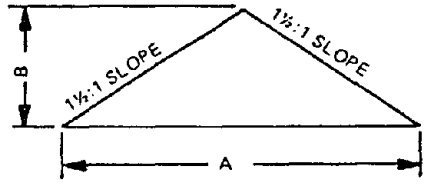

SECTION

"A" Values are greater than
inside tire clearance dimensions

FIGURE 40. MEDIAN BERM DESIGN CONFIGURATION

phase. The resulting bearing strength of the berm was then recorded by use of a soil penetrometer. Figure 41 illustrates the strengths for both packed and non-packed berm configurations. Packing of the berm produced a strength of 2.5 to 3 times that of the unconsolidated configuration.

The stopping distances at zero percent grade associated with these different strength berms for various vehicle load conditions and impact velocities are presented graphically in Figure 42. The results indicate approximately the same stopping distance for either berm material. This anomaly is attributed to the geometric shape of the berm rather than to its strength characteristics. The wide base width of the berm is approximately 200 inches compared to the spacing of 134 inches between the front wheels, and 85 inches between the dual rear wheels. Consequently, during impact with either type of berm, the wheels compact the berm material and in turn, ride along the edges of the berm above the road surface. When the vehicle impacts a non-packed berm, the shearing resistance is less, but the rolling resistance is high. Similarly, impacting the packed berm allows the vehicle to "ride higher" on the berm, shearing off a reduced width and volume of higher strength material. The resulting effect appears as an even trade between increased rolling resistance and reduced shearing area.

Straddling a berm which is too wide can result in the vehicle overturning; this happened during model testing. Essentially, localized failure of the berm material occurs when the vehicle is riding high, allowing either the front and/or rear wheels on one side of the vehicle to drop. The vehicle is then misaligned with the berm, with one set of wheels being in contact with the road surface, and the other side being three to four feet on top of the berm, resulting in an unstable condition.

3.4.2 Construction of Median Berms

Ideally, the median berm should be constructed from unconsolidated material, having a berm height as specified in Figure 40, but with a base width **less** than the narrowest tire spacing. This geometric configuration would initially be difficult to construct since loose material will naturally form at the angle of repose, approximately 33° or a slope of 1.5:1. In actual practice, this narrow berm is unintentionally obtained by the action of the road grader as it performs daily maintenance of the haul road. The grader blade constantly cuts away at the base of the median berm, which has been in existence for some time, allowing it to stand at a steeper angle and, consequently making it narrower.

After observing the model vehicle overturn when operating along the wide berm, additional tests were conducted employing a narrower berm which allowed the vehicle's rear track to completely straddle the berm. The construction of the berm required some compaction of the material to retain

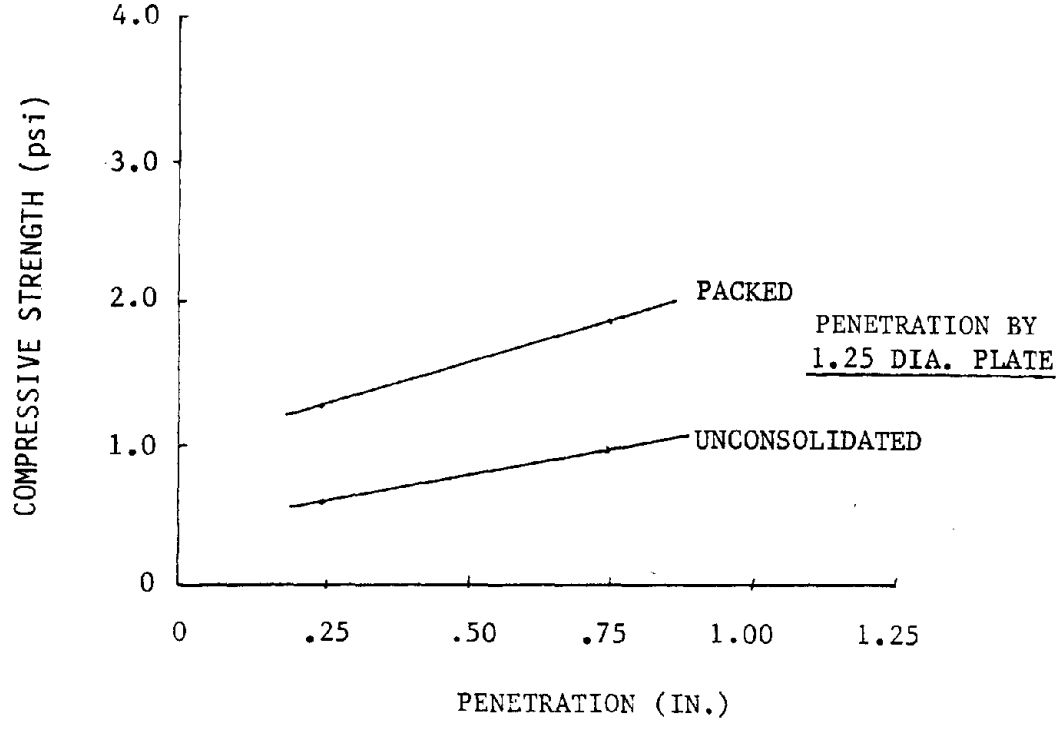

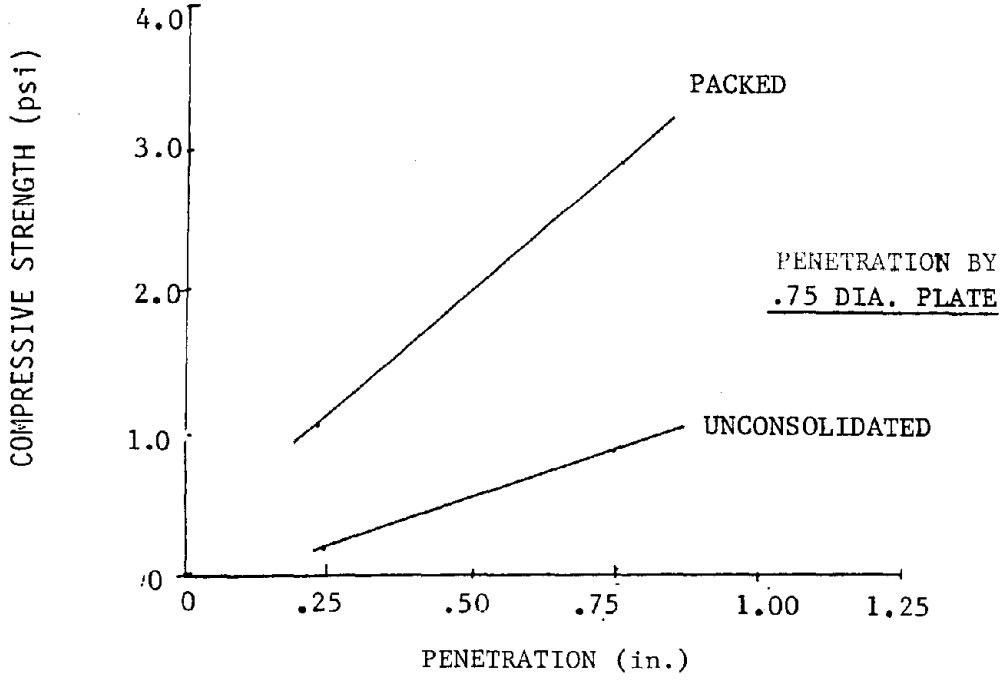

FIGURE 41. STRENGTH CHARACTERISTICS OF MODEL MEDIAN BERMS

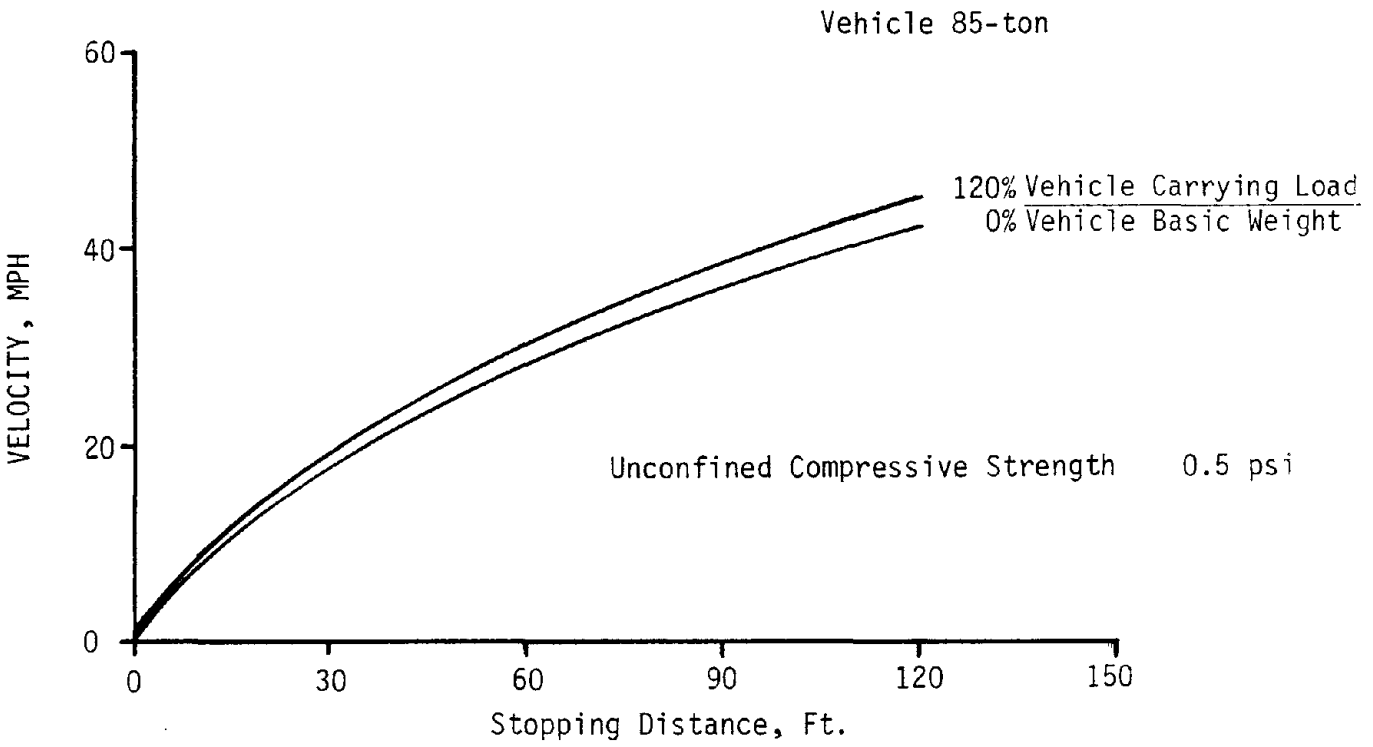

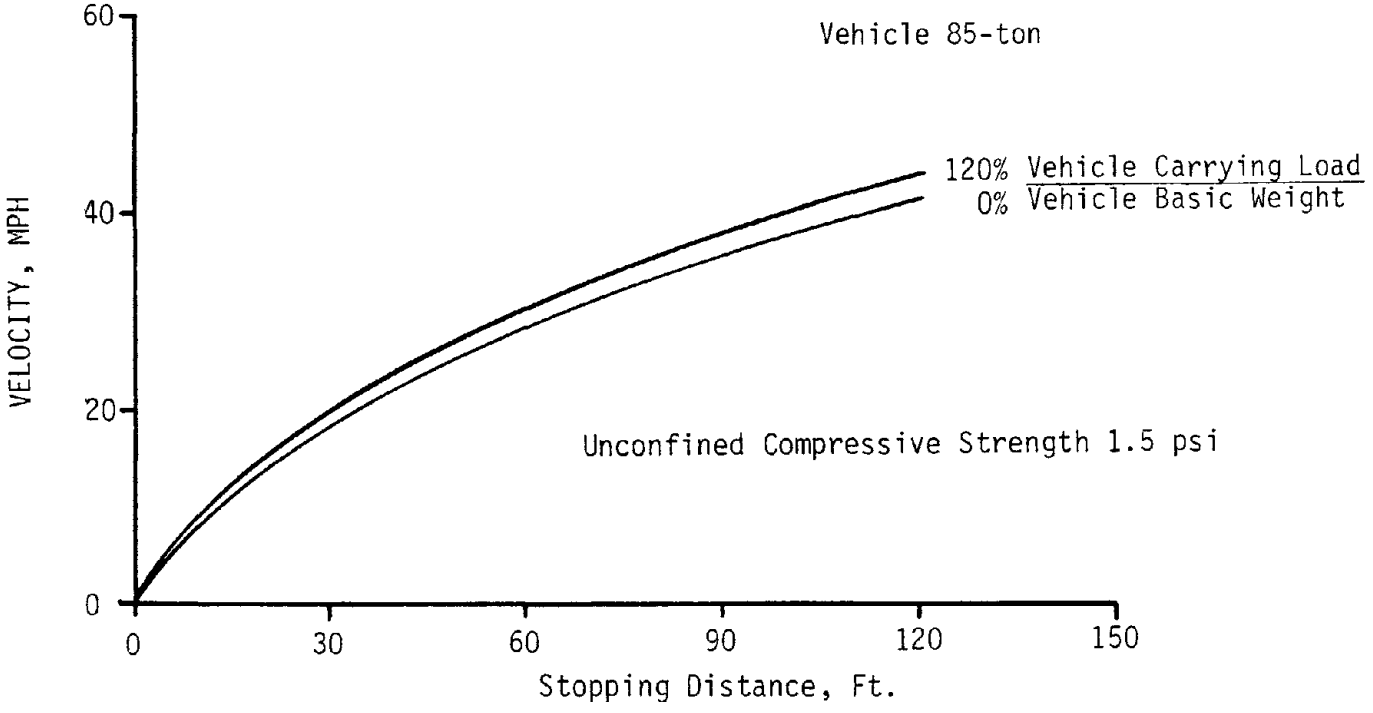

FIGURE 42. STOPPING DISTANCE FOR WIDE MEDIAN BERM OF VARIOUS STRENGTHS AT ZERO PERCENT GRADE

the desired shape. The results of the narrow berm tests are illustrated in Figure 43 and are compared to the previous wide berm design. Both tests were conducted on an 8 percent downgrade. The narrow berm stopped the vehicle in a shorter distance, particularly at the higher impact speeds. The increased shear area and, to a lesser extent, the shear strength of the compacted material were responsible for the reduction in travel. One observation during these tests was that, for a narrow berm, turning and misalignment of the vehicle was minimized by the restraining action of the berm. At high speeds, with the vehicle having more momentum, it could become misaligned, break through the berm, or ride up the berm placing the vehicle in an unstable condition.

Comparison of the median berm stopping requirements for zero percent, Figure 42, grade and the data for an 8 percent downgrade, Figure 43, illustrates the effect of grade on stopping distance. As expected, the stopping distance is increased for a negative or downgrade situation.

Determining the median berm length necessary to stop each of the various categories of haulage vehicles is beyond the current scope of work of this project. The haul road design manual[14] specifies a length of approximately 150 feet for all vehicle categories. Actual length depends upon available space along the haul road and intersections. However, a length of 150 feet is considered to be a maximum. Based on the model test, a full-scale stopping distance for a fully loaded 85-ton vehicle traveling at 40 mph down an 8 percent grade would require approximately 150 feet for a wide unconsolidated berm and 100 feet for a narrow compacted berm.

Based on the results of these model tests, a narrow compacted median berm is recommended because the decreased potential for rolling the vehicle over with the narrow berm outweighs the increased potential for damage to the engine as it shears the berm material. Entryways must be provided along the median berm to allow the driver to align the vehicle with the berm when the situation arises. Shaping the berm with a road grader to produce a base width equivalent to the vehicle rear track is considered feasible with current methods of production.

3.5 BARRIERS

Utilization of a concrete barrier, similar to the barriers employed along public highways, was studied during this project. The requirements of a barrier are analogous to boulders; however, the overall mass of the barrier is considerably larger and the shape well defined. Nevertheless, the kinetic energy of the vehicle must be absorbed by the action of the barrier.

The redirectional capability of a highway type barrier is a function of its shape and the particular design of the vehicle involved in the impact. While the majority of the highway barriers are of similar design,

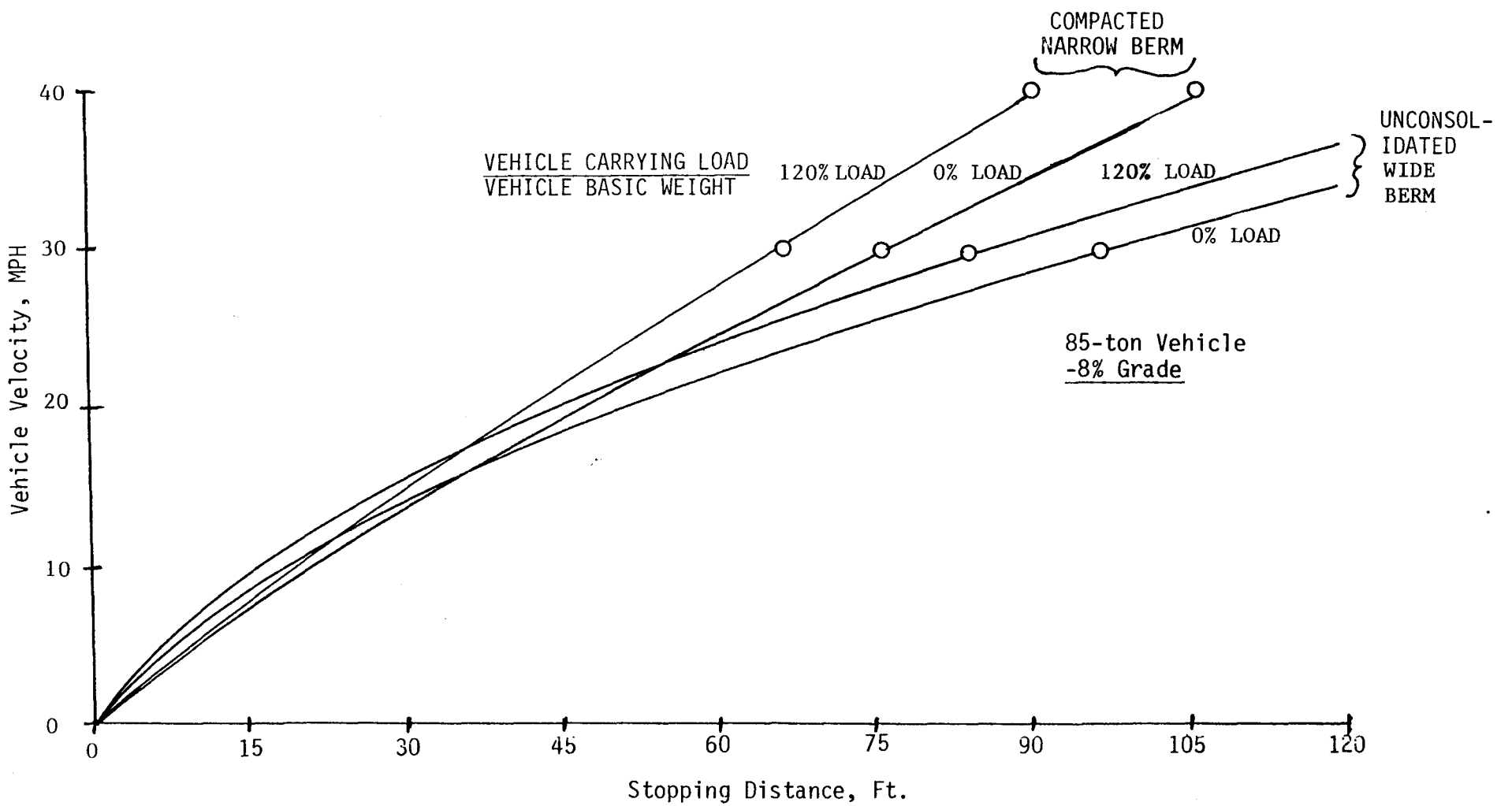

FIGURE 43. COMPARISON OF STOPPING DISTANCES

the trajectory is different for the various classes of vehicles. The specific design employed is the result of a substantial investigation of various designs using a "typical" highway vehicle. To simply illustrate a massive sloped concrete barrier as a recommendation for use on a mine would be a gross over-simplification of the problem. Any proposed concept must be validated through full-scale testing.

The advantages of these rigid type systems are:

- capable of being designed to withstand severe impact without penetration,
- result in negligible vehicle damage for impacts of low severity,
- can be reused at other locations.

Among the disadvantages are:

- relatively unyielding, tending to aggravate the deceleration environment of the vehicle occupant
- material and installation cost higher than conventional berms.

The various barrier combination design concepts illustrated in Figure 44 through 48 are intended to restrain the various categories of haulage vehicles as indicated on each illustration. The category of vehicle listed on the design concepts represents the maximum size vehicle which the barrier combination is expected to restrain based on the frictional restraint generated by the weight of the restraining system. The berm concepts specified for a large vehicle can be reduced in physical size and utilized for a smaller vehicle. Physically increasing the size of a small berm, however, would not restrain a larger vehicle. Again, these concepts represent preliminary designs which require further evaluation to validate their effectiveness in restraining the various categories of haulage vehicles.

The design objective of the proposed barrier combination is to eliminate the possibility of a vehicle vaulting the berm, and to either redirect or arrest the motion of the vehicle. This is accomplished by providing a near vertical face on the berm, with the energy of the vehicle impact being dissipated by displacement of the berm, and the berm reaction with the road surface.

Barrier Combination I, illustrated in Figure 44, consists of structural steel reinforced concrete sections backed by a soil embankment. The unique feature of this concept is to use the wheel loading along the base of the concrete structure to resist movement of the system during an impact. Also illustrated in Figure 44 is a slightly modified configuration of the initial concept using cleat plates along the bottom edge of the concrete section to increase the friction resistance.

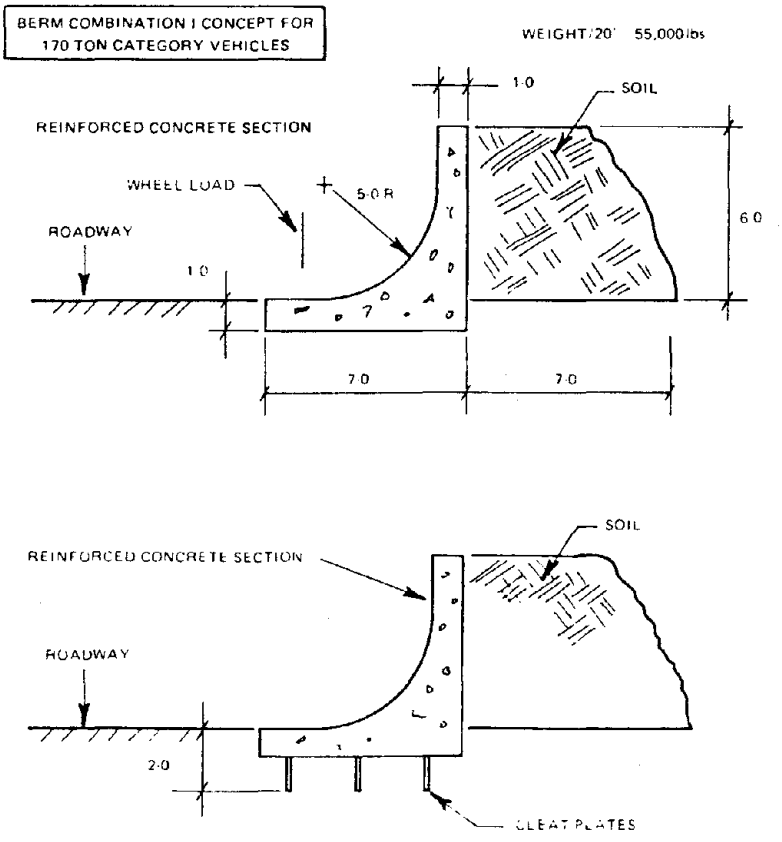

FIGURE 44. BERM COMBINATION DESIGN 1

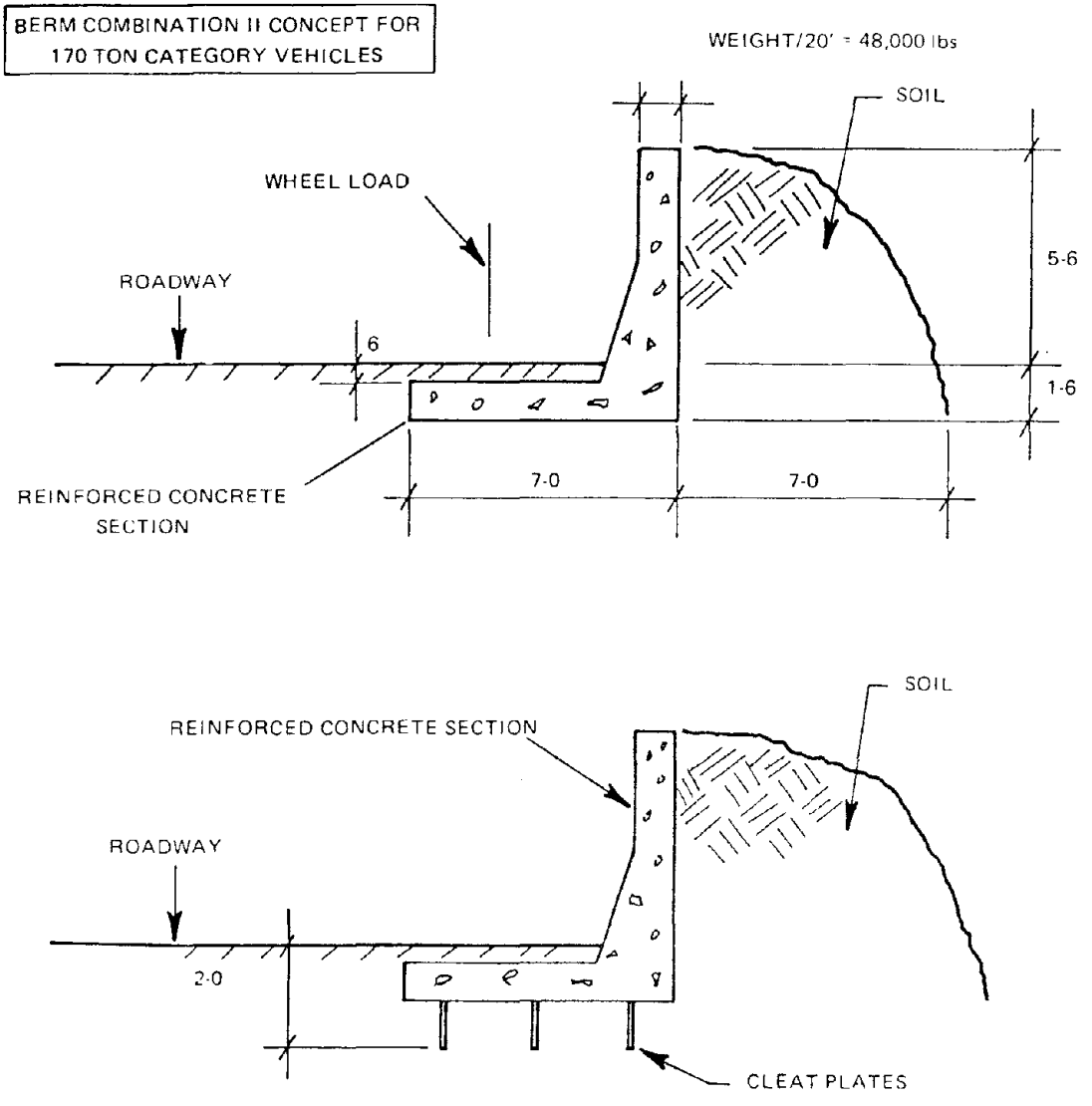

FIGURE 45. BERM COMBINATION DESIGN II

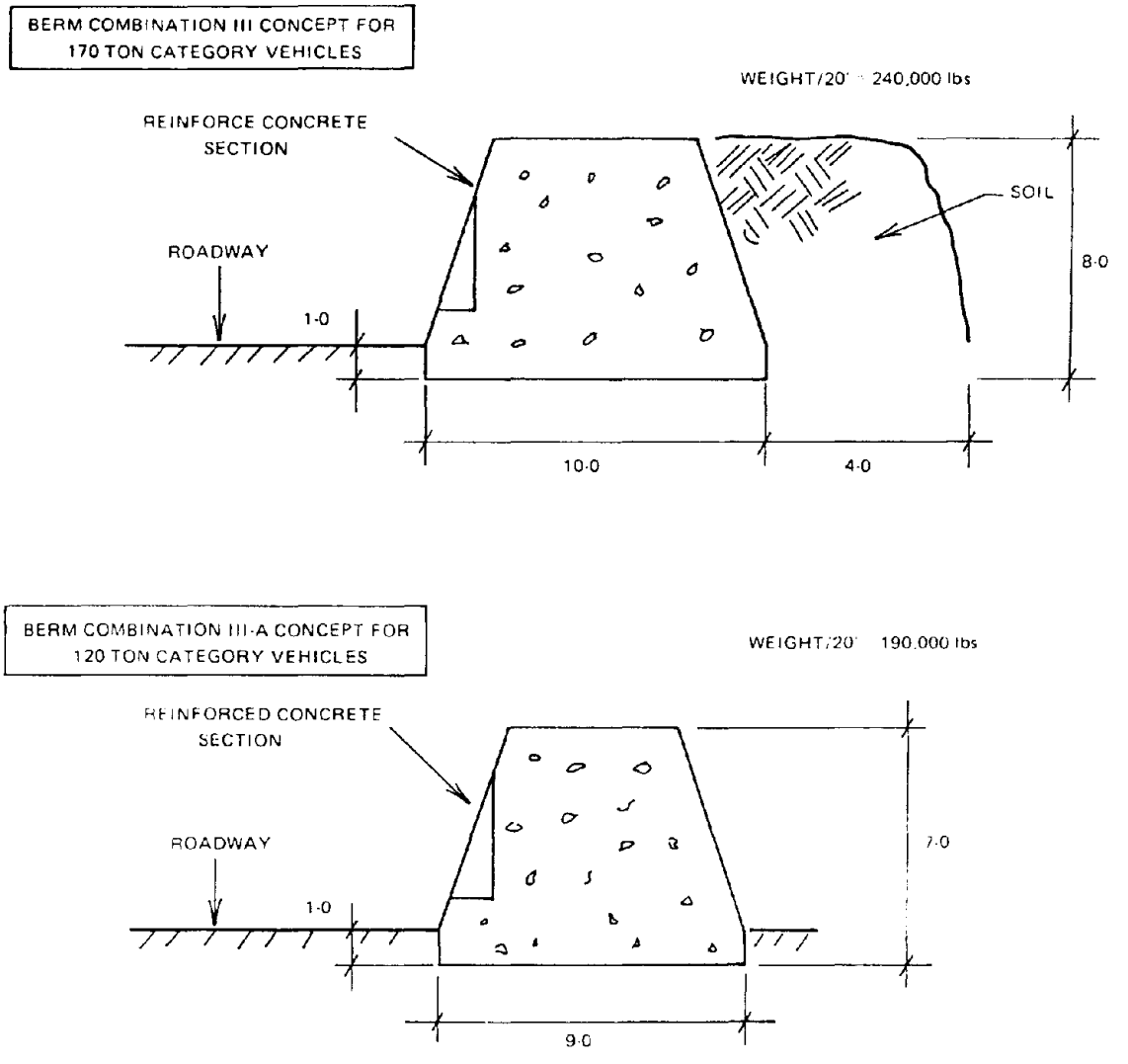

FIGURE 46. BERM COMBINATION DESIGNS III AND III-A

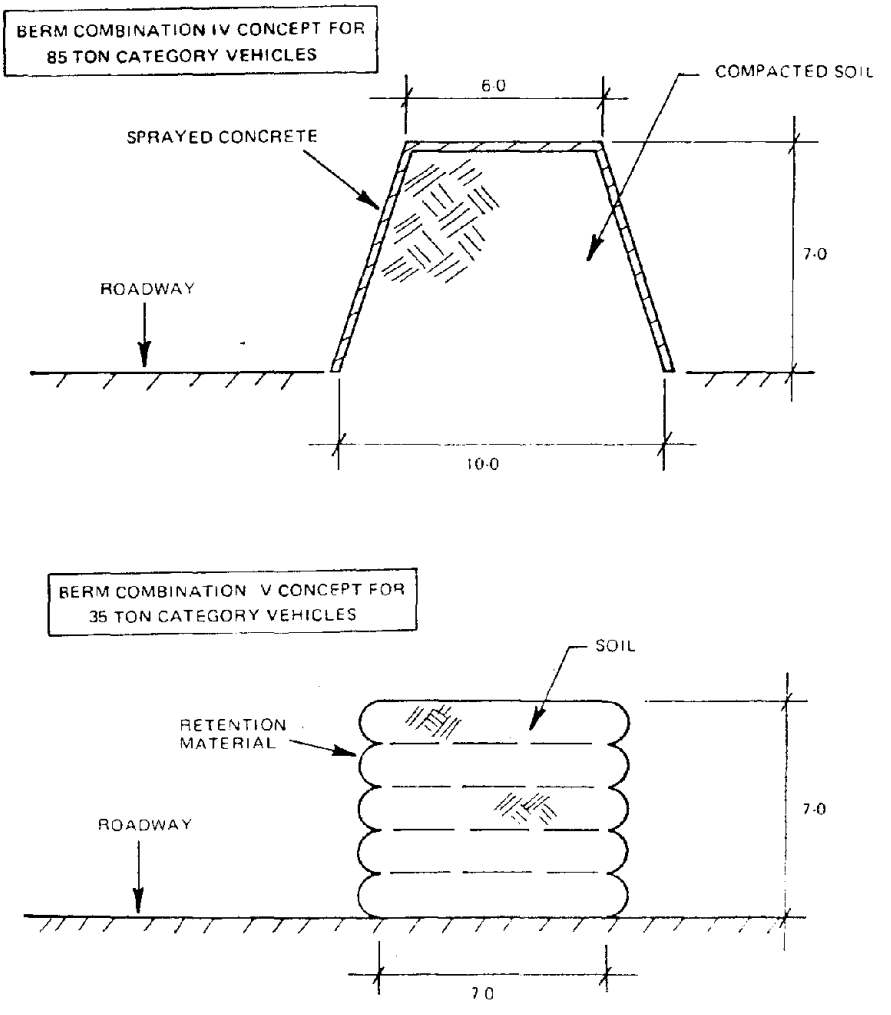

FIGURE 47. BERM COMBIANTION DESIGNS IV AND V

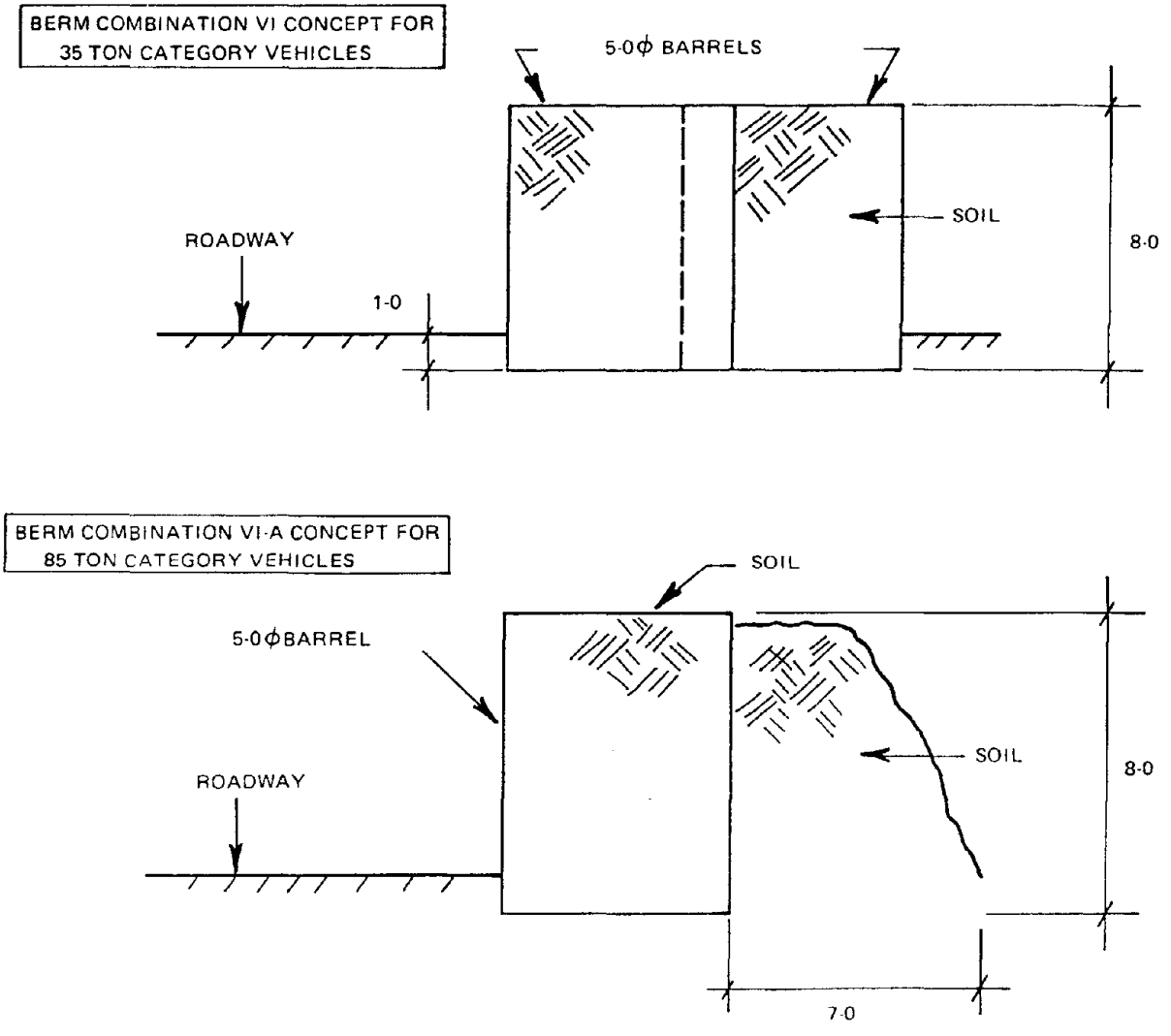

FIGURE 48. BARRIER DESIGN VI

The possibility of soil erosion along the roadway/concrete interface can be a drawback to this concept depending upon the placement of the system. Under normal mining operations, the vehicle would not be expected to operate along the apron section. With sufficient road width, a drainage ditch could be positioned between the barrier and the normally traveled segment of roadway. Under this type of installation, any erosion occurring at the roadway/concrete interface would have an insignificant effect on an errant vehicle.

Barrier Combination II, illustrated in Figure 45, is similar in concept to the previous design but is for application along a narrower roadway. In this concept, the concrete segment would be recessed in the roadway, allowing the vehicle to travel above the apron section. Soil erosion would also be a possible problem; however, the vertical section of the barrier could function as one side of a drainage ditch. Cleating plates along the bottom side of Barrier Combination II-A can also be utilized to increase the resistive force.

Barrier Combination III and III-A, illustrated in Figure 46, are representative of the concepts originally proposed in this program. These systems each consist of structural steel reinforced concrete sections recessed in the roadway. The mass of System III being less than III-A requires the addition of backfill to provide the additional resistive force required at impact. The use of only a concrete segment, without soil backing, as illustrated in Figure 46, would be restricted to applications wherever smaller vehicles are involved. Erosion along the roadway/concrete interface will occur; however, drainage ditches adjacent to the barrier will minimize this problem.

The advantages of these rigid type systems are: (1) they can be designed to withstand severe impact without penetration, (2) they can be designed to cause negligible vehicle damage for impacts of low severity, (3) they can be reused at other locations. Among the disadvantages are: (1) being relatively unyielding, they tend to aggravate the deceleration environment of the vehicle occupant and, (2) their material and installation cost would be higher than conventional berms. The economics associated with the various barriers will be discussed in a later section of this report.

Barrier Combination IV, illustrated in Figure 47, represents a means of utilizing existing overburden material while obtaining a near vertical face. Construction of this system would consist of compacting layers of existing material to gain additional soil strength to resist impact. The shape retention material, pneumatically-sprayed concrete, would then be applied to the finished, shaped berm.

Barrier Combination V, illustrated in Figure 47, represents a variation of this concept using a reinforced earth structure(18). The principle involved in this design is an increase in the berm strength arising from

soil friction acting against the reinforcement members. Transmission of forces by friction between the grains of soil and the reinforcements introduces a cohesive strength to the entire mass.

In actual construction, the berm is composed of overburden material and reinforcing elements in the form of strips disposed in horizontal layers. In these layers, the strips are set at certain intervals to obtain maximum transmission of frictional force. Construction could be simplified to some extent by the use of burlap or tight mesh for the skin element and wire mesh for the reinforcement element. In either case, construction of this device would be labor intensive.

Barrier VI, illustrated in Figure 48, consists of two staggered rows of barrels or pipe sections filled with overburden material, the barrels being recessed in the road surface for additional stability and strength. Barrier VI-A represents a similar design using a single row of barrels with an overburden backfill.

The intent of the designs illustrated in Figures 44 through 48 is to obtain a vertical facing to eliminate the possibility of a vehicle vaulting the berm. The primary advantages of several of these systems are: (1) reduced material cost compared to concrete systems and, (2) the yielding action of the berm would produce a less severe deceleration environment for the vehicle occupant. Among the disadvantages are: (1) corrosion of the metallic elements resulting in maintenance problems and need for periodic inspections. However, plastic barrels could be used in place of steel ones, (2) labor requirements to construct the systems, and (3) the system would not be salvageable for reuse.

3.6 Boulders

The ability of a berm, fabricated from a continuous line of large boulders to restrain or redirect an errant haulage vehicle will depend upon several factors, primarily the size of the vehicle, the size of the boulders, and the approach angle. The physical requirement for a boulder to restrain a haulage vehicle can be approximated by the following assumptions:

- collision of the vehicle and boulder is inelastic, the coefficient of restitution is small, so that there is a common velocity between the vehicle and boulder after impact,
- the boulder remains whole both during and after impact and remains in contact with the vehicle,
- the retarding or stopping forces developed are attributed to the frictional forces involved in sliding the boulder along the road surface.

Figure 49 illustrates the assumed vehicle-boulder positions resulting from an impact and the corresponding velocity-time diagram.

During the initial impact with the boulder, the collision is assumed to be inelastic, so there is a common velocity of the vehicle and boulder after impact. For analysis purposes, a single boulder of mass equivalent to the number of boulders capable of being intercepted by the front of the vehicle is assumed. Applying the principle of conservation of momentum where,

$$M_1 V_1 + M_2 V_2 = (M_1 + M_2)V_3 \qquad (22)$$

M_1 = mass of the haulage vehicle

M_2 = mass of the boulder

V_1 = initial velocity of the haulage vehicle

V_2 = initial velocity of the boulder

V_3 = common velocity of the vehicle and boulder after impact

Since the boulder is initially stationary, its velocity is zero and Equation (22) reduces to

$$V_3 = \left(\frac{M_1}{M_1 + M_2}\right) V_1 \qquad (23)$$

Equation (22) predicts the velocity of the vehicle after impacting a boulder or group of boulders having a total mass of M_2.

Consider the case of a vehicle impacting a large boulder mass equivalent to the vehicle mass. The vehicle will then experience a 50 percent reduction in velocity or a 25 percent reduction in vehicle kinetic energy. Impacting a boulder mass significantly larger than the vehicle mass, such as a solid structure, will essentially produce nearly an instantaneous stoppage of the vehicle.

Impacts of this magnitude, hitting a solid wall, would consist of dissipating the vehicle's total kinetic energy through the strain energy associated with deformation of the vehicle structure. Investigation of this severe type of impact is beyond the current scope of work of this contract. It should be remembered, however, that the deceleration forces experienced in any type of impact are directly related to the change in velocity of the vehicle and the time interval associated with this velocity change. The time period, Δt, associated with the deceleration period is of basic importance. This time period is normally obtained experimentally by instrumenting a test vehicle with accelerometers and obtaining the resultant deceleration/time curve for the specific type of impact.

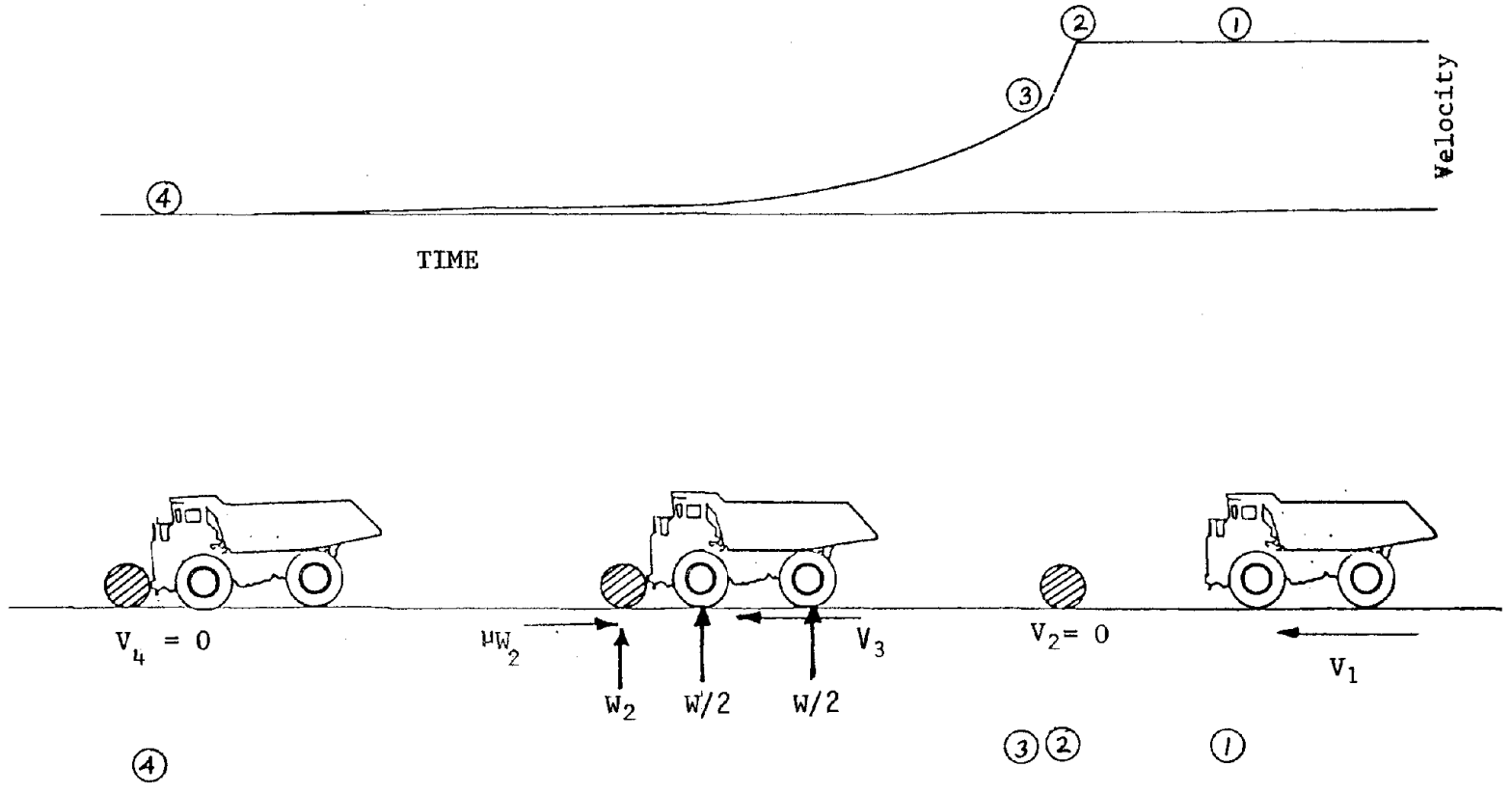

FIGURE 49. VEHICLE-BOULDER IMPACT

Typically, and also fortunately, a vehicle impacting a row of boulders or berm constructed from several large boulders will not be stopped instantaneously or within the short time periods associated with a totally rigid barrier impact. The impact sequence depicted in Figure 50 is more representative of what would acutally occur when a large mass such as a haulage vehicle impacts the significantly smaller masses of boulders. The vehicle's kinetic, rotational, and potential energy is dissipated in the work generated as the boulders slide along the road surface. The primary area of concern now becomes the distance associated with stopping various size vehicles by using typical size boulders.

The rotational energy of wheels, motors, and gearing is assumed to be 20 percent of the translational kinetic energy of the vehicle.(8) The energy relationships for the vehicle after impacting a boulder is

$$FS = \frac{(W_V + W_b)\ V_3^2}{2g} + \frac{20\%\ W_V\ V_3^2}{2g} \pm W_V\ S \sin\theta \qquad (24)$$

where,

F = total retarding force developed by the boulder/road contact, lb.

S = stopping distance, ft.

W_V = total weight of vehicle, lbs.

W_b = total weight of boulders, lbs.

V_3 = common velocity of vehicle and boulder, ft/sec.

g = acceleration of gravity, 32.2 ft/sec^2

θ = grade of roadway, degree (minus for a negative slope)

The total retarding force developed is a composite of all forces attributable to retarding the movement of the vehicle. They consist of braking, sliding friction, rolling resistance, and wind resistance.

For the case of an errant haulage vehicle, the only force being considered initially will be that developed between the boulder and the surface over which it slides. High rolling resistance and, to a lesser extent, air resistance forces will further reduce the stopping distance. Using these assumptions, Equation (24) for a vehicle operating on a level haulage road reduces to the following:

$$F = \mu\ W_b \qquad (25)$$

$$S = \frac{(1.2\ W_V + W_b)\ V_3^2}{2g\ \mu\ W_b} \qquad (26)$$

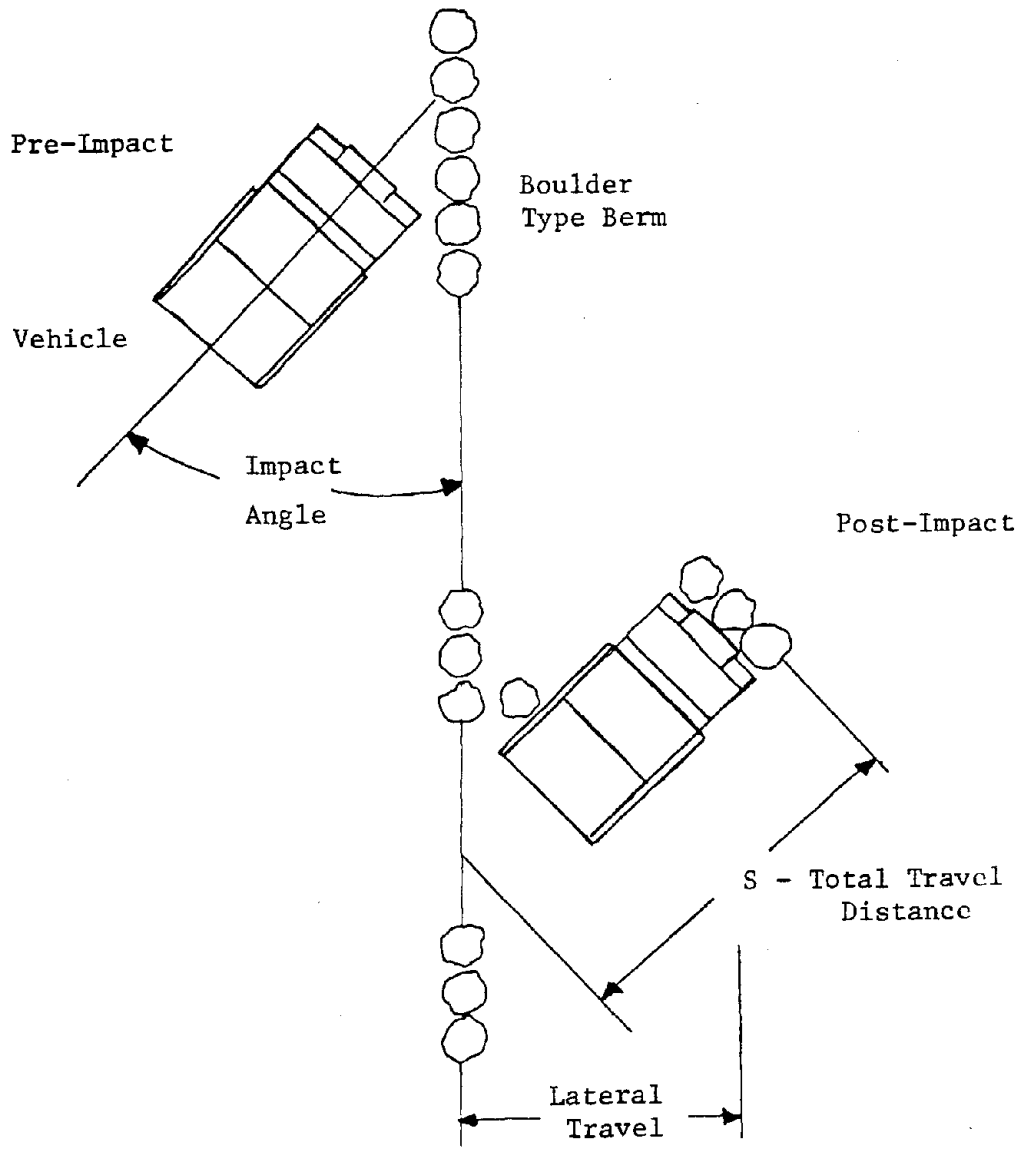

FIGURE 50. VEHICLE IMPACTING BOULDER BERM

where,

μ = coefficient of sliding friction, 0.5

This stopping distance equation can be further simplified by the following:

If

$$R = \frac{1.2\ W_v + W_b}{2g\ \mu\ W_b} \tag{27}$$

then,

$$S = \frac{R}{2\mu g}\ V_3^2 \tag{28}$$

The term R, therefore, represents a stopping distance coefficient relating the total mass in motion to the mass resisting this motion. This ratio will dictate the final stopping distance for the vehicle. Braking forces are not considered in this analysis.

For analysis purposes, it is further assumed that the boulders utilized are generally spherical in shape with constant mass density and diameter. The maximum number of boulders intercepted by the impacting vehicle is then a function of the vehicle width, boulder diameter, and number of boulder rows. If boulders are staggered in successive rows, the maximum number of boulders intercepted would be reduced by one for each succeeding row. Consequently, the restraining force would be proportionally increased for this type of impact.

Since it is being assumed that the boulders are not capable of developing a force sufficient to redirect the vehicle, the direction of motion remains along the initial vehicle trajectory and the vector component of the travel distance normal to the haulage road becomes significant. This lateral travel distance defines the minimum road width requirements when boulders are used as a berm to restrain haulage-type vehicles. Figure 50 illustrates pre- and post-impact conditions associated with this analysis, and further illustrates the significance of the impact angle and lateral components of the travel distance.

Table 32 illustrates several vehicle parameters, boulder size, and corresponding R-value for various size haulage vehicles in both empty and loaded conditions. Also listed in this table is the percent reduction in vehicle velocity as it makes initial contact with the boulder mass. For the data presented in this table, an empty vehicle would experience approximately a 20 percent reduction in velocity upon initial impact, the loaded vehicle velocity reduction would be approximately 10 pecent.

The results of this analysis and the corresponding stopping distances for various impact velocities, angles, vehicle weights and boulder sizes are illustrated graphically in Figure 51. Under these assumptions, the distance required to stop an empty 85-ton vehicle impacting a 20 mph and an angle of 20° with the boulder would result in a total vehicle travel

Table 32. Vehicle Boulder Parameters

Vehicle Size	Vehicle Weight, lb	Load* Factor	Vehicle Width, in	Boulder Dia. in	No. of Boulders Intercepted	Equivalent** Boulder Weight, lb	R	% Velocity Reduction
35-ton	60,000	1.0	145	48	3	17,600	5	23%
35-ton	60,000	2.2	145	48	3	17,600	8.5	12%
85-ton	115,000	1.0	200	60	3	34,400	4.3	23%
85-ton	115,000	2.5	200	60	3	34,400	9.4	11%
120-ton	170,000	1.0	235	60	4	45,800	4.7	21%
120-ton	170,000	2.4	235	60	4	45,800	9.9	10%
170-ton	210,000	1.0	250	72	3	59,400	4.5	21%
170-ton	210,000	2.6	250	72	3	59,400	10.2	10%

*Load Factor = 1.0 for empty vehicle

**Boulder Density = 175 lb/ft^3

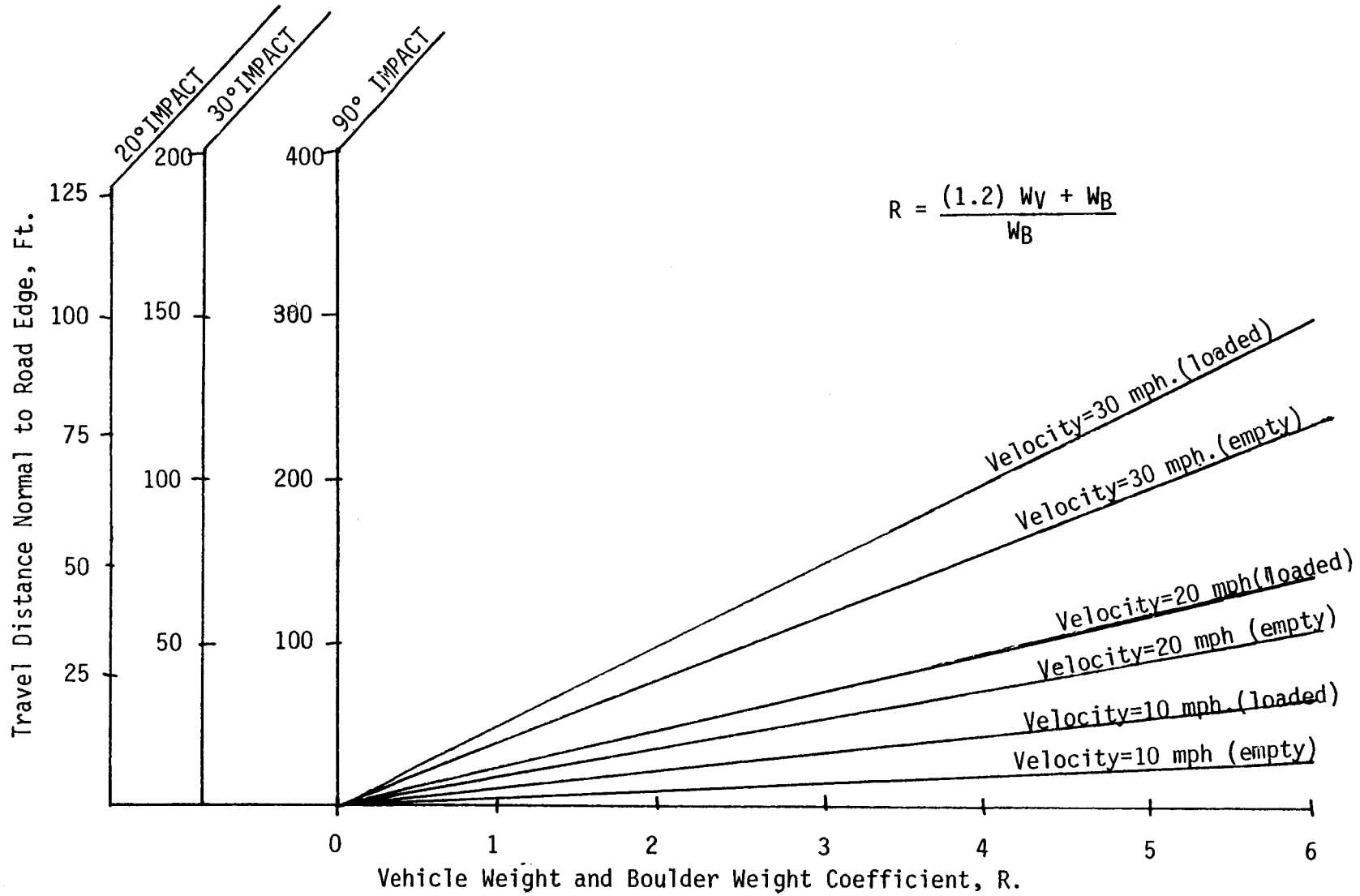

FIGURE 51. VEHICLE STOPPING DISTANCE FOR BOULDER IMPACTS BY 85-TON VEHICLE

distance of nearly 80 feet after impacting the boulders. This distance would necessitate positioning the boulder approximately 25 feet inside the edge of the elevated roadway. Construction of a boulder-type berm 25 feet from the edge of the roadway is totally unrealistic. Application of the vehicle's service brakes will provide an additional retarding force and, therefore a reduction in travel distance. However, the use of brakes is something that may or may not be available to the operator and, therefore has not been considered in this analysis.

Effective use of boulders as a restraint system compromises the intended vehicle action during an accident. If the boulders are sized to stop a vehicle in a short distance, they will probably cause considerable damage. If they are sized to reduce the deceleration forces, the distance that they must be placed from the edge of the road becomes excessive. The recommended alternative is to incorporate them into an earthen berm.

When incorporated into a berm, the effective restraint capability is enhanced because the berm material supports the boulder. Additionally, the berm material provides a measure of shock absorption during the initial stages of interaction. The berm size requirement to provide effective restraint should be determined from the strength characteristics of the parent berm material. This will provide a conservative design and allow for the effective disposal of the large boulders.

3.7 Cost Effectiveness of Restraint Systems

The cost effectiveness of guardrails, concrete embankments, and soil composite berms must be evaluated in respect to expected mine life, length of haulage road, expected life of the haulage road, and anticipated maintenance cost of each system.

The results of this program indicate the use of any of these devices as restraint systems is feasible. Both guardrails and concrete barriers require the acquisition of materials for their implementation. Soil berms, by comparison, may use waste material available at the mine site if it can conform to the strength recommendations outlined. Overall costs can be evaluated by comparing the costs of installing guardrails or concrete barriers to the costs of constructing berms from waste material or specially prepared material. All cost comparisons are based on the requirements for restraining a 170-ton haulage vehicle at the approach conditions of 30 mph and 30°. The costs are further defined as the average costs for restraint installations of 1000 feet in length.

Cost information for each restraint system is presented in Table 33. This information indicates that berms constructed of available waste material is by far the most economical method of constructing a restraint system. Constructing berms from special materials is as costly as guardrail installations which is 12 times as expensive as berms constructed of waste material. Concrete barriers are shown to be the most costly restraint system.

Table 33. Estimated Installed Cost of 1000 Feet of Various Systems to Restrain 170-Ton Vehicle, 30 mph, 30°

Restraint System Type	Particular Requirements	Sub System Cost
Guardrail (Fig. 27)	$26.25/ft-10 gage tubular Thrie beam	$ 26,150
	167 14-inch square x 15 foot long wood posts	43,921
	40 splices for thrie beam	950
	Installation at $5/ft.	5,000
	TOTAL	76,021
Concrete Barrier (Fig. 44)	$82.17/ft. reinforced concrete barrier	82,170
	Installation at $3.5/ft. 200 yd^3 waste material for additional reinforcement by dumping waste material and grading at $1.30/yd	7,000
		2,600
	TOTAL	91,770
Berm (Waste Mat'l)	Material Placement Cost Cat 777 22.28 hrs at $148/hr	3,315
	Compaction Costs Cat D7 pulling sheeps foot 16 passes for 6 hrs at $54/hr	327
	Grading Cost Cat 120G for 60 hrs at $40/hr.	2,400
	TOTAL	6,042
Berm (Special Mat'l)	Material Procurement 20,000 tons at $3.5/ton	70,000
	Spreading Costs Cat D9 for 40 hrs at $97/hr	3,880
	Compaction Costs Cat D7 pulling sheeps foot 16 passes for 6 hrs at $54/hr.	327
	Grading Cost Cat 120G for 6 hrs at $40/hr.	2,400
	TOTAL	$ 76,607

These costs clearly indicate why mine operators are reluctant to use anything other than available waste material. What is not reflected in this table is the maintenance cost associated with each system and the possible cost involved in widening the haulage road to accommodate a 38 foot wide berm.

Maintenance costs for the guardrail and concrete barrier restraint systems can be assumed to be zero as compared to berm restraint systems. If the berm restraint system has to be completely rebuilt three times a year, after five years of operation the costs would equate the cost of installing a guardrail. Since haul road changes can be expected to occur more often, berm restraint systems constructed of waste material would still be preferable.

Costs associated with widening the roadway cannot be generalized in respect to the overall cost picture. Each situation must be independently evaluated to determine the most economical system applicable.

This cost comparison indicates the economic impact of regulations requiring effective restraint systems. Not reflected is the overall economic analysis of mine operation. If a mine has 15 miles of elevated roadways and the cost is six dollars per foot the total cost to the mine would be $475,200. This would about cover the cost of replacing a medium size haulage vehicle.

4. CONCLUSIONS AND RECOMMENDATIONS

4.1 CONCLUSIONS

4.1.1 Current Restraint Practices

There are very few regulations which address the use of restraint systems on elevated roadways, and they are very general.

Mine utilization of berms vary considerably between mine operations and at different locations for any single operation. This may be attributed to the perceived ineffectiveness of berms constructed to the current rule of thumb recommendations (axle height of largest haulage vehicle).

Mine operators have a vast amount of working experience with their equipment. They probably know more about the capabilities of their equipment than the respective manufacturers. Numerous interviews with mine personnel have indicated the perceived ineffectiveness of berms constructed to the current rule of thumb, axle height, recommendations. Mine operators, therefore, tend to have one of the following three distinct attitudes toward berm construction.

- Current rule of thumb recommendations are judged to be inadequate and to compensate, mine personnel construct berms to a height of between two and three times the axle height, hoping to improve berm effectiveness.

- Current rule of thumb recommendations are accepted or at least not questioned and built to current recommendations in order to avoid confrontation with inspectors.

- Current rule of thumb recommendations are judged to be inadequate but operators continue to construct berms to minimum standards.

4.1.2 Interaction Analysis Capabilities

Interactions between haulage vehicles and guardrails were analyzed using the BARRIER VII computer program to determine the required guardrail configuration. Interactions between haulage vehicles and berms were simulated by scale and computer modeling techniques. The accuracy of the resulting interaction depends on the accuracy of the model used. Model tests performed indicated the mode of the interaction of various vehicles during accident situations. Computer simulations, using the HVOSM computer program performed for the 35-ton haulage vehicle correlates with the field test results. Predicting the interactions of other haulage vehicles is most economically performed by using this simulation technique. The installed restraint system cost ranges from $76 to $92 per foot to restrain a 170-ton haulage vehicle at approach conditions of 30 mph and 30°.

Full scale testing provides the most conclusive information on the interactions between haulage vehicles and berms. Tests were performed to relate the berm size and strength characteristics to vehicle response.

4.1.3 Restraint System Recommendation

Berms are the most economical of the systems which can effectively restrain haulage vehicles from leaving an elevated roadway, if they are constructed to certain height and strength requirements.

Berms must be constructed to a height versus strength relationship that will assure restraint by redirection, rollover, penetration, or berm climb. Generally, vehicles larger than 85 tons require berms constructed to a height of four times the axle height, while vehicles 85 tons or smaller require berms constructed to a height of three times the axle height. Berms must also be constructed to have a slope greater than 40°.

An alternate method of qualifying the berm strength was developed. It provides an acceptable evaluation of the berm strength. By driving a fully loaded haulage vehicle onto the berm at a 45° angle acceptable berm strength measures were obtained that can be related to the corresponding height requirement.

Guardrails which vary from a tubular thrie berm design to a simpler "I" beam/wooden post design were analyzed for effective restraint of haulage vehicles. The choice of a particular guardrail design depends on the vehicle size and the velocity and angle of the approach. Installation costs of guardrails limit their application to situations where there may not be enough room for berm construction, or where the installation may be considered permanent, such that the higher initial cost can be justified on the basis of lower maintenance costs.

The best alternative for effective vehicle restraint involves the use of escape lanes. Escape lanes ideally should be located where required changes in vehicle direction can be accompanied with increasing vehicle speed, such as at the location of a downhill switch-back. Escape lanes should be clearly marked and should provide a smooth transition from the haulage road. The length requirement has been developed for general conditions and depends on the incline of the escape lane, the maximum possible vehicle speed, and the material used to construct the escape lane.

Median berms provide effective restraint when used in combination with escape lanes or when used independent of other restraint systems. Results obtained during this project indicate that a compacted median berm constructed to a width narrower than the inside tire clearance and a height of at least 1.5 times the clearance of the haulage vehicle will provide the safest overall restraint of a runaway haulage vehicle.

Boulders are not considered to be a very effective means of providing vehicle restraint when used by themselves because of the distance required to stop the vehicle after contacting a boulder and the damage which may be incurred by the vehicle. A viable alternative to the independent use of boulders includes the burial of boulders in an earthen berm. This combination reduces the distance required to stop the vehicle and also reduces the severity of the impact.

Barriers can provide effective restraint for the range of approach conditions and vehicle sizes studied during this project. Their advantages include relative indestructibility and the capability of being reused. Their main disadvantages include probable aggravated vehicle damage as a result of an interaction and their high initial cost. Barriers should be used only in areas where maintenance of the restraint system will cause a great economic burden, such as a very heavily traveled, permanent haul road.

4.1.4 Restraint System Applications

Restraint systems should be used on all elevated roadways.

The required size of the berm, if used as the restraint system, is dependent on the maximum possible approach conditions. Declined roadways can generate the maximum approach conditions and require maximum restraint capability. Sharp turns or banked turns on an decline will also require maximum restraint capability. Flat elevated roadways must have berms constructed to restrain the largest haulage vehicle at the maximum approach conditions which can be exhibited.

When guardrails are used as the restraint system, the design requirements are specified by the CSI (Collision Severity Index) values which are a function of the vehicle's parameters and approach conditions. The same roadway description which can result in maximum restraint requirements for berm usage applies to guardrail usage.

4.2 RECOMMENDATIONS

The present attitudes of the mine operators in regard to perceived effectiveness of berms constructed to current recommendations will affect the acceptance of any change to the regulations which may be proposed on the basis of this research effort. In order to gain industry acceptance, investigative results of this project must be publicized to inform the industry of anticipated improvement in the regulations.

Publicizing the results of this project will produce two desirable effects. It will inform the mining industry that active research is being performed which addresses the questions they have asked. Specifically,

is there anything to substantiate the current requirements for berm construction? Secondly, it will inform them of the results of the research and allow them to respond to the information presented before any changes are made in the regulations.

The probability that any one mine would benefit from an effective restraint system is almost a certainty. Accidents summarized in Section 1.3 indicate that a large portion of mine accidents were berm related. Over a period of a few years the number of accidents could equal to the number of mines. These statistics indicate the likelihood of an accident situation occurring at some time for every mine.

Uncertainty of the accident location is the basis for requiring maximum restraint capability at all locations. It can be argued that certain locations, sharp curves or inclined grades are more susceptable to accident situations, but the fact that mechanical failure, environmental conditions, or human error can be the cause of the accident discounts the exclusive location of accident situations.

Restraint system capability is the key to maintaining control of an accident situation so that damage to the vehicle and operator can be minimized. Construction recommendations presented in this report, when implemented, will result in the required restraint capability. Mine safety will be improved if all haul roads are viewed as potential accident locations and restraint systems are constructed to effectively control accidents occurring at the maximum possible approach conditions. Vehicle operators must reflect this accident potential in their routine job performance which should include the use of seat belts and shoulder straps to restrain the operator from leaving the cab during an accident.

5. RECOMMENDATIONS FOR FUTURE RESEARCH

This project has provided the guidelines and recommendations to improve the safety of the surface mine environment by the appropriate application of restraint systems. To further enhance the safety of the mining environment, improvements in the use of dump site restraint systems and the design of the operator's environment are needed.

Safety of the mining environment can be further enhanced by an effective program to delineate the requirement for effective use of restraint systems at the dump site. This location is second only to haul road berms in the frequency of haulage accidents. Present regulations do not provide adequate guidance for the prevention of an accident situation from developing at this location.

Evaluating the requirements for effective restraint systems must begin with a detailed review of the accident reports to determine the particular cause of the accident. Identification into either inadequate restraint system design or back slope failure will provide the statistical basis for the improvement which should result from this program.

The research program should address the soil parameters and geometric design of the dump site to minimize the potential of back slope failure. Additionally, the program should evaluate the requirements for both dump site berms, or mechanical restraint systems. The economic ramifications of each system should be obtained for all restraint systems to provide a statement of economic alternatives based on the user requirements.

A detailed evaluation of the operator's environment is needed which will not only study the structural integrity of the cab, but also address the potential damage which can be incurred if foreign objects penetrate the cab during a rollover. Cab integrity has long been of primary concern in the mining industry where the cabs are fully exposed during a rollover. Haulage vehicles, however, provide a measure of protection to the cab by their design, and thus have not been fully scrutinized as to their capability for operator protection.

The primary concern of cab integrity receives additional emphasis when related to the possible intrusion of foreign objects during a rollover. It has been commonplace to find batteries and fuel tanks mounted adjacent to the cab. These articles can become projectiles during a rollover if not adequately anchored. A program is needed to fully evaluate the structural integrity requirement of the cab and to evaluate the cab and vehicle design for the prevention of cab intrusion by foreign objects.

(THIS PAGE INTENTIONALLY LEFT BLANK)

REFERENCES

1. Code of Federal Regulations, Title 30, section 57.9, Paragraph 22, 1978.

2. Baker, W. E., Westine, P. S., and Dodge, F. T., "Similarity Methods in Engineering Dynamics", Spartan Books, Rochelle Park, New Jersey, 1973.

3. Construction Machinery 1975, U.S. Department of Commerce, Bureau of the Census, Industry Division, Washington, DC 20233.

4. Construction Machinery 1976, U.S. Department of Commerce, Bureau of the Census, Industry Division, Washington, DC 20233.

5. Construction Machinery 1977, U.S. Department of Commerce, Bureau of the Census, Industry Division, Washington, DC 20233.

6. Segal, D. J., "Highway-Vehicle-Object-Simulation Model--1976, Volume 4 Engineering Manual-Validation", Calspan Corporation, Report No. FHWA-RD-76-165, February 1976.

7. Powell, C. H., "BARRIER VII: A Computer Program for Evaluation of Automobile Barrier Systems", University of California, Berkeley, Report UC SESM 70-17, August, 1970.

8. Dawson, V. E., "Observations Concerning On-Site Brake Testing of Large Mining Tracks in British Columbia", SAE paper No. 750560.

9. Caterpillar Performance Handbook, Ed. 9, Caterpillar Tractor Company, October 1978.

10. Nichols, H. L., "Moving the Earth", 2nd Edition, North Castle Books, Greenwich, Connecticut, 1962.

11. Bekker, M. G., "Tire Selection for Off-Road Vehicles Part 1: Homogenous Soils", Design News, OEM 9-17-73.

12. Bekker, M. G., "Tire Selection for Off-Road Vehicles Part 2: Non-Homogenous Soils", Design News, OEM 12-17-73.

13. "Mechanics of Vehicles", Penton Education Division, Penton Publishing Company, 1957.

14. Kaufman, Walter W., and Ault, James C., "Design of Surface Mine Haulage Roads - A Manual," Information Ciruclar 8758, U.S. Bureau of Mines, 1977.

15. Gill, William R. and Vandenberg, Glen E., "Soil Dynamics in Tillage and Traction", U.S. Department of Agriculture, Agriculture Handbook No. 316.

List of References (Cont'd)

16. Bekker, M. G., "Theory of Land Locomotives", the University of Michigan Press, Ann Arbor, Michigan, 1956.

17. Bekker, M. G., "Tire Selection for Off-Road Vehicles", Design News, September 17, 1973, and December 17, 1973.

APPENDIX A

DETERMINATION OF MODEL VEHICLE MASS MOMENT OF INERTIA

(THIS PAGE INTENTIONALLY LEFT BLANK)

The equation of motion for any shape body oscillating about a fixed point of rotation is defined by the following relationship:

$$\omega^2 = \frac{WL}{J_X} = \frac{4\pi}{\tau^2} \qquad \text{(Eq. A-1)}$$

where,

J_X = mass moment of inertia of the system about the axis of rotation, in-lb-sec^2.

L = distance from the center line of rotation to the center of gravity of the suspended mass, in.

W = weight of suspended object, lbs.

τ = duration of one complete oscillation, sec/cycle

ω = natural frequency of oscillating mass, rad/sec

π = dimensionless constant

If a body whose mass moment of inertia is to be determined is suspended horizontally on knife edges as illustrated in Figure B-1, and if the system is displaced from its equilibrium position through an angle of less than five degrees and allowed to swing free, the natural frequency of the body can be determined by timing the duration of the oscillation. In actual practice, the frequency is determined as an average value associated with 20-30 cyclic oscillations. The mass moment of inertia of the body about its own axis or center-of-gravity is then determined by using the parallel axis theorem:

$$J_O = J_X - \frac{WL^2}{g} \qquad \text{(Eq. A-2)}$$

where,

J_O = mass moment of inertia of the system about the center of gravity of the system, in-lb-sec^2.

g = gravitational constant

Combining equations (B-1) and (B-2) results in the following relationship:

$$J_O = WL\left(\frac{\tau^2}{4\pi^2} - \frac{L}{g}\right) \qquad \text{(Eq. A-3)}$$

Preceding page blank

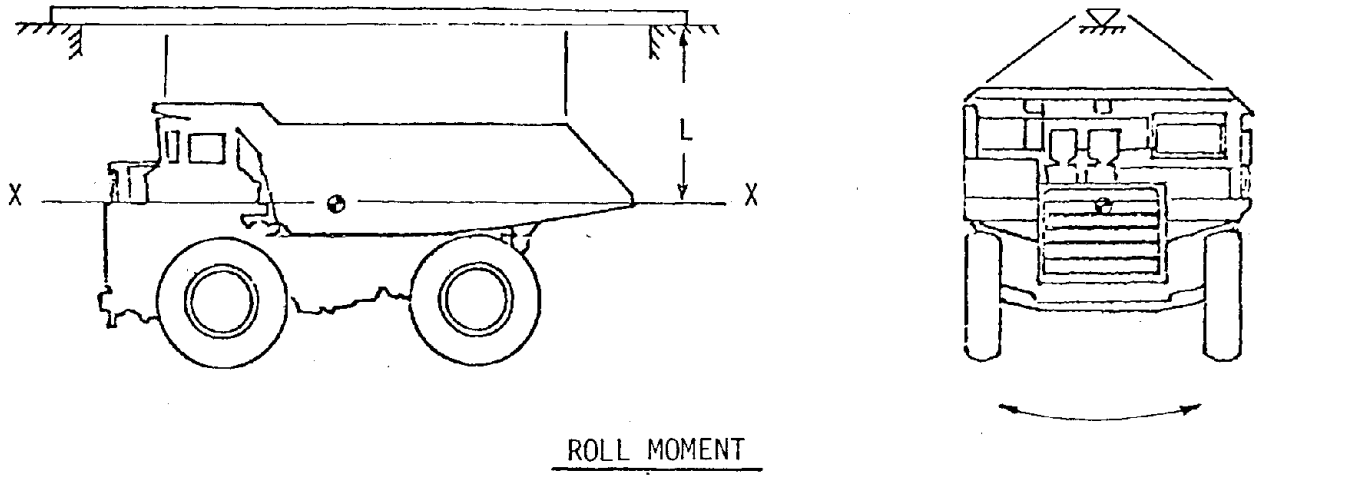

FIGURE A-1 VEHICLE POSITIONS FOR DETERMINING MASS MOMENT OF INERTIA

By selecting the axis of rotation parallel to the major axis of the model vehicle using either an empty or loaded vehicle configuration, the mass moment of inertia about the respective axis for each configuration can be determined.

The mass moment of inertia of a body as determined by Equation B-3 is dependent upon the suspended length, L, and the corresponding system oscillation, τ. During model testing, a 35-ton haulage vehicle was suspended as illustrated in Figure A-1 and A-3 arbitrarily selected suspension lengths employed, the frequency of oscillation recorded, and the resulting inertia terms evaluated by Equation A-3. The corresponding test data for the various size vehicles, representing a loaded condition, are summarized in Table A-1. The inertia terms were averaged for the three different suspension lengths and considered as representative value for each category of haulage vehicle.

TABLE A-1 - SUMMARY OF VEHICLE MASS MOMENTS OF INERTIA FOR SCALE MODELS

TEST NO.	VEHICLE	WEIGHT (LB.)	AXIS	SUSPENSION LENGTH (IN.)	FREQUENCY (CYCLE/SEC)	INERTIA (LB-SEC^2-IN)	AVG. INERTIA (LB-SEC^2-IN) MODEL	INERTIA (LB-SEC^2-IN) FULL-SCALE EQUIVALENCE
1	35-ton	17.18	X-X	4.3125 11.0 8.5625	1.3269 0.9219 1.0298	.252 .239 .254	.25	0.8×10^6
2	35-ton	17.18	Y-Y	6.0625 8.5625 10.8125	1.0684 0.9639 0.8785	.677 .751 .899	.78	2.5×10^6
3	35-ton	17.18	Z-Z	8.0625 10.1875 12.5625	1.0070 0.9252 0.8495	.570 .564 .560	.56	1.8×10^6
4	85-ton	40.5	X-X	9.125 7.750 12.625	0.9804 1.0336 0.8474	1.01 1.15 1.32	1.16	3.7×10^6
5	85-ton	40.5	Y-Y	7.750 10.6875 13.0	0.9412 0.8826 0.8192	2.68 2.10 2.16	2.31	7.4×10^6
6	85-ton	40.5	Z-Z	9.5625 7.625 11.625	0.8960 0.9422 0.8399	2.64 2.72 2.74	2.72	8.6×10^6
7	170-ton	67.5	X-X	11.124 15.50 18.625	0.9000 0.7804 0.7174	1.86 1.56 1.27	1.56	5.0×10^6
8	170-ton	67.5	Y-Y	14.75 18.75 18.375	0.7692 0.6984 0.7013	4.62 4.30 4.89	4.60	14.7×10^6
9	170-ton	67.5	Z-Z	13.75 17.375 21.125	0.7811 0.7154 0.6591	5.51 5.30 5.20	5.30	17.1×10^6

APPENDIX B

HAULAGE VEHICLE DATA

(THIS PAGE INTENTIONALLY LEFT BLANK)

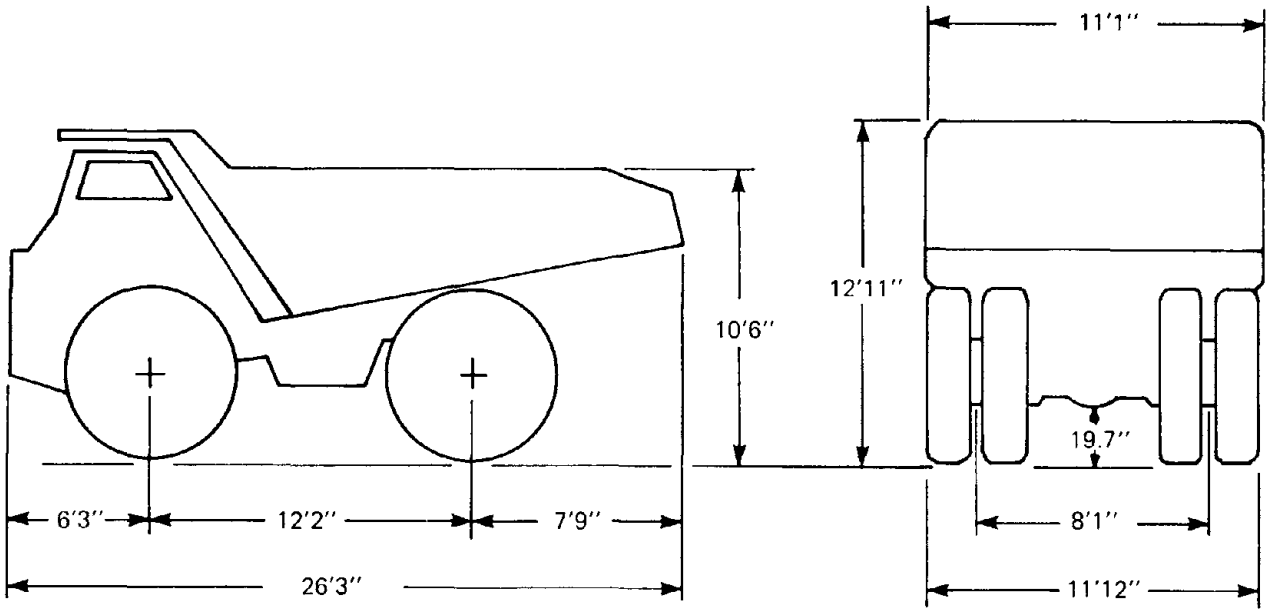

SPECIFICATIONS

CARRY CAPACITY: 35 tons	**EMPTY WEIGHT:** 61,800 lb
TIRE TYPE: 18.00 × 33, 28PR	**TURNING CIRCLE:** 709 in.

CENTER OF GRAVITY (in.)	Empty	Loaded
Vertical (above ground)	60	86
Horizontal (from rear axle)	72	50

WEIGHT DISTRIBUTION (lb)	Empty	Loaded
Front Axle	30,470	44,100
Rear Axle	31,330	87,670

Preceding page blank

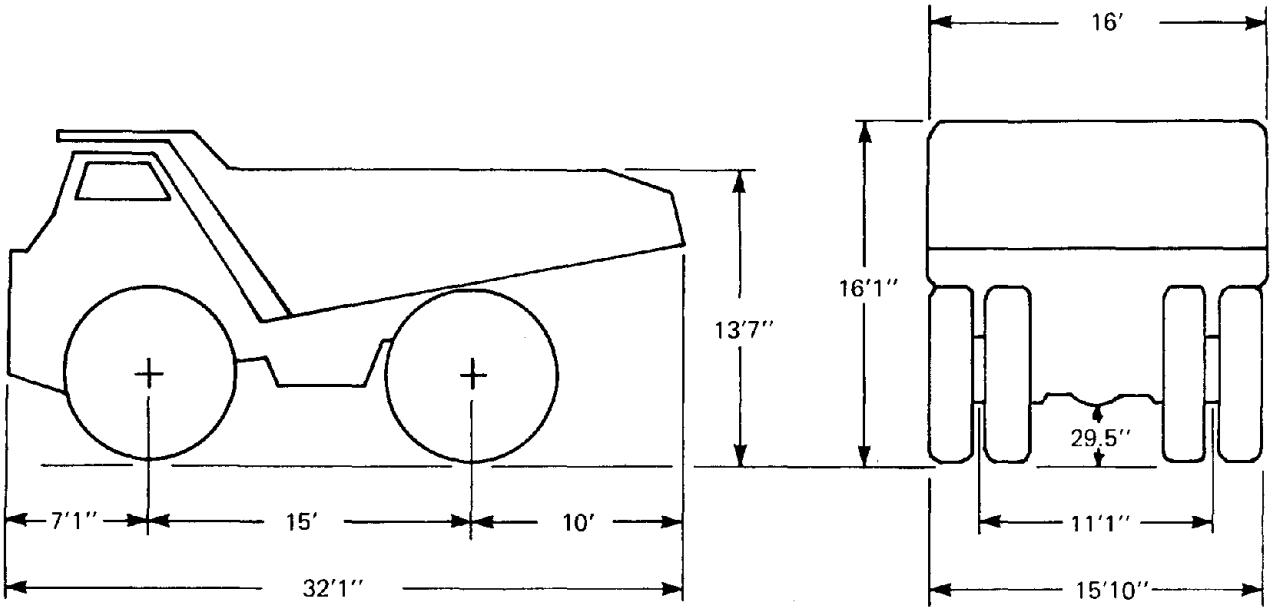

SPECIFICATIONS

CARRY CAPACITY: 85 tons
EMPTY WEIGHT: 140,000 lb
TIRE TYPE: 24.00 × 49, 42PR
TURNING CIRCLE: 1056 in.

	Empty	Loaded
CENTER OF GRAVITY (in.)		
Vertical (above ground)	76	117
Horizontal (from rear axle)	83	55
INERTIA DATA (lb-sec^2/in.		
Sprung Mass	230	710
Unsprung Front Mass	33	33
Unsprung Rear Mass	100	100
Moment of Inertia (I_x:lb-sec^2/in.)	1.5×10^6	3.9×10^6
WEIGHT DISTRIBUTION (lb)		
Front Axle	66,400	94,720
Rear Axle	73,600	215,280

	Empty	Loaded
SUSPENSION DATA		
Front Spring Rate (lb/in./strut)	4,290	14,200
Rear Spring Rate (lb/in./strut)	4,950	10,000
Velocity Squared Damping (lb-sec^2/in.^{2}/strut)		
Front Strut Extension		
Front Strut Compression	275	275
Rear Strut Extension	25	25
Rear Strut Compression	275	275
Front Friction (lb/strut)	25	25
Rear Friction	5,000	10,000
Front Suspension Travel (in.)		
Extension		
Compression	4.0	7.0
Rear Suspension Travel (in.)	8.5	5.5
Extension	2.25	5.25
Compression	4.25	1.25

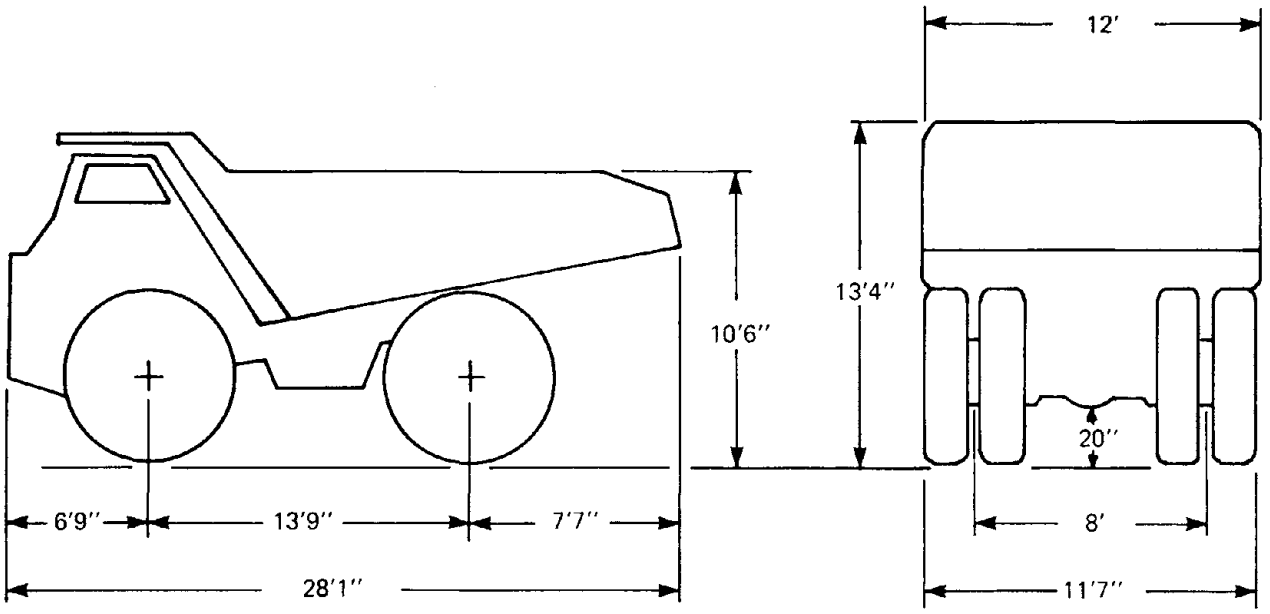

SPECIFICATIONS

CARRY CAPACITY: 35 tons	**EMPTY WEIGHT:** 61,000 lb
TIRE TYPE: 18.00 × 33, 28PR	**TURNING CIRCLE:** 720 in.

CENTER OF GRAVITY (in.)	Empty	Loaded
Vertical (above ground)	80	80
Horizontal (from front axle)	89.26	112.73

WEIGHT DISTRIBUTION (lb)	Empty	Loaded
Front Axle	28,000	41,500
Rear Axle	33,000	89,500

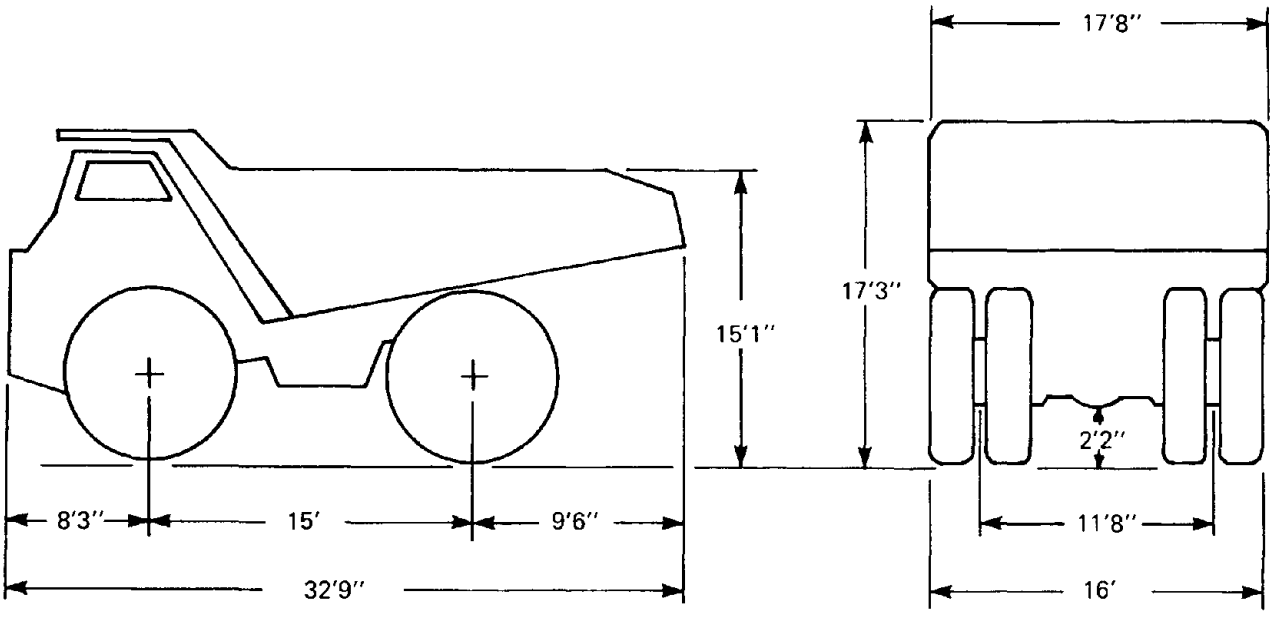

SPECIFICATIONS

CARRY CAPACITY: 85 tons
EMPTY WEIGHT: 128,200 lb
TIRE TYPE: 24.00 × 49
TURNING CIRCLE: 720 in.

	Empty	Loaded
CENTER OF GRAVITY (in.)		
Vertical (above ground)	62	97
Horizontal (from rear axle)	85	65
INERTIA DATA (lb-sec^2/in.		
Sprung Mass	253.9	694.3
Unsprung Front Mass	8.0	8.0
Unsprung Rear Mass	69.9	69.9
WEIGHT DISTRIBUTION (lb)		
Front Axle	60,542	107,683
Rear Axle	57,658	190,517

	Empty	Loaded
SUSPENSION DATA		
Front Suspension Travel (in.)		
Extension	1.1	5.1
Compression	11.3	7.3
Rear Suspension Travel (in.)		
Extension	0	4.1
Compression	11.0	6.9
Front Spring Rate (lb/in./strut)	2,400	7,300
Rear Spring Rate (lb/in./strut)	4,000	24,000

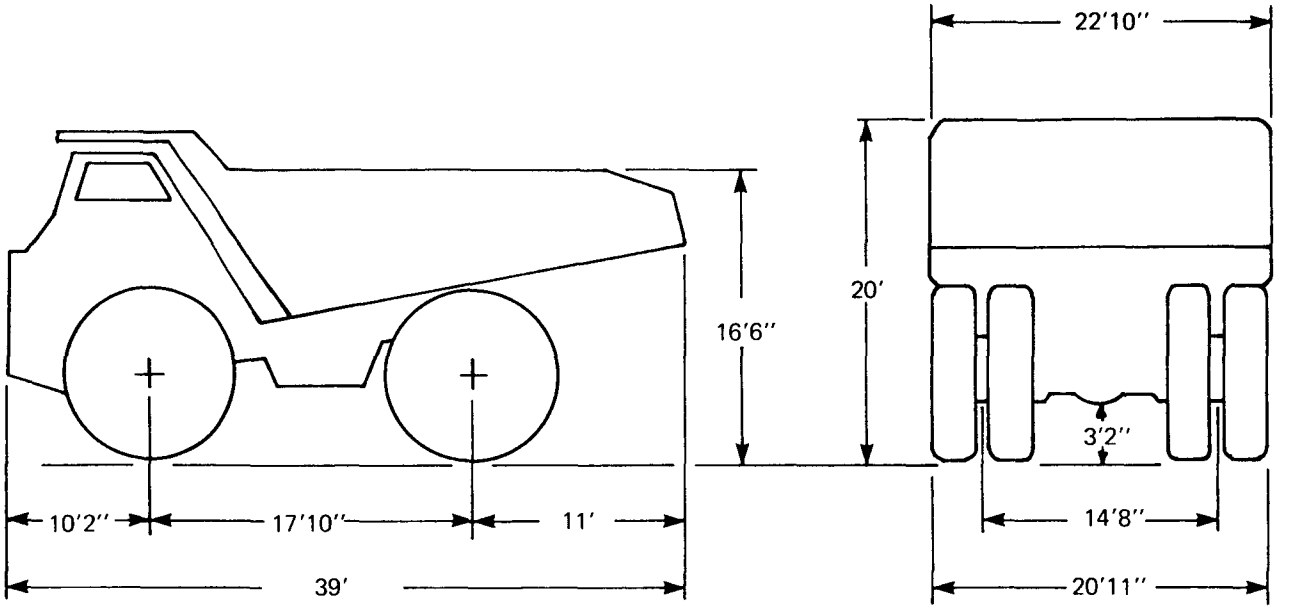

SPECIFICATIONS

CARRY CAPACITY: 170 tons
EMPTY WEIGHT: 212,500 lb
TIRE TYPE: 36.00 × 51, 50PR
TURNING CIRCLE: 972 in.

	Empty	Loaded
CENTER OF GRAVITY (in.)		
Vertical (above ground)	*	*
Horizontal (from rear axle)	100.4	71.3
INERTIA DATA (lb-sec^2/in.		
Sprung Mass	307.7	1,188.5
Unsprung Front Mass	75.4	75.4
Unsprung Rear Mass	178.3	178.3

	Empty	Loaded
WEIGHT DISTRIBUTION (lb)		
Front Axle	99,700	184,200
Rear Axle	112,800	275,823
SUSPENSION DATA (lb/in./strut)		
Front Spring Rate	9,165	29,762
Rear Spring Rate	47,010	124,921

(THIS PAGE INTENTIONALLY LEFT BLANK)

APPENDIX C

HVOSM COMPUTER PROGRAM SYMBOLOGY

(THIS PAGE INTENTIONALLY LEFT BLANK)

The HVOSM symbology is presented in this section. The listing of symbols is ordered with respect to analytical symbol and includes a corresponding program symbol, a brief definition and an equation number referencing the calculation of the variable. Input variables are indicated by an I in the equation number column.

ANALYTICAL SYMBOL	PROGRAM SYMBOL	EQN NO.	DEFINITION	UNITS
a	A	I	Distance along vehicle fixed x axis from the sprung mass center of gravity to the center line of the front wheels	in.
a_i, b_i, c_i		155	Directional components of a line perpendicular to both the normal to the wheel plane and the radial tire force, F_{R_i}	---
APD APDMAX	APD APDMAX	345 I	Accelerator pedal deflection and maximum accelerator pedal deflection	in
$a_{s_i}, b_{s_i}, c_{s_i}$	AS(4) BS(4) CS(4)	258	Directional components of a line perpendicular to both a normal to the tire-terrain contact plane and the line of intersection of the wheel and ground planes	
$a_{x_i}, b_{x_i}, c_{x_i}$	AX(4) BX(4) CX(4)	99	Direction components of a line perpendicular to both a normal to the tire-terrain contact plane and the vehicle fixed y axis	
$a_{y_i}, b_{y_i}, c_{y_i}$	AY(4) BY(4) CY(4)	104	Direction component of a line perpendicular to both a normal to the tire-terrain contact plane and the vehicle fixed x axis	
[A]	AMTX(3,3)	53	Transformation matrix from vehicle fixed to space fixed coordinate systems	
$(A_{INT})_i$	AINTI	267	Intersection area of cutting plane i with the sprung mass	in^2
$[A_j]$	AJMTX(3,3)	134	Transformation matrix from wheel fixed to vehicle fixed coordinate systems	
AMU	AMU	I	Tire-terrain friction coefficient at zero speed and nominal tire loading	
AMUG	AMUG(5)	I	Tire-terrain friction coefficient factor for 5 terrain tables	
$(AP)_F$	APF(21)	I	Anti-pitch coefficients for front suspension positive for anti-pitch for forward braking	lb/lb-ft
$(AP)_R$	APR(21)	I	Anti-pitch coefficients for rear suspension, effective at the wheels; positive for anti-pitch effect for forward braking	lb/lb-ft

ANALYTICAL SYMBOL	PROGRAM SYMBOL	EQN NO.	DEFINITION	UNITS
$(AR)_j$	ARBRF ARBRR	I	Drive axle ratio (propeller shaft speed/wheel speed). Default of 1.0	
A_0, A_1, A_2	A0,A1,A2	I	Constant coefficients for tire side force due to slip angle	
A_3, A_4	A3,A4	I	Constant coefficients for tire side force due to camber angle	
b	B	I	Distance along the vehicle fixed x axis from the sprung mass center of gravity to the centerline of the rear wheels (entered positive)	in.
[B]	BMTX(3,3)	134	Transformation matrix from wheel fixed to space fixed coordinate systems	
B_{FP1} B_{FP2}	BFP1 BFP2	I	First and second order coefficients for relationship between brake pedal force and brake system pressure	psi/lb psi/lb^2
$[B_n]$	BNMTX(3,3)	60	Transformation matrix from orientation of vehicle axes at indexing to space fixed axes (Euler angles= $\psi_n', \theta_n', \phi_n'$)	
C_{co}		215	Small angle camber stiffness	lb/rad
C_F, C_R	CF CR	I	Front and rear viscous damping coefficient for a single wheel, effective at the wheel for the front and at the spring at the rear	lb-sec/in
C'_F, C'_R	CFP CRP	I	Front and rear coulomb damping for a single wheel, effective at the wheel for the front and at spring for the rear	lb
$[C_i]$	CMTX(3,4)	110	Coefficient matrix for simultaneous solution of the ground contact point	
$\overline{CONS}$	CONS	I	Ratio of conserved energy to total energy absorbed by the sprung mass	
$[C_n]$	CNMTX(3,3)	60	Transformation matrix from vehicle fixed axes to most recently indexed axes (Euler angles= $\psi_r', \theta_r', \phi_r'$)	
C_{RRMi}	RRMC(4)	I	Rolling resistance moment coefficient	lb-in/lb
C_{So}		214	Small angle cornering stiffness	lb/rad
(CT_i)	TCT(12)	I	Closed throttle engine torque	lb-ft

ANALYTICAL SYMBOL	PROGRAM SYMBOL	EQN NO.	DEFINITION	UNITS
C_{Ti}	CT(4)	I	Circumferential tire force stiffness	lb
C'_{ψ}	CPSP	I	Coulomb resistance torque in the steering system effective at the wheels	lb-in
C_1, C_2, C_3	CONE CTWO CTHREE	I	Coefficients in relationship approximating aerodynamic and rolling resistance	
[D]	DMTX(10,11)	140	Mass matrix of coupled second order differential equations. Column 11 contains the forcing functions	
Dax	DELTAX	342	Desired vehicle acceleration	in/sec^2
DELB DELE DDEL	DELB DELE DDEL	I I I	Beginning, end, and incremental wheel deflection for entered front wheel camber table	in
DIST	DIST	I	Desired speed differential nulling distance	in
DRWHJ	DRWHJ	I	Incremental tire deflection for calculation of the equivalent tire force-deflection characteristic in the radial mode	in
D_{1i}, D_{2i}, D_{3i}	D1(4) D2(4) D3(4)	87	Direction components of a line perpendicular to the normals of both the wheel plane and the tire-terrain contact plane	
e_i	EI	320	Error between predicted and desired path at the ith viewing position	in
EN	EN	I	Number of points at which e_i is determined	
F_{APi}	APITCH	288	Anti-pitch force at wheel i	lb
F_{ARi}		267	Force at wheel i due to auxiliary roll stiffness	lb
F_B	FB		Resistance force normal to the contact surface of a deformable barrier	lb
FBRK	FBRK	346	Brake pedal force	lb
F_{c_i}	FC(4)	225	Circumferential tire force	lb
F_{cxui} F_{cyui} F_{czui}	FCXU(4) FCYU(4) FCZU(4)	254	Components of the circumferential tire force along the x,y, and z axes	lb
F_j	FJP(35)	144	Table of equivalent radial spring forces as a function of deflection	lb
F_{JFi}	FJF(4)	179	Jacking force at wheel i	lb
$(Fn)_t$	FN	298	Vehicle force produced by deformation of the vehicle structure normal to the contacted surface	lb

ANALYTICAL SYMBOL	PROGRAM SYMBOL	EQN NO.	DEFINITION	UNITS
F_{NSTi}	FNSTI(3)	300	Structural hard point force	lb
F_{R_i}	FR(4)	114	Radial tire force in the plane of the wheel	lb
F'_{Ri}	FRCP(4)	212	Tire force perpendicular to the tire-terrain contact plane	lb
(FRICT)	FRICT	306	Friction force acting between the vehicle sprung mass and barrier	lb
F_{Rxui} F_{Ryui} F_{Rzui}	FRXU(4) FRYU(4) FRZU(4)	253	Components of F'_{Ri} along the sprung mass axes for wheel i	lb
$\Sigma F_{Rx'i}$	SFRX(4)	144	Summation of the components of radial spring mode forces over tire i, with respect to space	lb
$\Sigma F_{Ry'i}$	SFRY(4)	145		
$\Sigma F_{Rz'i}$	SFRZ(4)	146		
F_{Si}	FS(4)	227	Tire side force in the plane of the tire-terrain contact patch perpendicular to the line of intersection of the wheel plane and ground plane	lb
F'_{Si}		220	Resultant side force corresponding to small angle properties for slip and camber angles	lb
$(F_{si})_{max}$		219	Maximum achievable side force as limited by the available friction	lb
ΣF_{xs}	SFXS	337 351	Sprung mass impact force or combination of rolling resistance and aerodynamic drag acting along the vehicle x axis	lb
F_{sxui} F_{syui} F_{szui}	FSXU(4) FSYU(4) FSZU(4)	256	Components of tire side force, F_{si} along the sprung mass axes	lb
F_{xui} F_{yui} F_{zui}	FXU(4) FYU(4) FZU(4)	259 260 261	Total tire force components along the vehicle axes	lb
ΣF_{xu} ΣF_{yu}	SFXU SFYU	353 354	Resultant forces acting on the vehicle through the unsprung masses in the x and y directions	lb
ΣF_{ys}	SFYS	307	Sprung mass impact force acting along the vehicle y axis	lb
ΣF_{zs}	SFZS	307	Sprung mass impact force acting along the vehicle z axis	lb
ΣF_{Z1}	SFZ1	356	Resultant force transmitted through the suspensions in the z direction	lb
F_{1Fi} F_{1Ri}	F1FI(2) F1RI(2)	174 184	Front and rear suspension coulomb damping forces for a wheel, effective at the wheel for the front and at the spring for the rear	lb

ANALYTICAL SYMBOL	PROGRAM SYMBOL	COMMON	DEFINITION	UNITS
F_{2Fi} F_{2Ri}	F2FI(2) F2RI(2)	175 185	Front and rear suspension spring and bumper forces for a wheel, effective at the wheel for the front and at the spring for the rear	lb
g	G	I	Acceleration due to gravity	in/sec^2
$GEAR_1$ $GEAR_2$ $GEAR_3^2$ $GEAR_4$	GEAR1 GEAR2 GEAR3 GEAR4	I	Transmission gear ratios	—
G_{1j}	GN(1,J)	I	Lever arm lengths in brake types 1,2 and 3	in
G_{2j}	GN(2,J)	I	Brake actuation constant, assumed to be equal for both shoes of brake types 1 and 2	
G_{3j}	GN(3,J)	I	Effective lining-to-drum or lining to-disk friction coefficient at design temperature for all shoes or disks in types 1,2 and 4 and for the primary shoe of type 3	
G_{4j}	GN(4,J)	I	Cylinder area for actuation of leading shoe of brake type 1, or for each shoe in types 2 and 3. Also used for total cylinder area per side of disk in type 4	in^2
G_{5j}	GN(5,J)	I	Cylinder area for actuation of trailing shoe of brake Type 1	in^2
G_{6j}-G_{11j}	GN(6,J)-GN(11,J)	I	Brake dimensions for type 3.	in
G_{12J}	GN(12,J)	I	Effective lining to drum friction coefficient for secondary shoe of brake type 3	
G_{13J}	GN(13,J)	I	Mean lining radius for brake type 4	in
G_{14j}	GN(14,J)	I	Coefficient of heat transfer for convective losses	
G_{15j}	GN(15,J)	I	Specific heat of brake assembly	BTU/lb/°F
G_{16j}	GN(16,J)	I	Effective weight of brake assembly for heat absorption	lb
h_i	HI(4)		Tire rolling radius	in
I_{Dj}	FIDJ(2)	I	Driveline inertia for front or rear (Note that a value of zero is entered at the non-driving end of the vehicle)	$lb\text{-}sec^2\text{-}in$

ANALYTICAL SYMBOL	PROGRAM SYMBOL	COMMON	DEFINITION	UNITS
I_R	XIR	I	Rear unsprung mass moment of inertia about a line through its center of gravity and parallel to the vehicle x axis	$lb\text{-}sec^2\text{-}in$
I_{wj}	FIWJ(4)	I	Rotational inertia of an individual wheel at the front or rear	$lb\text{-}sec^2\text{-}in$
Ix,Iy,Iz	XIX XIY XIZ	I	Spring mass moments of inertia about the vehicle axes	$lb\text{-}sec^2\text{-}in$
Ixz	XIXZ	I	Spring mass roll-yaw product of inertia	$lb\text{-}sec^2\text{-}in$
(I'x)t		47	Effective inertial term due to time varying positions of the unspring masses	
(I'z)t		47	Effective inertial term due to time varying positions of the unspring masses	
(I'xz)t		47	Effective inertial term due to time varying positions of the unspring masses	
(I'yz)t		47	Effective inertia term due to time varying positions of the unspring masses	
I_Ψ	XIPS	I	Moment of inertia of the steering system effective at the front wheels (includes both wheels)	$lb\text{-}sec^2\text{-}in$
K_d	FKD	I	Performance parameter characterizing understeer/oversteer properties of the vehicle	sec^2/in
K_F,K_R	AKF AKR	I	Front and rear suspension load deflection rate in the quasi-linear range about the design position effective at the front wheels and the rear springs	lb/in
K_{FC},K_{RC}	AKFC AKRC	I	Coefficients for the compression bumpers of the front and rear suspension effective at the front wheels and rear springs	
K'_{FC},K'_{RC}	AKFCP AKRCP	I	Coefficients for the cubic terms of the suspension compression bumpers	
K_{FE},K_{RE}	AKFE AKRE	I	Coefficients for the extension bumpers of the front and rear suspension effective at the front wheels and rear springs	

ANALYTICAL SYMBOL	PROGRAM SYMBOL	ECON INPUT	DEFINITION	UNITS
K'_{FE}, K'_{RE}	AKFEP AKREP	I	Coefficients for the cubic terms of the suspension extension bumpers	
K_P	FKP	328	Driver steer control gain	
K_{RS}	AKRS	I	Rear axle roll-steer coefficient, positive for roll understeer	
K_{S1}, K_{S2}	FKS1 FKS2	I	Drivers estimate of vehicle braking and accelerating gains	
K_{ST1}	AKST(3)	I	Structural hard point spring rates	lb/in
K_T	AKT	I	Radial tire rate in the quasi-linear range	lb/in
K_V	AKV	I	Load-deflection characteristic of the vehicle structure	lb/in^3
$K_{\delta S}, K_{\delta S1}, K_{\delta S2}, K_{\delta S3}$	AKDS AKDS1 AKDS2 AKDS3	I	Coefficients of the cubic representation of rear wheel steer as a function of deflection for independent rear suspension	
K_ψ	AKPS	I	Load-deflection rate for the linear steering stop, effective at the wheels	lb-in/rad
K_1	AK1	I	Slope of P_R vs P_F for values of P_F between P_1 and P_2	
K_2	AK2	I	Slope of P_R vs P_F for values of P_F greater than P_2	
$(LF)_i$	FLF	I	Fade coefficient for brake at wheel i	
M_S	XMS	I	Sprung mass	$lbsec^2/in$
M_{UF}, M_{UR}	XMUF XMUF	I	Front (both sides) and rear unsprung masses. Note $M_1=M_2=M_{UF}/2$, $M_3=M_{UR}$	$lbsec^2/in$
M_1, M_2	$\frac{XMUF}{2}$		Right and left front unsprung masses	$lbsec^2/in$
M_3	XMUR	I	Rear unsprung mass	$lbsec^2/in$
NBX	NBX(5)	I	Number of x' boundaries supplied for 5 terrain tables	
NBY	NBY(5)	I	Number of y' boundaries supplied for 5 terrain tables	
NDEL	NDEL		Number of entries in the front wheel camber table	
NX	NX(5)		Number of x' grid points in 5 terrain tables	
NY	NY(5)		Number of y' grid points in 5 terrain tables	
NZTAB	NZTAB	I	Number of terrain tables entered	

ANALYTICAL SYMBOL	PROGRAM SYMBOL	ECON INPUT	DEFINITION	UNITS
P_1, P_2	PONE PTWO	I	"Break" pressures for brake system proportioning valve	psig
$(RATIO)_i$			Factor used to modify the nominal tire-terrain friction coefficient at wheel i to reflect the effects of vehicle speed and tire loading	
R_{BB}	RBB	280	Constant for barrier bottom plane	in
R_{BI}	RBI	269	Constant for barrier face plane	in
R_{BT}	RBT	284	Constant for barrier top plane	in
R_{B_1}	RB1	273	Constant for the plane perpendicular to the barrier face plane and containing the axis of rotation	in
NZS	NZS	I	Flag to indicate whether the variable increment terrain table is supplied, =0,no,≠0, yes	
$\Sigma N_{\phi F}$	SNPF	347	Roll moment acting on the front axle	lb-in
$\Sigma N_{\phi R}$	SNPR	360	Roll moment acting on the rear axle	lb-in
$\Sigma N_{\phi S}$	SNPS	308	Roll moment on the sprung mass resulting from sprung mass impact forces	lb-in
$\Sigma N_{\theta S}$	SNTS	309	Pitch moment on the sprung mass resulting from sprung mass impact forces	lb-in
$\Sigma N_{\psi S}$	SNPSS	310	Yaw moment on the sprung mass resulting from sprung mass impact forces	lb-in
$\Sigma N_{\phi U}$ $\Sigma N_{\theta U}$ $\Sigma N_{\psi U}$	SNPU SNTU SNPSU	357 358 359	Moments acting on the sprung mass produced by forces acting on the unsprung masses	lb-in
P,Q,R	P,Q,R	+8	Scalar components of the sprung mass angular velocity along the vehicle x,y and z axes	rad/sec
P_C	PC	I	Hydraulic pressure in brake system master cylinder	psig
P_j	PP(2)	197	Hydraulic pressure in brake cylinders at front or rear brakes	psig
(PS)			Prop shaft speed	rpm

ANALYTICAL SYMBOL	PROGRAM SYMBOL	EQN NO	DEFINITION	UNITS
(PT)	XPS	I	Pneumatic trail of front tires	in
R_F, R_R	RF, RR	I	Auxiliary roll stiffness of the front and rear suspensions	lb/in/rad
(RPME)	RPME	211	Engine speed	rpm
$(RPS)_i$	RPSI(4)	44	Rotational velocity of wheel i, positive for forward motion of the vehicle	rad/sec
R_{RMi}	RRM(4)	352	Rolling resistance moment acting on wheel i	lb-in
R_W	RW	I	Undeflected tire radius	in
RWHJB RWHJE	RWHJB RWHJE	I	Beginning and ending radii for calculation of the radial tire force-deflection characteristic used in the radial tire mode	in
SET	SET	I	Ratio of permanent deflection to maximum deflection of deformable barrier	
S_i	SI(4)	173 183	Total suspension force for a wheel, acting at the front wheels and rear springs	lb
$(SLIP)_i$	SLIP(I)	241	The amount by which the rotational speed of wheel i is less than that of free rotation expressed as a decimal portion of the speed of free rotation	
$(SLIP)_{\mu i}$	SLIPP	198	The value of (SLIP)i, at a given wheel center speed U_{Gi} for which the value of μ_{x_i} is a maximum	
SP_n	ST(5,2)	I	Coefficients for straight line segments defining the desired path	
$(S_1)_i$, $(S_2)_i$, $(S_3)_i$	S1I S2I S3I	284 285 286	Characteristic lengths of intersection area between the sprung mass and barrier	in
t	T		Time	sec
T_b	TESTB	I	Braking indifference level	in/sec
T_B, T_E TINCR	TB, TE TINCR	I	Beginning, ending and incremental times for entry of control tables $(TQ)_F$, $(TQ)_R$ and Ψ_F	sec
T_F, T_R	TF, TR	I	Front and rear track	in
T_i	TI(4)	225	Circumferential tire force resulting from applied torque	lb
T_I, T_L	TIL TL	I	Driver steering model lag and lead times	sec
$(TQ)_{Bi}$	TQB(4)	204	Brake torque at wheel i	lb-ft
$(TQ)_{Dj}$	TQD(4)	211	Drive line torque at prop shaft at vehicle end j	lb-ft
$(TQ)_E$	TQE	210	Engine torque	lb-ft
$(\overline{TQ})_F$ $(\overline{TQ})_R$	TQF(50) TQR(50)	I	Front and rear torque tables for a single wheel and effective at the wheel (positive for traction, negative for braking)	lb-ft
(TR)	TTTR	I	Transmission ratio (speed ratio of engine to prop shaft)	
T_{R_1}, T_{R_2}	TESTR1 TESTR2	I	Lower and upper skid thresholds	
T_S	TS	I	Distance between spring mounts for a solid rear axle	in
T_{SF}	TSF	I	Distance between spring mounts for a solid front axle	in
(TS)	TTTS	I	Throttle setting expressed as the decimal portion of wide open throttle	
T_{S1}, T_{S2}	TESTS1 TESTS2	I	Driver threshold/indifference levels for positive and negative speed errors	in/sec
(TYPE)	NBTYPE	I	Brake type indicator	
$T_{1\Psi}$	T1PSI	36	Coulomb friction torque in steering system effective at the wheel	lb-in
$T_{2\Psi}$	T2PSI	36	Resistance torque produced by the front wheel steer stops, effective at the wheel	lb-in
u,v,w	U,V,W	48	Scalar components of linear velocity of the sprung mass along the sprung mass x,y and z axes	in/sec
u',v',w'	DXCP DYCP DZCP	64	Scalar components of linear velocity of the sprung mass along the space fixed x',y' and z' axes	in/sec
u_i, v_i, w_i	UI(4) VI(4) WI(4)	90-98	Scalar components of the tire contact points linear velocity along the vehicle axes	in/sec
U_{Gi}	UG(4)	103	Wheel center forward velocity in direction parallel to the tire-terrain contact plane	in/sec
U_{Gwi}	UGW(4)	195	Ground contact point velocity along the circumferential direction of the wheel	in/sec
u'_n v'_n w'_n	UNP(17) VNP(17) WNP(17)	282	Components of the velocity of the three or four points that define the intersection area of the barrier and vehicle along the space-fixed axes	in/sec

ANALYTICAL SYMBOL	PROGRAM SYMBOL	EQN NO	DEFINITION	UNITS
u'_r v'_r w'_r	URP VRP WRP	303	Components of the velocity of the point of application of the sprung mass impact force along the space-fixed axes	in/sec
U'_{ST1} V'_{ST1} W'_{ST1}	UPT(4) VPT(4) WPT(4)	299	Components of the velocity of the deformed structural hard points along the space fixed axes	in/sec
U_T	UT	313	Total vehicle velocity	in/sec
v_{Gi}	VG(4)	106	Contact point lateral velocity in the direction parallel to the tire-terrain contact plane	in/sec
VGR_{12} VGR_{21} VGR_{23} VGR_{32} VGR_{34} VGR_{43}	VGR12 VGR21 VGR23 VGR32 VGR34 VGR43	I	Vehicle speed at which transmission upshifts and downshifts occur	mph
(VTAN)	VTAN	305	Tangential velocity between the vehicle and barrier	in/sec
WE_i	WEIGHT(I)	328	Driver steering error weighting function	
WI_i	XIMPOR(I)	I	Driver steering error importance weighting function	
(WOT)	TWOT		Wide open throttle torque	lb-ft
X_B, X_E XINCR	XB(5) XE(5) XINCR(5)	I	Beginning, ending and incremental x' for terrain tables	in
x_{BB}, y_{BB} z_{BB}	XBB YBB ZBB	279	Coordinates of the intersection of the z' axis with the barrier bottom plane in the vehicle axes	in
X_{BDRY}	XBDRY(4,5)	I	x' intercept for angled boundaries within terrain tables	in
x_{Bi} y_{Bi} z_{Bi}	XBI YBI ZBI	267	Coordinates of the intersection of the y' axis with cutting plane i, in the vehicle axes	in
x_{BT} y_{BT} z_{BT}	XBT YBT ZBT	278	Coordinates of the intersection with the barrier top plane in the vehicle axes	in
x'_C, y'_C, z'_C	XCP YCP ZCP	65 66 67	Coordinates of the origin of the vehicle axes (sprung mass center of gravity) with respect to the space fixed axes	in
x_{cpn} y_{cpn} z_{cpn}	XCPN(3) YCPN(3) ZCPN(3)	214	Coordinates of the vehicle corner n in the vehicle axes	in
x'_{cpn} y'_{cpn} z'_{cpn}	XCPNP(3) YCPNP(3) ZCPNP(3)	214	Coordinates of the vehicle corner n in the space-fixed axes	in
X'_{GP_i}, Y'_{GP_i} Z'_{GP_i}	XGPP(4) YGPP(4) ZGPP(4)	150 151	Coordinates of the ground contact points with respect to the space-fixed axes	in
x'_i, y'_i, z'_i	XP(4) YP(4) ZP(4)	68- 82	Coordinates of the wheel centers with respect to the space fixed axes	in

ANALYTICAL SYMBOL	PROGRAM SYMBOL	EQN NO	DEFINITION	UNITS
x_n y_n z_n	XNN(17) YNN(17) ZNN(17)	276	Coordinates of intercept points between the barrier and sprung mass in the vehicle axes	in
X'_{P1} y'_{P1}	X Y	318	Coordinates of the location on the desired path at which the ith error is determined	in
x_{Ri} y_{Ri} z_{Ri}	XRI YRI ZRI	294	Coordinates of the centroid of the intersection area on cutting plane i, projected on to the actual vehicle barrier interface of the previous time increment	in
$(\Sigma x_R)_t$ $(\Sigma y_R)_t$ $(\Sigma z_R)_t$	SXR SYR SZR	295 296 297	Coordinates of the point of application of the sprung mass impact force	in
X_{ST1} y_{ST1} z_{ST1}	XSTI(3) YSTI(3) ZSTI(3)	301	Coordinates of the deformed structural hard points in the vehicle axes	in
X_{ST1_o} y_{ST1_o} z_{ST1_o}	XSTIO(3) YSTIO(3) ZSTIO(3)	I	Coordinates of the underformed structural hard points in the vehicle axes	in
x_{VF}	XVF	I	Distance from the sprung mass c.g. to the vehicle front along the x axis	in
x_{VR}	XVR	I	Distance from the sprung mass c.g. to the vehicle rear along the x axis	
X'_{VP_i}	XVP	312	Driver prediction of vehicle location at the ith sample increment in the future	in
y'_{VP_i}	YVP	313		
X_1, Y_1, Z_1 X_2, Y_2, Z_2	X1,Y1,Z1 X2,Y2,Z2	I	Coordinates of accelerometer positions with respect to the vehicle axes for which acceleration components are output	in
$\{y\}$	VAR		System dependent variable, integral of $\{\dot{y}\}$	
$\{\dot{y}\}$	DER	47	First derivatives with respect to time of the system dependent variables	
$Y_B\ Y_E$ YINCR	YB(5) YE(5) YINCR(5)	I	Beginning, ending and incremental y' for terrain tables	in
Y_{BDRY}	YBDRY(4,5)	I	Lateral position of y' terrain boundaries with respect to space	in
y'_B	YBP	I	Lateral position of the barrier face plane with respect to space	in
y'_{C1}, y'_{C2} y'_{C3}, y'_{C4} y'_{C5}, y'_{C6}	YC1P YC2P YC3P YC4P YC5P YC6P	I	Lateral positions of slope changes defining a curb	in
y_v	YV	I	Distance from the sprung mass c.g. to the vehicle side	in
z'_{BB}	ZBBP	I	Elevation of the bottom barrier plane in space	in

ANALYTICAL SYMBOL	PROGRAM SYMBOL	ECON NO	DEFINITION	UNITS
Z'_{BT}	ZBTP	I	Elevation of the top barrier plane in space	in
Z'_{C2}, Z'_{C3}	ZC2P	I	Elevation of curb at slope$_{C2}$	in
Z'_{C4}, Z'_{C5}	ZC3P ZC4P	I	Change lateral positions	
Z'_{C6}	ZC5P ZC6P			
Z_F	ZF	I	Static distance along z axis between the sprung mass center of gravity and the center of gravity of the front unsprung masses	in
$\bar{Z}'_G$	ZGP(21,21,5)	I	Input elevations of the terrain table grid points	in
Z'_{Gi}	ZPGI(4)	126	Ground elevation with respect to the space axes of the point beneath the wheel centers	in
Z'_{Gi}			A vector through the ground contact point normal to the actual or equivalent ground contact plane	
Z_R	ZR	I	Static distance along the z axis between the sprung mass center of gravity and the rear axle roll center	in
Z_{VB}	ZBV	I	Distance from the sprung mass c.g. to the plane defining the bottom of the vehicle along the z axis	in
Z_{VT}	ZVT	I	Distance from the sprung mass c.g. to the plane defining the top of the vehicle, along the z axis	in
$\alpha_{B'}, \beta_{B'}, \gamma_{B'}$		266	Direction angles of a normal to the barrier face plane in the vehicle axes	
$\alpha_{BT'}, \beta_{BT'}, \gamma_{BT'}$		277	Direction angles of a normal to the barrier top plane in the vehicle axes	
$\alpha_{B1'}, \beta_{B1'}, \gamma_{B1'}$		273	Direction angles of a normal to the plane perpendicular to the barrier face plane and containing the axis of rotation	

ANALYTICAL SYMBOL	PROGRAM SYMBOL	ECON NO	DEFINITION	UNITS
$\alpha_{ci}, \beta_{ci}, \gamma_{ci}$		255	Direction angles of a line perpendicular to the normals of both the wheel plane and tire-terrain contact plane with respect to space	rad
$\alpha_{GZ_i}, \beta_{GZ_i}, \gamma_{GZ_i}$		84	Direction angles of a normal to the tire-terrain contact plane at wheel i with respect to space	rad
$\alpha_{R_i}, \beta_{R_i}, \gamma_{R_i}$		176	Direction angles of the resultant radial force on wheel i with respect to the vehicle axes	rad
$\alpha_j, \beta_j, \gamma_j$		143	Direction angles of a line from wheel center i to the ground contact point of tire radial spring j with respect to the vehicle axes	
$\alpha_{R_i}, \beta_{R_i}, \gamma_{R_i}$		148	Direction angles of the resultant radial force on wheel i with respect to the space axes	rad
$\alpha_{S_i}, \beta_{S_i}, \gamma_{S_i}$		257	Direction angles of a line perpendicular to both a normal to the tire-terrain contact plane and the wheel axis with respect to space	rad
$\alpha_x, \beta_x, \gamma_x$		102	Direction angles of the x axis with respect to space	
$\alpha_y, \beta_y, \gamma_y$		100	Direction angles of the y axis with respect to space	
$\alpha_{y_{wi}}, \beta_{y_{wi}}, \gamma_{y_{wi}}$		85	Direction angles of a normal to the wheel i with respect to space	
$\alpha_{w_i}, \beta_{w_i}, \gamma_{w_i}$		88	Direction angles of kingpin axis of wheel i	
β_i			Slip angle at wheel i	rad
β'_i	BETP(4)	219	Equivalent slip angle produced by camber of wheel i	rad
$\bar{\beta}_i$	BETBR(4)	223	Non dimensional slip angle variable for wheel i	
γ_1	GAM1	47	Inertial expressions	
$(\gamma_2)_t$	GAM2			
$(\gamma_3)_t$	GAM3			

ANALYTICAL SYMBOL	PROGRAM SYMBOL	COM NO	DEFINITION	UNITS
$(\tau_4)_t$	GAM4			
$(\tau_5)_t$	GAM5	+7		
$(\tau_6)_t$	GAM6		Inertial expressions	
$(\tau_7)_t$	GAM7			
$(\tau_8)_t$	GAM8			
$(\tau_9)_t$	GAM9			
	DELBB		Barrier deflection	in
δ_1	DEL1		Right front suspension deflection for independent front suspension or front axle roll center deflection relative to the vehicle from position of statis equilibrium	in
δ_2	DEL2		Left front suspension deflection relative to the vehicle from static equilibrium position	in
δ_3	DEL3		Right rear suspension deflection for independent rear suspension or rear axle roll center deflection relative to the vehicle from static equilibrium position	in
δ_4	DEL4		Left rear suspension deflection relative to the vehicle from static equilibrium position	in
Δ_G	DELG	I	Distance between road roughness input points	in
Δi	DELTA(4)	112	Distance between the wheel center and ground contact point	in
Δt	DT	I	Numerical integration step interval	sec
Δt_B	DELTB	I	Time increment for use during barrier impacts	sec
Δt	DELTC	I	Numerical integration step size for curb impact option	sec
Δt_n	DTR		Integration step size for use with wheel spin equations of motion	sec
ΔT_{HF1} ΔT_{HR1}	DTHF1 DTHF2 DTHR3 DTHR4	I	Front and rear half-track changes with suspension deflection	in
$\Delta y'_B$	DELYBP	I	Incremental deflection of the barrier position	in
$\Delta\psi_{fj}$	DPSILF	526	Ideal steer angle change	rad
$\bar{\epsilon}_B$	EPSB	I	Acceptable error in the force balance between the vehicle structure and barrier	lbs
ϵ_F, ϵ_R	EPSF EPSR	I	Friction lag in front and rear suspensions	in/sec
ϵ_n	EPSL		Permanent set of the barrier for secondary impacts	in
ϵ_v	EPSV	I	Friction lag in the vehicle-barrier friction force	in/sec
ϵ_w	EPSPS	I	Friction lag in steering system	deg/sec
ζ_B	ZETAB	I	Threshold value of wheel rotational velocity below which logic is applied to limit brake torques	rad/sec
ζ_i		771	Suspension displacement of the relative to the vehicle from the position of static equilibrium	in
$(\zeta_0)_n, (\zeta_1)_n$ $(\zeta_2)_n$	CD0 CD1 CD2		Coefficients for unloading force deflection characteristic of the barrier	
θ_c	THESKD	336	Vehicle slip angle	rad
θ_{G_i}	THG1(4)	124	Pitch angle of terrain under wheel i relative to the space axes	rad
θ'_n	THETN		Value of θ at t=0 or at the nth indexing of the axes	rad
ϕ'_t	THETT	57	integrated value of $\dot{\theta}$ from t=0 or the nth indexing of the axes	
θ'_{xG_i}		101	Angle between the x axis and the tire-terrain contact plane at wheel i	rad
λ_B	TLAMB	204	Coefficient for inertial coupling terms in relationships for driving end of vehicle	
λ_F, λ_R	XLAMF XLAMR	I	Ratio of conserved to absorbed energy in the front and rear suspension bumpers or multiple of K_F, K_R for use in simulating suspension bumpers	
λ_T	XLAMT	I	Multiple of K_T for use in non-linear range of tire deflection	
$\lambda_{1i}, \lambda_{2i}$ λ_{3i}	XLM1(4) XLM2(4) XLM3(4)	107 108 109	Contants for simultaneous solution of the ground contact point	
μ_B	AMUB	I	Effective coefficient of friction between the vehicle sprung mass and barrier	
μ_c	AMUC	I	Tire-curb friction factor	

ANALYTICAL SYMBOL	PROGRAM SYMBOL	COM NO.	DEFINITION	UNITS
μ_{G_i}	XMUGI(4)	I	Nominal coefficient of friction between tire i and ground	
μ_i	XMUI(4)	I	Peak value of friction coefficient for side forces for prevailing conditions of speed and load at wheel i	
μ_{m_i}	XMUM(4)	I	Nominal test surface friction coefficient on which tire properties were measured	
μ_{x_i}	XMUX(4)	240	Effective friction coefficient between tire and terrain at wheel i in the direction along the tire circumference	
$\mu_{x_{p_i}}$	XMUXP(4)	I	Peak circumferential friction coefficient for tire i	
$\mu_{x_{s_i}}$	XMUXS(4)	I	Sliding circumferential friction coefficient for tire i	
π	PI		3.14159...	
ρ	RHO	I	Distance between rear axle center of gravity and roll center, positive for roll center above c.g.	in
ρ_F	RHOF	I	Distance between front axle center of gravity and roll center, positive for roll center above c.g.	in
ρ_{s_i}	RHOS(I)	198	Ratio of circumferential to peak side force friction coefficients for prevailing conditions of speed and load	
$(\rho_{s_i})_{max}$	RHOMAX	196	Maximum value of ρ_{s_i} at the existing forward velocity of wheel i	
σ_R	SIGR	I	Coefficients for the polynominal form of barrier load deflection characteristic	
σ_T	SIGT	I	Maximum radial tire deflection for quasi-linear load-deflection characteristic	in
τ_A	TAUA	I	Ambient temperature	°F
τ_i	TAU(4)		Temperature of brake assembly	°F
τ_{i_o}	TAUO(4)	I	Initial temperature of brake assembly	°F
ϕ, θ, ψ	PHIT THETT PSIT		Euler angles of sprung mass axes relative to inertial axes	rad
ϕ_C ϕ_{C_R}	PHIC(50) PHIRC(50)	I	Table of front and rear wheel camber as a function of deflection	deg
$\phi_{C_{G_i}}$	PHICI(4)	86	Camber angles of wheels relative to the normal to tire-terrain contact plane	rad
ϕ_{C_1}, ϕ_{C_2} ϕ_{C_3}, ϕ_{C_4} ϕ_{C_5}, ϕ_{C_6}	PHIC1, PHIC2 PHIC3, PHIC4 PHIC5, PHIC6	I	Curb slope angles	rad

ANALYTICAL SYMBOL	PROGRAM SYMBOL	COM NO.	DEFINITION	UNITS
ϕ_F	PHIF		Angular displacement of front axle relative to the vehicle about a line parallel to the x-axis through the front roll center	rad
ϕ_{G_i}	PHGI(4)	125	Camber angle of terrain under wheel i	rad
ϕ_i	PHII(4)		Camber angles of four wheels relative to vehicle	rad
ϕ'_n	PHIN		Value of at t=0 or at the nth indexing of the axes	rad
ϕ_R	PHIR		Angular displacement of rear axle relative to the vehicle about a line parallel to the x - axis through the rear roll center	rad
ϕ'_T	PHIT	58	Integrated value of $\dot{\phi}$ from t=0 or the nth axis indexing	rad
ϕ_{yG_i}		125	Angle between y axis and tire-terrain contact plane	rad
ψ_{BDRY}	PSBDRY(4,5)	I	Angle of interpolation boundaries in terrain tables, measured from the x'axis	rad
ψ_f	PSIF(50)	I	Table of front wheel steer angle vs time	rad
ψ_i	PSII(4)		Steer angles of wheels relative to vehicle (positive-clockwise as viewed from above)	rad
ψ'_{i_p}	PSIIP(4)	109	Steer angles of wheels in tire-terrain contact plane	rad
ψ'_n	PSIN		Value of ψ at t=0 or the nth indexing of the axes	rad
ψ'_t	PSIT	59	Integrated value of $\dot{\psi}$ from t=0 or the nth axis indexing	rad
Ω_F Ω_R	OMEGF OMEGR	I	Maximum suspension deflections from the equilibrium position for linear load-deflection characteristic of the springs	in
Ω_{FC} Ω_{RC}	OMEGFC OMEGRC	I	Front and rear suspension deflections at which the compression bumpers are contacted, measured at the front wheels and the rear springs	in
Ω_{FE} Ω_{RE}	OMEGFE OMEGRE	I	Front and rear suspension deflections at which the extension bumpers are contacted, measured at the front wheels and rear springs	in
Ω_T	OMEGT	I	Multiple of A_2 at which the assumed parabolic variations of small angle cornering and camber stiffnesses with tire loading are abandoned	
Ω	OMGPS	I	Front wheel steering angle at which the linear steering stops are engaged	rad